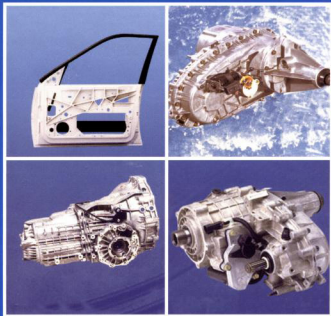


# Magnesium – Alloys and Technologies

Edited by K.U. Kainer



# **Magnesium – Alloys and Technology**

Edited by  
K.U. Kainer



**WILEY-  
VCH**

**WILEY-VCH GmbH & Co. KGaA**

**DGM**

Further titles of interest:

*K.U. Kainer (Ed.)  
Magnesium Alloys and their Applications  
ISBN 3-527-30282-4*

*H.P. Degischer, B. Kriszt (Eds.)  
Handbook of Cellular Metals  
ISBN 3-527-30339-1*

*G. Kosterz (Ed.)  
Phase Transformations in Materials  
ISBN 3-527-30256-5*

# Magnesium Alloys and Technology

Edited by  
K.U. Kainer

Translation by Frank Kaiser

**DGM**

Deutsche Gesellschaft  
für Materialkunde e. V.



WILEY-  
VCH

WILEY-VCH GmbH & Co. KGaA

Editor:  
Prof. Dr. K. U. Kainer  
GKSS-Forschungszentrum  
Institut für Werkstofforschung  
Max-Planck-Straße  
D-21502 Geesthacht  
Germany

Lectures from a workshop of the German Association for Material Science in cooperation with the Institute for Material Research at the GKSS Research Center Geesthacht GmbH.

This book was carefully produced. Nevertheless, editor, authors, and publisher do not warrant the information contained therein to be free of errors. Readers are advised to keep in mind that statements, data, illustrations, procedural details or other items may inadvertently be inaccurate.

British Library Cataloguing-in-Publication Data:  
A catalogue record for this book is available from the British Library

Bibliographic information published by Die Deutsche Bibliothek  
Die Deutsche Bibliothek lists this publication in the Deutsche Nationalbibliografie; detailed bibliographic data is available in the Internet at <<http://dnb.ddb.de>>.  
ISBN 3-527-30570-X

© 2003 WILEY-VCH Verlag GmbH & Co. KG aA, Weinheim

Printed on acid-free paper

All rights reserved (including those of translation in other languages). No part of this book may be reproduced in any form – by photoprinting, microfilm, or any other means – nor transmitted or translated into machine language without written permission from the publishers. Registered names, trademarks, etc. used in this book, even when not specifically marked as such, are not to be considered unprotected by law.

Translator: Frank Kaiser  
Composition: Strassner ComputerSatz, Leimen  
Printing: betz-druck GmbH, Darmstadt  
Bookbinding: Litges & Dopf Buchbinderei GmbH, Heppenheim  
Printed in the Federal Republic of Germany

# Preface

Magnesium alloys meet the demand for a combination of low specific weight, good machinability and handling, an interesting characteristic profile, and high recycling potential. Despite this, the application of magnesium still lags behind that of competing materials. Reasons for this are the high price, the limited availability of specific, custom-made magnesium materials, and to some extent also a lack of know-how as regards the handling and machining of magnesium. The automotive industry leads the way in the growing interest in magnesium alloys since this branch in particular is under public pressure to save scarce primary energy resources and to realize their environmentally friendly use.

The German Association for Material Science (DGM) has responded to the growing interest in magnesium materials by holding a workshop on this topic. At this workshop, the present state-of-the-art in magnesium materials was extensively described. Furthermore, the lectures detailed the application possibilities and the future potential of magnesium alloys. This book has emerged from the seminars and is based on them. The main focus of the summary lies in the processing technology, although wrought alloys, which are gaining interest, are also considered. Also covered is the use of progressive processing techniques. All articles are written by experts from research and development within the field of magnesium technology. The more application-oriented topics have been covered by experts from the industry. Through their expertise, they have contributed greatly to the success of the workshop.

The following topics are dealt with:

- basics of magnesium technology
- alloying systems
- melting metallurgical processing technologies (die-casting, squeeze-casting, thixo-casting)
- extrusion, forging, sheet-metal forming
- joining (welding)
- corrosion and corrosion resistance
- progressive technologies (powder metallurgy, spray-forming, magnesium composite materials)
- machining
- recycling
- economic aspects
- application examples and future potential

This book is addressed to engineers, scientists, and technicians from the fields of material development, production, and engineering. It may also be used as a source of information on magnesium for apprentice engineers and industrial engineers.

*Prof. K. U. Kainer*

GKSS Research Center Geesthacht GmbH

January 2003

# Content

1	The Current State of Technology and Potential for further Development of Magnesium Applications .....	1
	<i>K. U. Kainer, Institute for Materials Research, Center for Magnesium Technology, GKSS Research Center Geesthacht GmbH, Geesthacht</i>	
	<i>F. von Buch, Institute for Materials Research and Technology, Technical University of Clausthal, Clausthal-Zellerfeld</i>	
2	Die-Casting Magnesium .....	23
	<i>R. Fink, Oskar Frech GmbH, Schorndorf</i>	
3	Vacuum Die-Casting of Magnesium Parts with High Pressure .....	45
	<i>M. Siedersleben, Honsel AG, Meschede</i>	
4	Squeeze-Casting and Thixo-Casting of Magnesium Alloys .....	56
	<i>K. U. Kainer, T. U. Benzler, Institute for Materials Research, GKSS Research Center Geesthacht GmbH, Geesthacht</i>	
5	Deformation of Magnesium .....	72
	<i>E. Doege, K. Dröder, St. Janssen, University of Hannover</i>	
6	Manufacturing and Potential of Extruded and Forged Magnesium Products .....	90
	<i>J. Becker, G. Fischer, OTTO FUCHS Metallwerke, Meinerzhagen</i>	
7	High-Temperature Properties of Magnesium Alloys .....	106
	<i>F. von Buch, B. L. Mordike</i>	
	<i>Institute for Materials Research and Technology, Technical University of Clausthal</i>	
8	High-Tech Machining of Magnesium and Magnesium Composites .....	130
	<i>K. Weinert, M. Liedschulte, D. Opalla, M. Schroer</i>	
	<i>Institute for Metal Cutting Manufacturing, Dortmund University</i>	
9	Joining Magnesium Alloys .....	152
	<i>A. Schram, Chr. Kettler, ISAF, Technical University Clausthal</i>	
10	Rapid Solidification and Special Processes for Processing Magnesium Alloys .....	164
	<i>T. Ebert, Institute for Materials Research and Technology, Technical University of Clausthal</i>	
	<i>K. U. Kainer, Institute for Materials Research and Technology, Clausthal-Zellerfeld</i>	
	<i>GKSS Research Center GmbH, Geesthacht</i>	
11	Fibre-Reinforced Magnesium Composites .....	184
	<i>Ch. Fritze, BMW Group, München</i>	

<b>12 Particle-Reinforced Magnesium Alloys</b> .....	197
<i>F. Moll, Institute for Materials Research and Technology, Technical University of Clausthal</i>	
<i>K. U. Kainer, Institute for Materials Research, GKSS Research Center Geesthacht GmbH, Geesthacht</i>	
<b>13 Corrosion and Corrosion Protection of Magnesium</b> .....	218
<i>P. Kurze, AHC-Oberflächentechnik GmbH &amp; Co. OHG, Kerpen</i>	
<b>14 Magnesium Corrosion – Processes, Protection of Anode and Cathode</b> .....	226
<i>H. Haferkamp<sup>1</sup>, Fr.-W. Bach<sup>2</sup>, V. Kaese<sup>1</sup>, K. Möhwald<sup>2</sup>, M. Niemeyer<sup>1</sup>, H. Schreckenberger<sup>3</sup>, Phan-tan Tai<sup>1</sup></i>	
<sup>1</sup> <i>Institute for Materials Research, Technical University of Hannover</i>	
<sup>2</sup> <i>Chair of Materials Technology, Dortmund University</i>	
<sup>3</sup> <i>Volkswagen AG, Central Lab Wolfsburg</i>	
<b>15 Electroless Nickel-Phosphor Alloy Coatings for Magnesium</b> .....	242
<i>F. Leyendecker, AHC-Oberflächentechnik GmbH &amp; Co. OHG</i>	
<b>16 Recycling of Magnesium Alloys</b> .....	254
<i>Ditze, C. Scharf, Institute for Metallurgy, Technical University Clausthal, Clausthal-Zellerfeld</i>	
<b>Index</b> .....	279



# 1 The Current State of Technology and Potential for further Development of Magnesium Applications

*K. U. Kainer, Institute for Materials Research, Center for Magnesium Technology, GKSS Research Center Geesthacht GmbH, Geesthacht*

*F. von Buch, Institute for Materials Research and Technology, Technical University of Clausthal, Clausthal-Zellerfeld*

## 1.1 Introduction

High-technology companies increasingly rely on the technical and economic potential of innovative materials, as well as their workmanship and machining abilities, as a strategy for successful competition on the market. Additionally, politics and the public are demanding a more economical use of scarce primary energy sources.

One of the key goals for the next decades will be the further reduction of emissions to lower the growing environmental impact. Taking this into consideration, the use of light metals as construction materials is generally viewed as becoming of key importance in the future.

Although magnesium alloys are fulfilling the demands for low specific weight materials with excellent machining abilities and good recycling potential, they are still not used to the same extent as the competing materials aluminium and plastics. One of the reasons is the fairly high priced base material, coupled with the partial absence of recycling possibilities. On the other hand, the variety of magnesium available to the consumer is still limited to a few technical alloys. Unfortunately, there is a lack of know-how in the use of magnesium, not least within the companies dealing with the machining and application of construction materials. As a result, the industry still tends to use “conventional” materials instead of magnesium alloys.

Discovered in 1774 and named after the ancient city Magnesia, magnesium is found to be the 6<sup>th</sup> most abundant element, constituting 2% of the total mass of the Earth's crust. It belongs to the second main group in the periodic table of elements (group of alkaline earth metals) and is therefore not found in elemental form in nature, but only in chemical combinations. The silicates olivine, serpentine, and talc do not play any role in refining magnesium, although they represent the most commonly occurring natural magnesium compounds. More important are the mineral forms magnesite  $\text{MgCO}_3$  (27% Mg), dolomite  $\text{MgCO}_3 \cdot \text{CaCO}_3$  (13% Mg), and carnallite  $\text{KCl} \cdot \text{MgCl}_2 \cdot 6\text{H}_2\text{O}$  (8% Mg), as well as sea water, which contains 0.13% Mg or 1.1 kg Mg per  $\text{m}^3$  (3<sup>rd</sup> most abundant among the dissolved minerals in sea water). Magnesium is recovered by electrolysis of molten anhydrous  $\text{MgCl}_2$ , by thermal reduction of dolomite, or by extraction of magnesium oxide from sea water. The global production of roughly 436,000 t (1997) [1] is covered by melt electrolysis to 75% and by thermal reduction to 25% [2].

Considering the total energy needed to produce magnesium from its various raw materials, it consumes a relative large amount of energy compared to other metals as long as the calculation is based on the mass. Referring it to the volume of the gained primary material magnesium shows a contrary effect: in this case, magnesium uses much less energy than

e.g. aluminium or zinc and even competes with polymers. In addition, it is assumed that the present electrical energy of 40–80 MJ/kg (25 MJ/kg would be possible in theory) needed for electrolysis can be reduced to 40 MJ/kg or less by all the big producers in the near future. This would mean that the corresponding values for producing aluminium (electrolysis of  $Al_2O_3$  to yield aluminium consumes 47 MJ/kg) could be undercut [3]. Optimization or improvement of existing production methods and the establishment of a secondary recirculation could open new perspectives for reducing the cost of primary magnesium production.

## 1.2 Magnesium's Characteristic Profile

Magnesium crystallizes in the hexagonal closest packed structure and is therefore not amenable to cold forming. Below 225 °C, only {0001} <1120> basal plane slipping is possible, along with pyramidal {1012} <1011> twinning. Pure magnesium and conventionally cast alloys show a tendency for brittleness due to intercrystalline failure and local transcrystalline fracture at twin zones or {0001} basal planes with big grains. Above 225 °C, new {1011} basal planes are formed and magnesium suddenly shows good deformation behaviour, suggesting that extensive deformation only occurs above this temperature [2]. Table 1 shows the most important properties of pure magnesium.

Table 1: Properties of pure magnesium [1, 3, 6].

Crystal Structure .....	hcp
Density .....	1,738 g/cm <sup>3</sup> at RT
.....	1,584 g/cm <sup>3</sup> at T <sub>m</sub>
Young's Modulus .....	45 GPa
Ultimate Tensile Strength.....	80-180 MPa
Fracture Elongation .....	1-12 %
Melting Point.....	650 +/- 0,5°C
Boiling Point.....	1090°C
Specific Heat Capacity.....	1,05 kJ/(kg K)
Fusion Heat.....	195 kJ/kg
Heat Conductivity.....	156 W/(m·K) (RT)
Linear Expansion Coefficient.....	26·10 <sup>-6</sup> K <sup>-1</sup> (RT)
Shrinkage (solid-liquid) .....	4,2 %
Shrinkage (T <sub>m</sub> -RT) .....	ca. 5%
Specific Electrical Conductivity.....	22,4 m/(Ω mm <sup>2</sup> ) (RT)
Normal Potential.....	-2,37 V

Most magnesium alloys show very good machinability and processability, and even the most complicated die-cast parts can be easily produced. Cast, moulded, and forged parts made of magnesium alloys are also inert gas weldable and machinable. Another aspect is the good damping behaviour, which makes the use of these alloys even more attractive for increasing the life cycle of machines and equipment or for the reduction of sonic emission. Pure magnesium shows even higher damping properties than cast-iron [2], although these properties are highly dependent on the prior heat treatment.

Along with the excellent properties, there are some disadvantages to the application of these alloys. As already mentioned, the cold working abilities are very poor and the corrosion resistance of magnesium alloys is very low. Besides, magnesium is very reactive. When cast, magnesium has a high mould shrinkage of approximately 4% when solidifying and of about 5% during cooling [1]. This high degree of shrinkage leads to microporosity, low toughness, and high notch sensitivity that cannot be ignored. This behaviour, as well as

the high thermal expansion coefficient (ca. 10% above the corresponding value for aluminium), is often put forward as an argument against the use of magnesium alloys.

The negative properties mentioned above deter construction engineers from accepting magnesium alloys as a competitive replacement for aluminium or steel. Therefore, attempts have been made to improve the characteristic profile of magnesium alloys by employing different alloying elements so as to achieve better precipitation and solid-solution hardening.

In this way, all the advantageous properties listed below have been realized:

- lowest density of all construction metals at 1.8 g/cm<sup>3</sup>; light construction parts possible
- high specific strength (strength/density ratio)
- excellent casting ability; steel dies may be used
- good machining ability (milling, turning, sawing) [4]
- improved corrosion resistance with high-purity (HP) alloys [5]
- high damping properties
- good weldability under inert gases
- integrated recycling possible

The static and dynamic mechanical properties are inferior to the corresponding values for the competing aluminium, e.g. the Young's modulus. Nevertheless, magnesium is found in all places where weight saving takes priority over the other properties, mainly because the specific strength can reach and even exceed the values for aluminium and steel.

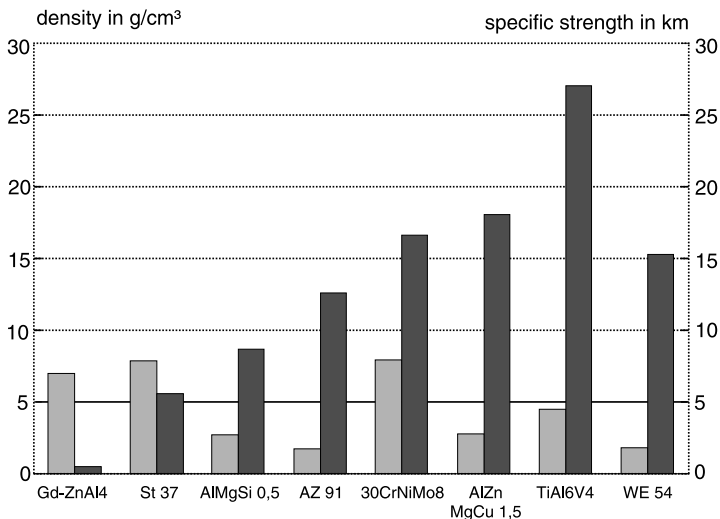


Figure 1: Densities and specific strengths of selected materials

## 1.3 Alloying Systems

To give a short overview of the different magnesium alloys, it is necessary to first show the identification of all kinds of alloys and the effect of each alloying element.

### 1.3.1 Identification of Magnesium Alloys

The identification of magnesium alloys is standardized worldwide in the ASTM norm; each alloy is marked with letters indicating the main alloy elements, followed by the rounded figures of each (usually two) weight in percentage terms. Table 2 shows the key letters for every available alloying element. The last letter in each identification number indicates the stage of development of the alloy (A, B, C,...). In most cases, these letters show the degree of purity. The alloy AZ91D, for example, is an alloy with a rated content of 9% aluminium (A) and 1% zinc (Z). Its development stage is 4 (D). The corresponding DIN specification would be MgAl9Zn1. ASTM dictates the following composition (all values weight-%): Al 8.3–9.7; Zn 0.35–1.0; Si max. 0.10; Mn max. 0.15; Cu max. 0.30; Fe max. 0.005; Ni max. 0.002; others max. 0.02. Iron, nickel, and copper have tremendous negative effects on the corrosion resistance and hence these values are strictly limited.

Table 2: ASTM codes for magnesium's alloying elements.

Abbreviation letter	Alloying element	Abbreviation letter	Alloying element
A	aluminium	N	nickel
B	bismuth	P	lead
C	copper	Q	silver
D	cadmium	R	chromium
E	rare earths	S	silicon
F	iron	T	tin
H	thorium	W	yttrium
K	zirconium	Y	antimony
L	lithium	Z	zinc
M	manganese		

### 1.3.2 Alloying Elements [3, 6, 11, 12]

Since the advent of magnesium alloys, there has been a lot of effort to influence the properties of pure magnesium with different alloying elements. The main mechanism for improving the mechanical properties is precipitation hardening and/or solid-solution hardening. While solid-solution hardening is determined by the differences in the atomic radii of the elements involved, the effectiveness of precipitation hardening mainly depends on a reduced solubility at low temperatures, the magnesium content of the intermetallic phase, and its stability at application temperature. Magnesium forms intermetallic phases with most alloying elements, the stability of the phase increasing with the electronegativity of the other element.

By the 1920s, aluminium had already become the most important alloying element for significantly increasing the tensile strength, specifically by forming the intermetallic phase  $Mg_{17}Al_{12}$ . Similar effects can be achieved with zinc and manganese, while the addition of silver leads to improved high-temperature strength. High percentages of silicon reduce the

castability and lead to brittleness, whereas the inclusion of zirconium forms oxides due to its affinity for oxygen, which are active as structure-forming nuclei. Because of this, the physical properties are enhanced by fine grain hardening. The use of rare earth elements (e.g. Y, Nd, Ce) has become more and more popular since they impart a significant increase in strength through precipitation hardening. Copper, nickel, and iron are very rarely used. All these elements increase susceptibility to corrosion, as established by the precipitation of cathodic compounds when they solidify. In contrast to regular cases, where a magnesium oxide or -hydride layer protects the metal and lowers corrosion rate, these elements increase the corrosion rate. This is one of the reasons why alloy development has been directed towards “high-purity” (HP) alloys with very little use of iron, nickel, or copper.

Below are the most important alloying elements in alphabetical order:

<i>Al</i>	The improvement of the physical properties with aluminium was already established in the 1920s. These alloys containing Al were sold as “Elektron”. Aluminium increases the tensile strength and the hardness, although the hardness effect caused by the precipitated phase $Mg_{17}Al_{12}$ is only observed up to 120 °C. These alloys are usually heat treated (T6), except under die-cast conditions, which hardly allow for heat treatment. Besides these improvements of the mechanical properties, there is the big advantage of better castability (eutectic system, $T_E = 437$ °C). This is the main reason why most technical alloys – especially casting alloys (mainly AZ91) – contain a high percentage of aluminium. The disadvantage is a higher tendency for microporosity.
<i>Be</i>	Beryllium is only supplied to the melt in small amounts (<30 ppm); the melt oxidation can be reduced dramatically.
<i>Ca</i>	Calcium has a positive effect on grain refining and aids creep resistance. On the other hand, calcium can lead to sticking to the tool during casting and to hot cracking [9].
<i>Li</i>	Lithium leads to solid-solution hardening at ambient temperatures, reduces density, and increases ductility. However, it has strong negative effects on the burning and vapour behaviour of the melt. Corrosion behaviour gets worse. Above 30% Li-content, the lattice structure changes to fcc.
<i>Mn</i>	Above 1.5 weight-% manganese, the tensile strength is increased. Alloying with manganese results in better corrosion resistance (Fe content is controlled by lowering the solubility), grain refinement, and weldability.
<i>RE</i>	All rare earth elements (including yttrium) form eutectic systems of limited solubility with magnesium. Therefore, precipitation hardening is possible and makes sense. The precipitates are very stable and raise the creep resistance, corrosion resistance, and high-temperature strength. Technical alloying elements are yttrium, neodymium, and cerium. Due to the high costs, these elements are mainly used in high-tech alloys.
<i>Si</i>	Silicon lowers the castability, but the creep resistance can be raised by stable silazide formation.
<i>Ag</i>	Silver, together with the rare earth metals, strongly increases the high-temperature strength and creep resistance, but also leads to low corrosion resistance.
<i>Th</i>	Thorium is the most effective element for increasing high-temperature strength and creep resistance of magnesium alloys. Unfortunately, however, it is radioactive and is therefore substituted by other elements.
<i>Zn</i>	Zinc induces the same behaviour as Al in terms of castability and strengthening. By adding up to 3% zinc, shrinkage can be compensated and tensile strength is raised. As with aluminium, there is a tendency towards microporosity, and on adding more than 2% hot cracking can also occur.
<i>Zr</i>	Addition of zirconium leads to an increase in tensile strength without a loss of ductility, because of its affinity for oxygen. The formed oxides are structure-forming nuclei and aid grain refining. Zirconium cannot be added to melts containing aluminium or silicon.

### 1.3.3 Casting Alloys

Aluminium is, as already described, the most frequently used alloying element for magnesium, with contents varying between 3 and 9 weight-%. These alloys have good mechanical properties and excellent corrosion resistance. The more aluminium the melt contains (eutectic system,  $T_E = 437\text{ }^\circ\text{C}$ ; Al content  $\sim 33\%$ ), the better the castability. The most widely used of magnesium die-casting alloys is AZ91 because of its superb castability even for the most complex and thin-walled parts. Table 3 gives a short overview of available alloying systems for pressure die-casting.

Table 3: Overview of all available casting alloys.

The most important die-casting alloy groups:			
AZ alloys			
– good room temperature properties			
– low heat resistance and creep resistance			
– limited ductility			
AM alloys			
– lower Al content and elimination of zinc improves ductility			
– limited room temperature properties and castability			
AS alloys			
– significantly higher heat and creep resistance through Mg-RE precipitations			
– only casting is possible			
– limited castability			
Consumption of the European automobile industry:			
2004	AZ: 61%	AM: 32%	AS/AE: 7%
1999	AZ: 67%	AM: 29%	AS/AE: 4%

As mentioned above, the negative effect of a high aluminium content is the formation of the interdendritic grain boundary phase  $\text{Mg}_{17}\text{Al}_{12}$ . It lowers the strength within the fine-grained crystal structure and leads to limited ductility of the alloy, as is also found for zinc components.

To improve the deformation behaviour of magnesium alloys, the Al content is decreased, the alloying with zinc is completely abandoned, and manganese is added instead. These alloys of the magnesium–aluminium–manganese family, e.g. AM20, AM50, AM60 (Mn contents between 0.2 and 0.4%) show lower strength at ambient temperature, but they are less brittle than the Al/Zn-based alloys. AMx alloys exhibit better deformation behaviour, but the low aluminium content limits their castability.

One of the most important criteria for magnesium alloys is the high-temperature and creep behaviour. For this reason, in earlier years attempts were made to reduce the aluminium content in the melt and to use different materials for alloying. During production of the VW-Beetle, the addition of silicon had already been established [13]. The resulting alloys, AS21 and AS41, were found to possess a much greater high-temperature strength and creep resistance than AZ91. The mechanism whereby high-temperature and creep behaviour is improved is based on a reduction of the aluminium content and the formation of the intermetallic phase  $\text{Mg}_2\text{Si}$  ( $T_m = 1085\text{ }^\circ\text{C}$ ), which shows good stability even at high temper-

atures. In this context, the AE alloys have to be taken into consideration, although they cannot be produced by die-casting because very stable Al-RE precipitates are formed on slow cooling. An overview of the tensile strength as a function of temperature for the most frequently used alloying systems is given in Fig. 2:

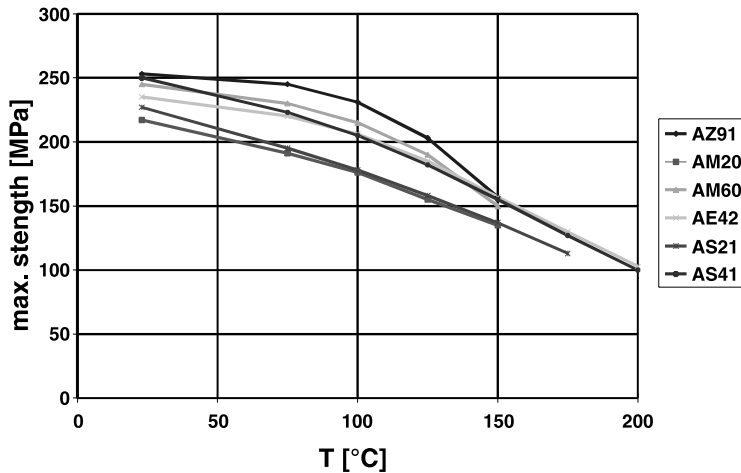


Figure 2: Tensile strengths of the most important Mg die-casting alloys as a function of temperature [2]

Applications at temperatures beyond 200 °C demand properties that can only be served by alloys containing silver and/or rare earths (Table 4). Specifically, this means the QE alloy group, which exhibit remarkable high-temperature properties, and the high-tech alloys WE-x, which allow applications up to 300 °C. The disadvantage of both series of alloys is their low castability; the production method is limited to sand and gravity casting. Additionally, the high costs have to be considered as a reason for many not to use them (e.g. 13 €/kg for QE22, 25 €/kg for WE54; compared to 2–3 €/kg for an AZ or AM alloy). For this reason, these alloys are mainly used in special applications such as in the aircraft and spacecraft industries. The falling prices for rare earths in the international markets may lead to a change in this trend in the future.

Table 4: Overview of the rare earth containing casting alloys (mostly sand/gravity casting).

<p><b>Rare earth containing casting alloys</b></p> <p>History:</p> <p>1937: good heat resistance Mg/Ce</p> <p>1947: influence of zirconium (EK, EZ, ZE series)</p> <p>1949: influence of La &lt; Ce &lt; Nd</p> <p>1959: influence of Ag (QE, EQ series)</p> <p>1979: system Mg-Y (WE series)</p> <p>Important alloys applied today:</p> <p style="padding-left: 20px;">ZE41</p> <p style="padding-left: 20px;">EZ33</p> <p style="padding-left: 20px;">EQ21</p> <p style="padding-left: 20px;">QE22</p> <p style="padding-left: 20px;">WE43</p> <p style="padding-left: 20px;">WE54</p> <p>The WE series represents the current stage of the material development:</p> <ul style="list-style-type: none"> <li>- good castability</li> <li>- highly heat resistant</li> <li>- highly creep resistant</li> <li>- ageing resistant</li> <li>- good fatigue strength</li> <li>- corrosion resistant</li> </ul>
---

### 1.3.4 Wrought Alloys

The poor cold workability of the hexagonal lattice structure and the formation of twins have resulted in a very limited usage of magnesium as a wrought material. Therefore, the range of available wrought alloys is still limited. Tables 5 and 6 give an overview of the compositions and properties of selected alloys. The Mg/Al series of alloys (AZ31, AZ61, AZ80) plays the most important role, being used on a scale comparable to that of the casting alloys.

Table 5: Summary of available magnesium wrought alloys [3]

alloy	Al	Ca	Zn	Mn	Cu	Zr	Y	Nd	Th
AZ21X1	1,6-2,5	0,1-0,25	0,8-1,6	0,15 max.	0,05				
AZ31	3,0		1,0	0,3					
AZ31B	2,5-3,5	0,04 max.	0,7-1,3	0,20-1,0	0,05				
AZ61A	5,8-7,2		0,40-1,5	0,15-0,5	0,05				
AZ80	8,5		0,5	0,12					
AZCOML	2,0-3,6	0,04 max.	0,3-1,5	0,15 min	0,10				
AZM	6,0		1,0	0,3					
ZC71			6,5	0,7	1,2				
ZK40			3,5-4,5			0,45 min			
ZK60A			4,8-6,2			0,45 min			
ZM21			2,0	1,0					
ZW3			3,0			0,6			
HM21				0,8					2,0
HM31						0,7			2,0
WE43						0,5	4,0	4,0	
WE54						0,5	5,25	3,5	



Table 6: Mechanical properties of various magnesium wrought alloys [3]

Alloy/condition	Tensile Strength [MPa]	0,2%-Yield Strength [MPa]	Fracture Elongation [%]	0,2%-Compression Strength [MPa]
<b>Solid Profile</b>				
AZ31B-F	262	193	14	103
AZ61A-F	317	228	17	131
AZ80-T5	379	276	7	241
HM31A-T5	303	269	10	172
ZK60A-T5	365	303	11	248
<b>Tubes/Hollow Profiles</b>				
AZ31B-F	248	165	16	83
AZ61A-F	283	165	14	110
ZK60A-T5	345	276	11	200
<b>Sheets/Bands</b>				
AZ31B-H24	290	221	15	179
AZ31B-0	255	152	21	110
HK31A-H24	262	207	9	159
HK31A-0	228	200	23	97
HM21A-T8	248	193	11	145

Alloys such as ZC71, ZW3, and ZM21 [12] are available, but are not used to any great extent. Wrought alloys are hot-worked by rolling, extrusion, and forging at temperatures above 350 °C. Additional cold-working procedures can be applied afterwards with low deformation rates to prevent the formation of cracks [3]. Since magnesium is envisaged for use in parts with high safety concerns, there has been a noticeable increase in interest in wrought alloys. The behaviour during crashing is an important criterion in such considerations.

## 1.4 Applications

In the past, the driving force behind the development of magnesium alloys was the potential for lightweight construction in military applications. Nowadays, the emphasis has shifted towards saving weight in automobile applications in order to meet the demands for more economic use of fuel and lower emissions in a time of growing environmental impact.

It is interesting to note that the use of magnesium in cars is by no means a recent innovation. As early as the 1930s, it was common to include magnesium cast parts in automobiles, with the VW-Beetle as the most famous example. Since the start of its production in 1939, more and more parts, such as the crank case, camshaft sprocket, gearbox housing, several covers, and the arm of an electric generator, were added until the total magnesium weight reached 17 kg in 1962, which meant a reduction of 50 kg in total mass compared to steel. The production of the VW-Beetle used almost 21,000 t of magnesium alloys in 1960 [19] and the Volkswagen Group reached a total consumption of 42,000 t of magnesium alloys in 1972 [13], until the change from air-cooled to water-cooled engines dramatically reduced the use of magnesium alloys.

Other manufacturers used magnesium in their technical applications, as well as in complex parts such as tractor hoods made of die-castings (dimensions: 1250 mm × 725 mm × 480 mm; weight 7.6 kg), main gear boxes for helicopters (casting weight 400 kg, machined 200 kg), crank cases for zeppelin engines, air intake cases for propjet engines (weight 42 kg), frames, rims, instrument panels, fan blades for cooling towers (weight 169 kg), etc.

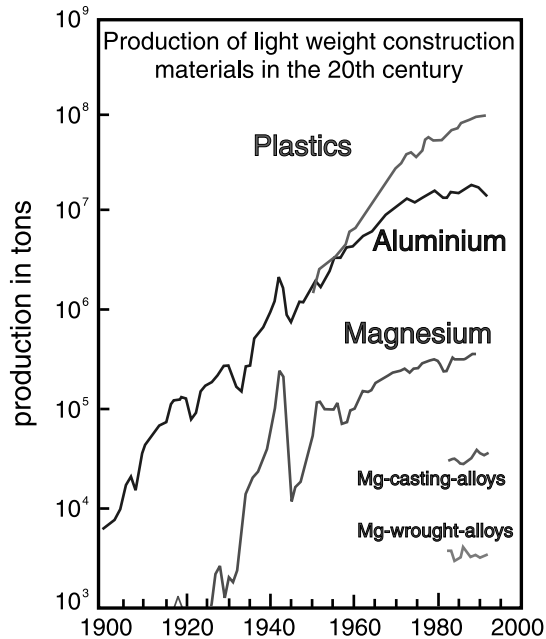


Figure 3: Production of materials with low density in the 20<sup>th</sup> century [3]

Why the trend of utilizing magnesium alloys did not continue in a straightforward manner is hard to explain today. A main factor was certainly the limited capacity of the few magnesium producers, as a result of which a low and constant price on the world market was not attained.

The development of high purity (HP) alloys, with their much improved corrosion resistance, contributed to a rapidly expanding production. In the past, the corrosion behaviour of available alloys had often been the overriding factor preventing their application. A further factor favouring magnesium use is that it counts as a substitute for polymers for which no satisfactory recycling solution has yet been found.

With regard to the processing of magnesium alloys, pressure die-casting is preferred in view of its advantages in the processing of aluminium and zinc, which are both amenable to this type of casting. Besides the specific properties of magnesium mentioned above, further favourable factors are its low casting temperature (650–680 °C, depending on the alloy) and the relatively low energy needed for melting. The energy needed for AZ91 (2 kJ/cm<sup>3</sup>) is about 77% of that required to melt the aluminium alloy AlSi12CuFe [3]. The high price of magnesium usually refers to its mass not its volume, and the lower density coupled with other factors can actually make it cheaper in real terms. Thus, the low thermal content allows the casting process to be 50% faster than with aluminium; a high clock cycle of parts is possible, maintaining high precision and good surface quality.

On freezing, the crystal structure is very fine grained, which results in good mechanical properties at room temperature but also leads to poor creep resistance. Moreover, the microstructure can be porous due to turbulences at high mould-filling speeds; subsequent heat treatments are useless since the pores would break apart. Magnesium does not attack iron moulds as much as aluminium does; the moulds can have steeper walls and the

potential savings in terms of tools can be as much as 50% compared with the use of aluminium [21]. Machine endurance is much higher as well (less retooling). The typical microstructure of an AZ91 alloy is shown in Fig. 4.

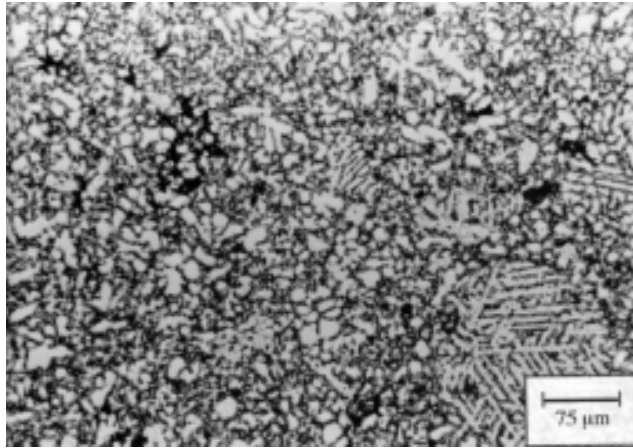


Figure 4: Microstructure of a die-cast AZ91 alloy

The automotive industry is by far the major user of magnesium alloys on a large scale, due to the possibility of mass-producing series parts by pressure die-casting with high quality at reasonable costs. Examples of magnesium parts in vehicles include:

- gearbox housing, e.g. in the VW Passat, Audi A4
- the inner tailgate in the Lupo (“3-liter car”), which is made of AM50 (3.2 kg)
- tank cover in the Mercedes-Benz SLK
- cylinder head caps, e.g. made of AZ91HP by cold-chamber casting, and having a weight of 1.4 kg [17]
- dashboard, e.g. in the Audi A8 and in the Buick Park Avenue/Le Sabre [22]
- seat-frames [23]
- steering wheels, e.g. in the Toyota Lexus, Celica, Carina, and Corolla [22]
- rims, e.g. in the Porsche Carrera RS (9.8 kg AM70 HP; low-pressure ingot casting) [17]

The list of magnesium parts in cars can be continued, e.g. in refs. [1,21,24], since new examples are constantly being added. Two recent applications of magnesium are illustrated in Figs. 5 and 6. The Mercedes-Benz SLK fuel tank cover is used as an example to show the consequences resulting from converting the construction from conventional materials to magnesium alloys. The part supports the car body’s web and serves as a separation between the trunk and the back seats. Previous solutions consisted of a welded conduit frame. The first alternatives were steel and aluminium weldings (7–8 kg each) and a magnesium cast part. The magnesium casting could be established as a serial part with a total weight of 3.2 kg, a decreased spatial requirement, and fewer components. Moreover, no post-processing was necessary and the part could be used uncovered. The use of magnesium in the gearbox housing in the VW Passat is also primarily based on the weight savings achieved on replacing aluminium alloys. The use of the AZ91 alloy instead of aluminium led to a

total weight reduction of almost 25%, and the geometry and production equipment remained identical. Since the introduction of repetitive work in 1996, 600 parts are manufactured at VW in Kassel per day [10]; an output of 1200 parts/day is projected for the future.

Magnesium's low density, its shielding against electromagnetic radiation, and the possibility of producing thin-walled parts has led to further use of die-cast parts in the computer industry [25], in mobile phones (Figs. 7 and 8), and in hand tools (e.g. chainsaws).

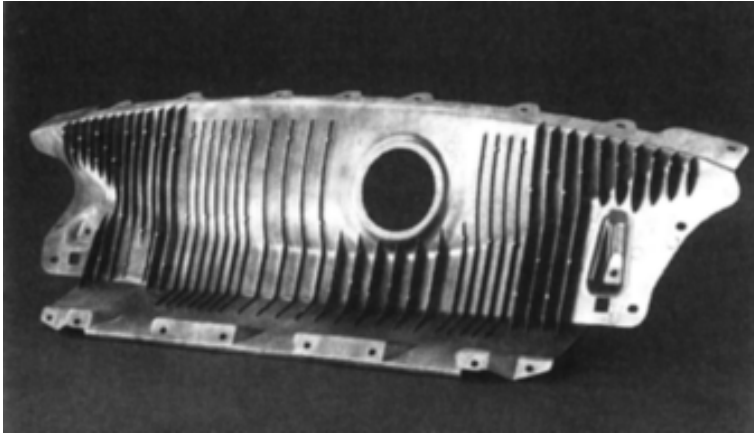


Figure 5: Fuel-tank cover (Mercedes-Benz AG)

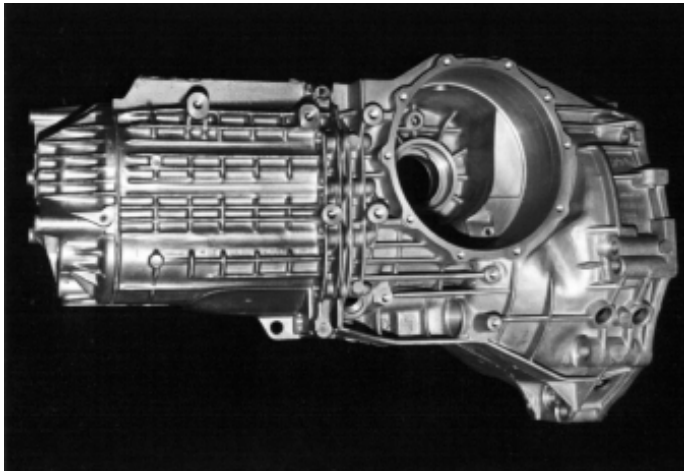


Figure 6: Gearbox housing in the VW-Passat (Volkswagen AG)

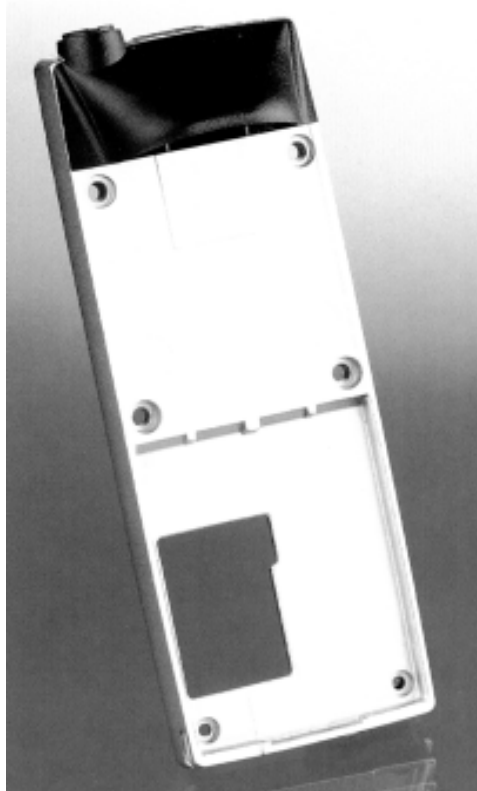


Figure 7: Mobile-phone case (Unitech Company)

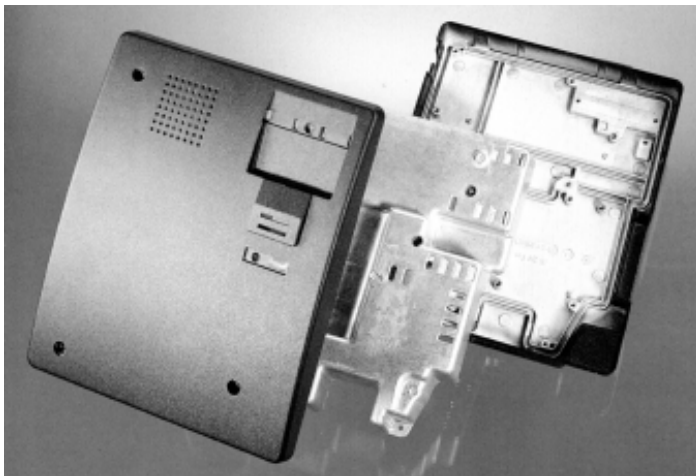


Figure 8: Parts for a telephone switchboard (Unitech Company)

## 1.5 Main Focuses in Research and Development

The main focuses within research and development are currently:

- alloy development
- rapid solidification
- production technology
- composites
- corrosion and its prevention
- recycling

### 1.5.1 Alloy Development

Having its golden years between 1930 and 1950, alloy development has again become one of the main focuses of contemporary research. One reason is magnesium's growing market segment, realized by the introduction of the corrosion resistant HP-alloys in the mid-1980s and followed by a demand for further alloys with specific characteristic profiles. Better creep and corrosion resistance, as well as even lower density, are the main targets for these alloys. The development of alloys with improved ductility and toughness and specific wrought alloys could support a growing magnesium market. The effect of different alloying elements and also micro-alloying, which has a tremendous effect on other materials, needs to be researched systematically.

### 1.5.2 Rapid Solidification

The technology of rapid solidifying plays an important role when it comes to materials with extraordinary profiles. A whole new series of structural effects can be observed when a metallic melting bath is cooled beyond its thermodynamic equilibrium extremely rapidly, as, for example, on sputtering.

This usually leads to an oversaturation of alloying elements, metastable phases within the microstructure, homogeneous distribution of elements and phases, an extremely fine-grained microstructure as well as minimized eliquations, and a high purity of the materials. Figure 9 shows two WE54 alloy microstructures that illustrate the difference between gravity casting and gas sputtering. Rapid solidification offers a link between production technology and alloy development since the development of new alloys, which cannot be accomplished by classical metallurgical procedures, is now possible. At the same time, the corrosion resistance is improved through a more homogeneous element distribution and a low eliquation microstructure.

Spray-forming is an attractive new technology for producing parts and near-complete products in almost final outline. Tubes, discs, rods, or sheets can technically be produced directly in one working step. The process is divided into the sputtering of a metal bath and the deposition of partly frozen drops on a substrate material. This technology is used successfully on an industrial scale for aluminium and copper alloys, and has recently been applied to steels as well. It is an advanced technology in which it offers a greater variety of alloying elements with different concentrations. At the same time, spray-forming allows any given solid particle portable within the gas flow to be introduced into the sputter-zone.

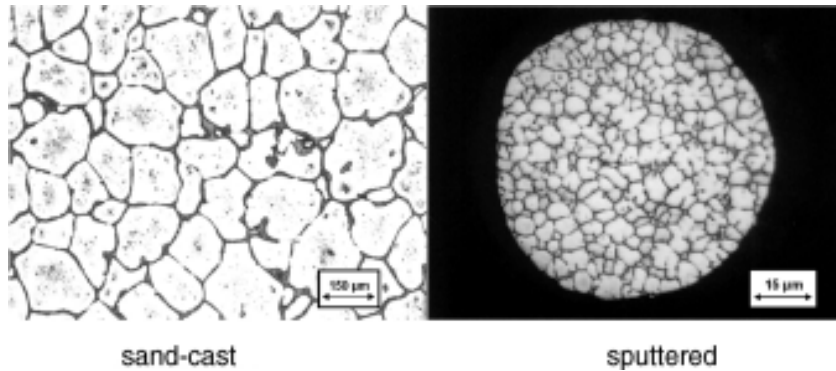


Figure 9: Comparison of the microstructures of sand-cast and sputtered WE54 [26]

In this way, composite materials with a homogeneous particle distribution (e.g. SiC, Al<sub>2</sub>O<sub>3</sub>) can be produced. Another possible application could be an in situ observation of the reaction between sputtered magnesium melts and nozzle gas components or injected materials for producing dispersion strengthened magnesium alloys. The development of magnesium wrought alloys also has tremendous potential in combination with rapid solidifying.

### 1.5.3 Production Technology

Another main emphasis of the research and development work towards magnesium alloys is their production technology. The main production methods, such as casting, joining, disconnection, and moulding, have been adapted without any material-specific optimization towards their use with magnesium. Material development (e.g. new alloys and composites) and the development of innovative procedures for producing and machining magnesium (primarily for automotive applications) represent a major part of magnesium's overall potential. For aluminium, these new procedures (e.g. squeeze-casting, rheo-casting, thixo-casting, thixo-forming, etc.) have already been successfully brought onto the market. Besides conventionally produced parts, pressure-cast or spray-formed aluminium materials are used in repetitive series production. Magnesium still lags behind this growth, but with further optimization of the process and the ongoing development of the materials, there will be a growth of magnesium die-cast parts unprecedented for any other metal.

Other innovative methods have been partly tested in research and development and it is assumed that they too will soon become established since the acceptance of magnesium alloys within the consuming industry is increasing. The possibilities of extending the applications of light metals will surely grow with the help of these new methods and materials.

### 1.5.4 Composite Materials

Metal composites based on magnesium offer well-defined material properties, such as high tensile strength, hot working abilities, or creep resistance; the Young's modulus or abrasion resistance may be directly matched to the required application profile. The reinforcement

of magnesium alloys with ceramic fibres (short or long fibres; usually made of aluminium oxide, silicon carbide, or carbon) or ceramic particles (mostly SiC [27], Fig. 10) must be mentioned first. These materials may be produced by squeeze-casting (preform infiltration from the reinforcement phase), by stirring during the reinforcement phase, or by spray-forming, each technique having its own advantages.

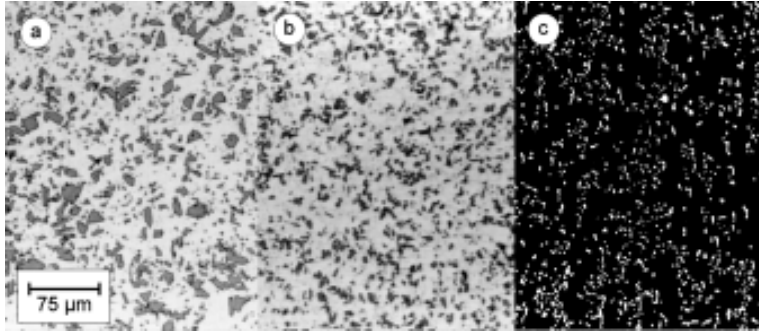


Figure 10: Micrographs of an SiC particle reinforced alloy QE22, produced by p/m methods [27]:  
a) AZ91 + 15 vol.% SiC (31 mm), cross-section polish (optical microscope)  
b) AZ91 + 15 vol.% SiC (8 mm), longitudinal polish (optical microscope)  
c) AZ91 + 15 vol.% SiC (8 mm), longitudinal polish (SEM)

## 1.5.5 Corrosion and its Prevention

The susceptibility of the surfaces of conventional alloys to corrosion has already been significantly lowered with the introduction of the HP alloys. The reduction of the critical contents of Ni, Fe, and Cu influenced the application of the alloys in a positive way (Fig. 11), but they still lack a passivating ability and a ‘self-healing’ passivating layer. In both the alloying and manufacturing steps, efforts need to be directed towards reducing the susceptibility to corrosion of Mg alloys. The process of rapid solidifying might offer advantageous features in this context.

With respect to appropriate organic or inorganic coatings, protection measures have been selected corresponding to those used for aluminium. The minimization of corrosion by surface conditioning or coating has given satisfactory results in some applications, but a systematic evaluation of the physical and chemical basis is still required for a full optimization.



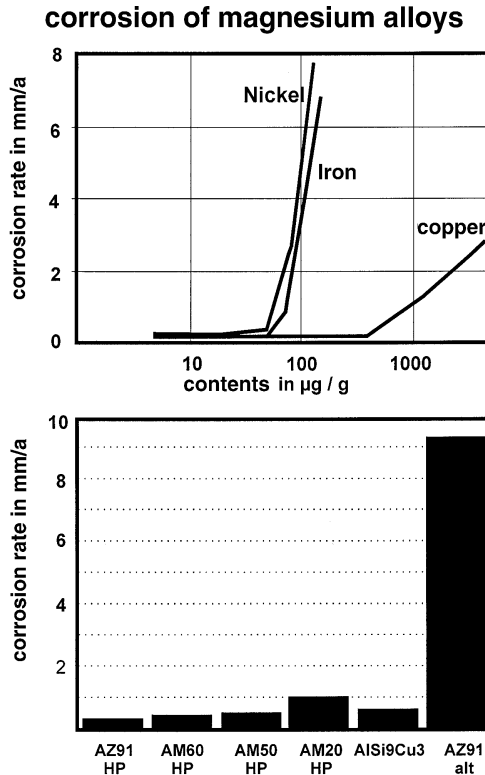


Figure 11: Influence of impurities on the corrosion behaviour of the alloy AZ91 (top) [3]; corrosion behaviour of various magnesium alloys compared to that of the aluminium alloy AlSi9Cu3 (bottom) [17]

## 1.5.6 Recycling

The recycling of conventional magnesium alloys is straightforward; scrap and melt residues can be directly reinserted into the process of the respective foundry, although contaminated or painted parts present bigger problems. A lot of magnesium leftovers have hitherto been used for steel desulfurization, but since magnesium has become a mass product, its secondary cycling is arousing interest on the part of producers and processors of magnesium. This is the reason why recycling activity has increased considerably in the last years. The recovery of the expensive rare earth metals is another important aspect, and this needs to be analyzed extensively.

It is assumed that all the aforementioned research and development work will yield further positive effects for the use of magnesium in the coming years. Therefore, an accelerated growth in its use can be expected.

## 1.6 Summary and Conclusion

Despite the evident advantages of magnesium parts, magnesium has yet to fulfil its full market potential. The advantages and limitations of its application, as described herein, are summarized in Fig. 12.

The driving force for an increasing use of magnesium alloys is still the automotive industry on the consumer side, urged by the public to meet the demands for a reasonable and limited exploitation of resources and primary energy, so as to reduce emissions and to stop further environmental impact. In the past, structural drive unit concepts and low aerodynamic drag were at the forefront of considerations for saving energy, while light construction remained a secondary concern. Figure 13 displays the average fuel consumption (values for passenger cars in Germany; Otto engines only) proving this fact. For a complete picture, however, the trend of vehicle weights shown in Fig. 14 needs to be taken into consideration. It becomes clear that, despite increasing vehicle weights, the average fuel consumption has been lowered significantly. The demand for a “3-litre-car” is growing and an increasing proportion of alternative materials are used to achieve this goal. This effect is clearly evident, for the industry is more interested in using magnesium – especially in the field of die-casting – and the magnesium market is growing. In this regard, the North American market is far ahead of the European one: the market for magnesium die-casting experienced an annual growth of more than 17% between 1984 and 1994 and a growth rate of 33% in 1994. At present, an annual growth of 12–20% is envisaged [31, 32].

The potential use of magnesium parts has been studied in more depth in [33]. The analysis showed that the following amounts of magnesium alloys could now be used, whereby the weight savings indicated would be realized (Fig. 15):

Table 7: Summary of the most important pros and cons of the construction material magnesium.

<b>Characteristic Profile of Magnesium Alloys</b>	
<p>(+)</p> <ul style="list-style-type: none"> <li>– lowest density of all metallic construction materials</li> <li>– high specific strength</li> <li>– good castability and suitability for pressure die-casting</li> <li>– easy machining with high cutting speeds</li> <li>– good weldability under inert gases</li> <li>– highly improved corrosion resistance</li> <li>– high availability</li> <li>– compared to plastics:               <ul style="list-style-type: none"> <li>– better mechanical properties</li> <li>– ageing resistant</li> <li>– better electrical and thermal conductivity</li> <li>– recyclability</li> </ul> </li> </ul>	<p>(–)</p> <ul style="list-style-type: none"> <li>– few optimized alloys</li> <li>– hardly any wrought alloys</li> <li>– low ductility and toughness at room temp.</li> <li>– limited high-temperature properties (heat – resistance, creep resistance)</li> <li>– high chemical reactivity</li> <li>– high shrinkage</li> <li>– no comprehensive recycling concepts</li> <li>– lack of knowledge in terms of combustibility, corrosion behaviour, and handling</li> <li>– limited number of producers, no low and stable price</li> </ul>

## Characteristic Profile of Magnesium Alloys

- lowest density of all engineering metals
- high specific strength
- good castability including die casting
- good machinability at high cutting speeds
- good weldability with inert gas
- highly improved corrosion resistance
- high availability
- compared to plastics:
  - better mechanical properties
  - aging resistant
  - better electrical and thermal conductivity
  - recyclable
- few optimized alloys
- wrought alloys
- low deformability at room temperature and low toughness
- limited high temperature properties (heat and creep resistance)
- high chemical reactivity
- high shrinkage
- no extensive recycling concepts available
- mind barriers with respect to handling, corrosion behaviour and burning
- limited number of producers, no stable and low price

**IWW  
TU Clausthal**

**Magnesium Alloys**

Figure 12: Progress of the average fuel consumption in Germany (passenger car figures; Otto engines) [29]

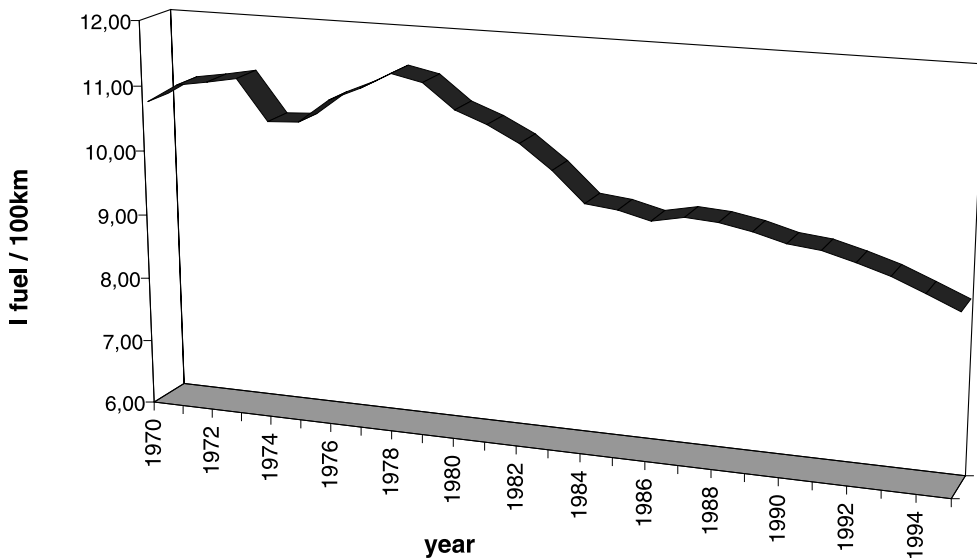


Figure 13: Development of weights of several vehicles [30]

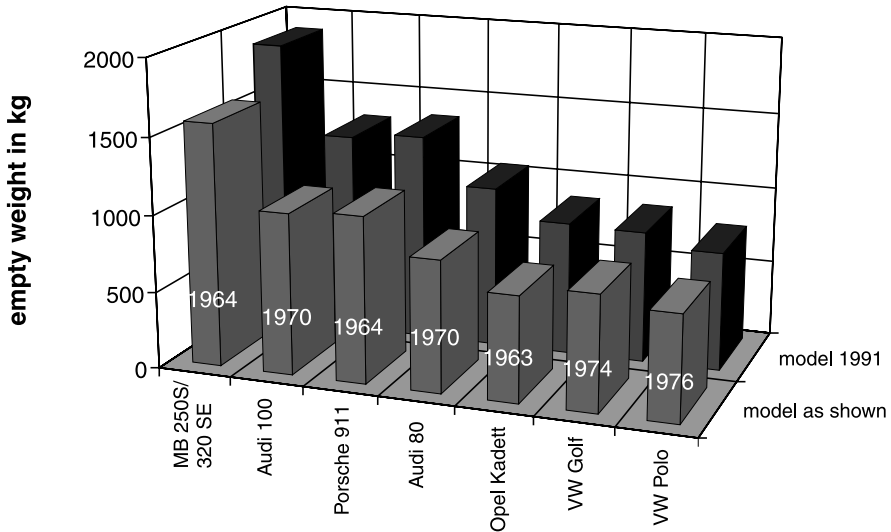


Figure 14: Possible application of Mg alloys in different vehicle classes and the projected weight savings [33]

In time, it will be possible to overcome the prevailing lack of knowledge and reservations concerning the application of magnesium alloys and to raise their acceptance in important fields of use. Research work must address the following goals:

- low and constant costs for the primary material,
- extended variety of alloys, with emphasis on better creep resistance, wrought alloys, and decreasing the specific weight,
- the use of new and innovative production methods,
- extension of the production variety (e.g. squeeze-casting, thixo-forming),
- further increase of the corrosion resistance by self-healing layers or improved coatings,
- exploitation of the rapid solidification process,
- development of application-optimized composites,
- comprehensive recycling concepts with the establishment of secondary cycling.

Once these goals are met, magnesium and its market will grow like no other material has grown before.

## 1.7 Literature

- /1/ BYRON B.: „Global Overview of Automotive Magnesium Requirements and Supply & Demand“, Automotive Seminar der International Magnesium Association (IMA); Aalen, 09.10.1997.
- /2/ Norsk Hydro Datenbank „NHMg.db (ext.)“, Norsk Hydro Research Centre Porsgrunn, 1996.

- /3/ CAHN, R.W.; HAASEN, P.; KRAMER, E.J. (EDS.): „Materials Science and Technology – A Comprehensive Treatment“, MATUCHA, K. H. (VOL. ED): Vol. 8: „Structure and Properties of Nonferrous Alloys“, VCH Weinheim, 1996.
- /4/ CAMERON, A.M.; LEWIS, L.A.; DRUMM, C.F.: „The thermodynamics and economic modelling of a novel magnesium production process“, Proceedings of the 3rd International Magnesium Conference, Manchester 1996.
- /5/ CELIK, C. ET AL.: „Magnola – an innovative process for magnesium production“, Proceedings of the 3rd International Magnesium Conference, Manchester 1996.
- /6/ ESCHELBACH, R.: „Taschenbuch der metallischen Werkstoffe“, Frankhsche Verlags-handlung, Stuttgart, 1969.
- /7/ EMLEY, E.F.: „Principles of Magnesium Technology“, Pergamon Press, Oxford 1969
- /8/ Analyse IMA und HMM, September 1995; in /2/
- /9/ „Spanabhebende Bearbeitung von Magnesium“, Informationsbroschüre der Hydro Magnesium Marketing GmbH, Eschborn.
- /10/ „Hochreine Legierungen für Magnesium Gußteile“, Informationsbroschüre der Hydro Magnesium Marketing GmbH, Eschborn.
- /11/ UNSWORTH, W.: „The role of rare earth elements in the development of magnesium base alloys“, Int. J. of Materials and Product Technology, Vol.4 No. 4, 1989.
- /12/ RAYNOR, G.V.: „Constitution of ternary and some more complex alloys of magnesium“, International Metals Review, Juni 1977.
- /13/ HÖLLRIGL-ROSTA, F.; JUST, E.; KÖHLER, J.; MELZER, H.-J.: „Magnesium im Volkswa-genwerk“, Metall 34 12 (1980).
- /14/ ALBRIGHT, D.L.; RUDEN, T.: „Magnesium Utilization in the North American Auto-motive Industry“, Light Metal Age, April 1994.
- /15/ „Elektron Database V 2.1“, Datenbank der Fa. Magnesium Elektron Ltd., 1994.
- /16/ HANAWALT, J.D., NELSON, C.E., PELOUBET, J.A.: „Corrosion Studies of Magnesium and it's Alloys“, Trans. AIME 147 (1942).
- /17/ OLSEN: „Korrosionseigenschaften von neuen Magnesiumlegierungen“, Metall 46 6 (1992).
- /18/ „Datamanual“, Informationsbroschüre der Hydro Magnesium Marketing GmbH, Eschborn.
- /19/ SERWE, G.: „Magnesiumgußteile im Volkswagen“, VDI-Berichte Nr. 58, VDI-Verlag Düsseldorf, 1962.
- /20/ BÜCHEN, W.: „Einige Beispiele für die Anwendung von Magnesiumguß im Maschi-nen-, Fahrzeug- und Apparatebau und in der elektrotechnischen und optischen Indu-strie“, VDI-Berichte Nr. 58, VDI-Verlag Düsseldorf, 1962.
- /21/ MÜLLER, C.M.: „Kostengünstige Druckgußteile aus Magnesiumlegierungen“, Gies-erei 78, 1991, Nr. 19.
- /22/ MAGERS, D.: „Einsatzmöglichkeiten von Magnesium im Automobilbau“, Leichtme-talle im Automobilbau (Sonderausgabe der ATZ und MTZ 1995), Franckh-Kosmos Verlags-GmbH, Stuttgart 1995.
- /23/ HECTOR, B.; HEISS, W.: „Magnesium Die-Castings as Structural Members of the New Mercedes-Benz Roadster“, SAE-Technical Paper Series No. 900798 (1990).
- /24/ POLMEAR, I.J.: „Overview – Magnesium alloys and applications“, Materials Science and Technology, Vol. 10 (1994).
- /25/ ANON.: „Magnesium the winner in computer housing cost study“, Modern Materials, Vol. 40 No. 1 (1984).

- /26/ EBERT, T.; KAINER, K.U.: „Use of spray forming in the development of new magnesium alloys“, Proceedings of the 3rd International Magnesium Conference, Manchester 1996.
- /27/ MOLL, F.; KAINER, K.U.: „Microstructure and Properties of Magnesium-SiCp-Composites influenced by Production Techniques and Particle Shapes“, Proceedings of the 29th ISATA, Florenz 1996.
- /28/ KING, J.F., HOPKINS, A., THISTLETHWAITE, S.: „Recycling of by-products from magnesium diecasting“, Proceedings of the 3rd International Magnesium Conference, Manchester 1996.
- /29/ RWE-DEA AG für Mineraloel und Chemie, Presse und Information, private Mitteilung, 1996.
- /30/ Auto Motor Sport 7/91 in MÜLLER, C.: „Magnesium – das umweltfreundliche Metall“, Metall 45 9 (1991).
- /31/ LUO, A.; RENAUD, J.; NAKATSUGAWA, I.; PLOURDE, J.: „Magnesium Castings for Automotive Applications“, JOM, Juli 1995.
- /32/ „World-wide Demand For Magnesium Diecastings“. Hydro Magnesium Press Information, 1997.
- /33/ DAVIS, J.: „The Potential for Vehicle Weight Reduction Using Magnesium“, SAE Technical Paper Series, No. 910551 (1991).

## 2 Die-Casting Magnesium

*R. Fink, Oskar Frech GmbH, Schorndorf*

### 2.1 Introduction

Magnesium has gained acceptance as a die-casting material and, together with the goal of lightweight construction, this has led to more aluminium and magnesium being used in automobiles. The demand for the 3-litre-car further emphasizes the trend towards the use of magnesium die-cast parts in cars. The development of the high-purity (HP) alloys AM20 HP, AM50 HP, and AM60 HP with an improved strain-to-failure ratio was an important step towards the increased use of magnesium in vehicles. New regulations concerning the electromagnetic radiation of consumer electronics opened the way for the application of magnesium die-cast parts. High-end mobile phones have been made of magnesium for many years, and this has now been extended to notebook and camera frames. These applications nicely highlight the advantages of magnesium; thus, it offers excellent castability, a high degree of stiffness, and the capacity to fashion thin-walled parts with high dimensional accuracy.

The use of magnesium die-cast parts in light construction and automotive applications has undergone a marked increase; the number of engineers knowing about the materials properties and the application possibilities as well as the advantages of magnesium parts in general is rising. Innovative and seminal solutions are the result of a close cooperation between raw material suppliers, founders, system suppliers, and the automobile industry. The potential for magnesium to benefit from the tendency towards the 3-litre car and the need for further weight savings looks promising. Some automobile producers sign long-running contracts with raw material suppliers or invest in production plants because they expect magnesium to become a material of enormous strategic importance.

**magnesium production plants 1998 (estimated)**

plant	country	metric tons
Hydro Magnesium	Norway, Canada	85.000
Northwest Alloys	USA	35.000
Magcorp	USA	42.000
Solikamsk	Russia	17.000
Avisma	Russia	16.000
Pechiney Electrometallurgie	France	13.000
Brasmag	Brazil	9.000
Timminco	Kanada	7.000
Kalush	Ukraine	4.000
Dead Sea Magnesium	Israel	24.000
Ust Kamenogorsk	Kazakhstan	4.000
Bela Stena	Serbia	4.000
Numerous	(People's Republic of) China	120.000
<b>sum</b>		<b>380.000</b>

Figure 1: Magnesium projects

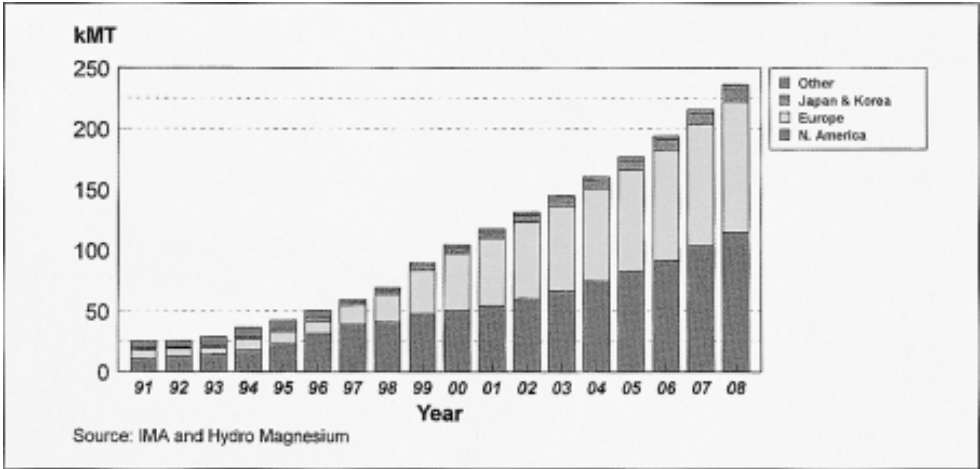


Figure 2: Worldwide magnesium consumption as Mg die-castings

Worldwide magnesium production amounted to 380,000 tons in 1998. The consumption of magnesium die-castings in 1997 amounted to 70,000 tons. Following North America, Europe has realized the potential of magnesium; therefore, a threefold increase in usage is expected by 2005. Magnesium and its alloys are still the metals with the lowest density and are perfectly suitable for advantageous lightweight constructions for automotive applications.

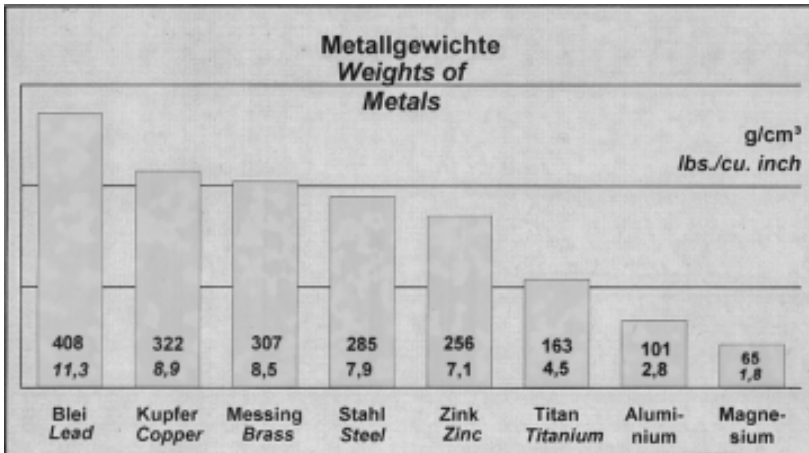


Figure 3: Densities of some important materials

As Fig. 3 indicates, aluminium is 50% heavier than magnesium, while zinc, cast-iron, and steel are four times heavier than magnesium.



## 2.2 Production Methods

The castability of magnesium using the die-casting process is excellent. Its flow properties are much better than those of the non-ferrous metals aluminium and zinc. The good flow properties allow the casting of thin-walled parts and costs are reduced due to the fact that less material is needed. Structural parts for automotive applications can be easily cast, resulting in a tremendous weight reduction.

Whether a part is produced using the cold- or hot-chamber die-casting process depends upon its mass. In the literature, it is usually advised that parts up to 1 kg should be produced with a hot-chamber machine, and that parts with a higher weight should be cast with a cold-chamber casting machine. The biggest hot-chamber machine currently available is the DAM 800, which has a clamping force of 9.300 kN and a rated shot weight of 6.4 kg (actually 5.5 kg).

### 2.2.1 Cold-Chamber Process

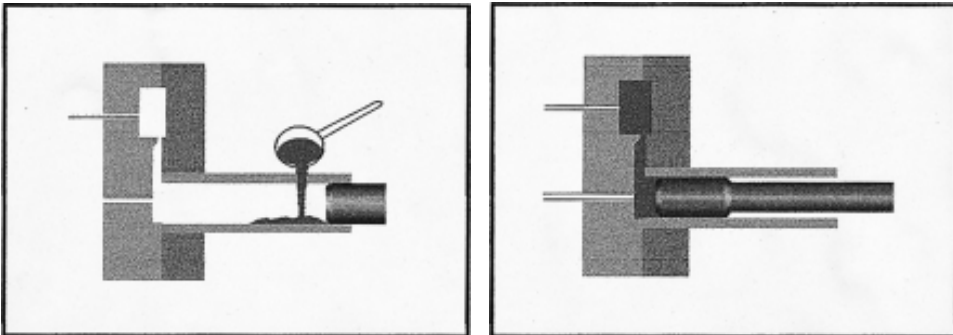


Figure 4: Schematic diagram of the cold-chamber process

“Cold chamber” means that the liquid metal is passed into the cold casting chamber by hand or by means of a proportioning furnace or a scooping tool.

## 2.2.2 Cold-Chamber Machine

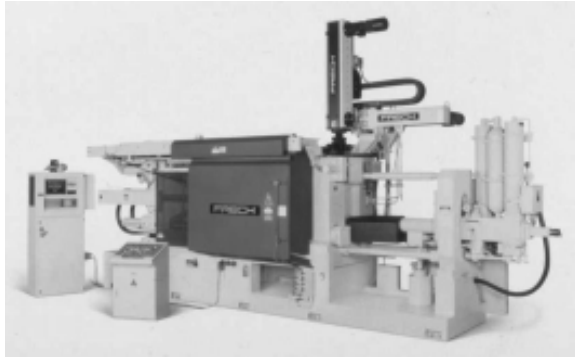


Figure 5: FRECH cold-chamber die-casting machine DAK 500/315 S

The high pressure (300 to 400 bar) applied in the cold-chamber process counteracts the shrinkage of thick-walled portions. However, this presumes a big gate cross-section. The flow properties of magnesium are superior to those of aluminium or zinc. To take advantage of this, the injection performance, i.e. the shooting speed of the second stage (filling stage), needs to be suitably high. The patented impression system ECOPRESS reaches plunger speeds of up to 10 m/s.

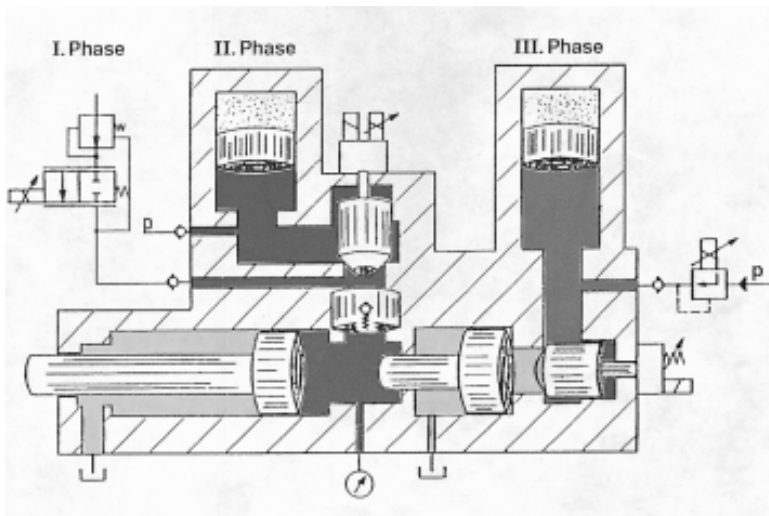


Figure 6: ECOPRESS

To cast magnesium using the cold-chamber process, a proportioning furnace infused with an inert gas is necessary. Latest developments have led to the two- or three-chamber furnace.

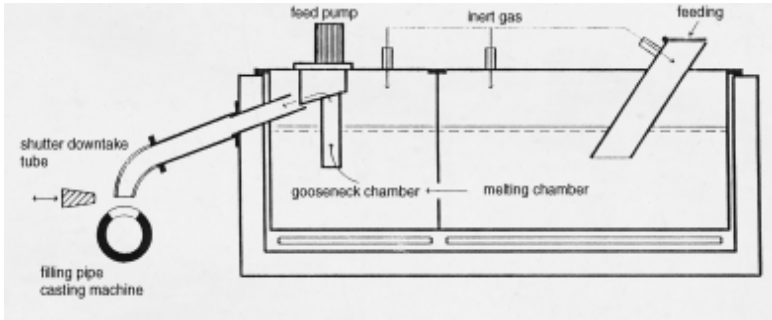


Figure 7: Two-chamber furnace for cold-chamber machines

The proportioning chamber of the furnace must contain only clean material without inclusions at a constant melt temperature to ensure a disturbance-free processing.

### 2.2.3 Hot-Chamber Process

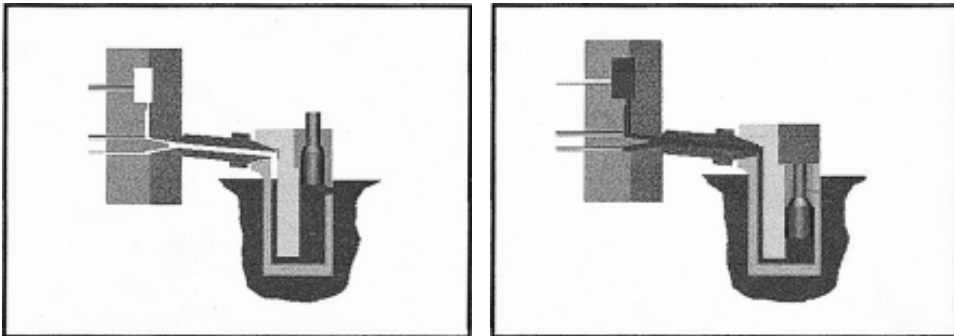


Figure 8: Schematic diagram of the hot-chamber process

“Hot chamber” means that the molten metal is transported directly to the die via the heated (hot) casting settings (casting container, nozzle). The flowing metal hardly comes into contact with air. The melting and warming furnaces are directly adjoining parts of the casting machine.

## 2.2.4 Hot-Chamber Machine

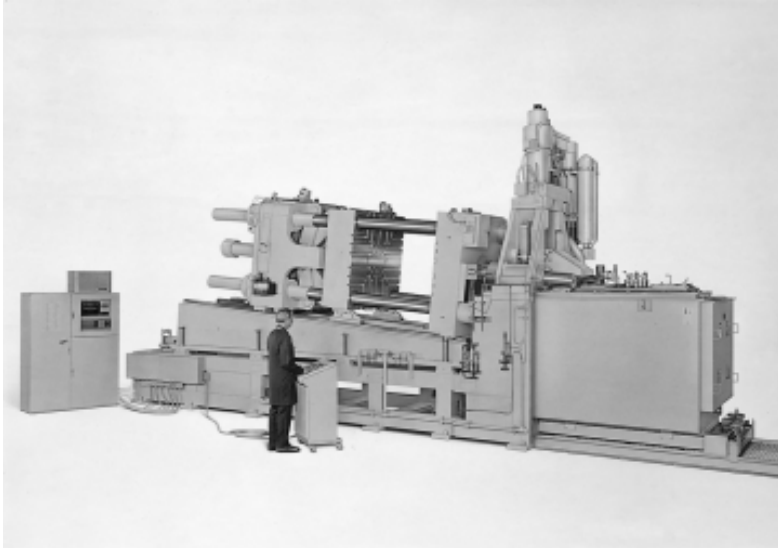


Figure 9: FRECH hot-chamber die-casting machine DAM 800 S

The most important technical facts can be summarized as follows:

clamping force:	9.300 kN or 1025 U.S. tons
closing stroke:	900 mm
rod distance:	900 ´ 900 mm
casting pressure:	400 kN
plunger diameter:	120, 130, 140, 150 mm
max. shot size:	3.800 cm <sup>3</sup>
specific casting pressure:	181–283 daN/cm <sup>2</sup>
max. mounting area:	4.100 cm <sup>2</sup>
separating stroke nozzle:	800 mm

Correct design of the gate allows for specific casting pressures ranging from 160 to 180 bar. The possible flowing distances are greater, allowing the casting of wide-area parts. Thin-walled parts (0.6 mm is possible nowadays) demand high injection speeds and require the use of a hot-chamber machine.

The use of a hot-chamber machine is much more economic in cases where the parts can be cast using this process.

Advantages	Hot-chamber	Cold-chamber
smaller machine	3.150 kN	6.000 kN
specific casting pressure	200 bar	400 bar
higher output rate	150 shots/h	70 shots/h
higher efficiency	0.85	0.8
thinner walls	0.6 mm	1.2 mm
surface quality	better	Plunger spray
die lifecycle	approx. 600,000 shots	approx. 400,000 shots
less recirculation material	approx. 40%	
	reduction of the production costs	

Figure 10: Advantages of the hot-chamber process

## 2.3 Application Fields

### 2.3.1 Automotive Branch

- gearbox housing VW (AZ91D)  
weight reduction  
vibration damping  
stiffness

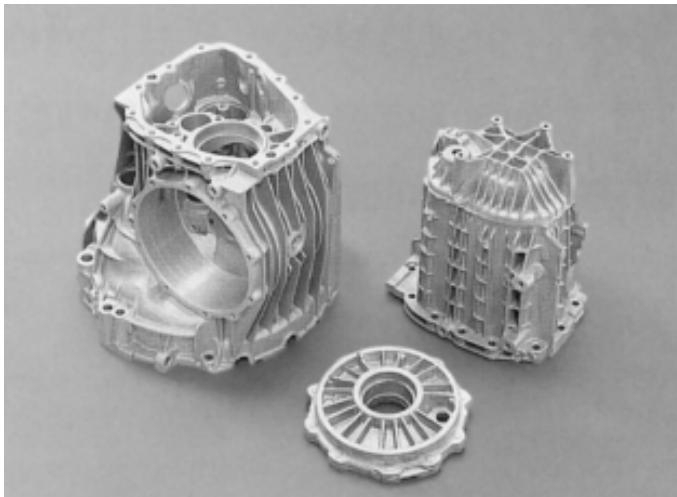


Figure 11: Gearbox VW

- fuel tank covering (AM60B)  
weight: 3.2 kg; weight reduction approx. 4 kg  
torsion resistance of the convertible frame

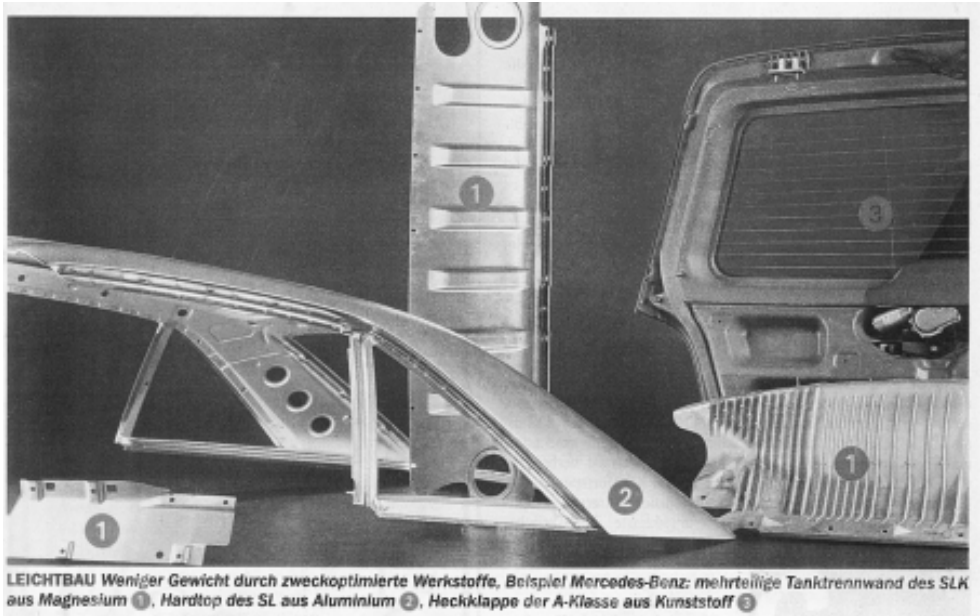


Figure 12: Fuel-tank cover

Lightweight construction; less weight through the use of optimized materials; examples shown (Mercedes-Benz): multipart magnesium fuel-tank separating plate of the SLK (1), aluminium hardtop of the SL (2), plastic tailgate of the A-class

- end plate , Audi Corp.



Figure 13: End plate, Audi-Corp.

- steering wheel

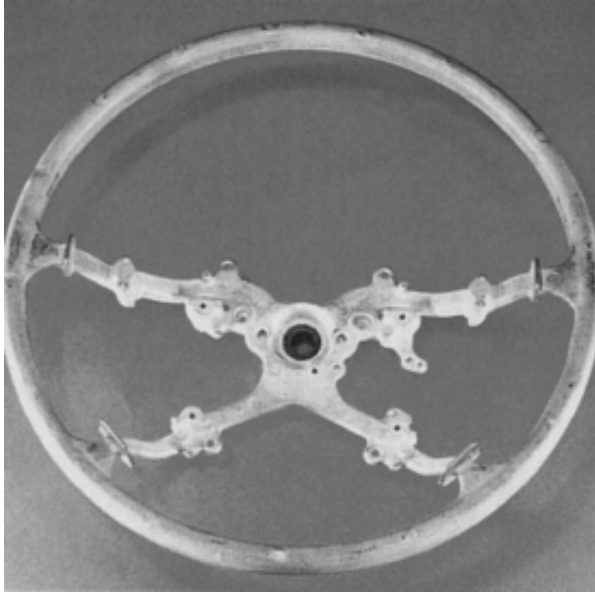


Figure 14: Steering wheel

- steering column holder and bracket – Audi/Zitzmann (AZ91D)  
weight reduction (approx. 20 kg)  
dimensional accuracy  
environmental aspects

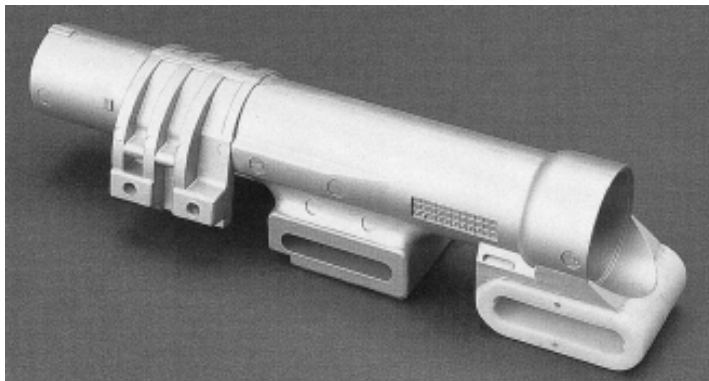


Figure 15: Steering column holder and bracket

- dashboard – Cadillac (AM50)  
deformation properties/ductility  
weight reduction  
dimensional accuracy/assembling accuracy  
simplified construction

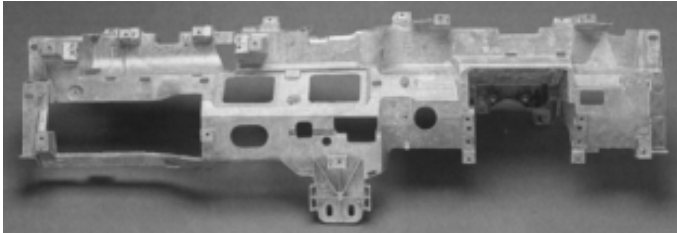


Figure 16: Dashboard

- seat frame – Alfa Romeo Meridian-MPI (AM60)  
deformation properties/ductility  
weight reduction  
simplified construction



Figure 17: Seat frame(s)



- tailgate – VW Lupo (Mössner AG)  
dimensions: 1350 ´ 800 mm, weight: 2.7 kg, average wall thickness: 1.6 mm



Figure 18: Tailgate

The concept study of a magnesium car door gives an example of the advantages of light metal construction. Magnesium rod profiles are combined with magnesium die-cast parts. The cast parts are smaller and therefore their production costs are lower. Smaller parts can be cast with even thinner walls, resulting in a better casting operating sequence and an even greater weight reduction.

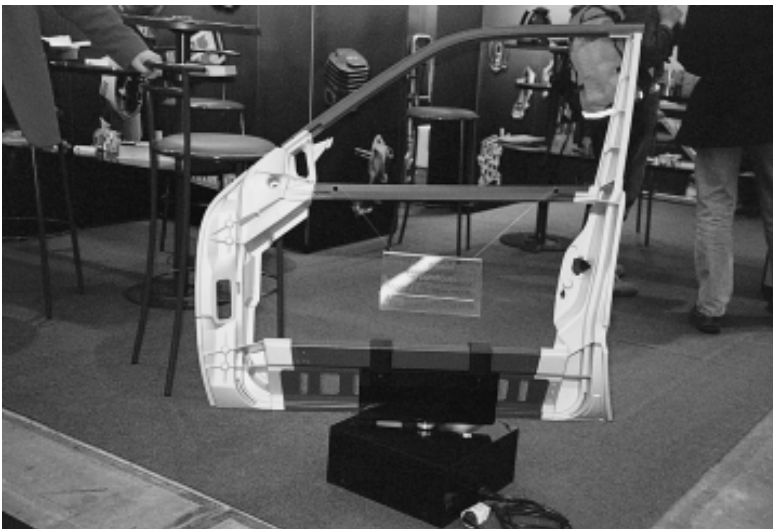
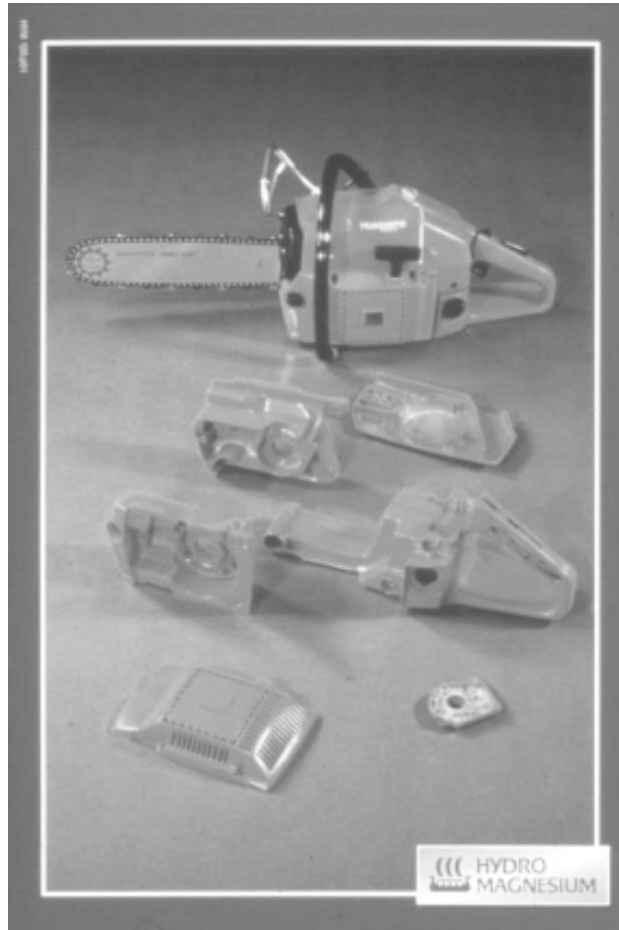
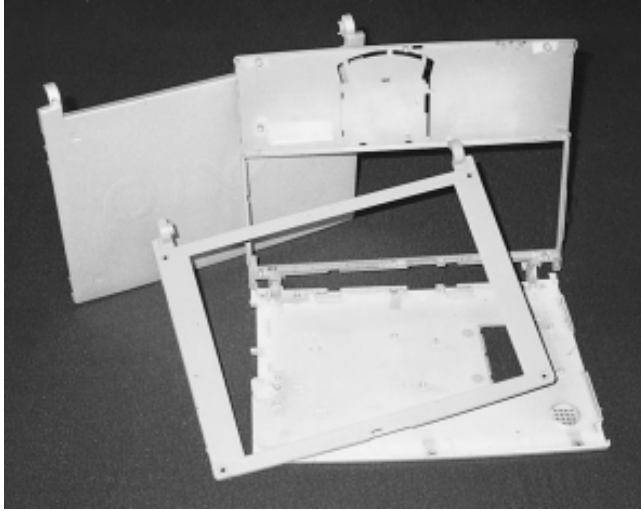


Figure 19: Car door in lightweight design

## 2.3.2 Tools, Electronics Industry, and Others







Figures 20–23: (chainsaws, video cameras, mobile phones, notebooks)

## 2.4 Casting Alloys

Modern casting alloys are summarized in Fig. 24:

Alloy Overview								
Alloy	UTS	0,2 % YS	Fracture Elongation	Hardness (Brinell)	Bending Fatigue Strength	Melting Range	Metal Bath Temperatur	
	N/mm <sup>2</sup>	N/mm <sup>2</sup>	0 %	HB-5/250	N/mm <sup>2</sup>	°C	KK °C	WK °C
AZ91 HP	200-250	150-170	0,5-3,0	65-86	50-70	420-600	660	630
AZ81 HP	200-240	140-160	1-3	60-85	50-70	425-615	660	635
AM60 HP	190-230	120-150	4-8	55-70	50-70	445-630	670	640
AM50 HP	180-220	110-140	5-9	50-65	50-70	440-625	680	650
AM20 HP	160-210	90-120	8-12	40-55	50-70	435-640	680	

Figure 24: An overview of alloys

Figure 25 shows the significant decrease in the corrosion rates of new HP alloys compared to their predecessors. Furthermore, a comparison with the aluminium casting alloy AlSi9Cu3 is given.

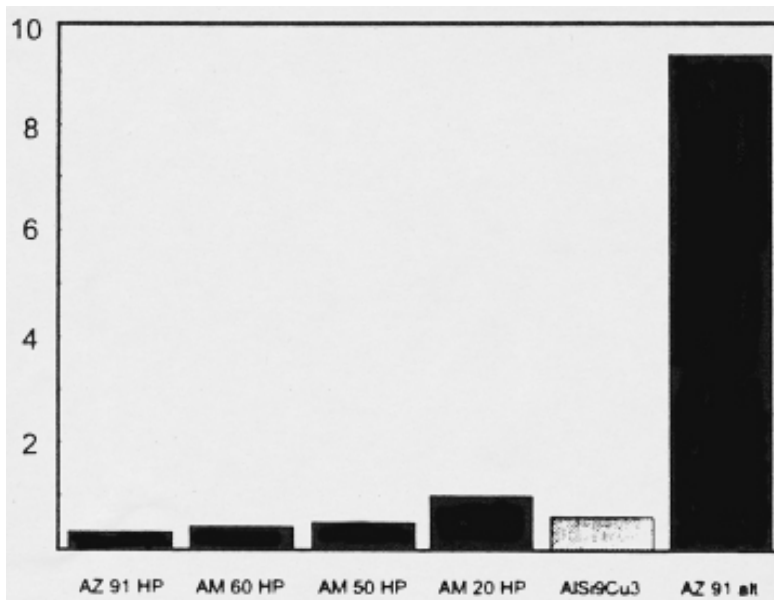


Figure 25: Comparison of corrosion rates of modern magnesium die-casting alloys with those of their predecessors and of typical aluminium casting alloys

### **2.4.1 AZ91 HP**

AZ91 HP is the most commonly used alloy; it has excellent castability and high strength.

Typical applications are automotive, computer, and mobile phone parts, body workout facilities, cases and plates, parts for chainsaws, hand tools, domestic equipment, etc.

### **2.4.2 AM50 HP and AM60 HP**

These alloys allow high-energy absorption and elongations at high strength and have good castability. The automotive industry offers typical applications, such as seat frames, steering wheels, dashboards, fans, etc.

### **2.4.3 AM20 HP**

This alloy is characterized by a high elongation capability together with a high shock resistance. Typically, it is used in automotive safety areas.

Technical hint:

In principal, an AM50 HP alloy can be cast with a hot-chamber machine, but the thermal load of machine parts within the casting unit is higher because of its higher melting point (650 °C, 1200 °F) compared to AM60 HP (640 °C, 1180 °F). Moreover, the leakage between the plunger bore and the piston ring is higher because of the higher melting bath temperature.

## **2.5 Mould-Making**

In contrast to aluminium, molten magnesium shows no affinity towards iron. This is an advantage in that it allows higher die life cycles. The thermal load (melting bath temperature is 650 °C, 1200 °F) and the mechanical load due to the specific pressure are the same for aluminium and magnesium. Magnesium freezes more rapidly within the die cavity. To counteract the high shrinkage, the casting duration is kept low and the plunger speed is about 30% higher. These parameters also facilitate the casting of thin-walled parts (down to 0.6 mm).

Tests have shown that the tensile strength is highly influenced by the plunger speed during the second stage of casting. This arises mainly from the short filling duration of the die and the higher turbulences during its filling. The melt jet is sputtered and oxide coatings, lubricants, and mould release agent carried with it are dispersed. The casting speed at the in-gate should be 90 to 100 m/s to achieve this fine dispersion. Magnesium allows high speeds at the in-gate without wearing it out.

The alloys AM50 HP and AM60 HP are recommended for parts with high degrees of elongation. Tests have proved that the elongation of an AM60 HP die-cast part can be increased from 13 to 16% using a vacuum.

## 2.5.1 Key Points Concerning Magnesium Die-Casting

- fill rates 30% lower than with aluminium
- in-gate speeds of 90–100 m/s
- in-gate thickness  $> 0.8$  mm
- temperatures of the die approx. 220–240 °C (430–465 °F). A temperature control device is mandatory.
- optimum gate
- amount of taper 1–2°
- magnesium is highly fluid and so a very heavy die is needed to prevent the formation of burrs.

## 2.5.2 Hot-Chamber Mould Conception

a) filling simulation

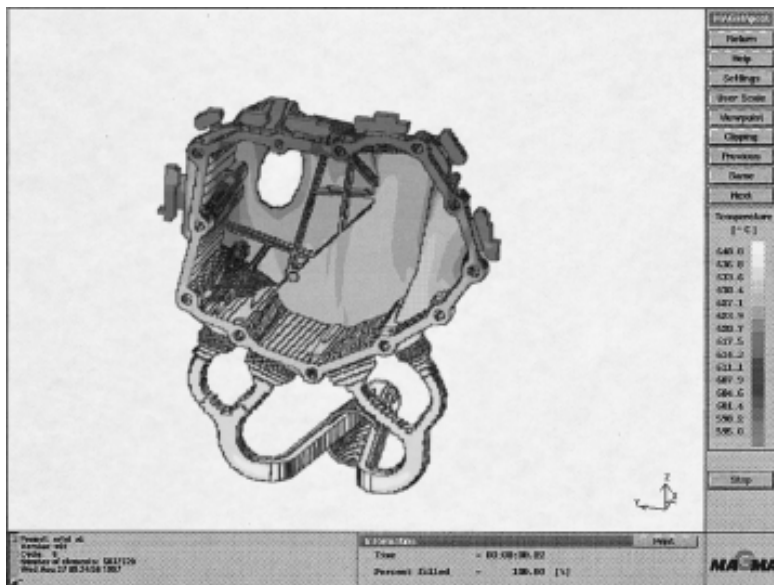


Figure 26: Temperature distribution through the mould filling after 36 ms. At this point, 100% of the part is already flooded. The filled portions are indicated.

b) die

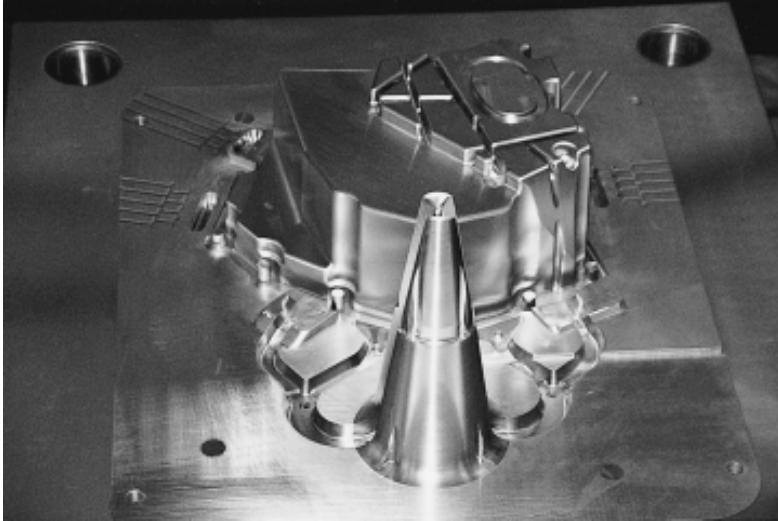


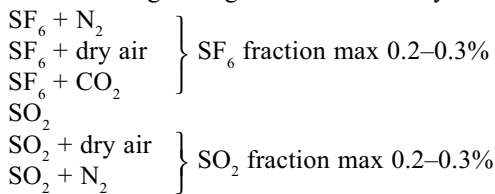
Figure 27: End plate, Audi Corp.

## 2.6 Safety

### 2.6.1 Inert gas

Magnesium is classified as dangerous because of its combustibility, but this danger does not arise during casting. The melt surface within the melting and heating furnaces is covered with an inert gas, protecting it from oxidation.

The following inert gases are used today:



### 2.6.2 Furnace

Because of the eliquations during the melting of magnesium, the two-chamber furnace offers advantages for the hot- and cold-chamber processes. The first chamber is for the melting of ingots; the clean melt then goes through a hole into the second chamber, the heating chamber. Both chambers are charged with inert gas.



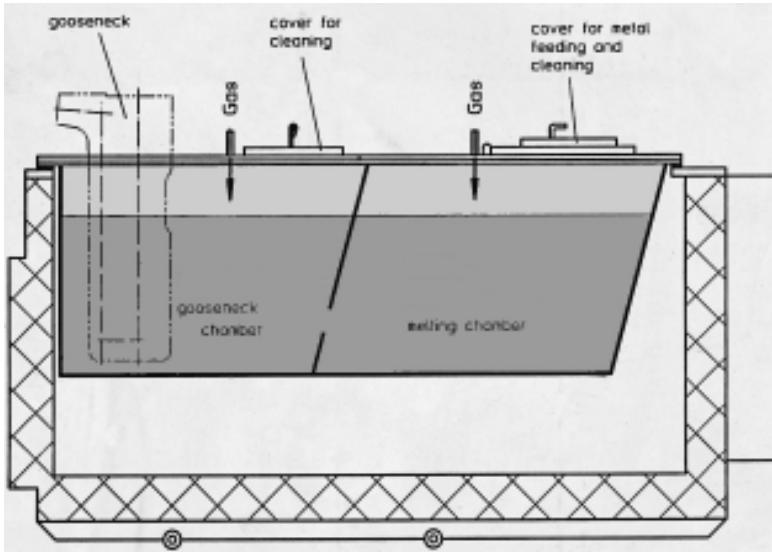


Figure 28: Two-chamber furnace

### 2.6.3 Ingot Feeding Device

For magnesium, an ingot-feeding device is recommended. The ingots are heated to 150 °C (300 °F) to dry them before they are fed into the melting bath. A bath sensor controls the belt-conveyor clocking. A very constant bath level in the machine furnace can be accomplished by this way of ingot feeding. A lock at the feeding cover prevents air from getting into the furnace and inert gas from leaking out.

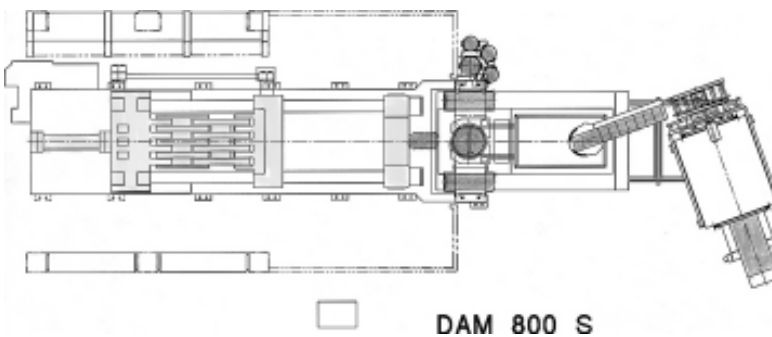


Figure 29: Schematic of the DAM 800 with ingot feeding device

### 2.6.4 Process Safety

A tremendous increase in the process safety was achieved with the advent of intelligent controls such as FRECH-DATACONTROL. The FRECH Company first sold machines with a screen control in 1983. Today, we have many different screen pages. The user interface is easy enough to be used by any trained founder; all the important casting parameters are to some extent recorded and displayed.

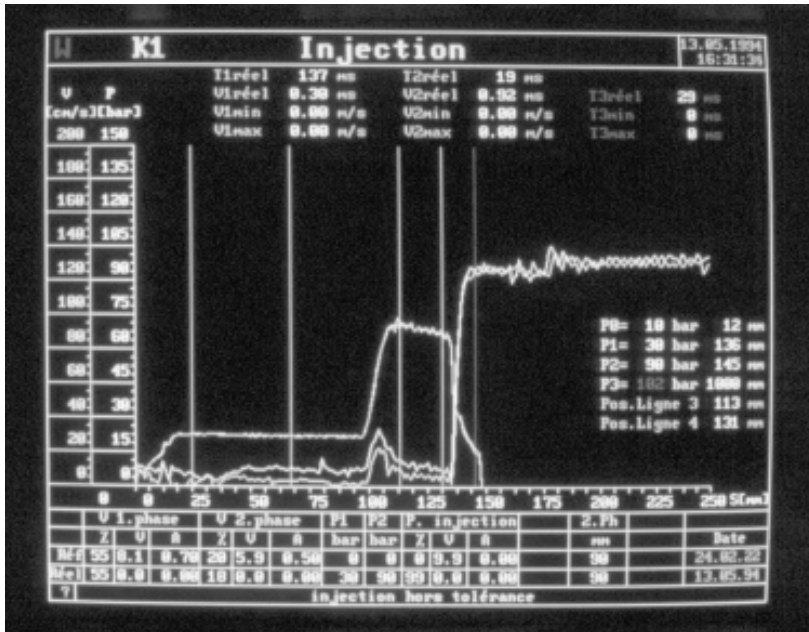


Figure 30: Pressurizing curve

The screen page “casting parameter calculation” allows the founder to enter in-gate cross-section and filling duration and to directly check the feasibility of the proposed process.

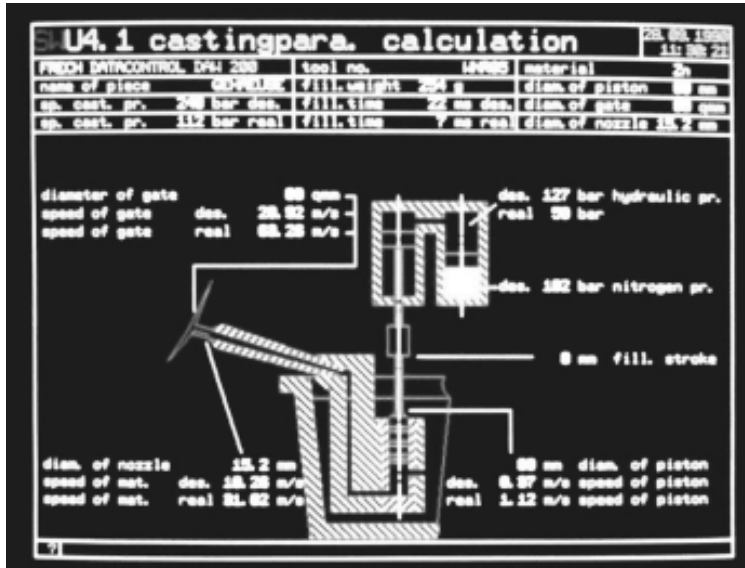


Figure 31: Calculation of casting parameters

The strict regulations within the scope of the product liability and the ISO9000 require documentation of the quality and the production process. The casting process is verified with the control charts; all eight of the casting and machine parameters are recorded and can be displayed on the screen. The values  $U_r$ ,  $x_{lateral}$ , and  $x_{lateral}/lateral$ , as well as the span are shown.

To check that the process is normally distributed, each parameter is additionally shown in a combined bell-shaped curve. All data curves can be plotted.

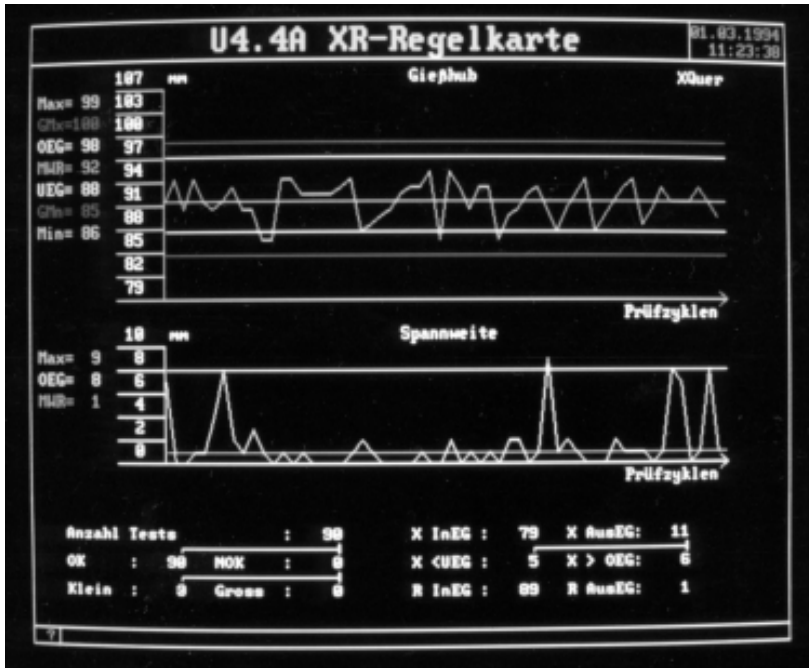


Figure 32: Screen XR-control chart

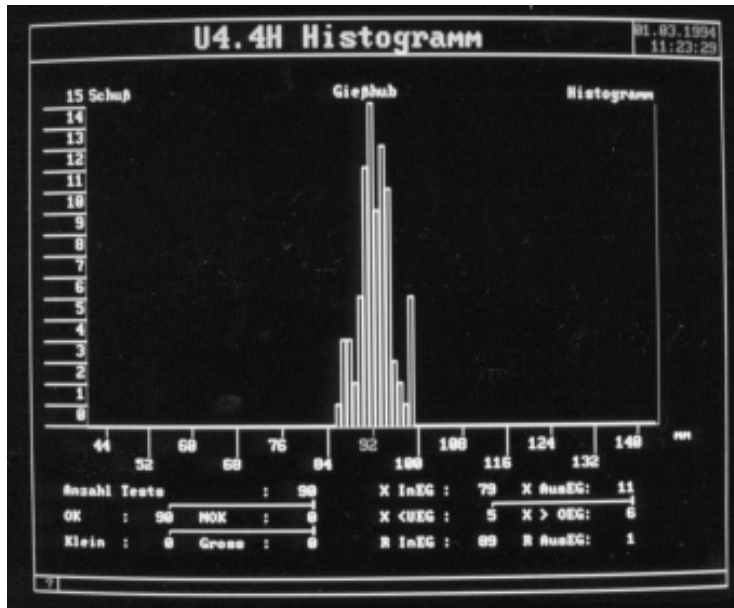


Figure 33: Screen histogram

# 3 Vacuum Die-Casting of Magnesium Parts with High Pressure

*M. Siederslebner, Honsel AG, Meschede*

## 3.1 Introduction

The classical and most economic procedure for processing magnesium is die-casting. It has advantages over the processing of aluminium and zinc, although these are also utilized quite well with this type of casting. In addition to the specific properties of magnesium mentioned in Chapter 1, other favourable features are its low casting temperature (650–680 °C, depending on the alloy) and the low energy needs for melting. The energy needed for AZ91 (2 kJ/cm<sup>3</sup>) is about 77% of the corresponding value for the aluminium alloy AlSi12CuFe [3]. The high price of magnesium is usually referred to its mass not its volume, and so it can actually be cheaper than other materials in terms of volume. The low thermal content allows the casting process to be 50% faster than that with aluminium; a high clock cycle of parts is possible, maintaining high precision and good surface quality. Additionally, magnesium does not attack iron moulds as much as aluminium does, the moulds can have steeper walls and the potential savings in terms of tools can be as much as 50% compared to the die-casting of aluminium [21] and machine endurance is much higher as well [3]. Pressure die-casting is a process whereby liquid metal is forced into a split permanent metal mould under high pressure. Compared to sand- or gravity casting, the mould filling does not occur simply under the force of gravity. Instead, the pressure on the melt is turned into kinetic energy, which results in high mould-filling speeds. Hence, there is much turbulence in the melt until the mould is filled and the metal pressure compacts everything. In brief, the advantages of pressure die-casting are mainly a high productivity and the possibility of producing thin-walled and near-net-shaped components. Moreover, the rapid solidification leads to a very fine-grained microstructure with good mechanical properties.

## 3.2 Die-Casting

There are several specific features that need to be considered when casting magnesium. Its high susceptibility to oxidation makes an inert atmosphere in the furnaces, pipes, and pumps essential. To ensure this, special casting set-ups have been developed.

Die-casting can be separated into two kinds of processes; cold-chamber and hot-chamber die-casting, depending on the machine used. Special processes, such as vacuum die-casting, are variations on these processes. The hot-chamber machine has a casting case with an integrated casting chamber that always stays within the casting furnace filled with molten metal (Fig. 1).

The furnace is used to keep the metal fluid; the melting is done in a separate furnace. The features of hot-chamber casting are:

- the proportioning unit lies within the melt
- the machine size extends up to 900 t clamping force

- the pressure of melt lies between 150 and 200 bar
- the shot is limited to 5–6 kg
- high productivity (more than 100 shots per hour is possible)
- typical wall thickness: 1 mm

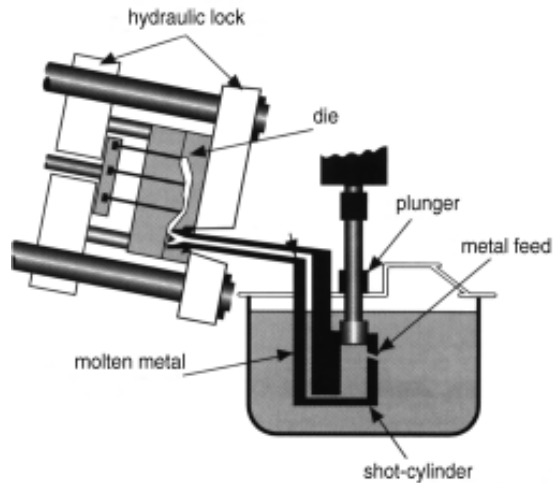


Figure 1: Schematic of hot-chamber die-casting

If a part has thin walls, it is more economical for it to be cast in a hot-chamber machine than by using the cold-chamber process. However, not all alloys can be processed in a hot-chamber machine.

The cold-chamber machine has its casting case outside of the melt. The metal is filled into the proportioning unit from an adjacent external furnace. The features of a cold-chamber machine are as follows:

- external proportioning unit
- lower productivity
- machine sizes up to 4,500 t
- pressure of the melt between 300 and 900 bar
- the shot is limited to 60 kg
- wall thickness from 1.5 to 2.5 mm

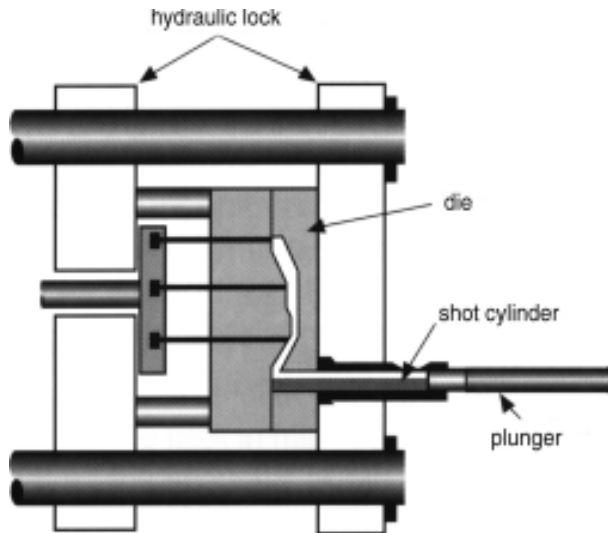


Figure 2: Schematic of cold-chamber die-casting

The high pressure is needed to compensate the high degree of shrinkage when casting thick-walled parts. After the transportation of the melt into the chamber, the conventional casting sequence consisting of three stages begins. The liquid metal reaches the gate in the first stage (duration approx. 20 ms), the second stage involves the filling of the mould, and during the third stage pressure is built up. With the simple casting procedure, a highly turbulent mould filling takes place and pockets of air, gas, and mould release agent can be encased within the metal. Therefore, the parts have limited ductility and lower strength, and subsequent heat treatment or welding is precluded. Furthermore, an air cushion is encountered during the mould filling, hindering the casting sequence. These problems can be overcome by vacuum die-casting, whereby the casting chamber and the mould are evacuated (remaining pressure below 80 mbar). The parts no longer contain any pockets of trapped air and show improved properties, such as weldability, and are now amenable to heat treatments. The formation of an air cushion, which disrupts the filling sequence, is prevented as well. In vacuum die-casting, the three sequences of the simple process are extended by closing the feeding cover and evacuating the mould cavity.

For aluminium and its alloys, the vacuum casting technology is already long-established. Interest in doing the same with magnesium has only arisen in the last few years. Various casting procedures have been developed, ranging from simply including a valve to the mould, to the use of a conventional casting machine with a sealed mould parting line (Fig. 2, Honsel system HOVAC), to the adaptation of the aluminium Vacural casting process. The change of the casting sequence and the mould sealing result in higher costs of the parts compared to a conventional procedure.

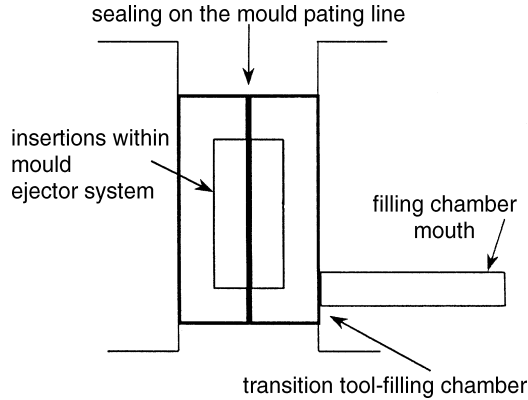


Figure 3: Schematic diagram of a tool-sealing during vacuum die-casting

### 3.3 Magnesium Casting Alloys

Aluminium is, as already described, the most extensively used alloying element for magnesium, with contents varying between 2 and 9 weight%. These alloys have good mechanical properties at ambient temperatures and excellent corrosion resistance. However, lowering the Al content also lowers the castability. Table 1 shows typical compositions of these alloys. Besides the improvements of the mechanical properties, there is the big advantage of better castability (eutectic system,  $T_E = 437\text{ }^\circ\text{C}$ , Al content  $\sim 30\%$ ). The more aluminium the melt contains, the better the castability.

By far the most widely used of magnesium die-casting alloys is AZ91 (Mg-9 weight-% Al-1 weight-% Zn) because of its superb castability even for the most complex and thin-walled parts.

The negative effect of the high aluminium content is the formation of the interdendritic grain boundary phase  $\text{Mg}_{17}\text{Al}_{12}$ . At a working temperature above  $120\text{ }^\circ\text{C}$ , it lowers the strength within the fine-grained crystal structure and leads to limited ductility of the alloy, as is also seen with zinc components.

Table 1: Compositions of common magnesium die-casting alloys.

alloy	Al [%]	Mn [%]	Zn [%]
AZ 91	8,5-9,5	0,17-0,40	0,45-0,9
AM 60	5,6-6,4	0,26-0,50	0,2
AM 50	4,5-5,3	0,28-0,50	0,2
AM 20	1,7-2,5	min. 0,20	0,2

To improve the deformation behaviour of magnesium alloys, the Al content is decreased, the alloying with zinc is completely abandoned, and manganese is added instead. The resulting alloys of the magnesium/aluminium/manganese family, e.g. AM20, AM50,



AM60 (Mn contents between 0.2 and 0.4%), show lower strengths at ambient temperature, but they are less brittle than the Al/Zn-based alloys. The dependence of the mechanical properties on the aluminium content is illustrated in Fig. 4. The increase in ductility with decreasing aluminium content in this series of alloys is obvious. One of the most important criteria for magnesium alloys is their high-temperature and creep behaviour, which is not very good for the magnesium/aluminium/zinc alloys. For this reason, in earlier years attempts were made to reduce the aluminium content in the melt and to use different materials for alloying. The resulting alloys AS21, AS41, and AE42 exhibit a much better high-temperature strength and creep resistance than AZ91. The relevant mechanical properties of the conventional magnesium casting alloys are listed in Table 2. All aluminium-reduced alloys show much worse castability.

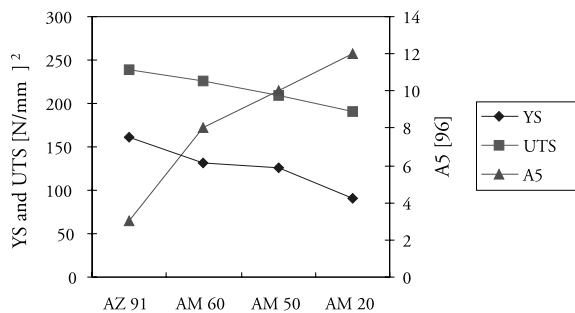


Figure 4: Influence of the aluminium content of Mg die-casting alloys on their mechanical properties

Table 2: Typical mechanical properties of conventional Mg die-casting alloys.

Alloy	UTS [MPa]	YS [MPa]	Compressive Strength [MPa]	Fracture Elongation [%]	Young's Modulus [GPa]	Impact Strength [J]
AZ 91	240	160	160	3	45	6
AM 60	225	130	130	8	45	17
AM 50	210	125	125	10	45	18
AM 20	190	90	90	12	45	18
AS 41	215	140	140	6	45	4
AS 21	175	110	110	9	45	5
AE 42	230	145	145	10	45	5

By applying the vacuum casting technology, the ductility properties of the AM alloy group can be further improved. The strain at fracture of the alloy AM50 could be raised from 15% with conventional casting to almost 19% with vacuum die-casting. In particular, the impact energy values are influenced, as shown in Table 3.

Table 3: Influence of the aluminium content and the vacuum die-casting process on the toughness of Mg die-casting alloys (individually cast Charpy specimen; according to [1]).

Alloy	Impact Energy		Fracture Elongation [%]	Remarks
	notched [J]	unnotched [J]		
AZ 91	1,4 (0,1)	9,3 (2,0)	7,0	9,2 % Al
AM 20	4,4 (0,2)	18,4 (4,8)	18,8	2,0 % Al
AM 50	3,3 (0,2)	18,3 (4,0)	15,2	4,8 % Al
AM 50	3,2 (0,3)	17,7 (5,2)	16,0	5,3 % Al
AM 50	5,4 (0,3)	36,8 (4,5)	19,3	4,8 % Al Vacuum
AM 60	3,1 (0,2)	16,7 (4,3)	16,1	5,8 % Al
AM 60	2,8 (0,2)	18,1 (5,0)	14,3	6,4 % Al
AM 70	2,4 (0,3)	18,0 (3,9)	12,8	6,9 % Al

Standard deviation in brackets

### 3.4 Application Examples

A variety of magnesium parts are already successfully produced using die-casting methods, e.g. gearbox housings, steering wheels, seat frames, cylinder head covers, and steering locks. Structural and car body parts are attracting ever increasing interest. In this context, vacuum die-casting might play an important role. Existing and potential parts include partition panels (tank cover and rear window shelf), dashboard frame and crossbar, frames for the roof and tailgate, as well as inner door and seat parts. The following advantages are most noteworthy:

- weight savings
- avoidance of joining working steps
- reduced processing effort
- less investment in tools than with sheet steel
- high tool lifecycles

Some examples of the potential of die-casting are listed below. One interesting example is the fuel tank cover manufactured on behalf of the DaimlerChrysler Corporation for its SLK model. The part supports the body stiffness and serves as a partition panel between the trunk and rear seats. Table 4 gives an overview of the different materials taken into consideration. Former solutions consisted of a welded conduit frame. First alternatives were steel and aluminium weldments and a magnesium cast part. Several advantages favoured the use of magnesium. With the part made of 3.2 kg magnesium AM60, a great weight saving could be accomplished. The spatial requirement is lower, the dimensional accuracy is excellent, and no post-processing or coating is necessary. Figure 5 shows the final operational part. Other application fields could be dashboard frames or crossbars; different concepts for this are already set up. The requirement and motivation for the use of magnesium alloys are listed in Table 5. Figure 6 shows two examples of different concepts from the USA and Europe, arising from different demands. Further application concepts are aimed at inner door parts. In the case of solution 1, the door consists of a cast part with a window frame made of an extruded or cast shape.

Table 4: Application example: fuel-tank cover.

Customer	DaimlerChrysler	Model: Mercedes SLK
function of component	car body stiffness separation: trunk/back seats	
former solution	welded conduit frame	
alternative concepts	2. steel weldment 3. aluminium weldment 4. magnesium die-casting for solution 1 and 2, a weight-saving of 7–8 kg each is obtained	
solution for series production	magnesium die-casting	
advantages	<ul style="list-style-type: none"> <li>– weight: 3.2 kg</li> <li>– dimensions: 1200 × 400 mm</li> <li>– wall thickness: 2 mm</li> <li>– alloy: AM60</li> <li>– dimensional accuracy (one cast part replaces a variety of single parts)</li> <li>– less space requirement</li> <li>– no post-processing</li> <li>– no coatings</li> </ul>	

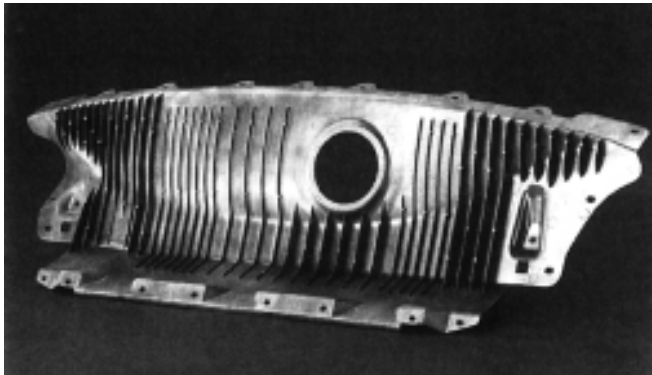


Figure 5: Fuel-tank cover Mercedes SLK

Table 5: Application example: dashboard holder/crossbar.

crossbar	dimensions: 1300 × 300 mm thickness: 2–3 mm weight: 3–4 kg
requirements	connection to A-column steering column fixing, connection to the tunnel air-bag fixture, air-conditioning, air ducts, etc. ductility for crash case
advantages of the Mg die-casting	dimensional accuracy interior component: no coating necessary pre-assembly outside cockpit
production	vacuum die-casting alloy AM50/AM60

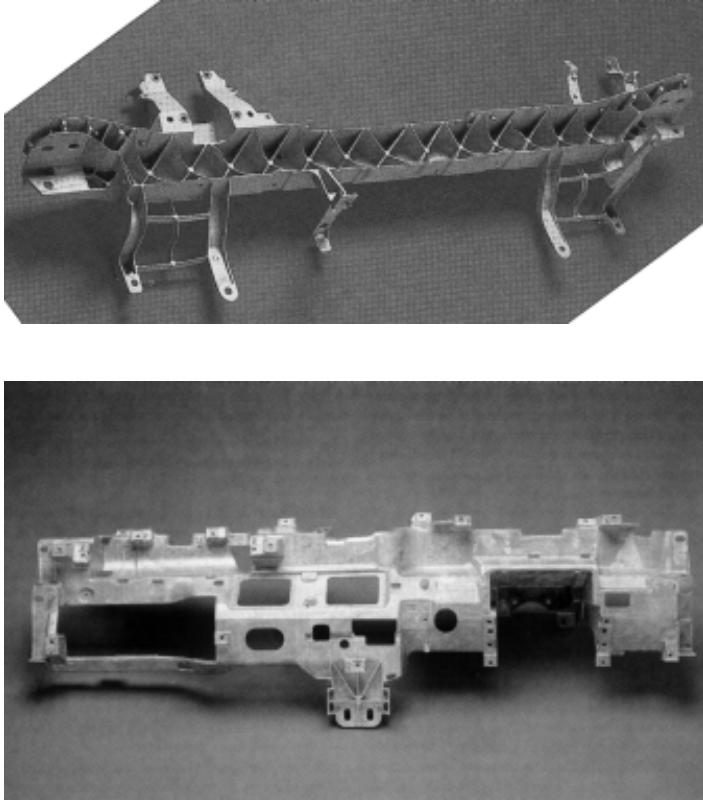


Figure 6: Examples of magnesium crossbars  
 top: manufactured by Median for Fiat Marena  
 bottom: manufactured by Gibbs for Cadillac Seville (AM50)

Magnesium cast parts and aluminium shapes in combination are the basis for solution 2 (Fig. 7). In the 3rd solution, the door consists entirely of a single magnesium cast part. More potential for high-performance parts is offered in the area of roof applications and tailgates (Fig. 9), where exterior sheet quality is partly required but is not yet available.

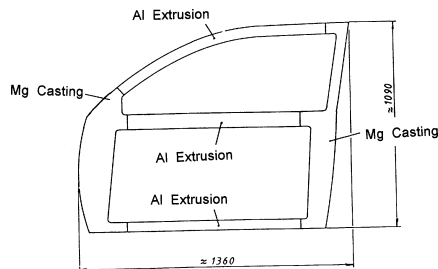


Figure 7: Concept for inner-door parts: version 2; composite construction

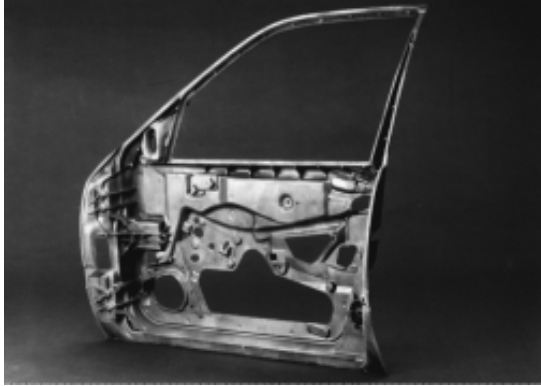


Figure 8: Concept for inner-door parts: version 3,  
Mg die-casting

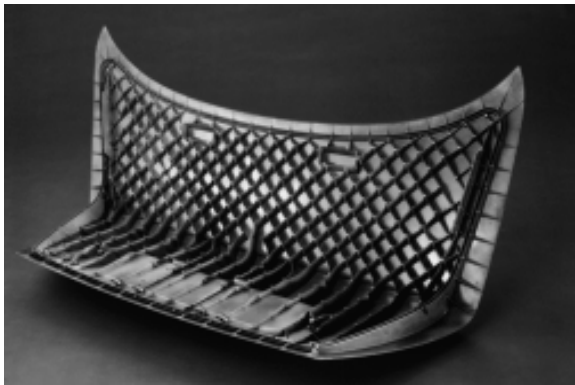


Figure 9: Prototype of a car tailgate made of AM60;  
Honsel AG

Several special features need to be considered when dimensioning such parts: abrupt transitions should be avoided and large radii are favourable, as shown in Fig. 5. The upper rib parts of the tank cover are 2 mm thick, and the drafts of the mould are  $1.5^\circ$  on each side. The mechanical properties meet the demand for an average tensile strength of 240 MPa, combined with an elongation of between 8 and 12% (values depend on the specimen orientation). The elongation values in particular are dependent on the orientation of the specimen, with the flow-path playing an important role. These concerns and the influence of the flow-path are considered in Fig. 10.

Table 6: Thoughts about influencing the strain values of components.

strain depends on the flow-path of the metal	
higher flow-path means:	<ul style="list-style-type: none"> <li>- lower strain</li> <li>- higher deviation of the strain values</li> </ul>
values depend on:	<ul style="list-style-type: none"> <li>- component geometry</li> <li>- mould-filling conditions</li> <li>- casting parameters</li> <li>- other factors</li> </ul>
strain for thin-walled cross-sections:	higher deviation because the microstructure inhomogeneity has a great influence on the results.

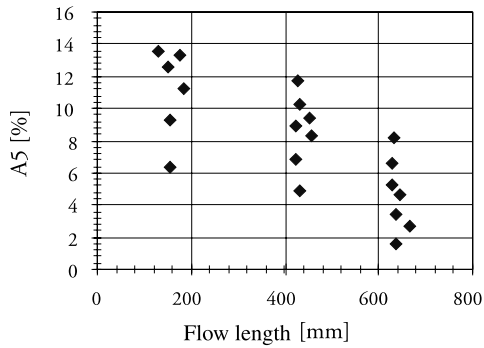


Figure 10: Strain-to-fracture ratios of magnesium alloys as a function of the flow-path

### 3.5 Costs

The application of magnesium in automotive technology can only be accomplished if a variety of material and processing based advantages contribute favourably. Table 7 shows a comparison of costs between an aluminium and a magnesium alloy in the form of a 3.5 kg sample part. The average price of an AM60 alloy is roughly 2.30 EUR/kg. The readapting costs of recycled materials are about 1 EUR/kg for external (Hydro Magnesium) and 80 Ct/kg for in-house recycling. This shows that the metal costs can be reduced significantly when using recycled material. Currently, a 3.5 kg magnesium die part would include 13 to 17 EUR for the pure metal, different portions of recycled material and melting costs already considered. Made of aluminium alloy 226, the part would cost from 10 to 11 EUR. On the other hand, magnesium allows longer tool life cycling and higher clocking, which can lead to a cost benefit of 2.50 to 3.50 EUR per part.

Table 7: Cost evaluation

metal costs		
costs AM60		2.90 €
readaption of recycled material:		Hydro Magnesium: ~ 0.80 €/kg In-house recycling: ~ 0.70 €/kg
example: part weight: 3.5 kg, i.e. metal costs:		9.45 €/part
fraction of recycled material:		
50%	1.75 kg × 0.80 €	1.66 €/part
150%	5.25 kg × 0.80 €	4.99 €/part
melting/heating costs		0.25 € / kg
melting loss		~ 5%
sum metal costs/component		13.14–17.81 €
compared to aluminium		
with same volume fraction aluminium, weight ~ 4.6 kg		
primary alloy, e.g. AlSi10Mg		2.00 €/kg
melting/heating costs		0.10 €/kg
melting loss		~ 2.5%
sum metal costs/component		10.24–10.93 €
production costs		
comparison of Mg die-casting and Al die-casting: approx. 2200 to DGM		
cycling times	Mg die-casting is about 10–20% faster than Al casting → lower casting costs, e.g. 2200 to DGM 4.10 €/part compared to 4.70 €/part	
tool life	Mg casting: ~ 150,000 shots Al casting: ~ 60–80,000 shots (depends on the alloy) → tool costs/part are less for Mg e.g. tool expenditures: 250,000 € costs/Mg part: 1.67 € ↔ costs/Al part 3.13–4.17 €	
tool maintenance	Mg casting ~20% less than Al casting e.g. 2.00 €/part ↔ 2.50 €/part	
result:	cost benefit of the Mg part compared to the Al part: 2.56–3.60 €/part	

## 3.6 Literature

- /1/ Norsk Hydro Datenbank „NHMg.db (ext.)“, Norsk Hydro Research Centre Porsgrunn, 1996.
- /2/ Cahn, R. W.; Haasen, P.; Kramer, E.J. (Hrsg.) in: Matucha, K. H. (Vol. Hrsg.): Vol. 8: „Structure and Properties of Nonferrous Alloys“, VCH Weinheim, 1996.
- /3/ Müller, C.M.: Giesserei 78, 1991, Nr. 19, p. 693-695.
- /4/ Hasse, S.: „Giessereilexikon“, Schiele & Schön, Berlin, 1997.

# 4 Squeeze-Casting and Thixo-Casting of Magnesium Alloys

*K. U. Kainer, T. U. Benzler, Institute for Materials Research, GKSS Research Center Geesthacht GmbH, Geesthacht*

## 4.1 Introduction

Extended use of magnesium in safety relevant parts of car body frames, the drive train, and the chassis requires parts with customized characteristic profiles. Combinations of cast parts, cast knots, sheet mould parts, and extruded profiles comparable to the aluminium space frame realized, are possible. Figure 1 shows a schematic view. The requirements for the materials cannot as yet be entirely fulfilled by magnesium alloys. The biggest problem is their limited ductility at room temperature. Magnesium crystallizes in the hexagonal closest packed structure and is therefore not amenable to satisfactory cold-forming. This is a problem of metal physics that can only be overcome by a change of the crystal structure by alloying (e.g. magnesium/lithium alloys [2]). Besides, the ductility is highly dependent on the grain size and the number of defects in the lattice, such as pores and enclosures. The grain size of both cast and wrought alloys can be reduced. With cast alloys, grain-refining additives are included, but they only work to a certain extent with machine-cast parts like die-cast parts. An adequate fine-grained microstructure can either be obtained by the rapid solidification of thin-walled parts or by applying new casting procedures such as squeeze-casting and thixo-casting.

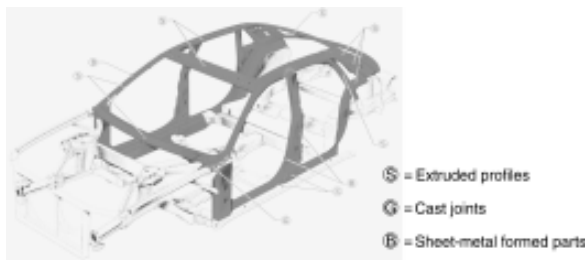


Figure 1: Potential body parts in a hypothetical magnesium car body shell (from [2])

The lattice structure can also be changed for wrought alloys, e.g. by adding lithium [2] (hcp » bcc). Another option is to induce precipitations that will interfere with grain growth during hot working or heat treatment and thereby stabilize the microstructure. All these alloying possibilities are supported by process development, since all new material designs require the development of new practices.



## 4.2 Process Development

The use of advanced casting processes offers a high innovation potential with regard to the ductility of die parts. Casting defects have a great influence on the mechanical properties, as shown in Fig. 2. Impurities and enclaves need to be prevented first, because these function as crack starting points. The reduction of the gas content and porosity will add to the positive effects.

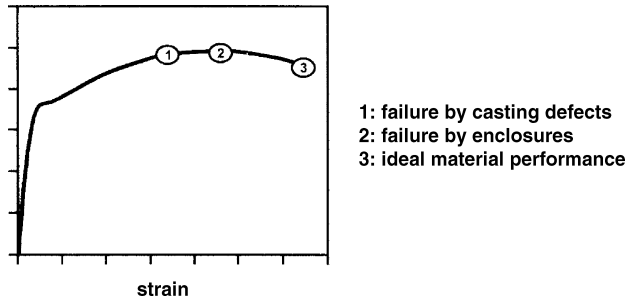


Figure 2: Influence of microstructure inhomogeneities on the stress–strain behaviour of magnesium casting alloys (schematic stress–strain curve)

The most common production method for magnesium alloys is die-casting. Further optimization of the process, accompanied by independent material development, especially the improvement of ductility and creep resistance, will lead to a growth in the use of magnesium die-cast parts never before seen for any other metallic construction materials. The acceptance of magnesium in industry is growing, and therefore the establishment of other innovative procedures currently being developed and tested can be anticipated.

A turbulent moulding process leads to the entrapment of pockets of air and residues of mould release agent. This leads to the disadvantage of a possible appearance of porosity. The parts lose their ductility, and heat treatments and welding become impossible.

Vacuum die-casting can solve these problems by evacuating the casting chamber and the mould (remaining pressure below 100 mbar). The parts no longer contain any enclaves of air and show improved properties such as weldability and amenability to heat treatments. The amount of trapped gas can be lowered to 3.5 cm<sup>3</sup>/100 g, compared to 10–40 cm<sup>3</sup>/100 g with conventional die-casting. The resulting parts show an increased strain at fracture. In research and development trials, it was found that vacuum cast magnesium parts have a much improved impact resistance (36.8 J compared to 17.7 J; AM50 alloy, unnotched specimen).

Besides the conventional casting procedure, various other manufacturing processes, such as squeeze-casting, thixo-casting or thixo-moulding, and spray-forming are currently in their testing phases. A leap to series production, as previously seen for aluminium in many fields, is sure to occur through the use of some of these processes. They greatly improve the characteristic profile of magnesium and so eventually its market segment will grow.

## 4.3 Process Description

### 4.3.1 Squeeze-Casting

Squeeze-casting is a special process with a vertical arrangement of a slewable casting unit and moulding direction. When the unit is filled, it closes and docks to the mould. Then, the piston rises up and the actual filling begins (Fig. 3). In contrast to die-casting, the moulding is done slowly (minimum turbulence and hence low porosity), though the final compression is the same. In squeeze-casting, however, the pressure is maintained until freezing is complete and even allows for further feeding in the half-frozen condition. Injection pressures are usually between 70 and 100 MPa (pressures of more than 300 MPa are possible) so as to obtain a compact, fine-grained microstructure. Squeeze-casting is an excellent method for producing pressure-sealed, low-porosity, weldable, heat-treatable parts with reproducible high quality. It is increasingly being used in place of classical gravity casting. Even T6 heat treatments for the improvement of mechanical properties are possible due to the low porosity [3]. Since the casting speed is very low, the parts do not have fin lines [4].

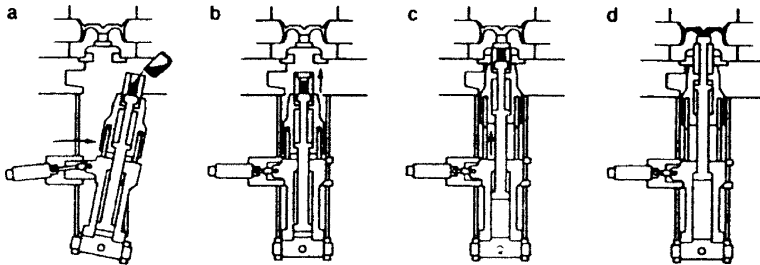


Figure 3: Schematic of the squeeze-casting process; a: proportioning; b: swinging to the vertical axis; c: hooking up to the mould; d: mould-filling and freezing [15]

The advantages of squeeze-casting are summarized below:

- reduced porosity
- hot cracking prevention for alloys with wide freezing range
- increase of strength and ductility by:
  - fine-grained microstructure
  - faultless microstructure
- possibility of heat treatment (e.g. T6)
- alloys difficult to cast can be processed
  - conventional creep-resistant alloys (WE54, QE22)
  - thixotropic melts
- alloy development
- production of magnesium composites

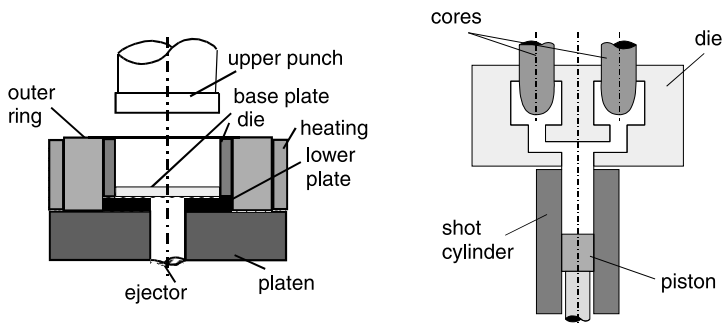
The process is separated into direct and indirect squeeze-casting.

### 4.3.1.1 Indirect squeeze-casting

In indirect squeeze-casting, the liquid magnesium is injected into the mould through a bigger injection canal compared to that used in die-casting. The flow rate of the melt is about 0.5 m/s, and is therefore significantly smaller than in die-casting (30 m/s). This low injection speed prevents the melt from absorbing air and the mould is filled without turbulence [4]. The pressure and temperature are constantly controlled, and so the pressure within the cavity stays almost constant both during and after the freezing. This also allows the use of cores and male moulds in the cavity, whereas in die-casting the high pressure would possibly destroy them.

Indirect squeeze-casting offers the possibility of infiltrating so-called preforms (porous fibre- or particle shapes) and of producing composites. The industry uses indirect squeeze-casting to produce various components in one step.

One disadvantage of the indirect process is the big gate needed for separation from the actual part. This takes a lot of material, but it can be used to host pores and micro-shrinkage when the freezing is properly controlled. Figures 4 and 5 show a schematic view of indirect squeeze-casting.



Figures 4 and 5: The left schematic depicts direct squeeze-casting, the right one shows the indirect process [6]

### 4.3.1.2 Direct squeeze-casting

In direct squeeze-casting, the punch that supplies the pressure is the lower part of the mould itself, whereas indirect casting needs a standard gate. This makes the manufacture of the moulds much easier. They can be made of either one or two parts. The pressure is applied by the upper punch; the lower one throws out the cast part. This simpler mould, compared to that needed for indirect casting, requires no clamping force and thus the costs are reduced.

On the other hand, direct squeeze-casting demands an exact determination of the amount of melt needed, since this will directly affect the shape of the cast part. Complex parts can be fashioned using additional punches or cores. The freezing of the part can be influenced by having different temperatures of the mould and punch. To obtain a non-porous part, the

freezing properties and pressure properties are not critical when using direct casting because there is no gate. Indirect casting, on the other hand, is more dependent on these factors [6]. A schematic view of direct squeeze-casting is shown in Fig. 4.

The heat transmission between the melt (i.e. cast part) and the mould is greatly improved by the high pressure of the squeeze-casting process because there is no air gap between the tool and the wall of the part. Consequently, high cooling rates are achieved and the microstructure will become very fine grained. The influence of the grain size on the yield strength of AZ91 (T6) is shown in Fig. 6.

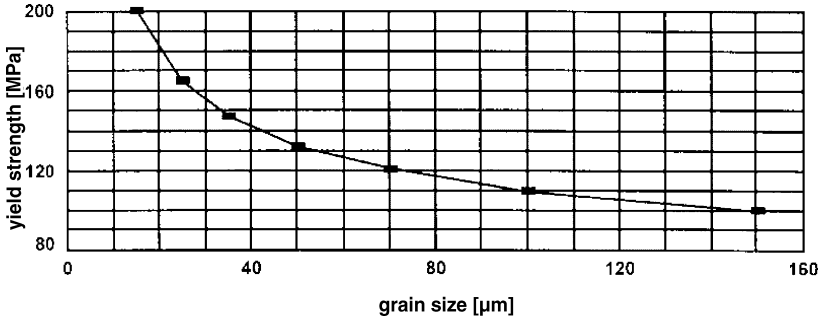


Figure 6: Influence of the grain size on the yielding of the alloy AZ91 (T6) [16]

The thermodynamics of the system is such that the applied pressure can influence the casting temperature. The melting point is shifted to higher temperatures and the melt is supercooled. The drift of the equilibrium of magnesium/aluminium alloys is shown schematically in Fig. 7. The influence of the casting pressure and the temperature of the mould on the freezing time in the middle of the cast part is shown in Fig. 8. These surrounding conditions additionally speed up the freezing; the resulting microstructure is then finely dispersed and has almost forged-like properties [6, 7].

Magnesium alloys made by squeeze-casting technology show good properties, and are even applicable for high security level parts [6]. The cast parts are almost non-porous, a further improvement on vacuum casting. Table 1 compares squeeze-cast and die-cast specimen porosities. Table 2 gives the gas volumes per 100 g for different processes and the maximum gas volume allowed for subsequent treatments.

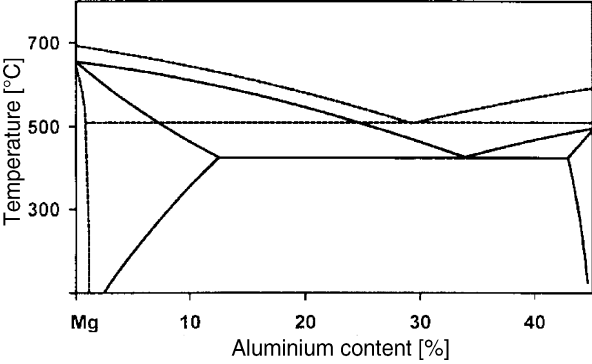


Figure 7: Equilibrium deviation in the Mg/Al phase diagram as a result of rapid freezing due to the high mould pressure.

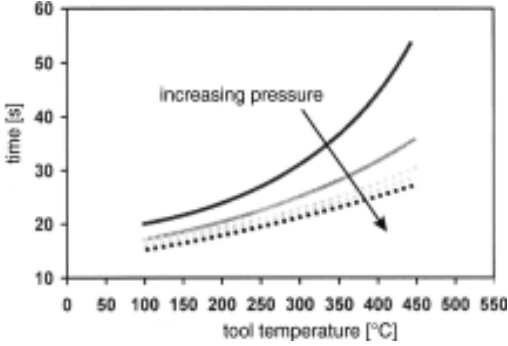


Figure 8: Influence of the mould pressure and the tool temperature on the freezing time in the centre of the casting

Table 1: Comparison of the porosities of squeeze-cast and die-cast components

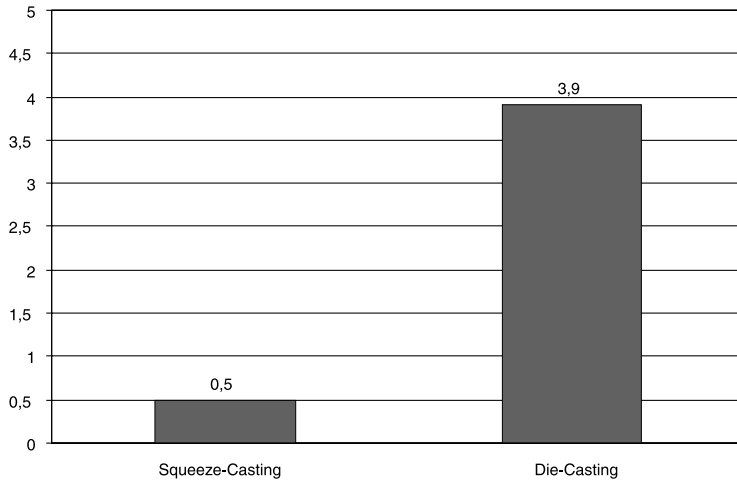


Table 2: Gas content for different casting methods and the maximum permissible contents for post-treatment.

casting technique	gas volume [cm <sup>3</sup> /100g]
low pressure casting	1-5
die casting (conventional)	10-40
die casting (vacuum)	<3,5
sand casting	1,8-12
direct Squeeze-Casting	1,2-3,5
indirect Squeeze-Casting	0,6-1,2

treatment	max. gas volume [cm <sup>3</sup> /100g]
welding	0,24-1,5
heat treatment	0,24-4,0

Hot cracking is prevented by a large freezing range. Alloys that are usually difficult to cast can be processed by squeeze-casting, opening new possibilities for alloy development. Another advantage is the production of composite materials by infiltration of ceramic preforms or by adding ceramic particles to the melt. Squeeze-cast parts have better mechanical properties compared to those cast by other processes such as sand-, ingot-, or die-casting.

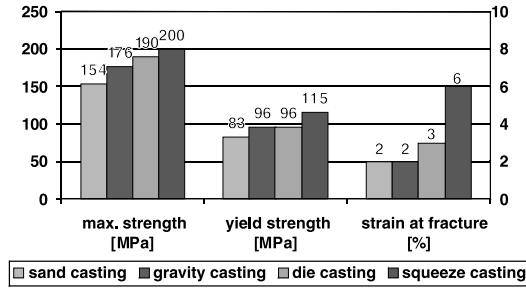


Figure 9: Comparison of the mechanical properties of cast AZ91 under T6 conditions [19]

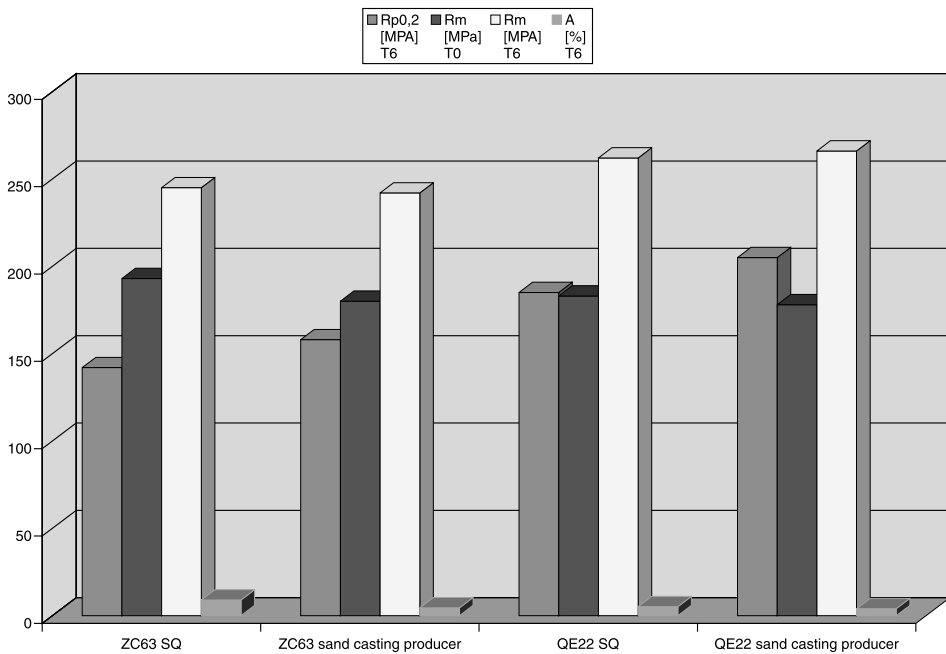


Figure 10: Diagram showing the mechanical properties of two magnesium alloys (ZC63 and QE22), cast using different processes

The improvements of the alloys ZC63 and QE22 can be seen by comparing Figs. 9 and 10. Both the maximum stress and the strain at fracture are raised. Table 3 shows that, in contrast to die-castings, squeeze-cast parts can be heat-treated.

Table 3: Comparison of mechanical strengths between squeeze-casting and die-casting

		yield strength [MPa]	tensile strength [MPa]	elongation at fracture [%]
Squeeze-Casting	as-cast condition	96	179	5,0
	T4	76	220	10,5
	T6	117	255	6,5
die casting	as-cast condition	150	230	3,0

The biggest advantage of squeeze-casting, however, is its capacity to produce metallic composites, even for series production. In the first step, a burned and re-heated porous fibre shape with specific dimensions is placed inside a pre-heated mould. After the deposition of the melt, the infiltration begins. A punch applies the pressure to the closed mould [9]. The tool consists of a heated single- or multi-part matrix with designated shape, an upper punch for the application of pressure, and an ejector to push out the solidified composite part. Since the wetting of magnesium on the ceramic materials is good, the infiltration pressure can be kept low and 50–130 MPa is sufficient. The air within the mould and preform can be expelled from the tool cavity through the slot and the venting gaps. At the same time, the air and the gases present react with the magnesium alloy to create a self-generated vacuum [10]. The time between positioning the preform and the ejection of the final part is approximately 120 seconds, whereupon the material is frozen. Cooling to room temperature is done in air. Even though the reactivity between the melt and the fibres is quite high; the short freezing time allows only little interaction at the fibre/matrix meeting planes. Squeeze-casting has a versatile application range and can readily be automated (for indirect squeeze-casting) for the production of partially or fully reinforced parts [11].

Metal composites are used in a great variety of application fields, where low density, mechanical compatibility (low but matrix-fitted thermal expansion coefficient), thermal stability, and, last but not least, a high Young's modulus together with high tensile and compression strength is required. Table 4 lists several metal matrix composites (MMCs) and their mechanical properties. The plot in Fig. 11 compares the values for the Young's modulus and the tensile strength of particle-reinforced and non-reinforced forms of the common alloy AZ91.

Table 4: Properties of short-fibre-reinforced magnesium composites (CTE = coefficient of thermal expansion; tensile strengths are measured parallel to the planar isotropic distribution)

	CP-Mg		AS41		AZ91		QE22	
	Matrix	MMC	Matrix	MMC	Matrix	MMC	Matrix	MMC
$R_{p,0.2}$ (MPa)	70	220	151	225	160	230	180	250
$R_m$ (MPa)	80	240	185	270	220	280	250	300
A (%)	5,0	2,2	4,3	1,5	4,8	1,8	4,5	1,6
E-Modul (Gpa)	46	56	49,8	77,7	46	64	46	74
$R_m$ (100 °C)(MPa)	65	240	175	250	200	270	240	285
$R_m$ (200 °C)(MPa)	45	180	150	240	120	220	200	245
$R_m$ (300 °C)(MPa)	30	120	70	145	60	130	125	180
HV10 (kp/mm <sup>2</sup> )	40	75	60	135	65	140	75	125
CTE (10 <sup>-6</sup> K <sup>-1</sup> )	26,5	21,5	24,0	18,0	27,0	20,5	26,0	20,0



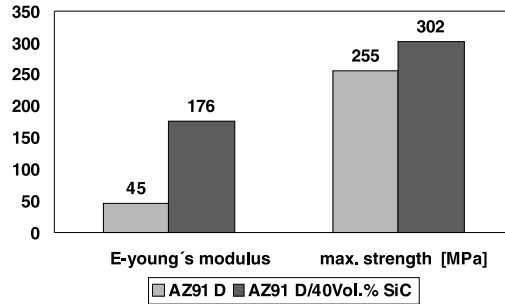


Figure 11: Mechanical properties of squeeze-cast AZ91D and AZ91D 40 vol.% SiC [18]

It can be seen from Fig. 11 and Table 5 that the Young's modulus can be up to three times higher with reinforcements; the maximum stress is raised as well. This gain is at the expense of limited ductility, i.e. the strain at fracture shown in Table 6. Table 6 shows two different reinforced alloys and a heat-treated aluminium alloy as possible materials for a piston. Aluminium is considered here as a competing material to magnesium and its alloys. The table also shows that the tensile properties of the composites with a magnesium matrix almost reach those of the aluminium alloy. The specific strength (strength referred to the density) is again seen to be increased compared to the non-reinforced magnesium materials. This proves that with squeeze-casting it is possible to produce parts from interesting materials.

Table 5: Properties of reinforced and non-reinforced magnesium materials

Material	$R_m$ [MPa] T0	$R_m$ [MPa] T6	$R_{p0.2}$ [MPa] T6	A [%] T6	E [GPa] T6	CTE [ $10^{-6}K^{-1}$ ]
QE22 SQ	183	262	185	5,2	48	
QE22 + 20% SiC-Hybrid	205	285	265	2,4	74	19
QE22 + 25% SiC-Hybrid	203	282	270	1	80	18
QE22 + 20% Saffil	230	290	270	1,2	70	20
QE22 + 20% $Al_2O_3$ platelets	240	250	240	0,5	88	21
AZ91 SQ	180 - 220	230 - 295	120 - 150	2 - 8	44	27
AZ91 + 20% C-Faser	225 - 260	230 - 270	200 - 240	0,5	66	19 - 20
AZ91 + 20% Saffil	295	260	200	2	69	20,5

Table 6: Properties of aluminium- and magnesium composite materials

Properties	Unit	AlSi12CuMgNi, heat treated	20 Vol.-% C-fibers + AS41	20 Vol.-% C-fibers + AZ91Ca1
Density	g/cm <sup>3</sup>	2,7	1,8	1,9
YS (RT)	MPa	275-335	149-160	200-240
UTS (RT)	MPa	295-360	175-196	225-260
YS (250 °C)	MPa	90-120	85-91	101-115
UTS (250 °C)	MPa	110-165	95-102	112-122
Fracture Elongation	%	1-3	-0,5	-0,5
Bending Fatigue Strength (200 °C)	MPa	85	75	60
Young's Modulus	GPa	79,5	78	55-60
Heat Conductivity	W/mK	155	n.n.e.	~140
CTE	10 <sup>-6</sup> K <sup>-1</sup>	20	19,7-19,3	19-19,8
Creep Rates (150 °C 70 MPa)	10 <sup>-9</sup> s <sup>-1</sup>	n.a.	1,3-2,9	13

### 4.3.2 Thixo-Casting

Thixo-casting is a fairly new method based on the thixotropic properties of semi-liquid alloys. The material has already reached liquidus temperature and consists of a mixture of solid and liquid phases (also known as semi-solid metal forming). The area of the magnesium/aluminium phase diagram in which a thixo-casting alloy is processed is indicated in Fig. 12. Intense stirring prevents the usual formation of dendritic grains and instead forms globular grains. Figure 13 shows the differences between dendritic and globular microstructures. This condition characterizes the thixotropic flow behaviour; with increasing viscosity the shearing strain falls off. Aluminium alloys are also suitable for this (e.g. G-ALSi7Mg).

The actual procedure requires suitably manufactured raw material. Technically, it is carried out by electromagnetic stirring (rheocasting) within a slab-casting machine. The cast bolts are heated up close to the liquidus temperature until the required ratio of liquid to solid phase is reached (approximately 30–40% melt). Such a bolt is then transferred into the casting chamber of the machine; it can still be handled like a solid material.

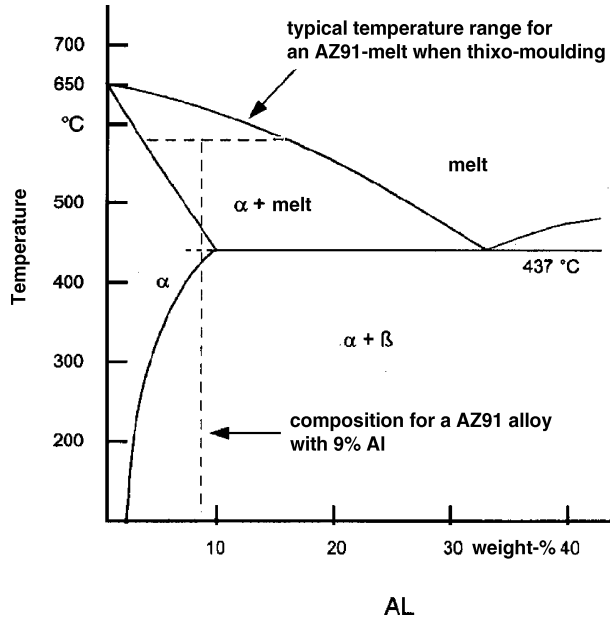


Figure 12: Typical alloy composition and associated temperature range, shown by the magnesium/aluminium phase diagram for the thixo-casting/moulding process [14]

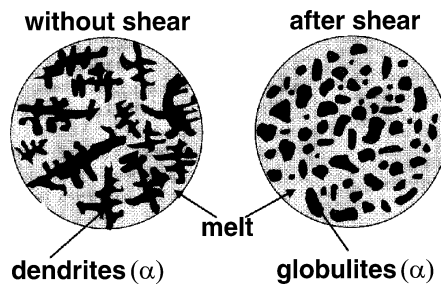


Figure 13: Dendritic and globular formations of an Mg/Al alloy

When pressure is applied to the bolt, the developing shearing stress decreases the viscosity and the bolt behaves like a fluid. Recently, much effort has been directed towards shortening the time required for the electromagnetic stirring so as to lower costs. A first step towards this goal is the so-called NRC process (new rheocasting process). This process tries to avoid dendritic growth by a customized cooling–melting process and simultaneous turning of the melting crucible [12].

The advantages of this procedure compared to conventional casting are as follows [22]:

- the production process can be fully automated
- high productivity

- cost savings due to low energy consumption
- higher tool lifecycles
- parts are free from gas inclusions and hence are weldable
- low cooling shrinkage and no blow holes
- parts have excellent mechanical properties
- final parts have near-net-shape quality

The thixo-casting process is outlined schematically in Fig. 14, while Fig. 15 compares the strength of a squeeze-cast and a thixo-cast AZ91 alloy (T4 conditions) [8]. Additionally, Fig. 16 shows the microstructure of a thixo-cast part.

Besides the thixo-casting process, there is a variation called thixo-moulding. The procedure is closely related to thixo-casting, but instead of a die-casting machine, an injection-moulding machine as used in the manufacture of plastics is used. Nevertheless, the hydraulic propulsion for the injection is based on the die-casting machine part. Figure 17 gives a schematic view of the injection unit.

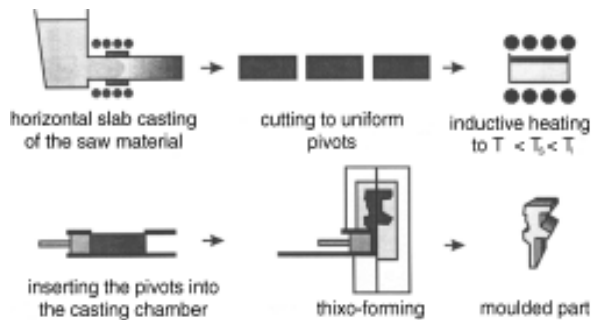


Figure 14: Schematic sequence of the thixo-casting/thixo-moulding process [20]

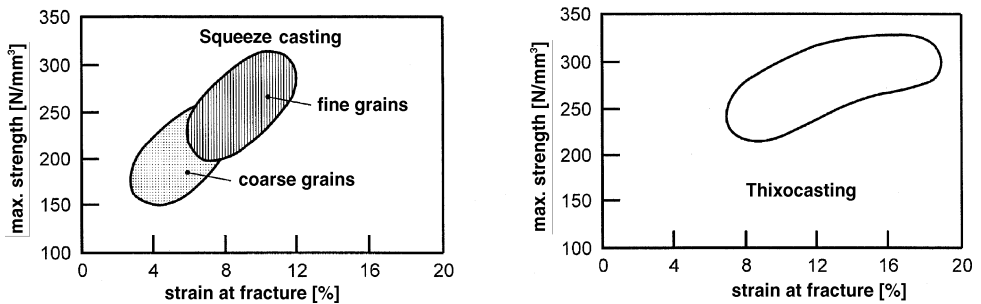


Figure 15: Correlation between strength and elongation at fracture for an alloy made by squeeze-casting and thixo-moulding (alloy AZ91 under T4 conditions) [21]



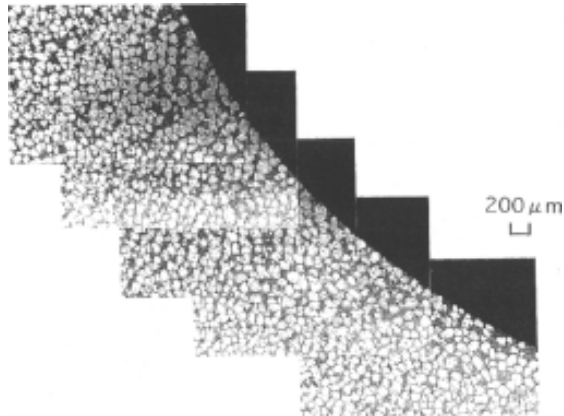


Figure 16: The crack-free surface of a thixo-cast component (AZ91D) [22]

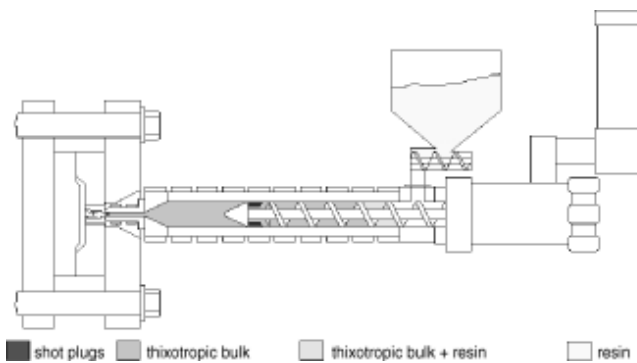


Figure 17: Thixo-moulding casting machine prior to the shot

The thixo-moulding granulate is melted in a screw conveyor, which leads directly to the chamber, and from there it is directly pressed into the mould. Care has to be taken to prevent bridging from occurring, as is known from experience with plastics. Additionally, the injection unit needs to be flooded with argon during heating and after turning off, i.e. on cooling down. This is necessary to prevent any contact with air, since the corrosion, i.e. oxidation activity, is high for the liquid alloy [13].

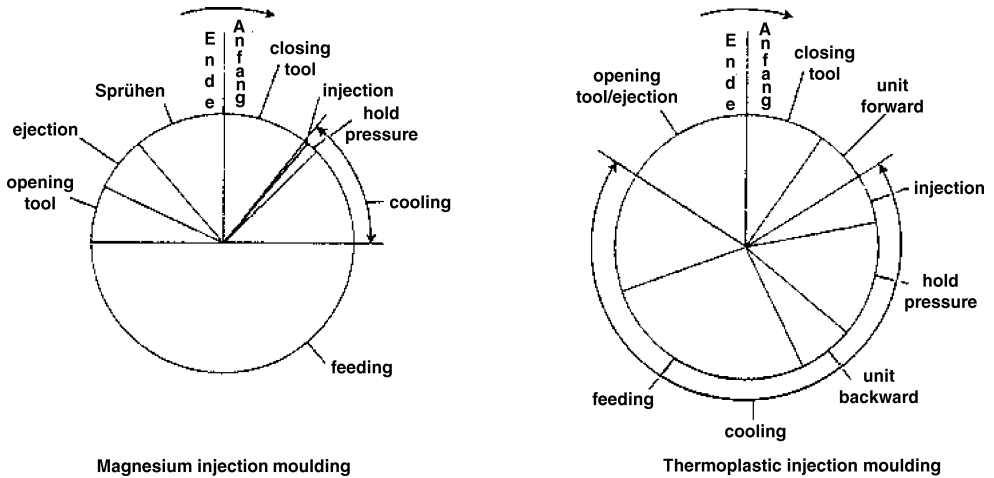


Figure 18: Schematic comparison of the injection-moulding cycles of magnesium injection-moulding/thixo-moulding and thermoplastic injection-moulding [13]

The screw conveyor transports the granulate slowly towards the end of the screw. During this transport, the granulate is melted, and the injection temperature lies between 560 and 620 °C. Remaining dendrites are formed into spherical solids by the shearing stress and are completely surrounded by the melt. The injection duration of the thixotropic mass is about 10–100 ms. The time for which the pressure is maintained after the filling process is shorter compared to the case of plastics. In Fig. 18, regular die-casting for plastics and thixo-moulding are compared [13].

## 4.4 Literature

- /1/ NN, Aluminium Technologie im Karosseriebau – Audi Space Frame (ASF), Firmenbroschüre Audi AG, Ingoldstadt.
- /2/ Haferkamp, H., Bach, Fr.-W., Juchmann, P.: „State, Development and Perspectives of Lithium Containing Magnesium Alloys, Proc. Int. Conf. on Magnesium Alloys and their Applications“, B.L. Mordike, K.U. Kainer (Hrsg.), Werkstoff-Informationsgesellschaft, Frankfurt, 1998, 157-162.
- /3/ Rajagopal, S.: „Squeeze-Casting: A Review and Update“, Journal of Applied Metalworking 4 (1981), ASM, Metals Park, Ohio, USA, 3-14.
- /4/ Kaufmann, H.: „Endabmessungsnahes Gießen: Ein Vergleich von Squeeze-Casting und Thixocasting“, Giesserei 81 (1994) 11, 342-350.
- /5/ Hasse, S.: „Giessereilexikon“, Schiele & Schön, Berlin 1997.
- /6/ Kainer, K. U.; Böhm, E.: „Preßgießen (Squeeze-Casting) von Magnesiumlegierungen“, VDI-Bericht Nr. 1235 (1995), 117-125.
- /7/ Degischer, H. P.: „Schmelzmetallurgische Herstellung von Metallmatrix Verbundwerkstoffen“, in Kainer K. U. (Hrsg.): „Metallische Verbundwerkstoffe“, DGM-Verlag, (1994), 139-144.
- /8/ Kaufmann, H.: „Endabmessungsnahes Gießen: Ein Vergleich von Squeeze-Casting und Thixocasting“, Giesserei 81 (1994), 342-350.

- /9/ Kainer, K. U. und Mordike, B. L., Metall 44 (1990), 438-443.
- /10/ Nientit, G.; Proc. Int. Conf. on Magnesium Alloys and their Applications, Garmisch-Partenkirchen, Mordike B. L. und Hehmann, F. (Hrsg.), DGM Informationsgesellschaft Oberursel (1992), 407-414.
- /11/ Henning, W.; C. Melzer, C.; Mielke, S.; Metall 46 (1992), 436-439.
- /12/ Kaufmann, H.; Wabusseg, H.; Uggowitzer, P. J.: „Metallurgical and Processing Aspects of the NRC Semi-Solid Technology“.
- /13/ Dworog, A.; Huppertz, R.; Hartmann, D.: „Magnesiumspritzgießen“, Kunststoffe, Carl Hanser Verlag, Jahrgang 89, Nr. 9, (1999), S. 75-78.
- /14/ Breuer, H.; Dolfen, E.: „Magnesium“, KU Kunststoffe, Carl Hanser Verlag, Jahrgang 89, Nr. 1, (1999), S. 64-66.
- /15/ Hasse, S.: „Giessereilexikon“, schiele & Schön, Berlin, (1997).
- /16/ Rozak, G. A.; Purgert, R. E.; Thomas, J.; Hale R.: „Metal Compression Forming [MCF]“, IMA 99 Annual World Magnesium Conf. IMA, McLean, USA, Toronto (1997), p 55-57.
- /17/ Lipchin, T. N.: „Alloy strengthening by solidification under pressure“, Russian Casting Produktion, (1973).
- /18/ Hu, H.: „Squeeze-casting of magnesium alloys and their composites“, Journal of Material Science 33 (1998), p. 1579-1589.
- /19/ Chadwick, G.A.: „Squeeze casting of magnesium alloys and magnesium based metal matrix composites“, (1998).
- /20/ Gabathuler, J-P. et al.: „Eigenschaften von Bauteilen aus Aluminium, hergestellt nach dem Thixoforming-verfahren“, VDI-Bericht Nr. 1235, 1995, p. 81.
- /21/ Sasaki, H.; Adachi, M.; Sakamoto, T.; Takimoto A.: „Einfluß des Erstarrungsgefüges auf die mechanischen Eigenschaften der Legierung AZ91“, Gießerei-Praxis, Nr. 15/16 (1997), p. 341-346.
- /22/ Sasaki, H.: UBE Industrie LTD.
- /23/ Steinscherer, A.: „Konzeption und Entwicklung eines Modellbauwerkzeuges für das Magnesiumspritzen (Thixomolding)“, unveröffentlichte Studienarbeit, Fochhochschule Niederrhein, IF-MSG, Willich, (1998).

# 5 Deformation of Magnesium

*E. Doege, K. Dröder, St. Janssen, University of Hannover*

## 5.1 Introduction

In the age of limited fossil energy resources, the demand for lightweight construction materials is growing in order to reduce energy consumption and to lower environmental impact. In this regard, magnesium and its alloys have attracted much attention recently. Magnesium is highly available (1.1 kg/m<sup>3</sup> in sea water) and possesses positive technological properties such as a low specific weight together with high strength (Fig. 1).

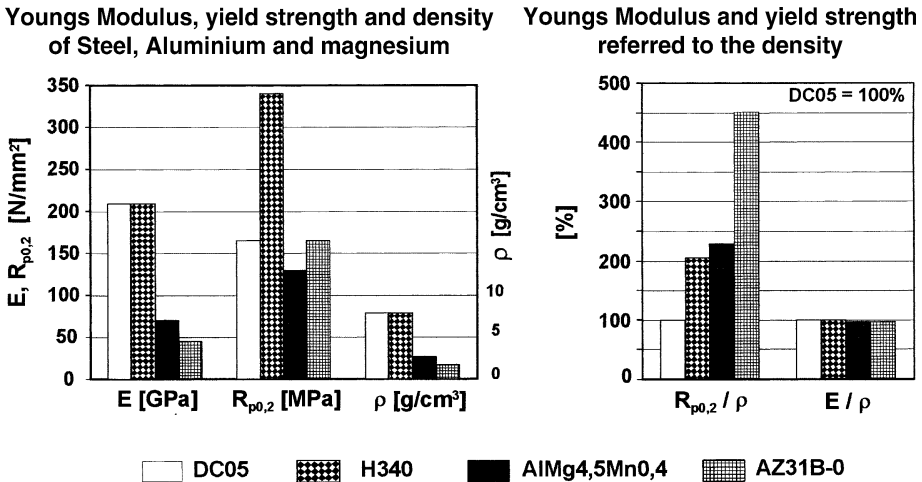


Figure 1: Mechanical properties of different sheet materials

Nowadays, magnesium is used for applications where the advantage of reducing the weight is more important than the relatively high cost [1]. With 1.75 g/cm<sup>3</sup>, magnesium's density is roughly 35% lower than that of the competing material aluminium. At present, the main applications of magnesium are as cast parts for the automotive industry. These cast parts can be most complex, but in many cases they lack the desired mechanical properties. Metal-formed magnesium parts are an alternative, and since they show a resilience that meets the application demands, due to a fine-grained microstructure with no eliquations or pores, the properties for applications are much better. Insufficient knowledge of the process parameters has hitherto limited the widespread use of magnesium on a massive scale. The potential for the application of shaped magnesium parts in a vehicle is great; the majority of the body shape consists entirely of formed parts, representing almost 25% of the vehicle weight (Fig. 2). Thus, the substitution of traditional steels with parts made of magnesium alloys may contribute to a significant weight saving.



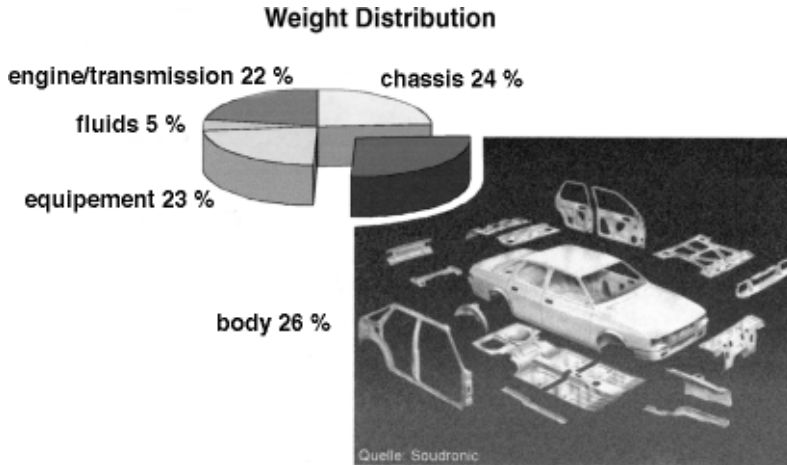


Figure 2: Use of sheets in automotive engineering

## 5.2 Procedures of Deformation

Hot mass forming, swaging of powder, and sheet forming have great potential to become the most important production methods for magnesium alloys.

The future potential for near-net-shape precision forging techniques is high, since they are very energy- and material efficient [3] and meet even the highest safety requirements for today's vehicle parts (Fig. 3).

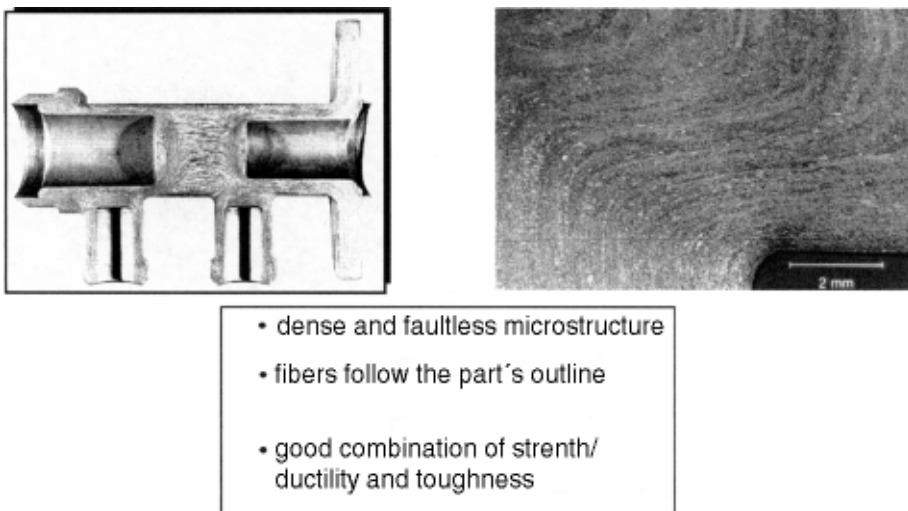


Figure 3: Advantages of drop-forged parts

Further fields of application were opened up by powder metallurgical processes such as swaging of powder (Figs. 4 and 5). Powder metallurgy allows one to work with alloys that are difficult to cast and to develop new alloying systems [4].

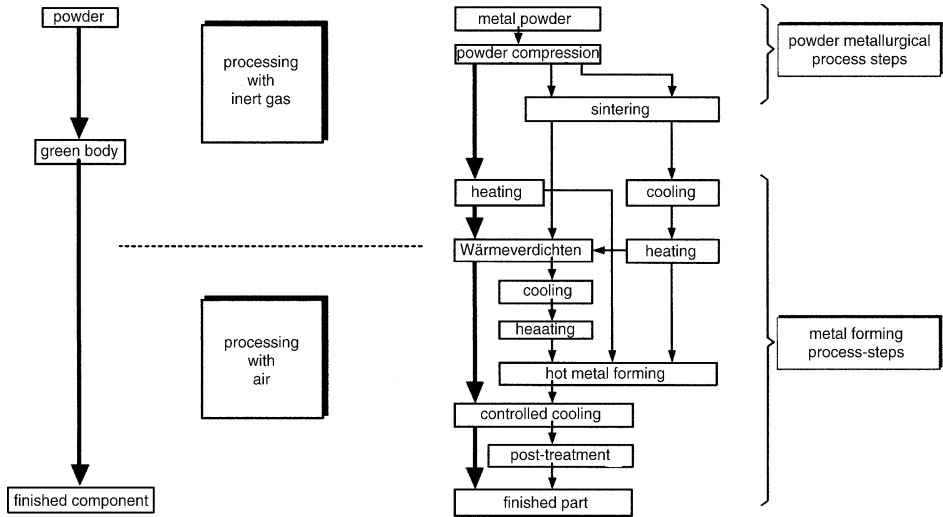


Figure 4: Process variations of the swaging of powder

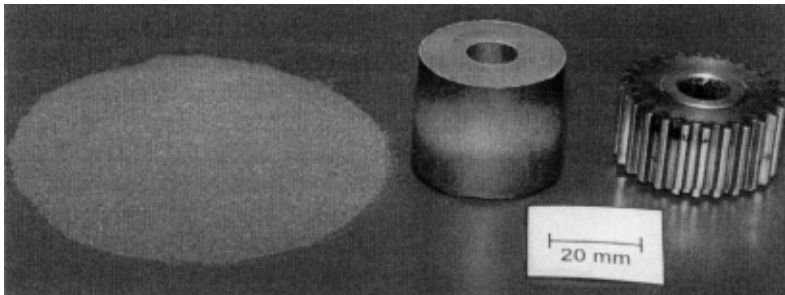


Figure 5: Stages of the swaging of powder

A hollow body is made out of a sheet cutting by deep drawing, whereby a characteristic tension-compression-stress condition occurs in the deformation zone. The direct force impact is typical for deep drawing; the force required for deformation is not directly induced by the tool in the deformation zone, but by the punch via the bottom and the can body. The actual shaping is done by radial tension and tangential compression stress inside the flange (Fig. 6). The maximum drawing ratio  $\beta_{0max}$  gives a measure of the deep drawing ability of a material.

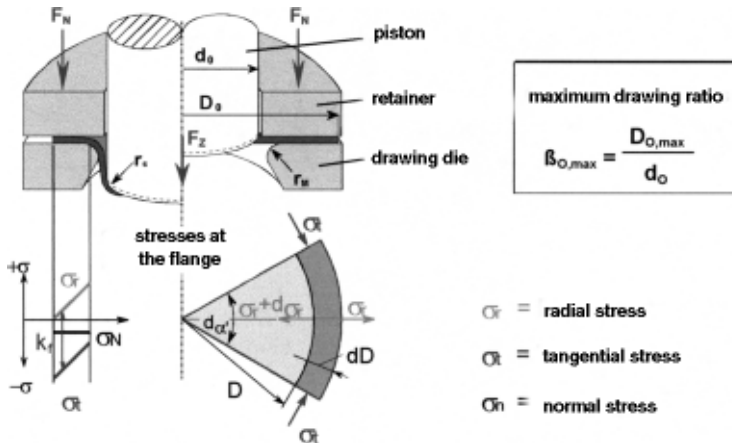


Figure 6: Basic tool set-up and stresses in the flange

## 5.3 Material Properties

### 5.3.1 Sheet Forming

One of the main focuses at the Institute for Metal Forming and Forming Machines is the characterization of the properties of magnesium that are relevant for forming issues. In this connection, the influence of temperature and deformation speed is closely scrutinized.

When the deformation abilities of classical steel and aluminium sheet materials are discussed, the vertical anisotropic exponent (“ $r$  value”) and the strengthening exponent (“ $n$  value”) are key parameters.

The vertical anisotropy  $r$  is a measure of the orientation dependence of the distortion of a material. It is the distortion ratio of width and thickness of a flat tensile specimen (Fig. 7). For deep drawing, an average anisotropy of  $r > 1$  is welcome, because then the material flows from the plane with only a slight change in thickness.

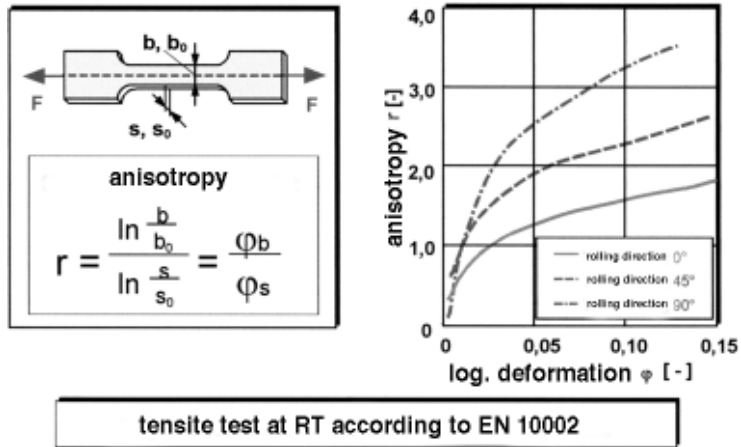


Figure 7: The anisotropy  $r$  for AZ31 at room temperature

At room temperature, AZ31 has a high average vertical anisotropy of  $r_m = 2.03$ . However, the scattering of the anisotropic values is unfavourable with regard to its forming ability [21].

The  $n$  value reflects the strengthening behaviour of a material. It is equal to the slope of the flow curve on a double logarithmic scale. The strengthening exponent gives a measure of the stress increase during forming. A high consolidation prevents an early local necking and thus leads to a higher forming limit during stress-forming. For AZ31, the average strengthening exponent in the rolling direction is considerably lower than for the common sheet-forming steels (e.g. DC04) (Fig. 8) [22].


 street thickness $s_0$ [mm]	material			
	AZ31	AlMg5Mn	DC04	DC06
max. strength $R_m$ [N/mm <sup>2</sup> ]	269	299	306	317
yield strength $R_{p0,2}$ [N/mm <sup>2</sup> ]	186	164	160	133
$R_{p0,2}/R_m$ [-]	0,691	0,548	0,523	0,419
strain hardening coefficient $n$ [-]	0,173	0,312	0,255	0,305
average anisotropy $r_m$ [-]	2,03	0,87	1,68	2,02

Figure 8: Characteristic parameters of different sheet materials, derived from the tensile test.

The influences of the metal-forming temperature and the deformation speed on the strength of magnesium alloy AZ31 were examined in further experiments. It could be shown that the flow stress is significantly lower for materials formed at higher temperatures. Starting at temperatures of  $T > 200\text{ °C}$ , the material softens due to recovery processes after an initial rise of the flow curve.

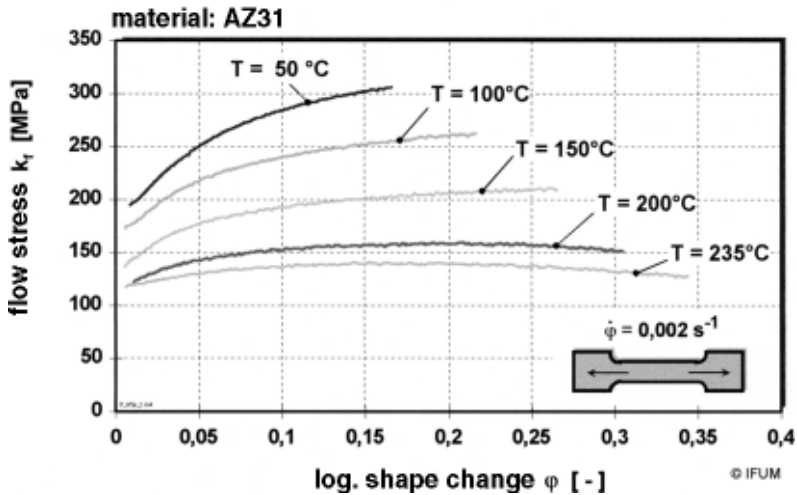


Figure 9: Temperature-dependent flow curve from the tensile test according to EN 10002

Further measurements revealed a great dependence of the flow stress needed for maximum deformation on the deformation speed. Figure 10 shows the measured flow curves for the magnesium alloy AZ31 at  $200\text{ °C}$  for different testing rates. The flow stress required for plastification rises with increasing deformation speed. Additionally, the strain at fracture decreases with increasing deformation speed.

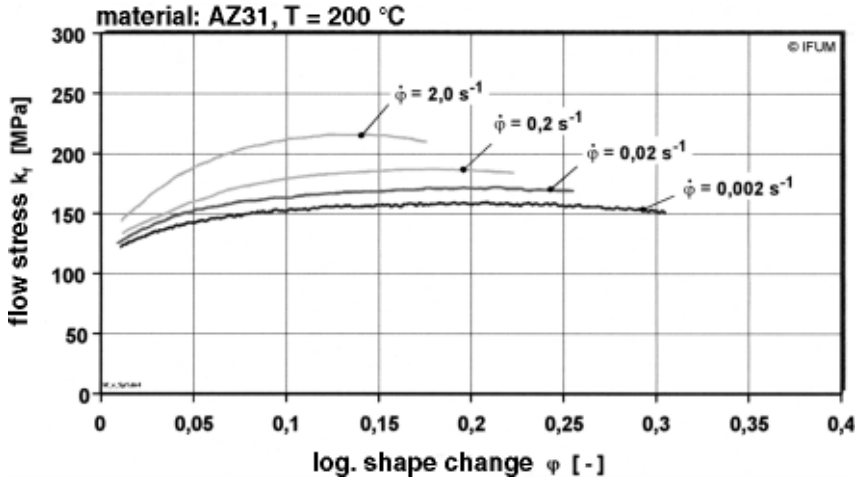


Figure 10: Influence of the deformation speed on the trend of the flow curve during the tensile test; testing temperature  $T = 200 \text{ °C}$

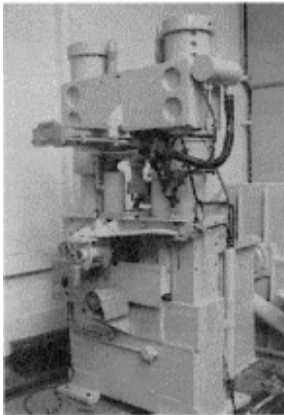
### 5.3.2 Massive Forming

The basic scientific background and process parameters for the forming of magnesium alloys and their powder metallurgical processing are now known. The knowledge gained from basic investigations (cylindrical compression test with a plastimeter) was applied in the design and construction of testing tools for the evaluation of massive forming and swaging of powder. In this way, the influence of the process parameters

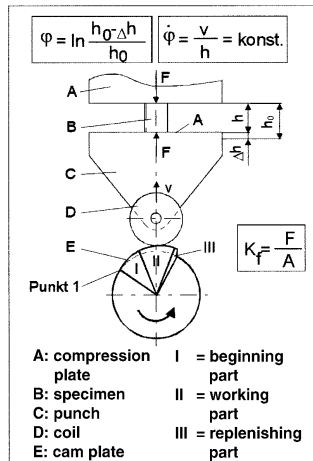
- raw part temperature
- tool temperature
- raw material
- deformation speed
- lubricant

on the material properties (e.g. hardness) and the process accuracy and mould-filling could be observed.

By means of the cylindrical compression test, flow curves of conventional and newly developed magnesium alloys were measured in order to describe and evaluate their deformation abilities. The flow stresses and curves are the experimental basis for the calculation of deformation force and deformation work, thus characterizing the plastic deformation ability of a material. The flow curves were recorded with a plastimeter (cylindrical compression test facility) developed at the IFUM (Fig. 11). This plastimeter allows the deformation of a cylindrical specimen with an almost constant deformation speed.



Test stand



Operating principle



Heat-protective case



Compression track

Figure 11: Plastimeter

The material behaviour of conventional magnesium alloys (AZ31, AZ61) was studied at 210–400 °C for two deformation speeds (1 s<sup>-1</sup> and 10 s<sup>-1</sup>). Figures 12 and 13 show the flow curves for AZ31 and AZ61 according to [6]. All curves show the same descending tendency at all temperatures. The slope gives a measure of the degree of crystal-structure softening. At temperatures below the recrystallization boundary, the curves descend more steeply. In the course of these tests, micro-cracking occurred to a certain extent, which could have led to significant softening or even fracture (dashed lines). The fractures at low temperatures and high degrees of deformation (up to  $\varphi = 0.8$ ) are obvious. Only beyond a deformation temperature of 300 °C are deformations at higher speeds possible, without shear fracture at an orientation of 45° (Fig. 14). The decline of the curves above the recrystallization temperature can be explained in terms of an overlay of the strengthening and recovery processes with a strong influence of the crystal structure recovery.

## AZ31

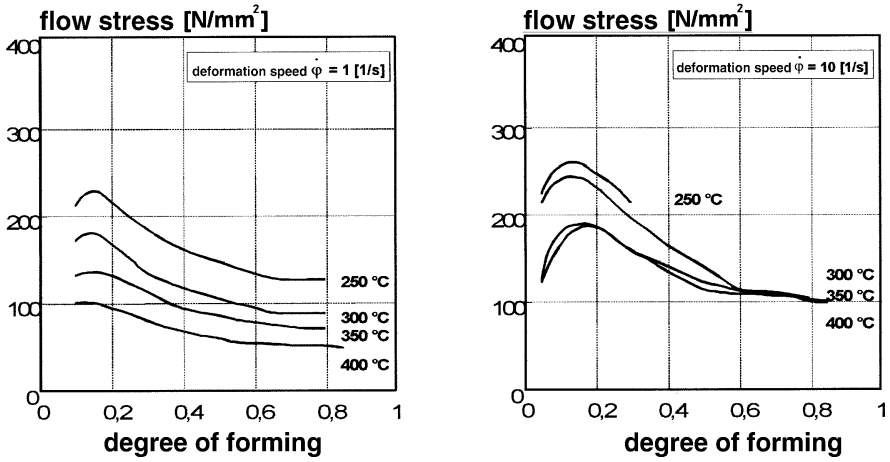


Figure 12: Flow curves for AZ31 derived from the cylindrical compression test [6]

## AZ61

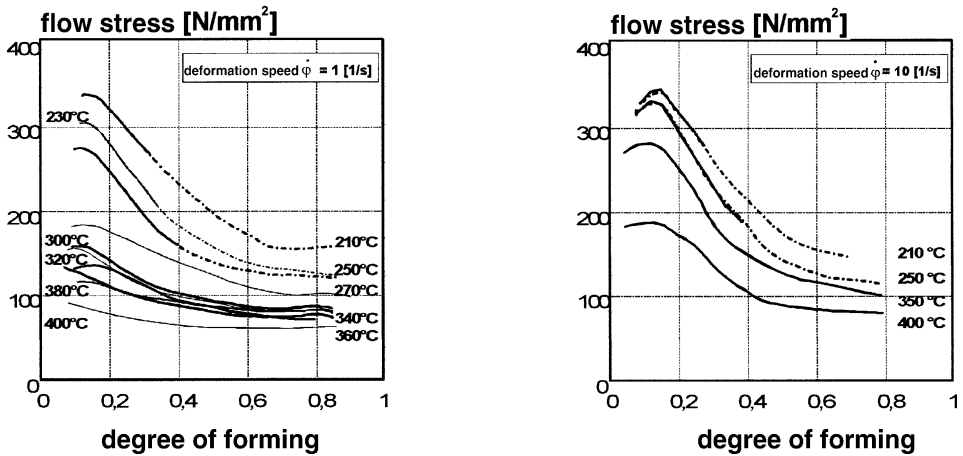


Figure 13: Flow curves for AZ61 derived from the cylindrical compression test [6]



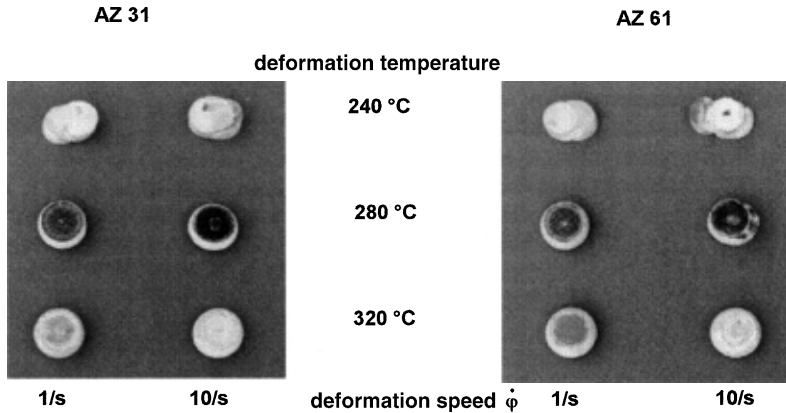


Figure 14: Deformed cylindrical compression specimen

## 5.4 Deformation Behaviour of Magnesium

A critical factor for the deformation of magnesium is the temperature, since magnesium shows only limited formability at ambient temperatures because of its hcp structure. Above 220 °C, however, additional gliding systems become thermally activated and magnesium becomes highly deformable [7–9,11,12].

Figure 15 lists the basic influencing factors for the deformability in hot metal forming according to Spittel [10], which are generally valid for magnesium as well.

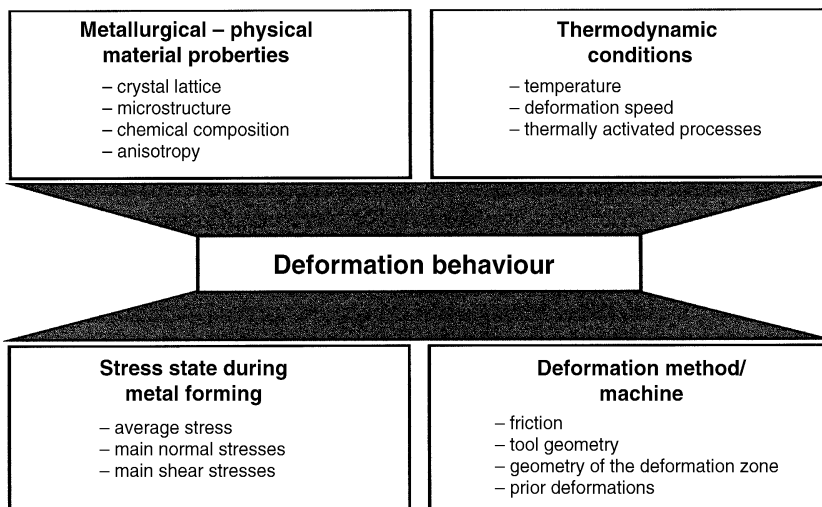


Figure 15: Parameters for tempered metal forming [10]

The temperature-sensitive processes that increase the formability have already been comprehensively discussed elsewhere. The increase in plasticity that occurs between 200 and 225 °C, depending on the alloy composition, has been described by Siebel [13]. For pure magnesium, this value is given as  $T = 225$  °C. Measurements by Roberts [14], Raynor [15], and Chapman [16] showed gliding of the basal crystal plane up to 225 °C.

The pyramidal planes, which lead to an erratic increase in the plastic formability, are only activated above 225 °C (Fig. 16).

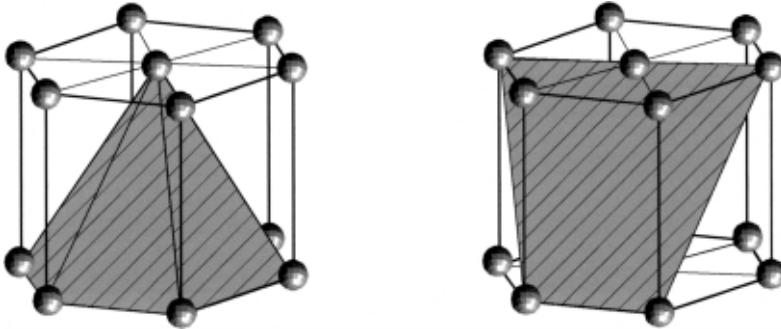


Figure 16: Pyramidal planes (first order)

Gliding of dislocations on prismatic planes is another deformation mechanism [17]. Low deformation speeds at approximately 160 °C result in wavy glide bands, which are possibly caused by alternating prismatic and pyramidal gliding [18].

### 5.4.1 Deep Drawing Magnesium Sheets

From the literature, it would appear that little is known about the deep drawing and stretching processes in relation to magnesium. AZ31 is listed as being capable of deep drawing and stretching [19]. Barnes introduced several examples of magnesium parts applied in the automotive and aeronautic industries.

Due to the limited deformability that results from the hexagonal structure, low deformation rates and big stretch radii are proposed [5,12,20].

Further proposals regarding the tool geometry for the bending and deep drawing of magnesium AZ31 have been given by the Dow Chemical Company [11]. They say that bending and deep drawing is possible at room temperature when the correct tool geometry is used.

The deformation behaviour of fine sheets made of AZ31 is indeed highly dependent on the temperature has been proven by tests at the IFUM (Fig. 17). The use of a rectangular tool geometry and a hypothetical stretch ratio of  $\beta_{10} = 1.5$  resulted in an early material fail caused by cracks at the punch's edge even before the bottom was completely stretched into shape. A temperature increase to 150 °C allowed a complete shaping of the bottom with the same stretch ratio as used before. However, the limited deformability led to cracks within the flange at a stretching depth of approximately 35 mm. At even higher temperatures, a sudden increase in the deformability of AZ31 was observed between 150 and 200 °C (Fig. 18) [23].

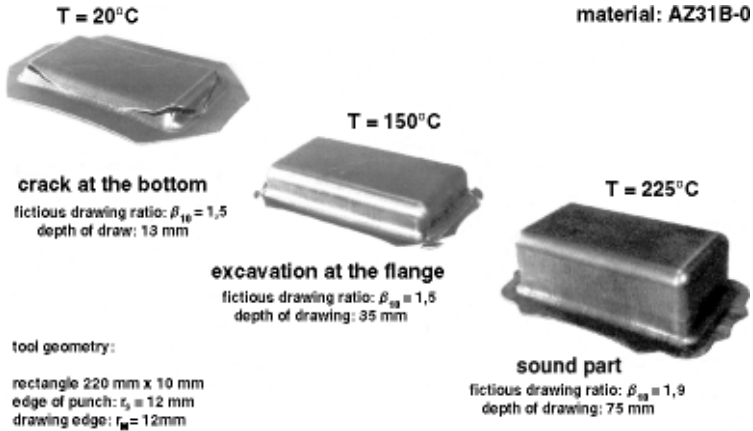


Figure 17: Temperature-sensitive deformation behaviour of the magnesium alloy AZ31

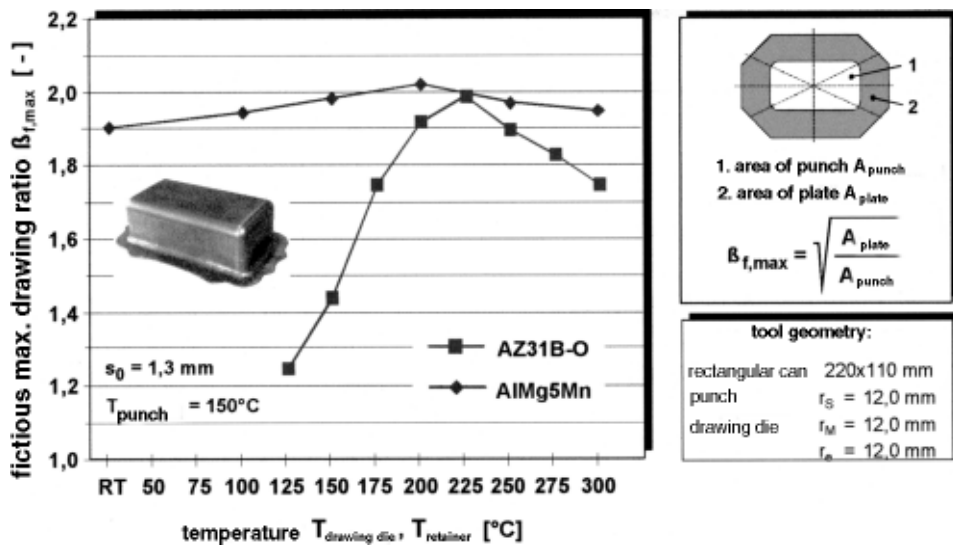


Figure 18: Hypothetical maximum drawing ratio of AZ31 and AlMg5Mn

The maximum deformability of  $\beta_{f,0max} \gg 2.0$  was reached in the flange area at 225 °C. The aluminium alloy AlMg5Mn was compared and was found to have a lower gradient of increase of the deformability over the temperature range and a maximum value of  $\beta_{max} = 2.02$  at  $T = 200$  °C. The hot forming of magnesium sheets thus offers a great potential for increasing the deformability and the manufacture of complex part geometries. Figures 19 and 20 show several trial parts made at the IFUM.

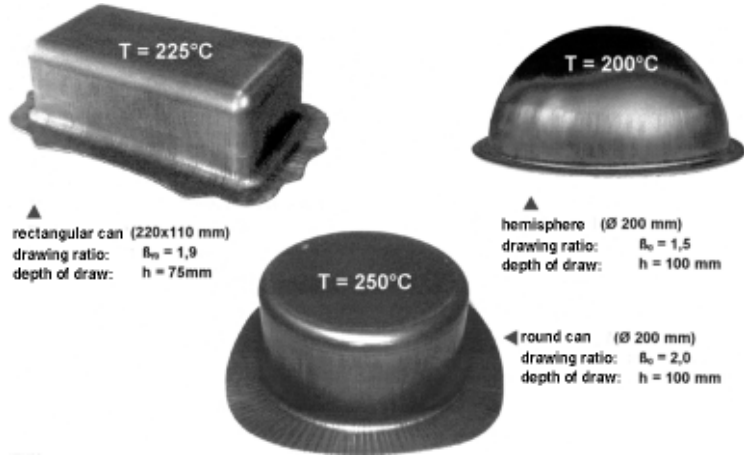


Figure 19: Deformation tests at high temperatures, thickness:  $s_0 = 1.35\text{ mm}$

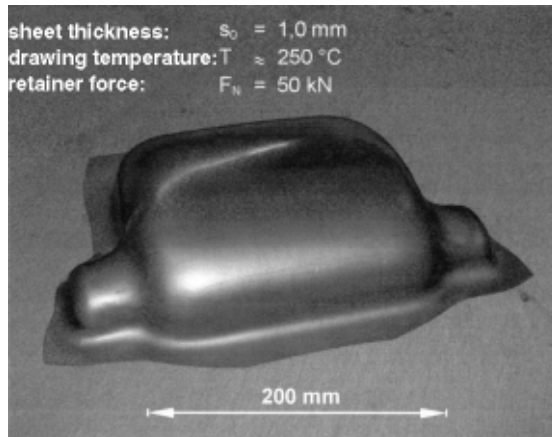


Figure 20: AZ31 deep drawing part,  $s_0 = 1.0\text{ mm}$

The studies showed that the manufacturing of component geometries from magnesium sheet requires heated tools. The set-up of a tempered tool is presented in Fig. 21.

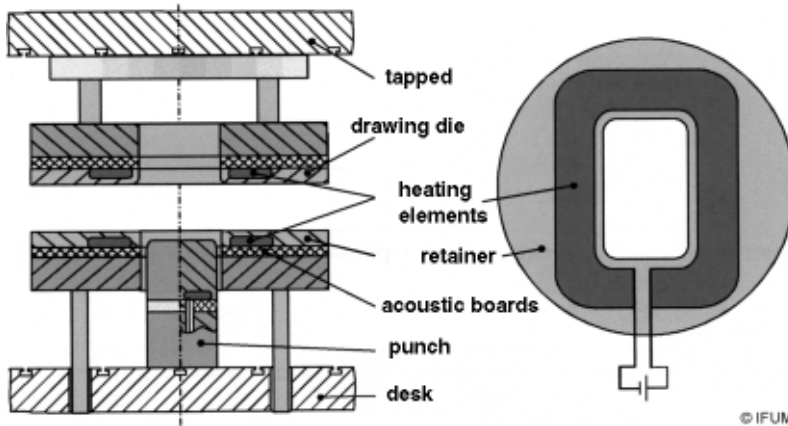


Figure 21: Principle tool set-up for deep drawing at elevated temperatures

## 5.4.2 Forging Magnesium Alloys

When forging magnesium alloys, a precise temperature control is again of critical importance. Low temperatures decrease the formability (Fig. 22), while at excessively high temperatures hot cracks appear in the forged part, which are partly caused by alloying elements or low melting points of secondary phases. Besides, magnesium has a high thermal conductivity therefore contact and handling times should be kept low in order to prevent greater temperature loss. Because magnesium alloys are very dependent on the temperature during deformation, several different tool systems with heatable die, punch, and ejector parts have been developed (Fig. 23). Figure 24 shows two examples of parts forged at the IFUM. The mould-filling behaviour of both AZ31 geometries at a tool temperature of 200 °C and a blank part temperature of 400 °C is also displayed. The specimen first gets thicker before the pivot goes up, and therefore the pivot can be seen as a measure of the mould-filling behaviour. While less energy is consumed to fill the mould with increasing temperature of the tool and the blank part, the maximum force for the final deformation stays the same (Fig. 25). The material properties and the processing loads need to be considered for an adjustment of the optimized forging parameters. Figure 26 shows the systematic procedure used to describe the deformabilities of various magnesium alloys.

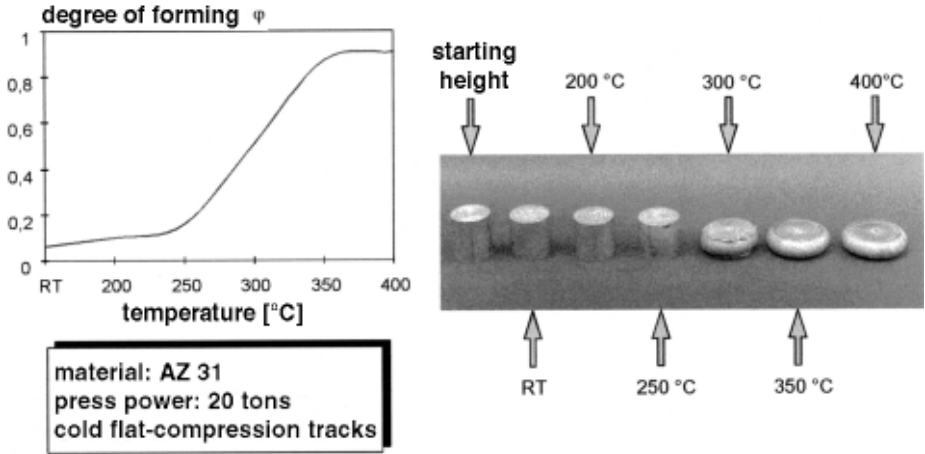


Figure 22: Deformation behaviour of conventional MgAlZn alloys

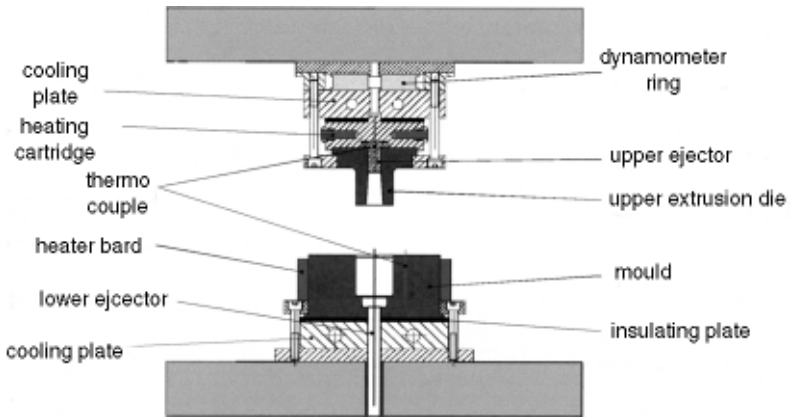


Figure 23: Heatable tool for forging

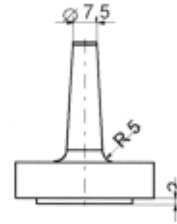
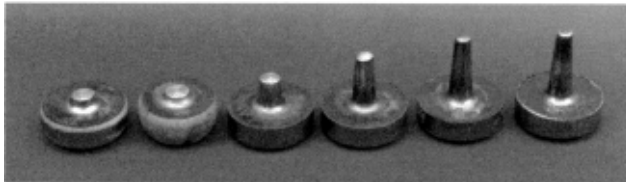
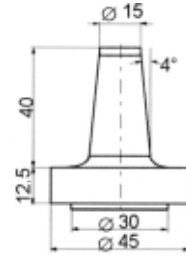


Figure 24: Mould filling

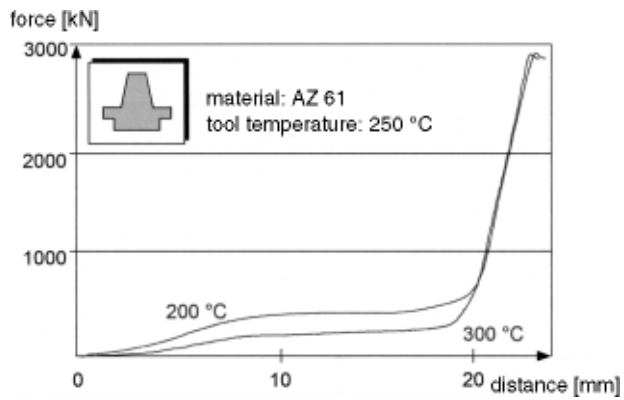


Figure 25: Force elongation diagram when forging AZ61

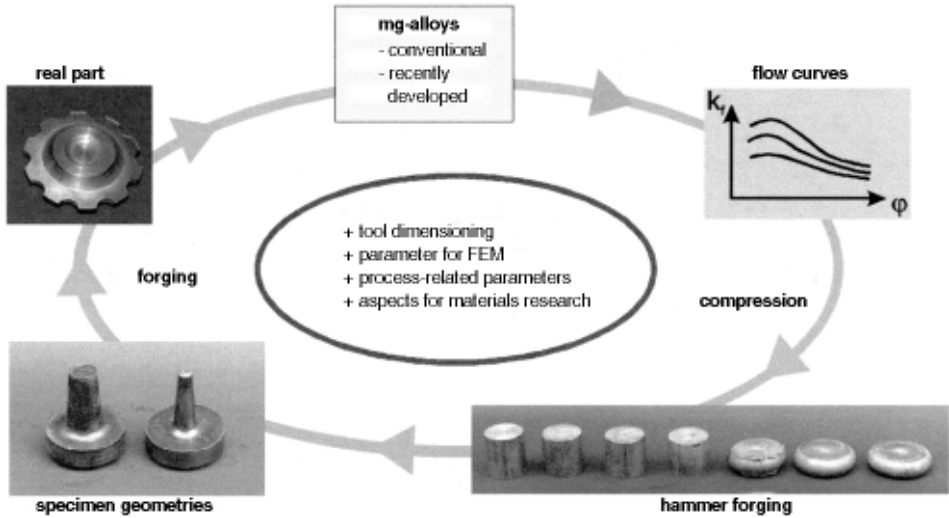


Figure 26: Assessment of the feasibility of the mass forming of magnesium wrought alloys

## 5.5 Summary

Research has proved the good deep drawing abilities of magnesium fine sheets with suitable process management. The temperature is a crucial parameter for the deformation, and hence it is necessary to use tempered tools in order to manufacture components with high draw depths.

Similar results were obtained for hot mass forming. With the developed heatable tool, used either in a hydraulic or mechanical press, it is possible to obtain optimized process parameters for precision forging. This is valid for both conventional alloys and magnesium alloys produced by powder metallurgy.

## 5.6 Outlook

The demands for lightweight construction, mass reduction, low energy consumption, and cost-effectiveness constantly have to be balanced with the handling and costs of alternative materials and material combinations, especially in the automotive industry. These demands have led to an extension of the manufacturing technology and the application of a variety of light metal alloys. Today, relevant knowledge is mainly based on experiments and experience. The aim of further research is to reach a scientific basis for process parameters instead. Additional studies of fundamental aspects of the material and the deformation process are aimed at extending the range of applications of magnesium alloys.



## 5.7 Literature

- /1/ Barnes, L.T.: Rolled Mg products – What goes around, comes around, Proc. of the 49th. Annual World Magnesium Conference, Chicago, USA, Mai 1993, Vol. 2, p. 29-43.
- /2/ Böndel, B.: Magnesium im Automobilbau, Ingenieur-Werkstoffe 4 (1992) 1/2, p. 60-61
- /3/ Gonia, D.: Präzises Verfahren liefert präzise Teile, Industrie-Anzeiger 73/1991, p. 19-22
- /4/ Kehler, H.; Bode, R.; Haddenhorst H.: Partikelverstärkte Leichtmetalle, Metall, 49 (1995) 3, p. 191-195
- /5/ Busk, R.S.: Magnesium Products Design, (Mechanical engineering 53) 1986, S. 123-149
- /6/ Papke, M.: Pulver- und Präzisionsschmieden von Superleichtlegierungen auf Magnesium Lithium-Basis Fortschrittsberichte VDI, Reihe 2: Fertigungstechnik Nr. 404; 1996
- /7/ N.N.: Forging of Magnesium Alloys, Metals Handbook, Ninth Edition, 4/1988, p. 260-261
- /8/ Solberg, J.K. et al.: Superplasticity in magnesium alloy AZ91, Materials Science and Engineering, A134, 1991
- /9/ Yang, H.S. et al.: High temperature deformation of a magnesium alloy with controlled grain structures, Materials Science and Engineering, A158, 1992
- /10/ Spittel, T., Spittel, M.: Mathematische Modellierung verfahrensunabhängiger Kenngrößen der Umformtechnik, Neue Hütte, 34. Jahrgang, Heft 1, Januar 1989
- /11/ Fabricating Magnesium, The DOW Chemical Company, 1984
- /12/ Ullmann: Magnesium and Magnesium Alloys, Ullmann's Encyclopedias of industrial chemistry, Reprint of articles from the fifth edition, VCH Verlagsgesellschaft mbH, Weinheim, 1990, p. 559-593
- /13/ Siebel, G.: Technology of Magnesium and its Alloys (Ed. Beck), Hughes, London, 1940
- /14/ Roberts, C.S.: Magnesium and its Alloys, Wiley, New York, 1960
- /15/ Raynor, G.V.: The Physical Metallurgy of Magnesium and Its Alloys, Pergamon Press, London, 1959
- /16/ Chapman, J.A.: Ph.D. Thesis, University of Birmingham, 1963
- /17/ Hauser, F.E.; Landon, P.R.; Dorn, J.E.: Trans. ASM, 1958, p. 50
- /18/ Chaudhuri, A.R.; Chang, H.C.; Grant, N.J.: Trans. AIME, 1955, p. 201
- /19/ Barnes, W.A. Barnes, L.T.: The Potential of Cast and Wrought Magnesium – Components Working Together in Automotive Applications Proceedings, 51st Annual World Conference, International Magnesium Association, 1994
- /20/ Polmear, I.J.: Physical Metallurgy of Magnesium Alloys; Department of Materials Engineering, Monash University, Melbourne, Australia
- /21/ Doege, E.; Dröder, K.: Processing of Magnesium Sheet Metals by Deep Drawing and Stretch Forming Matériaux & Techniques, No 7-8, 1997, p. 19-23
- /22/ Doege, E.; Dröder, K.; Janssen, St.: Umformen von Magnesiumwerkstoffen DGM-Fortbildungsseminar „Magnesium und seine Anwendung“, Clausthal-Zellerfeld, 28.-30.10.1998
- /23/ Doege, E.; Dröder, K.; Janssen, St.: Leichtbau mit Magnesiumknetlegierungen – Blechumformung und Präzisionsschmieden technischer Mg-Legierungen wt Werkstattstechnik, 11/12 1998, p. 465-468

# 6 Manufacturing and Potential of Extruded and Forged Magnesium Products

J. Becker, G. Fischer, OTTO FUCHS Metallwerke, Meinerzhagen

## 6.1 Introduction

Magnesium has been utilized in special application fields, such as aerospace, machinery, engineering, and automobile industries for decades [1]. The technical use of magnesium has a history of more than 70 years [2]. Despite this, the quantity of magnesium used is still behind that of other metallic materials such as steel and aluminium.

Recent goals for lightweight solutions of the automobile producers have revived the interest in magnesium [3]. Consequently, the development and application of magnesium materials has increased. Some manufacturers have already changed the production of components such as cylinder-head covers, gear housings, dashboard frames, and steering wheels from aluminium or steel to magnesium. Most components are die-cast, since this process takes most advantage of magnesium's good castability. Parts made by other production methods are used very rarely in automobiles. Possible reasons may be:

- the higher costs of the wrought semi-product compared to castings,
- insufficient knowledge and experience of the additional potential and security of semi wrought-products.

The latter point is particularly relevant with regard to the proposed use of magnesium wrought parts for applications with a high demand for security or dynamic strength (e.g. crash-relevant components). Wrought magnesium components could be an ideal complement to cast parts. Because of the hot deformation during extrusion and forging, the parts are free from any pores or cavities and at the same time the mechanical properties are

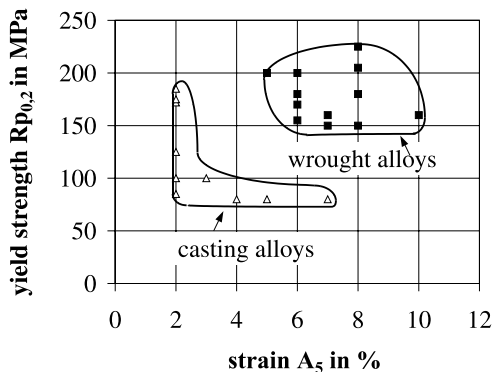


Figure 1: Strength ratio and strain ratio of magnesium wrought alloys and casting alloys. The listed values are the minimum values according to the specification, as measured in the fibre direction.

improved through a thermomechanical treatment leading to an ideal microstructure (Fig. 1). With this in mind, the Otto Fuchs Metallwerke can look back on several decades of experience giving an overview of production, design possibilities, and the potential applications of forged and extruded Mg products. Several examples show the advantages and limitations of magnesium components already used in the automobile industry, aeronautics, and machinery.

## 6.2 Magnesium Wrought Alloys

As for many other metals, only alloying can lead to sufficient strength for construction purposes [1]. Today's magnesium wrought alloys mostly contain the alloying elements aluminium (A), manganese (M), rare earths (E), yttrium (W), zirconium (K), and zinc (Z). Besides increasing the strength, these ensure sufficient hot deformability for forging and extrusion.

The letter code of the elements is followed by numbers, which give their rounded amounts in weight %. This is internationally standardized in the ASTM specification. Table 1 shows common established alloys separated into four main groups according to their alloying elements. The typical features of each alloy determine their application field. An alloy containing only manganese allows high pressing outputs with extrusion, but the low ductility limits the use of Mn-2 alloys and makes them rather minor. AZ alloys, on the other hand, distinguish themselves with high strength and good ductility. The high-purity versions of AZ alloys show the lowest Fe, Ni, and Cu contents and have greatly increased resistance against all types of corrosion. For deformation reasons, AZ alloys are especially suitable for extrusion, as well as for simple forged geometries. Compared to the others, AZ alloys are favoured for use because they are cheaper yet still have good properties.

The ZK alloys have a better hot deformability than AZ alloys and therefore play a more prominent role in the forging of complex parts.

Table 1: Magnesium wrought alloys for extruded and forged products

International indication	Chemical composition	Values from the tensile test $R_{p0.2}/R_m/A_s$ (MPa/MPa/%)	Characteristics
M 2	Mg-2Mn	160/215/4	Extrusion alloy for high performance with good weldability and corrosion resistance
AZ 31	Mg-3Al-1Zn	160/240/10	Extrusion and forging alloy with good strength and ductility; improved corrosion resistance in HP state
AZ 61	Mg-6Al-2Zn	190/270/9	
AZ 80	Mg-8Al-0,5Zn	215/300/8	Superb forging ability
ZK30	Mg-3Zn-0,6Zr	215/300/9	
ZK 60	Mg-6Zn-0,6Zr	235/315/8	Extrusion and forging alloy with good high-temperature strength
WE 43	Mg-4Y-3R.E.-0,5Zr	160/260/6	
WE 54	Mg-5,25Y-3,5R.E.-0,5Zr	180/280/6	

The WE alloys contain rare earths, which make them about ten times more expensive than AZ alloys, but this is justified in applications that require optimal ductility and heat resistance.

Recently, different institutions set their goals for increased research into alloy development, aimed at an improvement of the properties beyond today's limits. This could turn out to be an advantage for extruded and forged magnesium materials.

## 6.3 Raw Material Production for Extrusion and Forging

### 6.3.1 Melting

The alloys are cast from a charge made up of primary and secondary magnesium and pre-alloys. To achieve a low-oxide melt, the metal first undergoes a melt-treatment in the form of an extensive salt-wash. Liquid magnesium has a high affinity towards oxygen and it reacts with most core and mould materials, apart from steel. Therefore, oxidation prevention is required and the melting crucible is made of steel, in contrast to the situation with aluminium (Fig. 2). For a high-purity alloy, the purity of the raw material is irrelevant as any iron is eliminated from the melt by deposition. Fe contents below 0.004 weight % are achieved in this way. Chemical compounds containing carbon are added to melts of the Mg/Al alloy groups in order to obtain a small grain size of the casting [4,5].

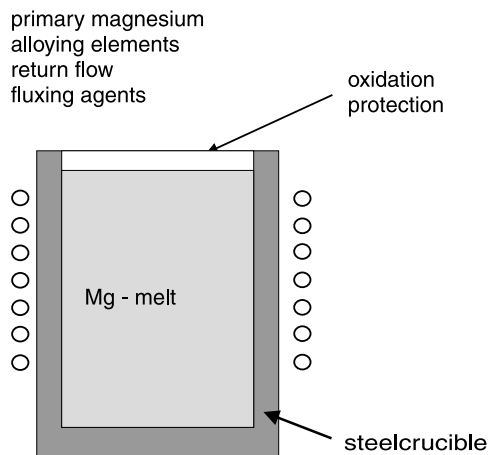


Figure 2: Schematic of the melting

## 6.3.2 Casting

Magnesium alloys are preferably cast using the water-cooled, slab-casting process, just like aluminium alloys. The standard procedures are the floater-nozzle process and the hot-top process. As for the melting, the casting needs an inert gas atmosphere to protect it from air (Fig. 3). The cast slabs are usually homogenized and the surfaces are machined to obtain a favourable deformability before further processing, such as by extrusion or forging [7].

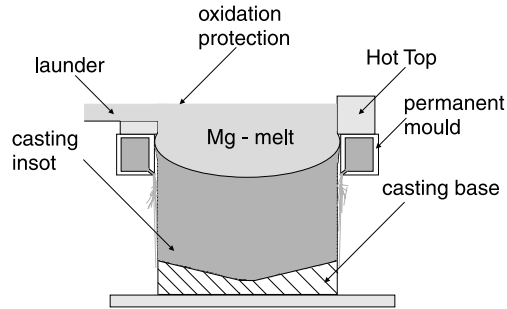


Figure 3: Schematic of the slab-casting process

## 6.4 Extruded Products

### 6.4.1 Production

The procedure for obtaining extruded magnesium wrought material is the same as that used for aluminium materials [8]. The most commonly used industrial process is direct extrusion without a lubricant, as shown in Fig. 4. Cylindrical ingots are heated to 300–400 °C depending on the alloy and pressed through matrices with manifold cross-sections. The maximum extrusion length is 50 m.

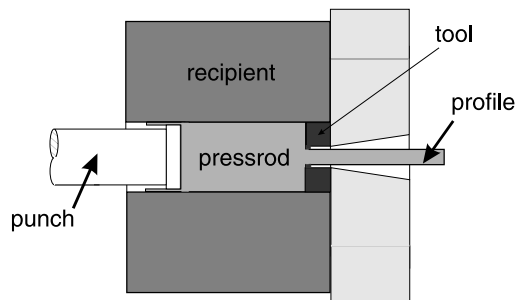


Figure 4: Schematic of the direct extrusion process

This procedure ensures a clean metallic surface and non-porous microstructures that are essential for high-tech materials and safety requirements. The maximum extrusion speed depends on the alloy and determines the price of the profile. The alloys AZ31 and M 2 allow the best extrusion speeds combined with good extrusion behaviour. Increasing alloying element content, as in the alloys AZ80, ZK60, WE43, and WE54, makes extrusion more problematic, resulting in extrusion speeds being ten times slower. For a rational general solution, this aspect needs to be considered when choosing the construction alloy.

The shapes or cross-sections of the magnesium extrusion profiles can be designed with considerable freedom and can be directly matched to their application. For high loads in the subsequent use, the walls are made thicker, whereas additional cavities will reduce the weight for parts not designed for high loads. Extrusion shapes are separated into solid and hollow profiles according to the complexity factors and the cross-sections. Rods and shapes without embedded planes (Fig. 5) belong to the first type, while hollow profiles include one or more completely enclosed cavity or bay region. Due to the required complexity, only AZ31 or M 2 alloys and, with restrictions, AZ61 alloys as well, can be extruded.

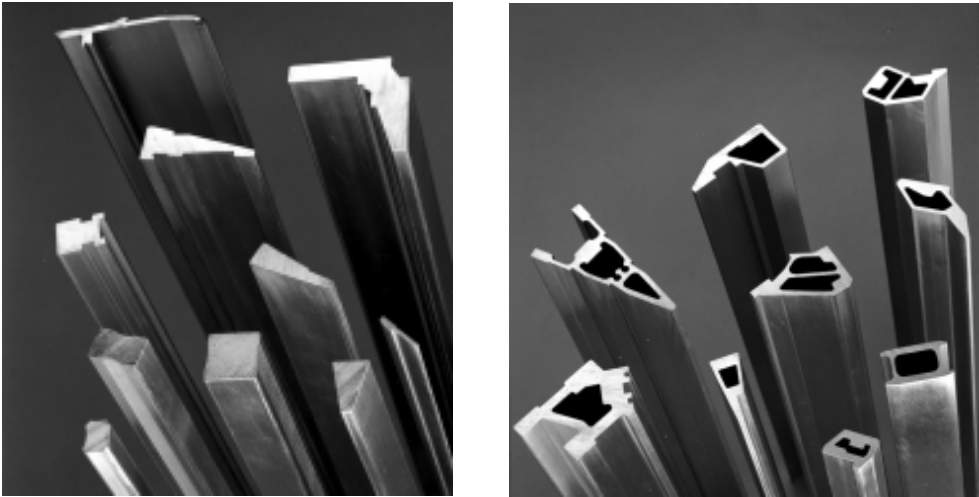


Figure 5: Examples of solid shapes (left) and hollow shapes (right) made of various Mg alloys

The minimum wall thickness is determined by the alloy, the type of profile, and the surrounding circle (Fig. 6). For small to medium-sized AZ31 profiles, the minimum wall thickness is 1.2 mm.

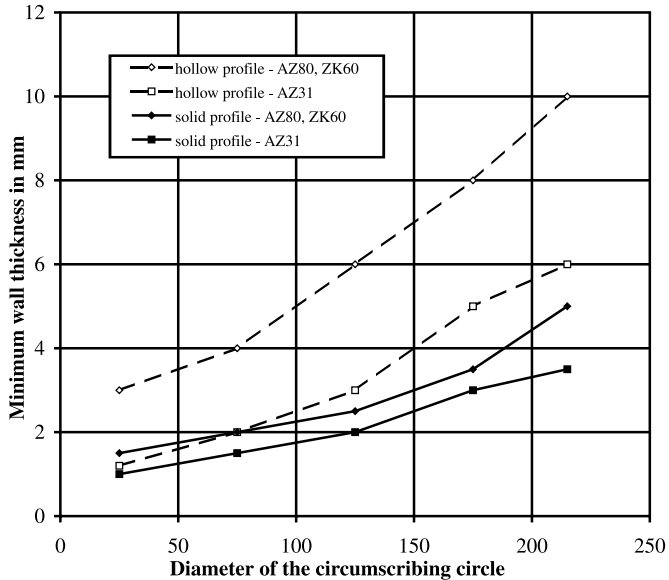


Figure 6: Minimum wall thickness of Mg profiles in terms of type and the alloy used

## 6.4.2 Further Processing

Several steps are necessary before the extruded profile can be used as a constructional component with the intended strength. The further processing includes stretching, heat treatment, sawing, bending, and machining. ZK and WE profiles may be heat treated, whereas AZ profiles already show favourable characteristics [9]. Magnesium has very good machining abilities (sawing, drilling, turning, milling) compared to other metals. The specific cutting power is low, the chips are short, and the surface is excellent. Short cut profile segments for use as levellers or engine housings are simple to build and offer a good alternative to cast components.

Depending on the alloy, magnesium profiles are hard to bend at room temperature. The hexagonal crystal structure limits the cold deformation, but elevated temperatures increase the deformation behaviour significantly [2]. Only AZ31 profiles may be bent with wide radii at ambient temperature; smaller radii and other alloys require higher deformation temperatures. Profiles can be joined among themselves, or with any cast or forged part. The most widely used joining methods are screwing, staking, gluing, MIG welding and TIG welding, as well as laser welding. Since magnesium has a high electron negativity, sufficient insulation is needed.

## 6.4.3 Properties

### 6.4.3.1 Static strength

Table 2 lists values derived from the tensile test of profiles according to the type of load applied and the specimen orientation. The tensile yield strength for profiles in the L-direction is 180 to almost 300 MPa. The yielding in the T-direction and for compression is lower because of the hexagonal structure. These differences are very important for the calculation of the profile's maximum surface pressing and compression load.

Table 2: Values of tensile and compression strengths of extruded Mg wrought-alloy products

alloy	condition	tension (L)			compression (L)	tension (T)		
		$R_{p0.2}$ (MPa)	$R_m$ (MPa)	$A_5$ (%)		$R_{p0.2}$ (D) (MPa)	$R_m$ (MPa)	$A_5$ (%)
M 2	F	180	250	4	110	–	–	–
AZ 31	F	180	250	14	110	110	225	13
AZ 61	F	220	300	12	130	137	294	12
AZ 80	F	240	340	10	145	170	323	11
ZK 30	T 6	240	290	14	190	220	280	16
ZK 60	T 6	280	320	12	230	250	310	14
WE 43	T 6	170	260	12	165	165	250	14
WE 54	T 6	190	280	10	180	185	275	13

The WE alloys have an almost constant strength between room temperature and 250 °C and a high creep resistance. This makes them suitable for applications at higher temperatures (Figs. 7 and 8). The low-temperature behaviour of magnesium is good as well; in contrast to carbon steels, there is no brittle fracture down to –200 °C.



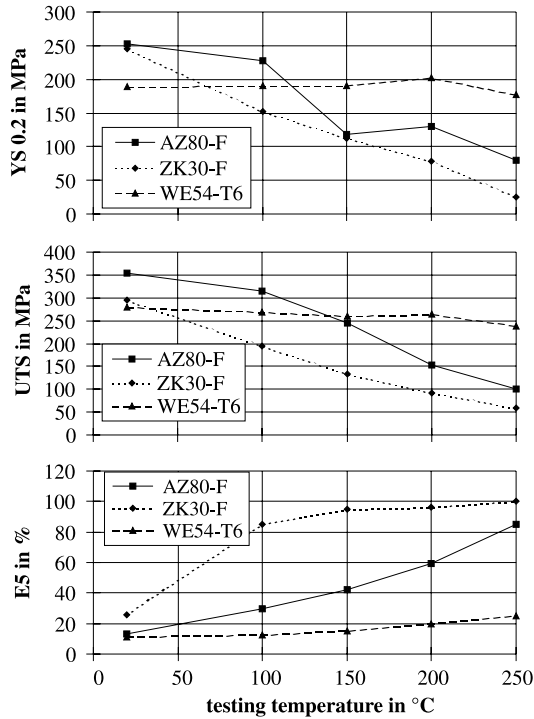


Figure 7: Tensile test results (elevated temperature) of extruded rods made of AZ, ZK, and WE alloys

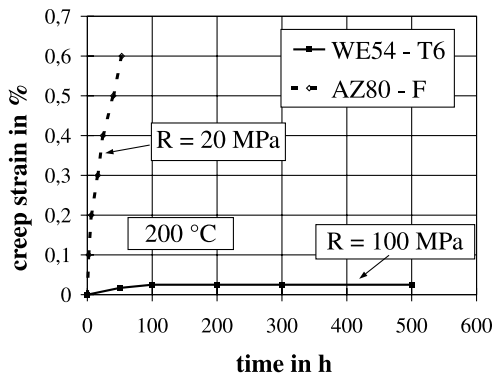


Figure 8: Creep behaviour of extruded rods made of WE54 T6 and AZ80-F

### 6.4.3.2 Toughness

The fracture toughness is a measure of a material's resistance against notches. Table 3 shows the fracture toughnesses of flat bars made of the alloys AZ80, AZ61, ZK30, and WE54 measured in individual experiments. The wrought alloys of the AZ group in F-condition show the best values, which are still below the values of the cured 6082-T6 and 7075-T6 aluminium alloys. In cured condition, the Mg alloys AZ80-T6, ZK30-T6, and WE54-T6 also attain acceptable values. Thus, in contrast to aluminium materials, magnesium components show favourable behaviour in case of cracks or defects.

Table 3: Fracture toughnesses of extruded flat rods made of various Mg and Al wrought alloys

alloy	condition	fracture toughness $K_{Ic}$ ( $\text{MPa m}^{1/2}$ )	
		L-T	T-L
AZ 80	F	23	20
AZ 80	T 6	16	14
AZ 61	F	24	20
ZK 30	T 6	16	16
WE 54	T 6	16	17
AA6082	T 6	36	29
AA7075	T 6	29	24

### 6.4.3.3 Dynamic strength

The following results, obtained from a rotating bending test using extruded rods, give an overview of the load-carrying capability of magnesium wrought alloys.

The fatigue limits of AZ80 (F and T6 conditions), ZK60, and WE54 (both T6) are comparable to that of the medium-strength AA 6082 aluminium alloy (T6).

Table 4: Fatigue strengths of extruded flat rods made of various Mg wrought-alloys and one Al wrought-alloy

$R = -1, k_f = 1$	AZ 80 - F	AZ 80 - T6	ZK 60 - T6	WE 54 - T6	AA6082 - T6
fracture strength at $5 \times 10^7$ load cycles (MPa)	145	145	140	160	150

### 6.4.4 Application Examples

Magnesium profiles offer great potential in a variety of application fields:

- fast-moving components with changing direction for computer hardware, textile printing, and boxing machines

- structural profiles for aircraft and space applications
- unit housings for the automotive industry, aircraft construction, and the military sector
- frames for suitcases and luggage cases

The good prospects are not only envisaged for stand-alone Mg profiles, but also for their use in a whole system together with weldable cast or forged parts, e.g. car body frames. If this concept is successful in the early research programs, the use of magnesium profiles will surely increase.

## 6.5 Forging Magnesium

In security related fields in particular, forged magnesium components have a number of advantages compared to the commonly used die-cast parts:

- excellent static and dynamic strengths, especially with the fibres lying parallel to the main load direction
- very good properties for pressure-sealed components because of a forging process that prevents a porous microstructure

### 6.5.1 Alloys and Basics

Only alloys with sufficient deformability can be used for forging magnesium semi-products. Adequate forging of the hexagonal crystal structured magnesium is only possible for a fine-grained microstructure. Among casting alloys, only the ZK and WE alloys meet the requirements, with Zr or rare earth phases that result in a fine-grained microstructure. This is only reproducible with special melting and casting techniques. These techniques make the components very expensive, and therefore ZK and WE alloys are reserved for special applications only.

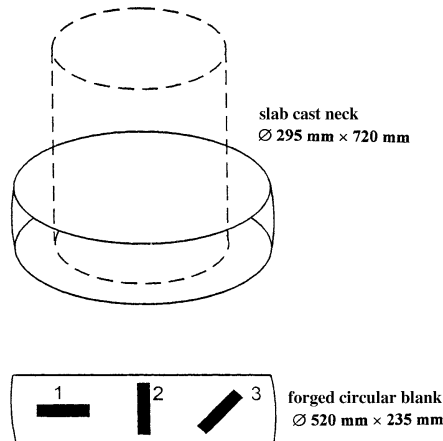
Despite grain refining during casting, a sufficient grain size for AZ alloys cannot be achieved with current methods. Another problem for forging is their multi-phase microstructure. However, with an additional extrusion process, a sufficient grain size for forging can be achieved even for these alloys [10]. Relatively low costs compared to the ZK and WE alloys and the much less complex treatment have led to widespread use of forged AZ alloys in small- and medium-sized components. For big forged parts, however, only ZK alloys can be used, since they do not need to be extruded first and are available in rods with greater diameters.

Forged magnesium components are primarily produced on hydraulic presses. These allow a controlled processing of the degree of deformation and the temperature compared to mechanical machines. Hydraulic machines can also hold a certain maximum load, which is beneficial for the squeezing of complex engravements.

Complex component geometries are usually produced in several forging steps.

## 6.5.2 Forged Components and their Properties

Magnesium parts forged in the direction of one axis show a higher tensile strength parallel to the flow direction compared to other orientations (Fig. 9). The reason for this is the hexagonal crystal structure, but this can be an advantage, e.g. for a radial compressor wheel. However, components loaded in equal directions show an anisotropic behaviour. It can be eliminated by cubic forging (Fig. 10), whereby the strength becomes almost isotropic and adequate for a multi-axle load.



orientation	yield strength Rp 0,02 [MPa]			yield strength Rp 0,2 [MPa]			strength Rm [MPa]		
	1	2	3	1	2	3	1	2	3
tension	94	85	58	181	140	117	230	160	185
compression	71	104	63	118	203	108	416	398	352
both	0,75	1,25	1,2	0,65	1,45	0,9	1,8	2,5	1,9

Figure 9: Dependence of the tensile and compression strength on the crystallographic orientation. Uniaxially compressed MgAl8Zn (AZ80) circular blank according to [4]

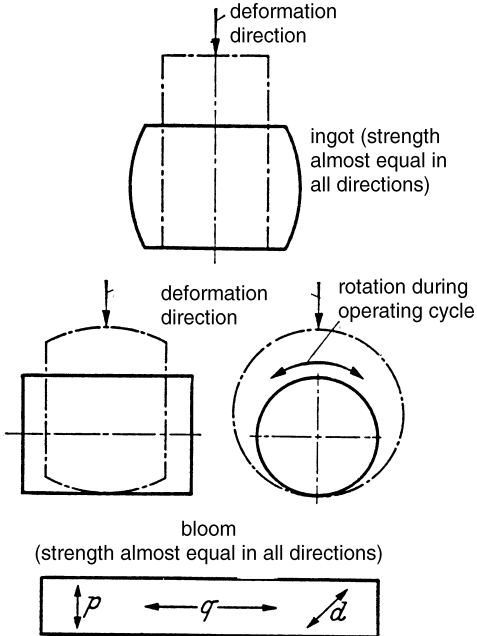


Figure 10: Three-axial dispersing (shown schematically) to avoid directional properties [2]

Figures 11, 12, and 13 show typical forged magnesium parts already used in helicopters and a racing engine. These parts are charged with extraordinary static and dynamic loads. Additionally, the racing engine is exposed to high temperatures.



Figure 11: Drop-forged component for a helicopter (ZK30-T6, Ø 700 mm)

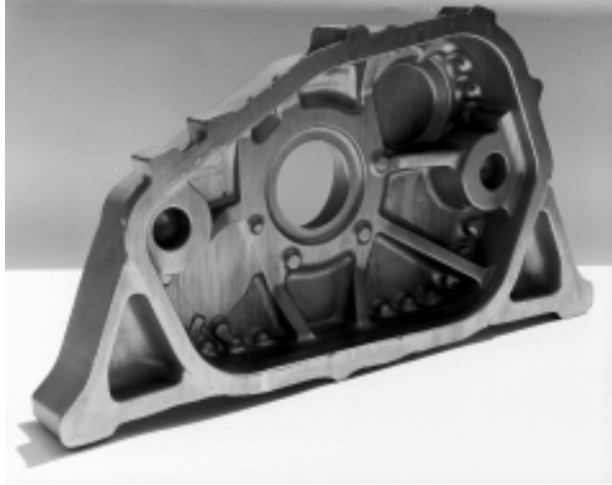


Figure 12: Drop-forged gearbox cover for a helicopter (ZK60-T6, 1020 × 445 mm, 44 kg)



Figure 13: VANOS housing of WE43-T5 (200 × 80 mm)

The forged magnesium wheel in Fig. 14 is another example of a component that requires much safety and performance.

The wheel was produced as a prototype at Otto Fuchs using a forgeable ZK30 alloy and the same tools as used for an aluminium wheel of identical structure that is already available in the market [11]. It weighs 6.8 kg, which is 35% less than the aluminium version. The strength is fairly isotropic since the deformation steps were uniaxial; the strain on all parts of the wheel was found to be between 12 and 14% (Table 5).



Figure 14: Prototype of a magnesium forged wheel (ZK30), produced on the basis of the corresponding aluminium part, which is already in series production for the Audi A8 (wheel size: 8Jx17)

Table 5: Strength properties of the magnesium wheel (ZK30)

Extraction point of the specimen	Orientation	Yield strength $R_p 0.2$ [MPa]	Tensile strength $R_m$ [MPa]	Elongation at fracture, $A$ [%]
rim	axial	248	302	13,7
	tangential	196	266	12,3
spoke/dish	axial	157	260	14,9
	tangential	203	265	12,3

To assess the fatigue strength, the wheel was tested on a rotating bending machine. The durability was found to be 8.5% of that of the corresponding AlMgSi1 wheel with equal cut-off criteria (Fig. 6).

Table 6: Results of the rotation-bending test for the forged magnesium and aluminium wheels (same design)

	forged magnesium wheel alloy: MgZn3Zr (ZK30)	forged aluminium wheel alloy: AlMgSi1 (AA6082-T6)
wheel weight	6,8 kg	10,5 kg
hardness	66,6 HRB	78 HRB
testing moment	3.000 Nm	3.000 Nm
load cycles	84.000	1.064.000

To attain the required durability through adjusting the specifications of the wheel, FEM methods were used to calculate the required increase in the wall thickness. In this way, using the same design, the weight saving dropped to 10–15% compared to the Al wheel.

Figure 7 shows a summary of the properties of forged Mg wheels in comparison to other wheel concepts.

Table 7: Characteristics of forged magnesium wheels (ZK30/ZK60) compared to other concepts

Properties of forged magnesium wheels
compared to cast magnesium wheels + 5–10% weight saving (identical design assumed) + better abusing behaviour due to higher strength and toughness + pressure-tightness because of a non-porous microstructure without cavities – higher costs
compared to aluminium forged wheels + 10–15% weight saving (identical design assumed) – worse abusing behaviour due to lower strength and toughness – marked tendency towards contact corrosion – lower surface pressure and different friction coefficient – much higher costs

## 6.6 Conclusion

The presented examples prove that it is possible to produce complex parts by forging.

Even though the potential for Mg parts seems to be high, short- and medium-term applications will be limited to specific cases. The main reason for this is the high price of alloys that can be forged. Future alloy development will hopefully yield reasonably priced alloys having the same properties. With higher batch sizes, the potential for price reduction will then surely become a reality.

The situation for the extrusion of material is much better. Very complex hollow and solid profiles can be manufactured, which contribute to lightweight construction due to their favourable combination of properties. Another advantage is the possibility of using the much cheaper standard wrought alloys, and so an increasing number of applications can be expected in the near future.

The most important factor for the future of both deformation processes is a close cooperation between producers and customers to determine the components' specifications and to guarantee a design appropriate for magnesium in an early stage of development. Only in this way the specific advantages of these materials can be fully exploited and the high price justified.

## 6.7 Literature

- /1/ Emley, E.F., Principles of Magnesium Technology, Pergamon Press, New York 1966
- /2/ Beck, A., Magnesium und seine Legierungen, Springer-Verlag, Berlin 1939
- /3/ Mordike, B.L., Kainer K.U., Magnesium Alloys and their Applications, Proc. of the Int. Conference in Wolfsburg, DGM, 1998
- /4/ Brit. Patent 606 948



- /5/ Brit. Patent 608 941/2
- /6/ Büschen W., Oxidationsschutz bei Al- und Mg-Formguss durch Schutzgase, Gießerei 77 (1990), p. 581-587
- /7/ B. Kittilsen, P. Pinfield, Magnesium Extrusion – Recent Developments, DGM-Tagung, 1992, Proc. p. 85-92
- /8/ Laue, K., Stenger, H., Strangpressen, Aluminium-Verlag GmbH, Düsseldorf 1976
- /9/ Rosenkranz, W., Ein Vergleich der Eigenschaften verschiedener hochfester Magnesiumknetlegierungen, Metall 9 (1959) 824-830
- /10/ Rosenkranz, W., Das Schmieden und Gesenkpressen von Magnesiumlegierungen vom Mg-Al-Zn-Typ, Z. Metallkunde 47 (1956) 107-117
- /11/ Schemme, K., Lowak, H., Manufacturing of Light Weight Wheels by Forging and Flow-Forming, in: H.-D. Kunze (ed.), Competitive Advantages by Near-Net-Shape Manufacturing, DGM-Informationsgesellschaft mbH, Frankfurt/Main 1997, 115-120

# 7 High-Temperature Properties of Magnesium Alloys

*F. von Buch, B. L. Mordike*

*Institute for Materials Research and Technology, Technical University of Clausthal*

## 7.1 Introduction

The increasing use of magnesium alloys, especially in the automotive industry, will reach a limit when the currently available alloys can no longer meet the projected properties. For this reason, efforts in alloy development have been growing in recent years. The aim is to obtain alloys with improved ductility, corrosion resistance, and hot working abilities, which also includes creep resistance.

This chapter gives an overview of the reasons why conventional alloys can only be used to a certain extent at higher temperatures, and speculates on solutions for improving the creep resistance of existing alloys. A short introduction to the relevant basic aspects of material science is mandatory for an understanding of this.

## 7.2 Phenomenological Description of Creep

Creep is defined as the time-dependent plastic deformation of a material under constant mechanical load (and at higher temperature). The result of measurements with creep testing machines (a typical set-up is given in Fig. 1) is the creeping curve  $\epsilon(t)$ . Usually,  $\epsilon(t)$  describes the strain as a function of time at a constant temperature and load (Fig. 2). The derivative of the (true) strain with respect to time gives the creep rate  $\dot{\epsilon}$ , which is dependent on the stress, the temperature  $T$ , and the time  $t$ , i.e. the strain  $\epsilon$  reached after a certain time  $t$ .

If the creep rate is plotted against time for higher temperatures, it becomes obvious that for sufficiently high temperatures (for pure metals, the following is valid:  $T > 0.4 T_m$  in Kelvin, which is approximately 100 °C for Mg), the creeping speed can be separated into three stages, the primary (or sliding), secondary (or “steady-state”), and tertiary (or accelerated) creep. On applying a load, the creep rate first decreases (i.e. with  $\ddot{\epsilon} < 0$ ) in the primary stage, and then becomes a constant deformation speed in the secondary stage ( $\ddot{\epsilon} = 0$ ,  $\dot{\epsilon} = \dot{\epsilon}_s$ , secondary (steady-state) creep rate). The following tertiary stage ( $\ddot{\epsilon} > 0$ ) ends with the failure of the material (Fig. 4).

The material becomes increasingly strain-hardened in the primary stage, and thus the deformation speed steadily decreases. In the secondary stage, the deformation speed reaches a constant value, which is indicative of an equilibrium between strengthening and softening mechanisms in the material.

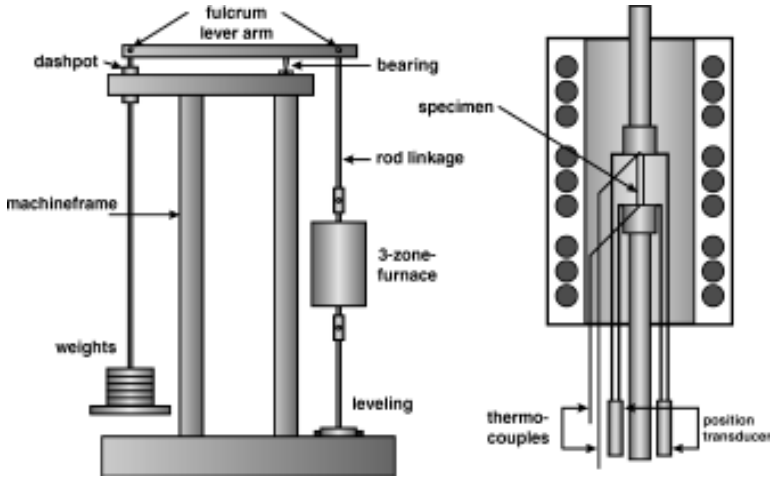


Figure 1: Typical test arrangement for the recording of creep curves

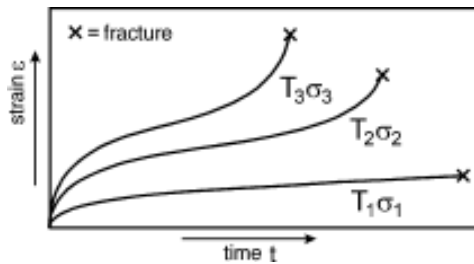


Figure 2: Ideal creep curve of a material effected by the stress  $s$  and temperature  $T$  ( $\sigma_3 > \sigma_2 > \sigma_1$ ;  $T_3 > T_2 > T_1$ )

The tertiary stage, characterized by a dominant contribution from softening mechanisms until fracture occurs (e.g. because of mechanical instabilities such as necking, microstructural instabilities such as grain growth, recrystallization, and ageing, or the forming and growing of cracks) is reached after passing through the steady-state deformation. The strain in this area increases exponentially with time. The different failure mechanisms are listed in [83Ash]. For a wide range of temperatures and stresses, the major part of the deformation occurs in the secondary (“steady-state”) stage, in which the deformation speed remains constant.

This stage is the technically most important one, and hence some further information about secondary creep is given below.

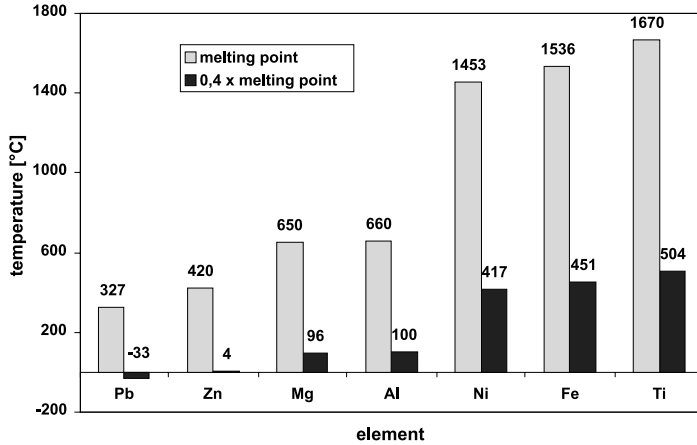


Figure 3: Relationship between the melting temperature  $T_m$  and  $0.4 T_m$  in K for different pure metals

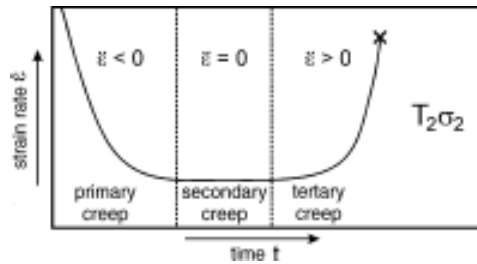


Figure 4: Derivation of the creep curve for  $T_2, s_2$ , taken from Fig. 1, after time  $t$ ; primary, secondary, and tertiary creep

### 7.2.1 Temperature-Sensitivity of the Secondary Creep

If it is assumed that the influences of temperature and stress on the secondary creep rate are mutually independent, experiments concerned with the dependence of the secondary creep rate on the temperature have proven that it can be described in a similar manner to oxidation and diffusion procedures, using an Arrhenius approach:

$$\dot{\epsilon}_s \sim \exp(-Q_c/RT) \tag{7-1}$$

with:

$\dot{\epsilon}_s$  = secondary creep rate

$Q_c$  = activation energy for creep

R = general gas constant

This approach towards the analysis of creep of pure metals at higher temperatures has shown that the activation energy for creep,  $Q_c$ , for a given material is different for each creep mechanism.  $Q_c$  can be viewed as a measure of the speeds determining the diffusion processes. Additionally, the temperature dependence is determined by the Young's modulus and the stacking fault energy.

## 7.2.2 Stress Dependence of the Secondary Creep Rate

For the relationship between the stress and the secondary creep rate of many metals and alloys, a similar description called "Norton's Law" is used:

$$\dot{\epsilon}_s \sim s^n \quad (7-2)$$

with:  $n$  = stress exponent

This expression is the basis for considering the "power-law creep", which is often used to describe high-temperature creep and has proved its utility through many explanations of experimental results. The values of the stress exponent  $n$  vary with changing creep mechanism and other factors. The value of  $n$  can be seen as an indicator of atomic-scale creep.

The combination of both dependences led to the following approach, which is capable of describing real creep processes:

$$\dot{\epsilon}_s = A s^n \exp(-Q_c/RT) \quad (7-3)$$

with:  $A$  = a constant

## 7.2.3 Creep Mechanisms

For creep, three basic mechanisms are relevant:

- diffusion creep
- dislocation creep
- grain boundary gliding

Diffusion creep is usually of no interest with regard to the technical application of magnesium materials, since the stresses in the components are too high. However, dislocation creep and grain boundary gliding have a fundamental significance.

Grain boundary gliding is based upon elixation of the grain boundaries at high temperatures. It can either result from a low heat resistance of the boundary phase and a disturbed lattice close to the boundary area, or from complex and local solution/precipitation processes and dislocation responses. During grain boundary gliding, the grains glide over each other without undergoing any marked deformation (not mentioning geometrical necessities). Grain boundary gliding seems to be the main reason for the low creep resistance of aluminium-containing magnesium die-casting alloys.

Dislocations carry the plastic deformation through the material and cause a deformation of the whole sample. Dislocation creep is based on this effect, which leads to hardening at low temperatures because the dislocations dam in front of material barriers (precipitations, grain boundaries, other dislocations, etc.). At higher temperatures, the dislocations can bypass these barriers. Besides the so-called cross-slip, the main mechanism for by-passing is the heat-activated "climbing" of dislocations, which is close to diffusion processes. For this reason, the creep rate depends not only on temperature and stress, but also on material-specific properties, especially the Young's modulus (which seems to be the main reason for

aluminium having a much higher creep resistance than magnesium), the diffusion coefficient, and the stacking fault energy. While alloying cannot change the Young's modulus, the other two parameters may be greatly influenced. Besides, alloying elements (as solid solutions or precipitations) can interact with moving dislocations and the resulting effects may be efficiently used to prevent dislocation creep (Section 7.2.4).

## 7.2.4 Options for a Reduced Creep Rate

Apart from making reinforced materials and composites, the main options available for reducing the creep rate in metals are precipitation and solid-solution crystal formation. In alloy development, the main focus lies in adding elements to the melt that induce solid-solution formation or precipitations. Solid solutions thus formed may have the following advantages:

- a positive influence on the melting- and solidus temperature, as well as on the interdiffusion coefficient
- reduction of the dislocation mobility since gliding is impeded
- lowering the stacking fault energy and stabilizing stacking faults by introducing impurity atoms limits cross-slip

Precipitations within a grain and/or on the grain boundaries are another way of improving creep resistance. In this way, the dislocation movement is complicated and grain boundary gliding is minimized. Dislocations, on the other hand, have no influence on diffusion creep. The precipitations need to fulfil the following requirements for an optimized effect:

- The distribution of the precipitations must be sufficiently dense that they cannot be avoided. This is possible for precipitations that contain a major constituent of the matrix, because even low concentrations of the element will allow a high volume fraction of precipitations.
- The precipitations must be stable at high temperatures. The melting points of the intermetallic phases and the binding enthalpies give first indications in this regard. Another possibility is sequential precipitation, which means that new precipitations are formed as soon as the first breaks down.
- The precipitations should be coherent with low interfacial energy and their components should only diffuse to a small extent within the matrix. In this way, obsolescence of the precipitations ("Oswald maturation") is complicated and is shifted to longer times and higher temperatures.

In this regard, as long as suitable alloying elements are used, precipitation hardening is superior to solid-solution hardening because the effect of the latter is reduced with increasing temperature. The best solution is a combination of both effects, i.e. a high density of heat-stable and uncuttable precipitations and a solid solution that results in an increased liquidus temperature, a stabilization of stacking faults, and a limited diffusion.

The following statements may be made regarding the effect of precipitations and dispersoids as a barrier to the movements of dislocations:

- the creep rate is lowered by several orders of magnitude
- the finer the dispersion, the greater the creep resistance
- primary creep is less dominant

- the creep ductility is lower and the steady-state stage is shorter
- the stress exponent  $n$  and the activation energy  $Q_c$  may have higher values

Both the thermal stability of the particles and the strength play an important role, and thus another time-dependent factor is added to the creep process. The most important factors with regard to softening are:

- insufficient strength of the particles at higher temperatures
- a change in size and orientation of the strengthening particles (e.g. Oswald maturation)
- loss of metastable phases at the expense of the equilibrium phase.

The particle-hardening is very complex, hard to evaluate, and hard to describe in theory. During the creep test, the precipitation structure may change or become renewed through the induction of stress. The load, structure, coherence, and volume fraction are also relevant. Other indirect influences include stabilization of the dislocation orientations, the fixing of sub-grain boundaries (recovery processes are limited), and stabilization of the grain boundaries. These effects make the process even more complex. Precipitations at the boundaries can either slow down or speed up grain boundary gliding. In cases where the precipitations form a continuous seam at the grain boundaries, with low strength and high viscosity, an accelerated creep rate will result. Strong and thermally stable precipitations that remain at the boundaries will largely prevent grain boundary gliding and hence the creep resistance will increase.

## 7.3 High-Temperature Properties of Pure Magnesium

### 7.3.1 Deformation by Crystallographic Gliding

The only deformation mechanism for pure magnesium at low temperatures is a dislocation movement of the closest-packed basal planes (0001) in two linearly independent directions  $\langle 11\text{-}20 \rangle$ . The ability of polycrystalline materials to undergo plastic deformation is given by the “von Mises criterion”, whereby five independent gliding systems need to be activated in each crystal to perform any possible deformation without cracking at the grain boundaries. Lacking three systems, magnesium is very hard to deform at ambient temperatures. Therefore, other gliding systems, especially twinning, become very important [84Hul].

At higher temperatures, however, the arrangement of close-packed planes is no longer rigorously maintained, and three additional gliding systems become active, the simple prismatic and pyramidal gliding, as well as the  $\langle c+a \rangle$  pyramidal gliding. Through these additional systems, cross-slip during creep becomes possible and barriers cannot only be climbed but also passed by this means. This is the main reason for magnesium’s fairly low high-temperature strength. The temperature required for the activation of the supporting gliding systems partly depends on the alloying elements present and on the grain size. This temperature lies between 200 and 250 °C for most conventional magnesium alloys; for pure magnesium, 225 °C is necessary [69Eml]. Beyond this temperature, deformation processes, such as rolling or extrusion, are possible in principle. Lithium, for example, makes prismatic gliding possible at room temperature, and therefore alloys with Li have a high ductility [96Nei].

### 7.3.2 Deformation by Twinning

Besides crystallographic gliding, twinning is another possible means of plastic deformation in magnesium. At “normal” temperatures, twinning occurs on the pyramidal  $\{10\text{-}12\}$  planes [69Eml]. Twinning is only possible under compression stresses applied parallel or tension applied perpendicular to these planes because the  $c/a$  ratio is slightly smaller than the ideal value. This explains why textured magnesium components (e.g. extrusions) show differences in yielding for tension and compression. In [69Eml], further types of twinning are discussed, but these are of little importance for plastic deformation. Twinning is a thermal shear process and has little influence on high-temperature deformation, but a certain contribution towards primary creep cannot be neglected.

### 7.3.3 Creep Behaviour of Pure Magnesium

The most important research papers on the creep behaviour of pure magnesium (most notably [61Teg], [66Gib], and [72Cro]) published to date have been gathered in [82Fro] and a “deformation map” for pure Mg has been established (Fig. 5). The data were not only critically evaluated, but different statements were compiled. In deformation maps, areas of different creep mechanisms of pure metals, depending on the grain size, stress, and temperature, are plotted. All mechanisms are mutually independent, and the total creep rate is the sum of contributions from all the individual mechanisms. For a better comparison of different materials, the stress is normalized and the homologous temperature is used in the deformation map.

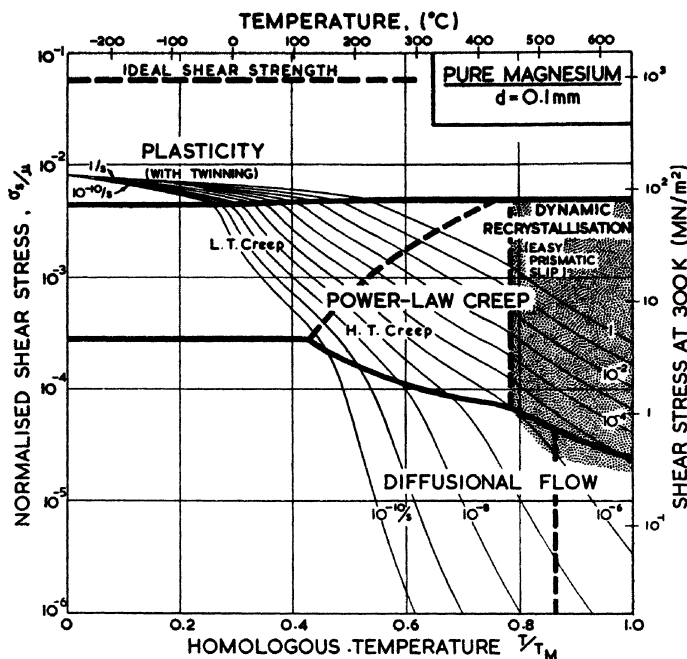


Figure 5: Deformation map for pure magnesium with a grain size of 0.1 mm [82Fro]



The maps are based on steady-state deformation conditions. The grain size is given as the most important criterion. The maps also include lines of equal creep rate. In many cases, the region of elastic deformation is also given. In theory, creep begins at 0 Kelvin, but it can be neglected since the creep rate can hardly be determined up to  $0.4 T_m$ . The idea of extending the maps to three dimensions, as proposed in [81Oik], has not yet been successfully accomplished. Nevertheless, maps for creep fracture already exist for a variety of different materials [79Ash].

The deformation maps can provide the engineer with useful information as to how the creep will behave at different temperatures and stresses. However, the maps are only available for pure magnesium and not for alloys.

## 7.4 High-Temperature Properties of Magnesium Die-Cast Alloys

### 7.4.1 General Issues

The strengthening effect of adding 4 to 9 weight % aluminium to the melt was known as long ago as the 1920s. The die-cast alloys were sold under the name “Elektron” [39Bec]. Aluminium increases the maximum strength and hardness, with the strengthening effect being based on solid-solution formation and an  $Mg_{17}Al_{12}$  phase. Besides improving the mechanical properties, aluminium significantly enhances the castability of magnesium (eutectic system;  $T_E = 437\text{ °C}$  [90Mas]). On the other hand, at high aluminium contents, an interdendritic  $Mg_{17}Al_{12}$  grain boundary phase is formed, which lowers the strength at application temperatures beyond  $120\text{ °C}$  (Fig. 6). This disadvantage has long been known [59Ray]. Moreover, alloys with Al and Zn show only limited ductility.

For this reason, in earlier years attempts were made to reduce the amount of aluminium in the melt and to use different materials for alloying. In the production of the VW-Beetle, the addition of silicon became established [80Höl]. The resulting alloys, AS21 and AS41, exhibit

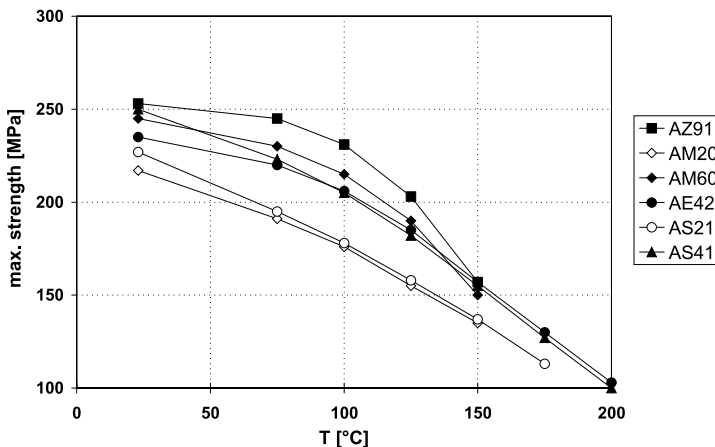


Figure 6: Tensile strength of magnesium die-casting alloys as a function of temperature [96NHM]

a much better high-temperature strength and creep resistance than AZ91. Experiments with Ca were abandoned at an early stage due to casting problems. The mechanism whereby high-temperature and creep behaviour is increased is based on the reduction of the aluminium content and the formation of the intermetallic phase  $Mg_2Si$  ( $T_m = 1085^\circ C$ ), which has a good stability even at high temperatures. This is only valid for stresses that do not cut the precipitations. Above  $120^\circ C$ , AZ91 again becomes more creep-resistant because there is a greater contribution from solid-solution hardening caused by aluminium [97Blu].

In this context, the AE alloys have to be taken into consideration [72Foe] (formation of Al/RE and Mg/RE precipitations [96Pet], perhaps also of  $Mg_{17}Al_{12}$  [96Wei]; no Mg/Sc precipitations as thought in [98Blu] since there is no Sc included), though they can only be produced by die-casting because of the formation of very large, stable Al/RE precipitations on slow cooling. The series of AE alloys, with AE42 being the best alternative, are superior to the AS series in terms of creep resistance [90Mer]. In [77Foe], the following classification of creep resistance for conventional alloys is proposed: AZ91 and AM60 up to  $110^\circ C$ , AS41 up to  $150^\circ C$ , AS21 up to  $175^\circ C$ . The measurements were made with a negligible creep strain of  $<0.1\%$  in 100 h at 35 MPa. The alloy AE42 was not commercially available at that time, but its maximum application temperature is comparable to that of the AS series. It should again be noted that creep is strongly dependent on the stress, and that creep resistance can only be compared under conditions of equal stress. Changing the stress may result in a shift of the application temperature and vice versa. This means that, for real applications, AZ91 could be more creep resistant at low temperatures and high stresses than AE42. The creep resistances of various casting alloys are given in Fig. 7.

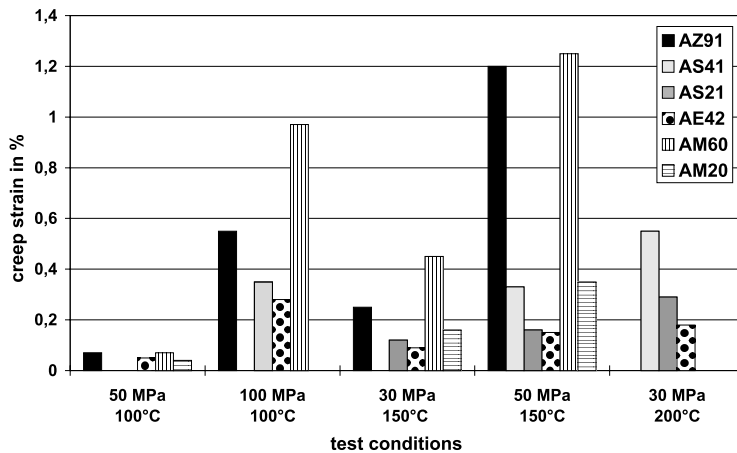


Figure 7: Creep resistances of various casting alloys

## 7.4.2 Overview of the Literature

Magnesium cast components, as mass-produced products with the lowest density, are of great technical importance, first and foremost in the automotive industry. Because strength and creep resistance are often the limiting factors for using magnesium, e.g. in engine-

related parts, much effort has been devoted to the observation of creep behaviour. Earlier research mostly concentrated on the qualitative comparison of different alloys, but during recent years the focus has shifted towards gaining an understanding of the working mechanisms and obtaining basic knowledge to aid in future alloy and process development.

The primary creep of the alloys AZ81, AS41, and AS42 at temperatures in the range 100–150 °C and stresses from 34 to 67 MPa has been thoroughly investigated [76Lö]. The results proved that alloys containing Si are far superior to the AZ alloy. They also showed an activation energy independent of the stress of approximately 37 kJ/mol and a stress exponent of  $n = 2.6$  for all the alloys. This behaviour was rationalized in terms of jumps in non-split screw dislocations representing the speed-determining step. The high  $A$  value of AZ81 was attributed to the high dislocation density around the prevalent  $Mg_{17}Al_{12}$  phase, which appears due to high differences in the Young's moduli. This research was later extended to the alloys AE41 and AE42 [92Aun], again showing their superiority. Subsequent work confirmed the superiority of the AE alloys [97Che]. In [91Sum], it was concluded from experiments on AZ91 and AM60 that below a load spectrum of 100 °C/25 MPa, no heat-activated but only logarithmic creep occurs in these alloys.

The alloy AZ61 in T6 condition has been studied with respect to its inner stresses [76Thr]. At 200 °C, the following stress exponents were observed:  $n = 4$  for  $s < 100$  MPa and  $n = 10$  for  $s > 100$  MPa. Similar results were obtained from studies on AZ91 at room temperature ( $n = 4.6$ ; [91Mil]). Diffusion-controlled dislocation climbing was proposed as the mechanism.

In [91Gje], the influence of extremely small grains on the creep behaviour of AZ91 was investigated. The creep rate of AZ91 RS was shown to be two orders of magnitude higher than that of the corresponding cast alloy. This behaviour was attributed to the very small grain size of 1.5 mm compared to 11.6 mm. The stress exponent of  $n = 2$  is suggestive of grain boundary gliding. Adding Ca to the AZ91 RS alloy resulted in a much improved creep resistance, comparable to that of the cast alloy. Very fine precipitations of  $Al_2Ca$ , which are stable at 150 °C, act as barriers to dislocation movements within the grain and limit grain boundary gliding.

The results of further tests on AZ91 (made by different processes) have been compared with the results of various other authors [97Mor]. From the almost identical  $n$  values, it was concluded that the dislocation movement on the basal plane is the speed-controlling factor, whereas precipitations that cannot be cut are more likely to act as barriers.

In many studies, the weakening effect of the  $Mg_{17}Al_{12}$  phase on the grain boundaries has been invoked as the limiting factor for creep resistance of AZ91. This has been called into question in [97Dar] because weakening is only observed beyond 260 °C, and a heat treatment usually contributes to the creep behaviour in a positive way, even though the amount of the intermetallic phase increases. Based on these experiments, it was assumed that creep resistance is caused by more pore formation in the material (growth of production-induced pores and pore formation on the  $a/b$  boundary surface), which was verified by electron microscopy. Investigations of the microstructure showed that distinctive basal gliding (or twinning at higher temperatures) occurred and that grain boundary gliding was only secondary. This hypothesis is supported by [97Gut] and [97Reg]. In further works [98Dar], the consequences of different structural constituents were demonstrated. Because of the small activation energies ( $Q_c = 30\text{--}45$  kJ/mol) and low stresses, it is assumed that the reason for this is a discontinuous precipitation of the  $\beta$  form in the supersaturated  $\alpha$ -solid solution (with the same activation energy). The precipitation is combined with a (large-angle) grain boundary movement, which supports the grain boundary gliding ( $n = 2$  in this area). The

alloys AS21 and AE42 are more creep-resistant because they not only contain less aluminum, resulting in less precipitations, but  $Mg_2Si$  rather than  $Al_4RE$  precipitations, which also prevent grain boundary gliding. At higher temperatures, the mechanism with the higher  $n$  value, namely the climbing of dislocations, becomes relevant in determining the speed.

Table 1 lists the most important results of the various studies. It can be seen that the values differ considerably between authors. The reason for this might be the different production histories of the specimens, leading to differences in their microstructures. As regards the actual mechanisms, there is no consensus between the authors. Nevertheless, an evaluation of the alloys is possible, and it is clearly evident that the volume fraction and dispersion of the  $Mg_{17}Al_{12}$  precipitations has a tremendous influence on the creep behaviour of the alloys. It is also clear that heat-stable precipitations within the AS and AE alloys positively affect creep resistance.

Table 1: Summary of the results of different authors in terms of creep of Al-containing magnesium alloys; authors statements

alloy	T [°C]	s [MPa]	n	Q [kJ/mol]	mechanism*	source
AE42	150	20-185	16,1	–	2	/97Che/
AE42	150	30-80	2	30-45	5	/98Dar/
AE42	175	20-185	17,6	–	2	/97Che/
AS21	100-150	34-67	2,6	36,9	1	/76Löv/
AS21	150	30-70	2	30-45	5	/98Dar/
AS21	150	70-80	5	94	2	/98Dar/
AS41	100-150	34-67	2,6	36,9	1	/76Löv/
AZ61	200	69-100	4	–	2	/76Thr/
AZ61	200	100-154	10	–	3	/76Thr/
AZ81	100-150	34-67	2,6	36,9	1	/76Löv/
AZ91	25	60-180	4,6	–	2	/91Mil/
AZ91	120-160	40-115	n. a.	190-220	n. a.	/98Reg/
AZ91	150	25-150	5,1	–	2	/97Mor/
AZ91	150	20-185	4,8	–	2	/97Che/
AZ91	150	30-100	6,9	–	2, 4	/97Reg/
AZ91	150	20-40	2	30-45	5	/98Dar/
AZ91	150	50-80	5	94	2	/98Dar/
AZ91	150-250	50	–	103	2	/97Mor/
AZ91	150-250	75	–	92	2	/97Mor/
AZ91	150-250	100	–	139	2	/97Mor/
AZ91	160-180	40-115	n. a.	94-105	n. a.	/98Reg/
AZ91	175	20-185	4,7	–	2	/97Che/
AZ91	180	30-100	5,4	–	2, 4	/97Reg/
AZ91	200	25-150	6,6	–	2	/97Mor/
AZ91	250	25-150	4,0	–	2	/97Mor/

\* mechanism (as given by the authors):

- 1: Formation of non-split dislocations out of dislocation jogs
- 2: diffusion-controlled climbing of dislocations on the base plane
- 3: intersecting/by-passing of dislocation obstacles
- 4: cross slip of dislocations
- 5: grain boundary gliding

## 7.5 High-Temperature Properties of Magnesium/ Rare Earth Alloys

Magnesium alloys containing aluminium lack thermal stability. Therefore, from the early days of alloy development, magnesium alloys were sought that could be applied at temperatures above 150–200 °C. Based on theoretical thoughts about developing creep-resistant alloys, the positive influence of rare earth elements on the high-temperature properties of magnesium was soon established (early summaries appeared in [37Hau], [38Bol], [39Bec], and [49Leo]).

According to their behaviour in binary magnesium alloys, rare earth elements can be divided into two subgroups, the Ce group (La to Eu) and the Y group (Y and Gd to Lu). These two groups differ from each other according to the number of valence electrons (Ce subgroup: 2, Y subgroup: 3), which leads to differences in their interaction with magnesium (“valence effect”). The solubilities of the Ce subgroup elements in solid magnesium are much lower than those of the Y subgroup. During the decay of a supersaturated solid-solution crystal of the Ce group, Guiner–Preston (GP) zones form with almost no incubation time, and turn into semi-ordered or incoherent precipitations [92Pol]. GP zones could not be confirmed in alloys with elements of the Y group; instead, metastable coherent precipitations appear after a certain incubation time [92Pol]. The rare earth elements of the Ce subgroup are the most effective solid-solution hardeners, while Y group elements are better suited for precipitation hardening. For both groups, it holds true that the solubility of the elements in solid magnesium and the stability of the supersaturated solid-solution crystal increase with increasing atomic number (“radius effect”) [98Rok]. With the help of the rare earth elements, solid-solution hardening as well as precipitation hardening is possible; the intermetallic phases have a low diffusion ability and show good coherence towards the matrix [92Pek].

All rare earth elements (including yttrium) form eutectic systems of limited solubility with magnesium. Therefore, advantageous precipitation hardening is possible and the castability is fairly good. The precipitations are very stable and increase the creep resistance, corrosion resistance [96Nei], and high-temperature strength. This is due to heat-stable precipitations on the grain boundaries, which limit grain boundary gliding, and by precipitations within grains, which act as barriers to dislocations. The most widely used technical alloying elements are yttrium and neodymium. Due to the high costs, these elements are mainly used to form solid-solution crystals in high-tech alloys (Ce crystal: 50%Ce/23%La/17%Nd/7%Pr; Nd crystal: 85 weight % Nd; Y crystal: 75 weight % Y [89Uns]).

The properties of different Mg/RE alloys (mostly Mg/Ce) and a comparison of the different rare earth elements were the subject of early studies [49Leo]. It was shown that La, Ce, and Nd improve the properties in the listed order. The influence of cerium has also been described in [54Sau] and [61Gsc]. In small amounts, cerium affects creep resistance in a positive way. At higher levels of cerium, the creep resistance increases but strength decreases. The reason for this is given in [61Gsc]; cerium is a very effective solid-solution hardener, but causes brittleness at higher amounts and failure occurs at the grain boundaries. Besides, cerium has little diffusion ability in magnesium [61Gsc]. In commercial alloys, more Nd solid-solution crystals (“dydimium”) have been applied than Ce crystals. Nd is more effective at improving creep resistance up to 260 °C [77Ray].

The effect of zirconium as a grain refiner was discovered in 1937 [54Sau] and this led to the first heat- and creep-resistant alloys of the EK, EZ, and ZE series (with Nd-rich rare

earth elements) [88Uns]. However, zirconium may only be used with alloys not containing Al, Si, Mn, Ni, or Sb [54Sau]. Thanks to Zr, all technical alloys used nowadays have sufficient strength [88Nai]. Adding zinc to these alloys improves the properties at room temperature. Since Zr and rare earth elements have different effects, ZE alloys have higher strengths but lower creep resistance than the EZ series alloys.

Later, silver was found to have a positive influence on the precipitation behaviour of Mg/RE alloys [59Pay]. The QE series of alloys was then developed, having a further improved creep resistance and high strength at room at higher temperatures, although the use of silver resulted in rather poor corrosion resistance. The QE alloys have a high temperature profile up to 200 °C, almost matching the alloys containing thorium [96Nei]. Thorium has become known as the best element for tremendously improving the high-temperature properties of magnesium. These alloys form precipitations that are very stable up to high temperatures (with Mg<sub>23</sub>Th<sub>6</sub> precipitations at its end, incongruent melting phase;  $T_m = 776$  °C). These precipitations can be induced by means of a specific heat treatment and they raise the recrystallization temperature and mechanically stabilize the grain boundaries [77Ray]. In commercial alloys (e.g. HK31, HM21), the precipitation sequence becomes more difficult with further alloying elements, but this has already been addressed in earlier work [72Str]. The properties of binary Mg/Th alloys are improved up to 4 weight % of thorium, beyond which no further improvements are possible [54Sau]. Since thorium-containing alloys are slightly radioactive, thorium is no longer used as an alloying element and such alloys are not commercially available. This restriction has made it necessary to develop new highly creep-resistant alloys.

The improvement of the Mg/Y phase diagram [61Miz] and first studies of the mechanical properties of binary Mg/Y alloys laid the foundations for further alloy research. Binary Mg/Y alloys have already been proposed as high-strength wrought alloys in [66Lon]. These materials show an extremely high specific strength never before seen for a magnesium alloy. First experiments involving a T6 heat treatment have been undertaken and the anticipated improvements in strength were indeed observed. These studies showed that heat treatments under normal atmosphere are possible, despite some formation of Y<sub>2</sub>O<sub>3</sub>, as was found later [71Wal]. The precipitation sequence, including the metastable and stable phases (e.g. [72Miz]), and the ternary phase diagrams [77Ray] were the topic of many subsequent investigations.

As reported in [71Svi], first studies of the constitution of the ternary system Mg/Y/Nd showed that the solubilities of the elements Y and Nd in the Mg solid-solution crystal could be reduced by first adding the other element. Thus, a greater volume fraction of precipitations is possible by adding equal parts of the alloying elements. These experiments, coupled with the fact that Nd has a positive influence on the mechanical properties, led to the first studies of the Mg/Nd/Y/Zr system [75Dri]. Further development of creep-resistant alloys led to multiple patents for this alloy series (e.g. [78Tik], [82Uns], [84Uns]) and the commercial introduction of the WE alloys [89Uns].

Studies of the influence of alloying variations on this series of alloys showed great potential. In [81Mor] and [82Mor], for example, the addition of 2 weight % each of Zn and Nd to an Mg/Y/Zr alloy proved to be very favourable and correlated with later studies on the influence of Nd on the mechanical properties [82Dri] and the formation of ternary precipitations in the Mg/Zn/Y system [82Pad]. Studies on the heat treatment of the alloys [82Mor] showed no influence at 300 °C because the precipitations are mainly formed at the grain boundaries. Zn lowers the solubility of Y in magnesium and has a positive effect on the alloy's creep resistance. The activation energy for creep was found to be between 165

and 212 kJ/mol at high temperatures. This was mainly attributable to the Y content of the alloy; other additions had no significant influence (Table 2).

Two activation energies for the alloys Mg–6.2 weight % Y–3 weight % Nd–0.4 weight % Zr and Mg–5.9 weight % Y–3 weight % Nd were determined in [83Mor]. Depending on the prior heat treatment, activation energies of 60–68 kJ/mol were found for temperatures ranging from 280 to 300 °C and 100–226 kJ/mol for higher temperatures. Between 200 and 280 °C, “jerky flow” occurred, but it could not be established which element had a sufficiently high mobility to be responsible for this. It would seem to be Y, since the effect was lower after a heat treatment, but other authors favour a hardening by Mg/Nd precipitations [88Vos]. The results were partly confirmed in [85Hen], [86Hen], and [87Mor]. In these studies, two different mechanisms, with two different activation energies, were found to be dominant in specific regions of stress and temperature. At lower temperatures, the mechanisms are mainly gliding (with dissolved impurity atoms limiting diffusion) and the climbing of dislocations with activation energies close to that for self-diffusion [90Mor]. At higher temperatures, there are two basic possibilities for interpreting the high activation energies, i.e. the movement of screw dislocations by either jumps or intense cross-slippage. A slight dependence of the activation energy is suggestive of the second mechanism [90Mor]. The change in the mechanism also results in different stress dependences of the creep rate. Heat treatment has no significant effect on the creep rate beyond 250 °C, which can be attributed to an insufficient heat resistance of the acting precipitations [86Stu]. In the alloys investigated in [83Mor], [85Hen], and [86Hen], no zinc was included so as to prevent the formation of ternary Mg/Y/Zn precipitations, which show poor heat stability [87Mor].

The alloys that emerged from these studies were introduced by Magnesium Elektron Ltd. (MEL) as WE54 (Mg–5.1 weight % Y–1.75 weight % Nd–1.5 weight % rare earths–0.5 weight % Zr) and WE43 (Mg–4 weight % Y–2.25 weight % Nd–1 weight % rare earths–0.5 weight % Zr). A number of experiments concerning creep resistance were carried out with these alloys.

At stresses between 180 and 225 MPa ( $T = 130$ – $170$  °C), WE43 was found to have an activation energy of approximately 140 kJ/mol and a stress exponent of  $n = 14$ , but with stresses from 32 to 80 MPa ( $T = 230$ – $270$  °C) the values changed to 170 kJ/mol and  $n = 4$  [92Ahm2]. During creep, some precipitation-free zones formed and the material failed at the grain boundaries. The creep behaviour of WE54 after different conditions of heat treatment and production has been studied at stresses in the range 32–80 MPa and temperatures of 230–270 °C [97Kho]. The stress exponent was 4.5 for each material, and the activation energies varied between 175 and 221 kJ/mol. No detailed explanation of the underlying cause or of the acting mechanisms was given. Since the influence of Y and Nd has only been discussed in the aforementioned earlier studies, [98Suz] investigated the Mg/Y system, in particular with respect to the creep behaviour at 275 °C and 50 to 200 MPa, to find out more about the mechanisms of creep. It was shown that small amounts of Y tremendously increase the creep resistance. This can again be explained in terms of the excellent ability of Y to act as a solid-solution hardener. A comparison with Al and Mn in other studies showed Y to be more effective than the two more traditional elements.

The WE series of alloys have good castabilities and, with a prior T6 heat treatment, they are very heat resistant, highly creep resistant, ageing resistant, corrosion resistant, and show good fatigue strength. At the present time, the WE alloys represent the state of the art of alloy development, having characteristic profiles comparable to those of aluminium alloys. They may be used as casting or wrought alloys (e.g. [92Kin]), but mainly in the

Table 2: Summary of the results of the creep behaviour of magnesium alloys with Y; author statements

alloy	T [°C]	s [MPa]	n	Q [kJ/mol]	mechanism*	source
Mg-0,7Y	277	50-70	5	–	1	/98Suz/
Mg-0,7Y	277	> 70	12	–	5	/98Suz/
Mg-3,9Y	277	50-100	5	–	1	/98Suz/
Mg-3,9Y	277	> 100	12	–	5	/98Suz/
Mg-5,6Y	277	50-120	5	–	1	/98Suz/
Mg-5,6Y	277	> 120	12	–	5	/98Suz/
Mg-8,3Y	277	50-150	5	–	1	/98Suz/
Mg-8,3Y	277	> 150	12	–	5	/98Suz/
Mg-5,9Y-3Nd	200-300	40	–	60-68	2	/83Mor/
Mg-5,9Y-3Nd	300-350	40	–	100-226	1	/83Mor/
Mg-6Y-4Nd	290-360	10-30	2-3	–	3	/85Hen/
Mg-6Y-4Nd	290-360	30-80	6-7	–	k.A.	/85Hen/
Mg-5,8Y-2,8Nd-0,9Zr	< 200	20	–	150	1	/97Mor/
Mg-5,8Y-2,8Nd-0,9Zr	< 200	40	–	135	1	/97Mor/
Mg-5,8Y-2,8Nd-0,9Zr	< 200	60	–	122	1	/97Mor/
Mg-5,8Y-2,8Nd-0,9Zr	< 300	–	3,1	–	k.A.	/97Mor/
Mg-5,8Y-2,8Nd-0,9Zr	> 200	20	–	257	2	/97Mor/
Mg-5,8Y-2,8Nd-0,9Zr	> 200	40	–	202	2	/97Mor/
Mg-5,8Y-2,8Nd-0,9Zr	> 200	60	–	179	2	/97Mor/
Mg-5,8Y-2,8Nd-0,9Zr	> 300	–	3,7	–	k.A.	/97Mor/
Mg-6,2Y-3Nd-0,4Zr	200-300	40	–	60-68	2	/83Mor/
Mg-6,2Y-3Nd-0,4Zr	300-350	40	–	100-226	1	/83Mor/
Mg-6Y-3Nd-0,5Zr	200-280	20	–	50-90	3	/85Hen/
Mg-6Y-3Nd-0,5Zr	280-350	20	–	200-300	2 oder 4	/85Hen/
Mg-1Y-Zn-Nd-Zr	250-350	40	–	212	1	/81Mor/
Mg-3Y-Zn-Nd-Zr	250-350	40	–	187	1	/81Mor/
Mg-5Y-Zn-Nd-Zr	250-350	40	–	165	1	/81Mor/
WE43	130-170	180-225	14	140	k.A.	/92Ahm2/
WE43	230-270	180-225	2-3	170	k.A.	/92Ahm2/
WE54	<200	100	–	150	k.A.	/97Mor/
WE54	<200	150	–	160	k.A.	/97Mor/
WE54	>200	100	–	14	k.A.	/97Mor/
WE54	>200	150	–	40	k.A.	/97Mor/
WE54	150	50-150	1,5	–	k.A.	/97Mor/
WE54	200	50-150	3,4	–	k.A.	/97Mor/
WE54	230-270	32-82	4-5	175-221	k.A.	/97Kho/
WE54	250	50-150	3,3	–	k.A.	/97Mor/

\* mechanisms (as given by the authors):

- 1: diffusion-controlled climbing of dislocations on the basal plane
- 2: cross slip of dislocations
- 3: dislocation gliding, hampered by solved impurity atoms
- 4: movement of jogged screw dislocations
- 5: Power-Law-Breakdown



aeronautics industry (e.g. [97Arl], [97Gea]). As regards the mechanical properties, WE54 is slightly superior to WE43, which is more ductile and does not lose its ductility upon prolonged heating [90Kin]. Nevertheless, WE43 is most widely applied in the industry. Figure 8 shows the strength properties of the WE alloys as a function of temperature compared to other magnesium alloys. Figure 9 compares the creep behaviour in the same way.

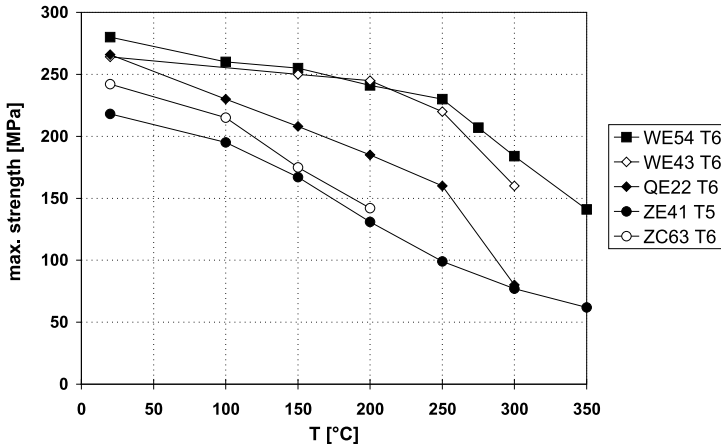


Figure 8: Tensile strength of magnesium sand-cast alloys as a function of the temperature [96MEL]

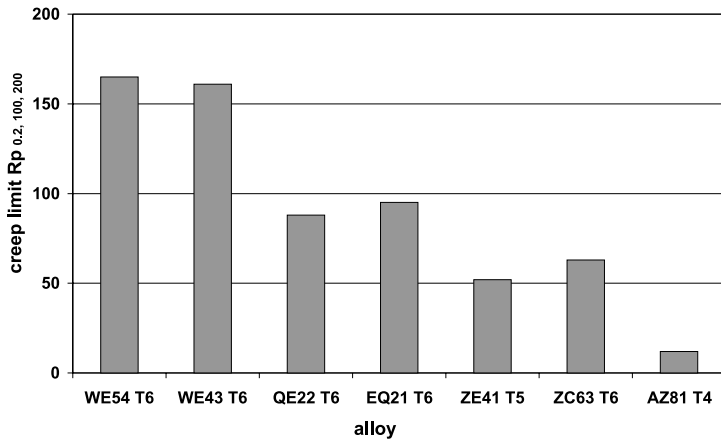


Figure 9: Time yield limit  $R_{p_{0.2, 100, 200}}$  of several magnesium alloys [96MEL]

In the last few years, many studies have dealt with the precipitation behaviour of the WE alloys, but they shall only be mentioned in passing here ([86Stu], [88Vos], [92Ahm1],

[92Pol], [92Wei], [97His]). There have been proposals to increase the number of precipitations by deformation with a two-stage heat treatment or by micro-alloying to further increase the mechanical properties [98Hi].

The listing of the most important results of different authors in the field of creep behaviour gives the impression that discussions concerning the mechanisms operative during creep are not yet at an end. The interpretation of the results is still sometimes controversial, despite the fact that a clear trend can be seen.

## 7.6 Potential Applications

### 7.6.1 Casting Alloys Containing Aluminium

Alloys containing a high proportion of zinc (e.g. ZA124) were proposed as early as the mid-1970s as alternatives to the conventional alloys [77Foe]. These alloys have higher creep resistance, excellent corrosion resistance, and good castability. Calcium was found to increase the creep resistance (Fig. 10) and heat resistance. However, such alloys were never introduced commercially. It is not clear today as to what initiated this development, but the good properties of Mg/Al/Zn are acknowledged in modern works [98Zha], [99Boh], with Ca again having a positive influence on creep [98Luo]. However, in contrast to [98Kin], this study did not highlight the problems of castability, hot cracking, and glueing that arise on adding Ca. As proposed in [94Luo], other strategies might be a change in the b-phase structure by micro alloying or the generation of bigger grains by adjusting the alloying contents.

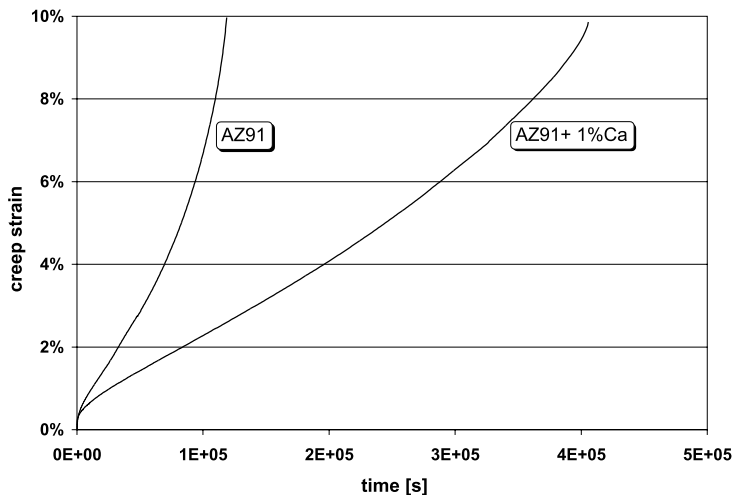


Figure 10: Creep curves for AZ91 and AZ91 + 1%Ca (200 °C, 60 MPa) [97Som]

In other studies, aluminium was completely removed from the casting alloys, and more rare earth elements were used instead [97Lyo]. On adding 2.5 weight % of rare earths and

0.3% each of zinc and manganese, the creep resistance was found to be increased greatly and reached values higher than that of the commercial creep-resistant alloy AE42 (Fig. 11). The rapidly falling prices for rare earth elements will support this development.

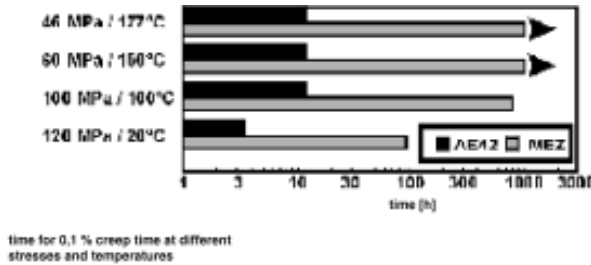


Figure 11: Creep behaviour of a new Mg die-casting alloy (MEZ) compared to that of AE42 [87Kin]

Magnesium’s significance in die-casting alloys is still rising and there are many developing institutions working in various research fields. Since magnesium/rare earth alloys do not have any commercial significance, their development lags behind that of other alloys.

### 7.6.2 Magnesium/Rare Earth Alloys

Several studies on the properties of new magnesium/rare earth alloys have been made in recent years, but their market segment and economic impact is very small and the amount and variety of research work cannot approach that of publications dealing with AZx alloys.

At present, gadolinium and samarium are the most promising candidates. They have a low solubility in magnesium and the alloys are therefore expected to be “reasonably priced”. With Gd and Dy, high-strength alloys are possible, but the matter of their creep resistance has not yet been addressed.

The binary system Mg/Sc and alloys based on it, such as Mg/Sc/Mn [99Buc1], Mg/Sc/Ce/Mn [98Buc2], and Mg/Sc/Gd/Mn [99Buc2] show far superior creep behaviour to WE43. Depending on the load spectrum and the alloy, the creep rates can be 100 times slower than those for WE43 (Fig. 12). There are definitely many more questions to be answered, but the high potential of this alloy system cannot be doubted.

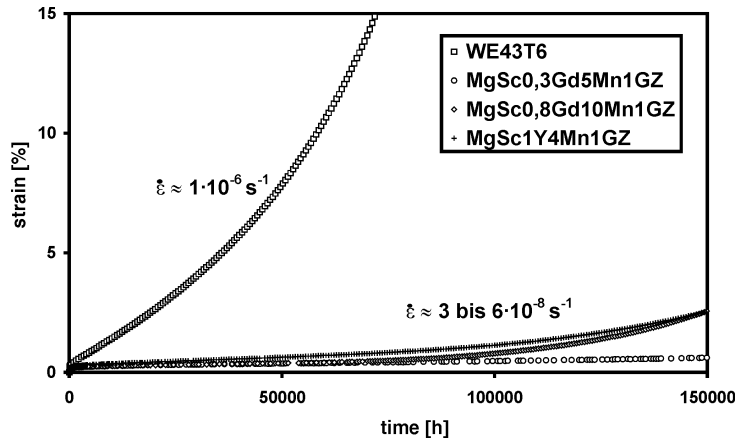


Figure 12: Creep behaviour of novel high-tech alloys compared to that of WE43 (350 °C, 30 MPa) [99Buc2]

Usually, the high cost is invoked as an argument against using rare earth elements for alloy development. However, with the break-up of the CIS, and China opening up to trade, the increasing demand for rare earths will eventually lead to stable prices and a consequent increase in research activity.

## 7.7 Literature

- /37Hau/ Haughton, J.L.; Prytherch, W.E., „Magnesium and its alloys“, His Majesty’s Stationery Office, London (1937)
- /38Bol/ Bollenrath, F., „Physikalische und mechanische Eigenschaften der Magnesiumlegierungen“, in „Werkstoff Magnesium“, VDI-Verlag, Berlin (1938), p. 5-28
- /39Bec/ Beck, A., „Magnesium und seine Legierungen“, Springer, Berlin (1939)
- /49Leo/ Leontis, T.E., „The properties of sand cast magnesium-rare-earth alloys“, Trans. AIME 191 (1949), p. 968-983
- /54Rob/ Roberts, C.S., „Creep behavior of magnesium-cerium alloys“, Trans. AIME 200 (1954), p. 634-640
- /54Sau/ Sauerwald, F., „Der Stand der Entwicklungen der Zwei- und Vielstofflegierungen auf der Basis Magnesium-Zirkon und Magnesium-Thorium-Zirkon“, Z. Metallkde. 45 (1954), p. 257-269
- /59Pay/ Payne, R.J.M.; Bailey, N., „Improvement of the age hardening properties of magnesium-rare-earth alloys by addition of silver“, J. Inst. Met. 88 (1959-60), p. 417-427
- /59Ray/ Raynor, G.V., „The physical metallurgy of magnesium and its alloys“, Pergamon, Oxford (1959)
- /61Gsc/ Gschneidner, K.A., „Rare earth alloys“, Van Nostrand, Princeton (1961)
- /61Miz/ Mizer, D.; Clark, J.B., „The magnesium-rich region of the magnesium-yttrium phase diagram“, Trans. Met. Soc. AIME 221 (1961), p. 207-208
- /61Teg/ Tegart, W.J.McG., „Activation energies for high temperature creep of polycrystalline magnesium“, Acta Met. 9 (1961), p. 614-617

- /66Gib/ Gibbs, G.B., „Creep and stress relaxation studies with polycrystalline magnesium“, *Phil. Mag.* 13 (1966), p. 317-329
- /66Lon/ London, R.V.; Edelman, R.E.; Markus, H., „Development of a wrought high-strength magnesium-yttrium alloy“, *Trans. ASM* 59 (1966), p. 250-261
- /69Eml/ Emley, E.F., „Principles of Magnesium Technology“, Pergamon, Oxford (1969)
- /71Svi/ Sviderskaya, Z.A.; Padezhnova, E.M., „Solid solubility of neodymium and yttrium in magnesium“, *Russ. Met.* (1971), p. 141-144
- /71Wal/ Waldman, J.; Schwartz, M.; Perez, J., „On the nature of the impurity phase in an age-hardenable Mg-10, 8 wt pct Y alloy“, *Met. Trans.* 2 (1971), p. 2942-2944
- /72Cro/ Crossland, I.G.; Jones, R.B., „Dislocation creep in magnesium“, *Met. Sci. J.* 6 (1972), p. 162-166
- /72Foe/ Foerster, G.S., „Designing die casting alloys“, *Light Met. Age* 30 (1972), p. 11-13
- /72Miz/ Mizer, D.; Peters, C., „A study of precipitation at elevated temperatures in a Mg-8.7 pct Y alloy“, *Met. Trans.* 3 (1972), p. 3262-3264
- /72Str/ Stratford, D.J.; Beckley, L., „Precipitation processes in Mg-Th, Mg-Th-Mn, Mg-Mn, and Mg-Zr alloys“, *Met. Sci. J.* 6 (1972), p. 83-89
- /76Lövl/ Lövlöf, K., „Transient creep in pressure die cast magnesium alloys“, *Z. Metallkde.* 67 (1977), p. 514-517
- /76Thr/ Threadgill, P.L.; Mordike, B.L., „Creep mechanisms in a Mg-Al-Zn alloy“, *Proc. 4<sup>th</sup> Int. Conf. Strength Metals & Alloys (ICSMA4) Vol. 3*, p. 1389-1392
- /77Foe/ Foerster, G.S., „Research in magnesium die casting“, *Die Cast Eng.* 21 (1977), p. 12-18
- /77Ray/ Raynor, G.V., „Constitution of ternary and some more complex alloys of magnesium“, *Int. Met. Rev.* 216 (1977), p. 66-96
- /78Tik/ Tikhova, N.M.; Blokhina, V.A.; Antipova, A.P.; Vasilieva, T.P., „Heat treated and aged magnesium-base alloy“, *US Pat.* 4.116.731 (1978)
- /79Ash/ Ashby, M.F.; Gandhi, C.; Taplin, M.R., „Fracture-mechanism maps and their construction for f.c.c. metals and alloys“, *Acta Met.* 27 (1979), p. 699-729
- /80Höl/ Höllrigl-Rosta, F.; Just, E.; Köhler, J.; Melzer, H.-J., „Magnesium im Volkswagenwerk“, *Metall* 34 (1980), p. 1138-1141
- /81Mor/ Morgan, J.E.; Mordike, B.L., „An investigation into creep-resistant, as-cast magnesium alloys containing yttrium, zinc, neodymium and zirconium“, *Met. Trans. A* 12A (1981), p. 1581-1585
- /81Oik/ Oikawa, H., „Deformation mechanism diagrams – modifications for engineering applications“ in Wilshire, B.; Owen, D.R.J. (Hrsg.) „Creep and Fracture of Engineering Materials and Structures“, Pineridge 1981, p. 113-126
- /82Dri/ Drits, M.E.; Rokhlin, L.L.; Oreshkina, A.A.; Nikitina, N.I., „Principles of alloying magnesium-based heat-resistant alloys“, *Russ. Met.* (1982), p. 83-87
- /82Fro/ Frost, H.J.; Ashby M.F., „Deformation-mechanism maps“, Pergamon, Oxford (1982)
- /82Mor/ Morgan, J.E.; Mordike, B.L., „Development of creep resistant magnesium rare earth alloys“, *Proc. 6<sup>th</sup> Int. Conf. Strength Met. All. (ICSMA6)*, p. 643-648
- /82Pad/ Padezhnova, E.M.; Mel'nik, E.V.; Miliyevskiy, R.A.; Dobatkina, T.V.; Kinzhibalo, V.V., „Investigation of the Mg-Zn-Y system“, *Russ. Met.* (1982), p. 185-188
- /82Uns/ Unsworth, W.; King, J.F.; Bradshaw, S.L., „Magnesiumlegierungen“, *Deutsches Patent DE 32 10 700 C2*

- /83Ash/ Ashby, M.F.; Brown, L.M. (Hrsg.), „Perspectives in creep fracture“, Pergamon, Oxford (1983)
- /83Mor/ Mordike, B.L.; Stulikova, I., „Mechanical properties of magnesium-yttrium-rare earth alloys“, Proc. Int. Conf. Met. Light All. (1983)
- /84Hul/ Hull, D.; Bacon, D.J., „Introduction to dislocations“, Pergamon, Oxford (1984)
- /84Uns/ Unsworth, W.; King, J.F.; Bradshaw, S.L., „Magnesiumlegierungen und Verfahren zu ihrer Wärmebehandlung“, Deutsches Patent DE 25 58 915 C2
- /85Hen/ Henning, W.; Mordike, B.L., „Creep in magnesium-rare earth alloys“, Proc. 7<sup>th</sup> Int. Conf. Strength Met. All. (ICSMA 7), p. 803-808
- /86Hen/ Henning, W., „Untersuchungen zum Aufbau und zum Hochtemperaturverhalten von Magnesium-Seltene-Erden-Legierungen des Typs Mg-Y-Nd(-Zr)“, Dissertation, TU Clausthal (1986)
- /86Stu/ Stulikova, I.; Vostry, P.; Mordike, B.L.; Smola, B., „Strengthening of creep resistant Mg-based alloys by thermo-mechanical treatment“, Proc. 5<sup>th</sup> Int. Cong. Heat Treatm. Mat. (1986), p. 1993-2000
- /87Mor/ Mordike, B.L.; Henning, W., „Creep and high temperature properties of magnesium based alloys“, Proc. Conf. Magnesium Techn. 1986; Institute of Metals (1987), p. 54-59
- /88Nai/ Nair, K.S.; Mittal, M.C., „Rare earth in magnesium alloys“, Mat. Sci. Forum 80 (1988), p. 89-104
- /88Uns/ Unsworth, W., „Developments in magnesium alloys for casting applications“, Met. & Mat. (1988), p. 83-86
- /88Vos/ Vostry, P.; Stulikova, I.; Smola, B.; Cieslar, M.; Mordike, B.L., „A study of the decomposition of supersaturated Mg-Y-Nd, Mg-Y, and Mg-Nd alloys“, Z. Metallkde. 79 (1988), p. 340-343
- /89Uns/ Unsworth, W., „The role of rare earth elements in the development of magnesium base alloys“, Int. J. Mat. Prod. Techn. 4 (1989), p. 359-378
- /90Kin/ King, J.F., „New advanced magnesium alloys“, Brook, G.B. (Hrsg.) Adv. Mater. Tech. Int. (1990), p. 12-19, Sterling (1990)
- /90Mas/ Massalski, T.B., „Binary Alloy Phase Diagrams, Vol. 3, 2<sup>nd</sup> edition“, ASM International, Materials Park, Ohio (1990)
- /90Mer/ Mercer, W.E. II, „Magnesium die cast alloys for elevated temperature applications“, SAE Techn. Pap. Ser. 900788 (1990)
- /90Mor/ Mordike, B.L., „Creep resistance of magnesium alloys at elevated temperatures“, Proc. 4<sup>th</sup> Annual World Magnesium Conf. (1990), p. 56-60
- /91Gje/ Gjestland, H.; Nussbaum, G.; Regazzoni, G.; Lohne, O.; Bauger, O., „Stress-relaxation and creep behaviour of some rapidly solidified magnesium alloys“, Mat. Sci. Eng. A134 (1991), p. 1197-1200
- /91Mil/ Miller, W.K., „Creep of die cast AZ91 magnesium at room temperature and low stress“, Met. Trans. A 22A (1991), p. 873-877
- /91Sum/ Suman, C., „Creep of diecast magnesium alloys AZ91D and AM60B“, SAE Tech. Pap. Ser. 910416 (1991)
- /92Ahm1/ Ahmed, M.; Lorimer, G.W.; Lyon, P.; Pilkington, R., „The effect of heat treatment and composition on the microstructure and properties of cast Mg-Y-RE alloys“, in Mordike, B.L.; Hehmann, F. (Hrsg.) Magnesium Alloys and Their Applications; DGM-Informationsges., Oberursel (1992), p. 301-308
- /92Ahm2/ Ahmed, M.; Pilkington, R.; Lyon, P.; Lorimer, G.W., „Creep Fracture in a Mg-Y-RE alloy“, in Mordike, B.L.; Hehmann, F. (Hrsg.) Magnesium Alloys and Their Applications; DGM-Informationsges., Oberursel (1992), p. 251-257

- /92Aun/ Aune, T.K.; Ruden, T.J., „High temperature properties of magnesium die casting alloys“, SAE Tech. Pap. Ser. 920070 (1992)
- /92Kin/ King, J.F; Thistlethwaite, p., „New corrosion resistant wrought magnesium alloys“, in Mordike, B.L.; Hehmann, F. (Hrsg.) Magnesium Alloys and Their Applications; DGM-Informationsges., Oberursel (1992), p. 327-334
- /92Pek/ Pekkülyüz, M.Ö.; Avedesian, M.M., „Magnesium alloying – some metallurgical aspects“, in Mordike, B.L.; Hehmann, F. (Hrsg.) Magnesium Alloys and Their Applications; DGM-Informationsges., Oberursel (1992), p. 213-220
- /92Pol/ Polmear, I.J., „Physical metallurgy of magnesium alloys“, in Mordike, B.L.; Hehmann, F. (Hrsg.) Magnesium Alloys and Their Applications; DGM-Informationsges., Oberursel (1992), p. 213-220
- /92Wei/ Wie, L.Y.; Dunlop, G.L., „Precipitation hardening in a cast Mg-rare earth alloy“, in Mordike, B.L.; Hehmann, F. (Hrsg.) Magnesium Alloys and Their Applications; DGM-Informationsges., Oberursel (1992), p. 335-342
- /94Luo/ Luo, A.; Pekkülyüz, M.Ö., „Cast magnesium alloys for elevated temperature applications“, J. Mat. Sci. 29 (1994), p. 5259-5271
- /94Pol/ Polmear, I.J., „Light Alloys – metallurgy of the light metals; 3rd edition“, Arnold, London (1994)
- /96MEL/ „Elektron Database V 2.2“, Datenbank der Fa. Magnesium Elektron Ltd., Manchester (1996)
- /96Nei/ Neite, G., Kubota, K., Higashi, K., Hehmann, F., „Magnesium-Based Alloys“, in Cahn, R.W.; Haasen, P.; Kramer, E.J. (Hrsg.) „Materials Science and Technology – A Comprehensive Treatment“, Matucha, K.H. (Vol. Hrsg.) Vol. 8 „Structure and Properties of Nonferrous Alloys“, VCH Weinheim, 1996
- /96NHM/ „NHMg.db (ext.)“, Datenbank der Fa. Norsk Hydro Magnesium, Porsgrunn (1996)
- /96Pet/ Pettersen, G.; Westengen, H.; Hoier, R.; Lohne, O., „Microstructure of a pressure die cast magnesium-4wt.% aluminium alloy modified with rare earth additions“, Mat. Sci. Eng. A207 (1996), p. 115-120
- /96Wei/ Wei, L.Y.; Dunlop, G.L., „The solidification behaviour of Mg-Al-rare earth alloys“, J. Alloys Comp. 232 (1996), p. 264-268
- /97Arl/ Arlhac, J.-M.; Chaize, J.-C., „New magnesium alloys and protections in new helicopters“, in Lorimer, G.W. (Hrsg.) Proc. 3<sup>rd</sup> Int. Magnesium Conf., The Institute of Materials, London (1997), p. 213-230
- /97Blu/ Blum, W.; Weidinger, P.; Watzinger, B.; Sedlacek, R.; Rösch, R.; Haldenwanger, H.-G., „Time dependent deformation of the magnesium alloys AS21 and AZ91 around 100 °C“, Z. Metallkde. 88 (1997), p. 635
- /97Che/ Chen, F.C.; Jones J.W.; McGinn, T.A.; Kearns, J.E.; Nielsen, A.J.; Allison, J.E., „Bolt-load retention and creep of die-cast magnesium alloys“, SAE Techn. Pap. Ser. 970325 (1997)
- /97Dar/ Dargusch M.; Hisa, M.; Caceres, C.H.; Dunlop, G.L., „Elevated temperature deformation of die cast Mg alloy AZ91D“, in Lorimer, G.W. (Hrsg.) Proc. 3<sup>rd</sup> Int. Magnesium Conf., , The Institute of Materials, London (1997), p. 152-165
- /97Gea/ Geary, B., „Advances in the application of magnesium in helicopter gearcases“, in Lorimer, G.W. (Hrsg.) Proc. 3<sup>rd</sup> Int. Magnesium Conf., The Institute of Materials, London (1997), p. 563-574
- /97Gut/ Gutman, E.M.; Unigovski, Y.; Levkovich, M.; Koren, Z.; Aghion, E.; Dangur, M., „Influence of technological parameters of permanent mold casting and die

- casting on creep and strength of Mg alloy AZ91D“, *Mat. Sci. Eng. A234-236* (1997), p. 880-883
- /97His/ Hisa, M.; Barry, J.C.; Dunlop, G.L., „Precipitation during age hardening of Mg-rare earth alloys“, in Lorimer, G.W. (Hrsg.) *Proc. 3<sup>rd</sup> Int. Magnesium Conf.*, The Institute of Materials, London (1997), p. 369-379
- /97Kho/ Khosrshohahi, R.A.; Pilkington, R.; Lorimer, G.W.; Lyon, P.; Karimzadeh, H., „The microstructure and creep of as-cast and extruded WE54“, in Lorimer, G.W. (Hrsg.) *Proc. 3<sup>rd</sup> Int. Magnesium Conf.*, The Institute of Materials, London (1997), p. 241-256
- /97Lyo/ Lyon, P.; King, J.F.; Nuttall, K., „A new magnesium HPDC alloy for elevated temperature use“, in Lorimer, G.W. (Hrsg.) *Proc. 3<sup>rd</sup> Int. Magnesium Conf.*, The Institute of Materials, London (1997), p. 99-108
- /97Mor/ Mordike, B.L.; Lukac, P., „Creep behaviour of magnesium alloys produced by different techniques“, in Lorimer, G.W. (Hrsg.) *Proc. 3<sup>rd</sup> Int. Magnesium Conf.*, The Institute of Materials, London (1997), p. 419-429
- /97Reg/ Regev, M.; Aghion, E.; Rosen, A., „Creep studies of AZ91D pressure die casting“, *Mat. Sci. Eng. A234-236* (1997), p. 123-126
- /97Som/ Sommer, B. (Institut für Werkstoffkunde und Werkstofftechnik, TU Clausthal), persönliche Mitteilung (1997)
- /98Blu/ Blum, W.; Watzinger, B.; Weidinger P., „Creep resistance of Mg-base alloys“, in Mordike, B.L.; Kainer, K.U. (Hrsg.) *Magnesium Alloys and Their Applications*, Werkstoff-Informationsges., Frankfurt, 1998, p. 49-60
- /98Buc1/ Buch, F.v.; Mordike, B.L., „Microstructure, Mechanical Properties and Creep Resistance of Binary Magnesium Scandium Alloys“, in Aghion, E.; Eliezer, D. (Hrsg.) „Magnesium 97-Proc. 1<sup>st</sup> Israeli Int. Conf. Magnesium Sci. Techn.“, Magnesium Research Institute, Beer-Sheva, Israel (1998), p. 163-168
- /98Buc2/ Buch, F.v.; Mordike, B.L., „Microstructure, Mechanical Properties and Creep Resistance of binary and more complex Magnesium Scandium Alloys in Mordike, B.L., Kainer, K.U. (Hrsg.) *Magnesium Alloys and Their Applications*, Werkstoff-Informationsgesellschaft, Frankfurt, 1998, p. 145-150
- /98Dar/ Dargusch, M.S.; Dunlop, G.L.; Pettersen, K., „Elevated temperature creep and microstructure of die cast Mg-Al alloys“ in Mordike, B.L.; Kainer, K.U. (Hrsg.) *Magnesium Alloys and Their Applications*, Werkstoff-Informationsges., Frankfurt (1998), p. 277-282
- /98Hil/ Hilditch, T.; Nie, J.F.; Muddle, B.C., „The effect of cold work on precipitation in alloy WE54“ in Mordike, B.L.; Kainer, K.U. (Hrsg.) *Magnesium Alloys and Their Applications*, Werkstoff-Informationsges., Frankfurt (1998), p. 339-344
- /98Kin/ King, J.F., „Development of magnesium diecasting alloys“, in Mordike, B.L.; Kainer, K.U. (Hrsg.) *Magnesium Alloys and Their Applications*, Werkstoff-Informationsges., Frankfurt (1998), p. 37-47
- /98Luo/ Luo, A.; Shinoda, T., „Development of a creep-resistant magnesium alloy for die casting applications“ in Mordike, B.L.; Kainer, K.U. (Hrsg.) *Magnesium Alloys and Their Applications*, Werkstoff-Informationsges., Frankfurt (1998), p. 151-156
- /98Reg/ Regev, M.; Aghion, E.; Rosen, A.; Bamberger, M., „Creep studies of coarse-grained AZ91D magnesium castings“, *Mat. Sci. Eng. A252* (1998), p. 6-16
- /98Rok/ Rokhlin, L.L., „Dependence of the rare earth metal solubility in solid magnesium on its atomic number“, *J. Phase Equil.* 19 (1998), p. 142-145



- /98Suz/ Suzuki, M.; Sato, H.; Maruyama, K.; Oikawa, H., „Creep behavior and deformation microstructures of Mg-Y alloys at 550K“, *Mat. Sci. Eng. A252* (1998), p. 248-255
- /98Zha/ Zhang, Z.; Couture, A.; Luo, A., „An investigation of the properties of Mg-Zn-Al alloys“, *Scripta Mat.* 39 (1998), p. 45-53
- /99Boh/ Bohling, P.; Schumann, S.; Aghion, E.; Bronfin, B.; Kainer, K.U.; Fiedler, J., „Entwicklung einer kostengünstigen, warmfesten und kriechbeständigen Magnesiumdruckgußlegierung“, in Stauber, R.; Liesner, C.; Bütje, R.; Bannasch, M. (Hrsg.): *Werkstoffe für die Verkehrstechnik/Werkstoffwoche '98, Symposium 2*, Wiley-VCH, Weinheim (1999)
- /99Buc1/ Buch, F.v.; Lietzau, J.; Mordike, B.L.; Pisch, A.; Schmid-Fetzer, R., „Development of Mg-Sc-Mn alloys“, *Mat. Sci. Eng. A*, in press
- /99Buc2/ Buch, F.v., „Entwicklung hochkriechbeständiger Magnesiumlegierungen des Typs Mg-Sc(-X-Y), Mg-Gd und Mg-Tb“, Dissertation 1999, TU Clausthal, in press

# 8 High-Tech Machining of Magnesium and Magnesium Composites

*K. Weinert, M. Liedschulte, D. Opalla, M. Schroer  
Institute for Metal Cutting Manufacturing, Dortmund University*

## 8.1 Introduction

Magnesium is constantly gaining importance as a lightweight construction material. The best known fields of application are vehicle construction, aeronautics, industrial handling (robots, automation), and communication technology. In particular, the automobile industry uses magnesium for gearbox housing, steering wheels, and body frames [4]. The main reasons for this development are a changed environmental legislation, the customer requirements, and corporate objectives, which require lower vehicle weights and thus lower fuel consumption.

Despite high die-casting performance, especially with respect to parts with near-net-shape properties, important functional surfaces such as sealing faces, bearing surfaces, etc., still need to be machined [1, 2, 6].

## 8.2 The Current State of Mechanical Treatment of Magnesium

Knowledge about the machining of magnesium has been at hand since the 1930s–1970s. However, the processing technology has advanced and new machine tools have higher performances, and the alloys show different properties, hence this knowledge can only be partly adapted [7]. In general, magnesium has very good machining properties, i.e. low tool wear at low cutting loads and high surface qualities. New skills are very limited, and hence the present study deals mainly with turning and milling [5, 8, 9].

An analysis of practices at different companies, all of which are engaged in the machining of magnesium in series, showed that currently only cutting alloys and synthetic isotropic diamonds (PCD) are used, with the PCDs becoming more important for special tools. The cutting parameters are related to those for aluminium. On the one hand, the machine speed and cutting speeds are pushed to their limits according to the machine capabilities, but the feed rate, with its influence on the essential operation time, is not used to its full extent [11].

Different cooling lubricants are preferred by each of the observed companies. Despite cautions against the use of water-miscible cutting fluids because of possible hydrogen formation, emulsions as well as oils are used. The decision of what to use is mainly determined by the cutting fluid policy within the individual companies.

## 8.3 Safety Engineering

The safety engineering is very significant for the machining of magnesium. Magnesium is dangerous when it has a big surface area, e.g. as a powder or small chips, because then it becomes highly flammable. Tool breaking, tool wear, or unfavourable machining conditions may result in heating beyond magnesium's ignition temperature and so chips or particles can catch on fire.

Taking a look at the production of magnesium gear components at VW in the 1970s, the manufacturing was done on non-enclosed transfer lines or revolving transfer machines without any lubricant. The machines and their peripherals were easily accessible. Machines and workholdings had chamfers. Flying chips were contained with baffles. Despite these precautions, chips collected in many places that could not be regularly cleaned. Small ignitions occurred routinely, but they were extinguished with arc extinguishing media (powder fire extinguisher and grey-cast iron chips) and with the help of the personnel [7].

Today's manufacturing of magnesium components differs considerably in the machines, tools, cutting parameters, and cooling lubricants employed. Currently, oil and emulsions are mostly used as cutting fluids for series production. High cutting speeds and encapsulated machines increase the danger of deflagrations with oily lubricants, whereas hydrogen evolution occurs with emulsions. Hydrogen has a low ignition energy, but also evaporates easily. In the case of a burning during machining with emulsion, magnesium reacts with the water [3].

The machine should have effective safety precautions for safely machining magnesium under today's conditions. A proper safety design includes a fire extinguishing device with nozzles inside the working space and maybe even in the exhaust unit. The fire alarm system should consist of a maximum heat sensor and an infrared sensor. Additionally, a hand lever for the extinguishing system should be present at the control desk. The machine should have a pressure valve at the ceiling to release overpressure in the case of evaporation. Besides the lubricant feeding through the mandrel, the walls of the working space should be watered continuously to remove chips and lower the load of combustibles [12].

## 8.4 Drilling

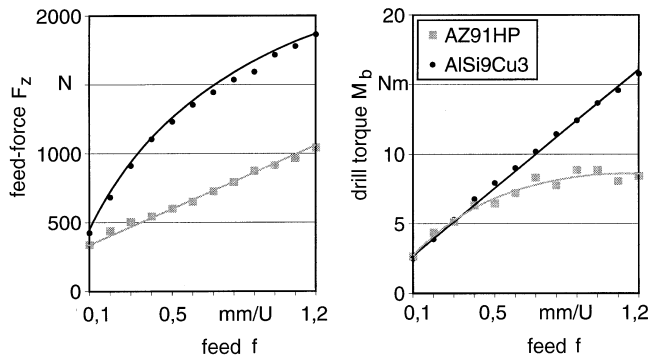
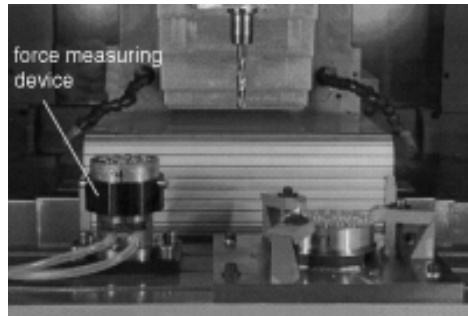
Drilling and fine-drilling is the main work involved in the production of many components. Compared to milling or turning, the working area is not freely accessible. This gives rise to many problems, such as the need for chip transportation and cooling, to mention only the most important ones. Compared to turning and milling, it is much more difficult to improve the parameters towards high-speed, high-performance drilling (high feeding speeds combined with high cutting speeds) and dry processing.

### 8.4.1 Mechanical Load on the Tool

A knowledge of the cutting forces that occur is important for many reasons. It is important for machine design (driving power), for tool design, and for clamping-piece design. It is also necessary to consider any deformations that could occur in the working piece due to these forces.

The mechanical load on the tool is determined by the parameters of cutting speed and feed rate, besides the properties of magnesium and the tool geometry. The feed forces and the drilling moment are measured and compared to the corresponding values of aluminium to obtain information on the influence of these parameters. The feed force and drill moment are almost constant for cutting speeds,  $v_c$ , between 100 and 700 m/min and a feeding of  $f=0.2$  mm/rotation. The feed force required for machining aluminium is roughly 1.5 to 1.6 times higher than that for magnesium. The drill moment is almost equal for the two materials.

Figure 1 shows the curve of the axial load and the drilling moment as a function of feed. Increasing the feed results in increasing feed force and drilling moment, and a significant influence of the material can be observed. The feed force at a feed of  $f=0.1$  mm/rotation is nearly the same for the two materials.



tool: VHM-drill uncoated  
 diameter:  $D = 14,5$  mm  
 cutting speed:  $v_c = 500$  m/min  
 drill depth:  $l = 40$  mm  
 cooling lubricant: Emulsion (Polinor FFY, 6%ig)

Figure 1: Comparison of the mechanical tool load when machining AZ91HP and AISi9Cu3

With increasing feed, the force also increases, which is again true for both materials, but at  $f = 1.2$  mm/rotation, aluminium has a feed force 1.7 times higher than that of magnesium. The drilling moment is determined by the cutting force, the friction between

the land and the drill hole, and the chip transportation. It shows a significant difference beyond a feed of  $f = 0.4$  mm/rotation; at  $f = 1.2$  mm/rotation, the drill moment for aluminium is 1.8 times higher than that with magnesium.

The mechanical load on the tool mainly depends on the tool geometry. In order to assess the influence of this factor, experiments with different tools of the same diameter were conducted. Figure 2 shows the feed force and the drill moment in relation to the feed. These values cannot be compared with those in Fig. 1 since the melts were different. The feed force is indeed highly influenced by the tool geometry, with the drill types II and III producing much higher loads. At a feed of  $f = 1.2$  mm/rotation, the feed force using the type II and III drills is 1.5 times higher than that using of a type I drill, which can be rationalized in terms of the size of the relief angle.

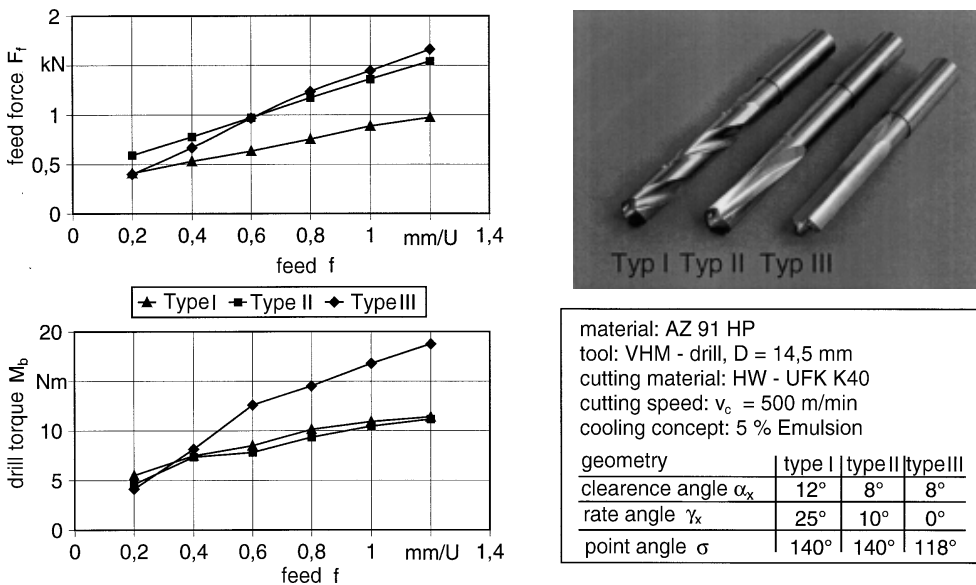
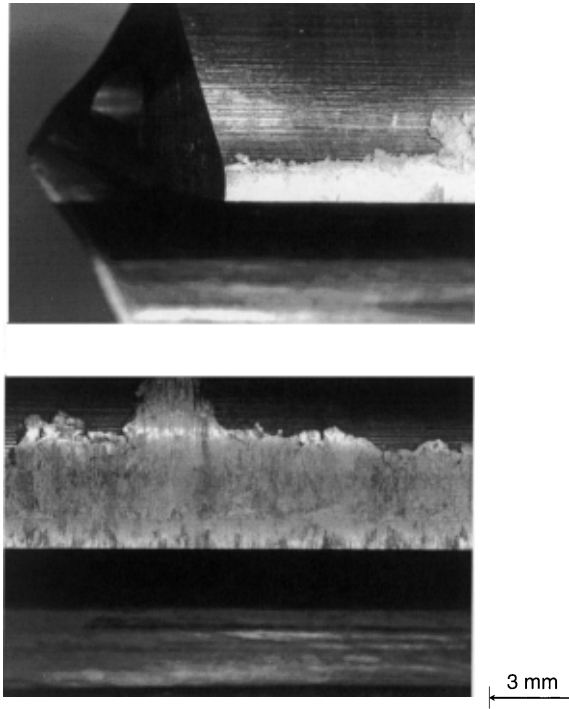


Figure 2: Effect of the drill geometry on the mechanical tool loads when drilling the magnesium alloy AZ91HP

The drilling moment is also influenced by the geometry and preparation of the effective surface. Measurements have shown that the drill types I and II have the same drill moments throughout the whole feed range, whereas the drill moment for type III significantly increases for feeds greater than  $f = 0.6$  mm/rotation. The high including angles of  $s = 140^\circ$  of drill types II and I are responsible for this divergent behaviour; they reduce the cutting force and the drill moment. Positive undercut angles also lower the drill moment, but this seems to be of secondary concern in this case. Another cause of the higher values of the drill moment are material segregations on the lands, which increase friction and thus the drill moment (Fig. 3).



material: AZ91 HP  
 tool: VHM - drill, uncoated  
 diameter:  $D = 14,5$  mm  
 cooling cubricant: Emulsion (Polinor FFY, 6%ig)

cutting speed:  $v_c = 500$  m/min  
 feed:  $f = 0,6$  mm/U  
 drilling distance:  $L_f = 0,4$  mm  
 drill depth:  $l = 40$  mm

Figure 3: Material deposits on the chamfers of the straight-notched drill (type III)

There are two main reasons for the segregations. The roughness of the type III tool lands is greater than that for those of types I and II, and therefore material can add more easily. The second reason is poor chip transportation with this tool, which could not be improved by adding more lubricant.

Figure 4 shows the feed force and drill moment for different cutting materials and coatings when machining magnesium. The parameters used were rather moderate. The lowest mechanical load was achieved with a non-coated hard metal drill. The use of a TiAlN coating resulted in a slight increase in the feed force, whereas a diamond coating led to a significant increase. The drill moment was only slightly affected. The increase in feed force was primarily based on the stronger roundings through the coating. The TiAlN coating was 1–5  $\mu\text{m}$  thick; the diamond coating was 3–5  $\mu\text{m}$ . With the diamond-coated drills, the edges in particular (e.g. the cutting edge) can have an even greater thickness. The coating also influences the friction behaviour and the surface structure. For an uncoated drill, the scoring and the chip-flow occur in the same directions. The score marks are still noticeable for a TiAlN coating, but are no longer seen at all with a diamond coating. This changes the conditions of the contact, thus influencing the resulting loads. For a PCD drill

with changed cutting lip geometry, the same feed forces occur as for a hard metal drill, only the drill moment is slightly higher.

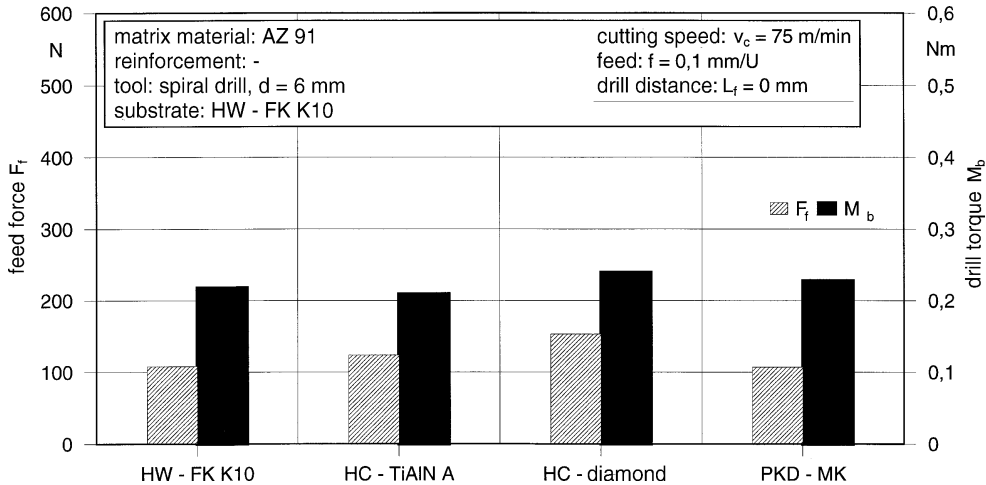


Figure 4: Influence of the cutting material and the coating on the mechanical tool load when drilling magnesium

Looking at the mechanical load on tools, it is obvious that, besides high cutting speeds, an increase of the feed is useful for machining magnesium. The tool geometry has a big influence on the load, whereas the cutting material, i.e. the coating, is rather unimportant. It remains to be verified that the form and size errors and the attainable roughness are still within the required tolerances.

## 8.4.2 Solid Drilling

The most important factors for evaluating the quality of a drilling are the deviation of the cross-section and the roughness of the drill hole. A type I drill was used for these studies, which turned out to be of no significance since even equal drills showed different concentricity faults of up to  $\Delta D = 25 \mu\text{m}$ .

Figure 5 shows the measured surface roughness as a function of the feed and cutting speed. Increasing the speed has only little effect on the average roughness height, which reaches good values irrespective of the cooling system used. The cutting speed was limited to the maximum mandrel speeds of the two machines used ( $n = 15,000 \text{ min}^{-1}$  and  $n = 24,000 \text{ min}^{-1}$ ). At cutting speeds of  $v_c = 900$  and  $1100 \text{ m/min}$ , the feed was increased to  $f = 0.4 \text{ mm/rotation}$  to avoid vibrations at  $f = 0.2 \text{ mm/rotation}$ .

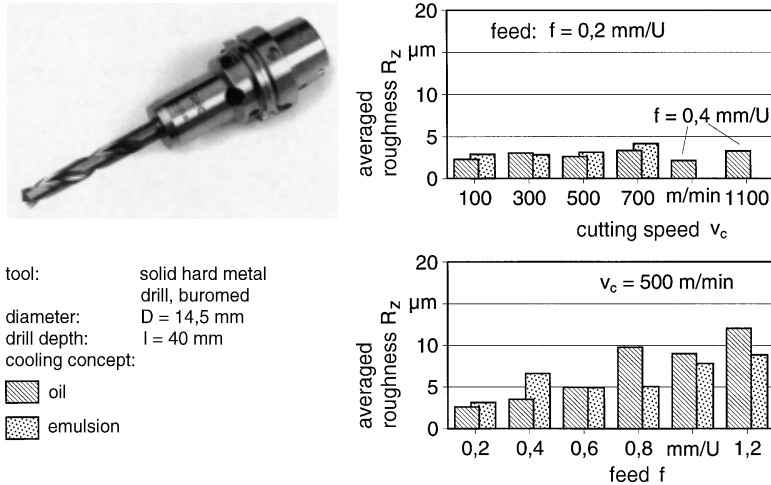


Figure 5: Influence of the cutting speed and the feed on the drill quality when drilling AZ91HP

Increasing the feed at constant cutting speed results in increased roughness. The maximum values for roughness amounted to  $R_z = 12 \text{ mm}$ . The small differences that resulted from a lubricant change cannot be completely explained in this way because several tools of the same geometry were used.

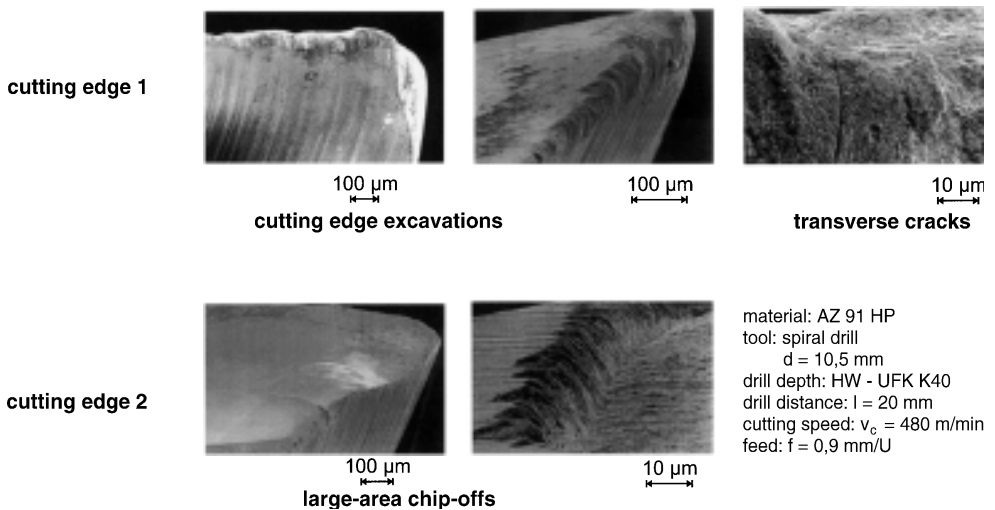


Figure 6: Solid hard-metal drill in used condition (mass production)

The transferability of the results towards serial production was tested. Figure 6 shows SEM images of a drill (type I) after a drill distance of approximately  $L_f = 3500 \text{ m}$ .



Production was carried out at a cutting speed of  $v_c = 480$  m/min and a feed of  $f = 0.9$  mm. Oil was used as the cutting fluid. Cutting edge no. 1 of the drill shows several small cracks and is damaged by flaking. Cutting edge no. 2 shows a large-area crack, as a result of which it could no longer be used. The diagonal cracks on the first edge are the first indications of further failure.

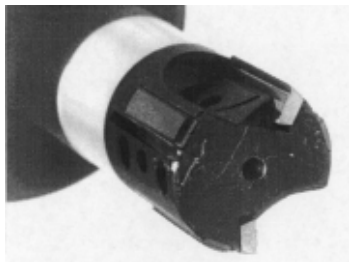
### 8.4.3 Reaming/Precision Boring

Figure 7 shows some examples of clearance holes made by precision boring and a single cutting edge reamer. A 15 mm diameter tool was used with emulsion as the lubricant, and a 20 mm tool was used with additional oil. The tool diameter, the maximum mandrel speed, and the resulting cutting speeds were again limited by the machine. Increasing the feed up to  $f = 0.3$  mm/rotation did not reduce the drilling quality. Axial overhang of the cutting edge towards the guide rail was used, which also limited a further increase of the feed.

The drill-hole diameter was within the tolerance limit IT7 for all tests. Using the cutting fluid oil, the average roughness value was between  $R_z = 0.6$  and  $1.6$   $\mu\text{m}$ , whereas using an emulsion it was between  $R_z = 1.1$  and  $3.2$   $\mu\text{m}$ . Because of the more effective lubrication, the roughness is lower for oil.

Additional tests with a “double-edged” reamer were carried out to realize feeds of greater than  $f = 0.3$  mm/rotation. This tool operates on the same working principle, but has an additional cutting edge on the perimeter. Furthermore, the axial leads of the cutting edges are changed with respect to the guide rails, allowing much higher feeds.

Figure 7: Influence of the cutting speed and the feed on the drill quality when reaming AZ91HP



double cutting-edge  
drill in single-block design

tool: fiddle drill 20H7  
 guide rails: PKD  
 material: AZ91HP  
 cutting speed:  $v_c = 500$  m/min  
 drill depth:  $l = 40$  mm  
 lubricant: emulsion

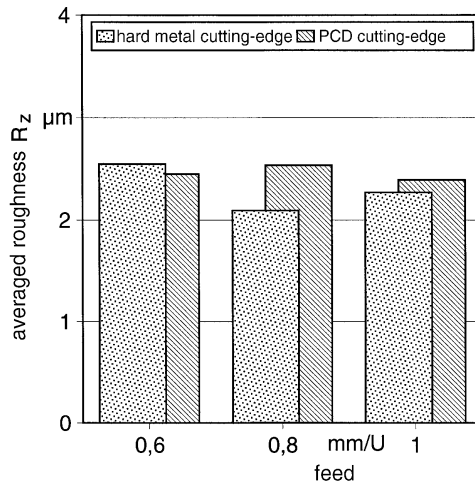
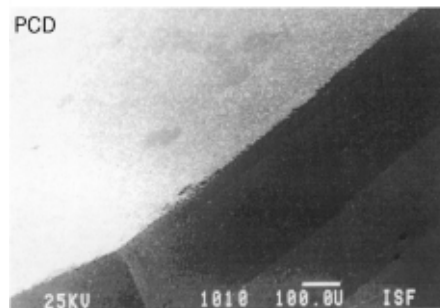
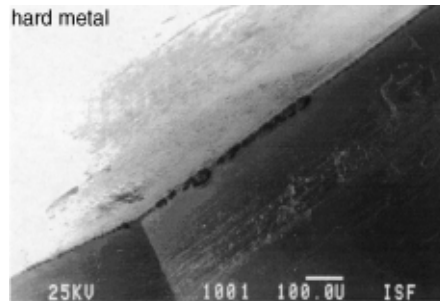


Figure 8: Averaged roughness when reaming AZ91HP with a “double-edged” tool

Figure 8 shows the average roughness heights of drillings made with this tool at cutting speeds of  $v_c = 500$  m/min and feeds up to  $f = 1$  mm/rotation. Hard metal and PKD were used as cutting materials, and the guide rails consisted of PKD. Both materials allow maximum feeds of  $f = 1$  mm/rotation, i.e. a feed rate of  $v_f = 8$  mm/min, with a high quality being achieved. However, analysis of the cutting-edge wear showed the appearance of cracks with these parameters (Fig. 9).



tool:	fiddle drill 20H7
guide rails:	PCD
material:	AZ91HP
cutting speed:	$v_c = 500$ m/min
feed:	$f = 0,6 - 1,0$ mm/U
drill depth:	$l = 40$ mm
drill distance:	$L_f = 1,5$ m
lubricant:	Emulsion

Figure 9: REM micrograph showing the cutting-edge wear

Figure 10 shows the drilling quality in terms of the diameter deviation and the average roughness when reborings AZ91HP with a solid tool tipped with four PKD cutting edges. The cutting edges are not distributed equally with this tool. The shaft is made of hard metal for stiffness. This tool could be used at cutting speeds up to  $v_c = 500$  m/min; at faster speeds it began to jar. The feed for reborings can be as high as that for drilling or reaming. When using oil, the drill quality is independent of the feed, the diameter deviation is in the range  $\Delta D = 2-7$   $\mu\text{m}$ , and the averaged roughness lies in the range  $R_z = 1-2$   $\mu\text{m}$ . The use of emulsion has a negative effect on the roughness, i.e. a decreased surface quality, in accordance with the results from reaming.

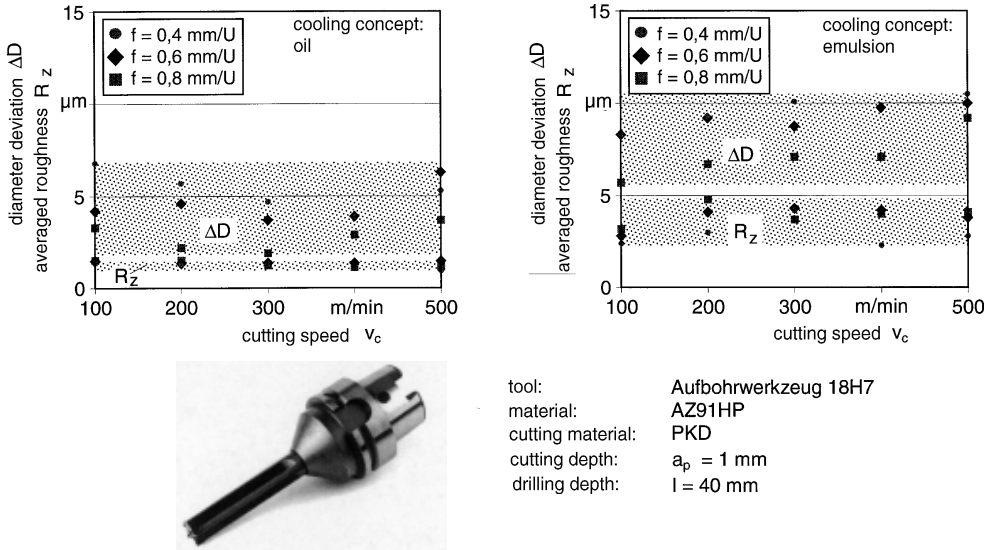


Figure 10: Influence of the cutting speed and the feed on the drill quality when reboring AZ91HP

Both increasing the cutting parameters and a change in the production strategy can optimize the processing time of a part. For machining magnesium, high cutting parameters may be used. The primary time required to reach a hole depth of 40 mm as a function of the applied tool and its different cutting parameters is given as an example in Fig. 11. All listed combinations of the tool and its parameters produce a part of almost equal quality. The comparison starts with a conventional multi-cutting-edge reamer that needs 16.8 s to drill such a hole. Use of an optimized multi-cutting-edge reamer already reduces the primary time to 2.5 s, while with a single-edged reamer and its specific cutting parameters, it only takes 0.3 s. The “double-edged” reamer, with its significantly higher feed, would even allow a theoretical time of 0.1 s. However, it is questionable as to whether this would reduce the overall cycling time since much time would be needed to reach the desired mandrel speed. Taking this acceleration time into consideration, the use of the “double-edged” tool with a reduced cutting speed but with a much higher feed would still be favourable. With this combination of parameters, the primary time rises by 0.2 s and the tool endurance is increased.

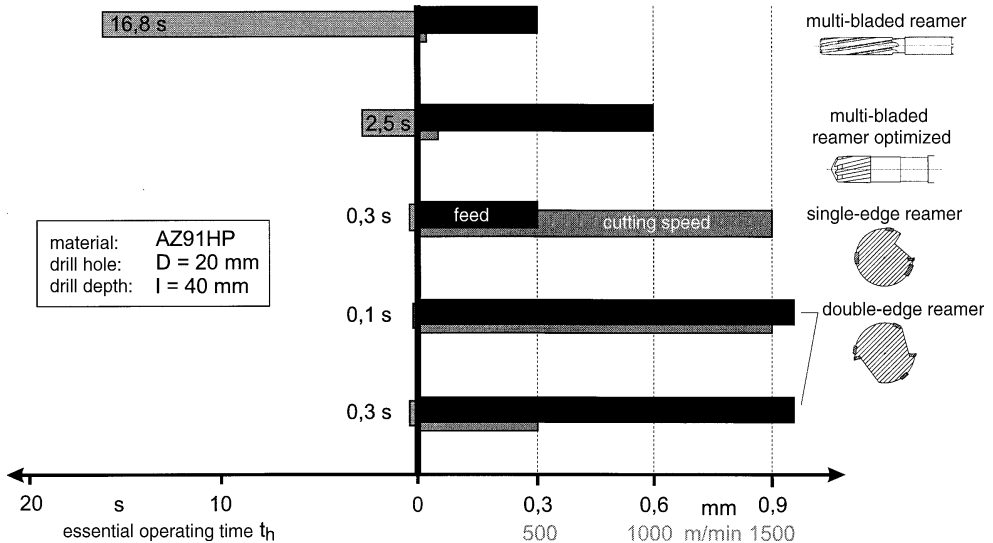


Figure 11: Primary processing times for several reaming methods

## 8.5 Micro Lubrication System (MLS) for Machining Magnesium

Disposal costs and ecological awareness are increasing and so the use of lubricants is questioned, especially in the machining branch. The aim is for dry lubrication, but this is still not possible for drilling and even less so for precision boring. The required quality is not attained and tool wear is severe. MLS represents an alternative in that only minimal amounts of lubricant are supplied ( $< 50$  mL/h). For the machining of aluminium, similar or even better results could be obtained for single cutting edge reaming with MLS instead of emulsion [10].

Experiments on drilling, reaming, and reborring were carried out with minimum lubrication. For this, the above-mentioned tools were used because their geometry is already adapted to the needs of MLS. Figure 12 shows the effect of the lubrication system on the averaged roughness. In the case of reborring, the same results are achieved with oil and MLS, while the use of emulsion results in worse roughness. This mainly stems from the fact that oil has the best lubrication efficiency. MLS also uses oil for lubricating, and despite the very small amount it is directly fed to the acting areas. With a 5% emulsion, the cooling comes to the fore.

The best procedure for machining magnesium in terms of safety is based on oil and emulsion lubrication. It has yet to be established whether a revised protocol is necessary for MLS, but it is obvious that higher temperatures occur in the tool, the workpiece, and the machine. Chip transportation out of the working zone is facilitated by the carrier medium, but chips will not be removed from the machine unless it is redesigned. The matter of the binding of the smallest chips or dust has yet to be addressed for MLS.

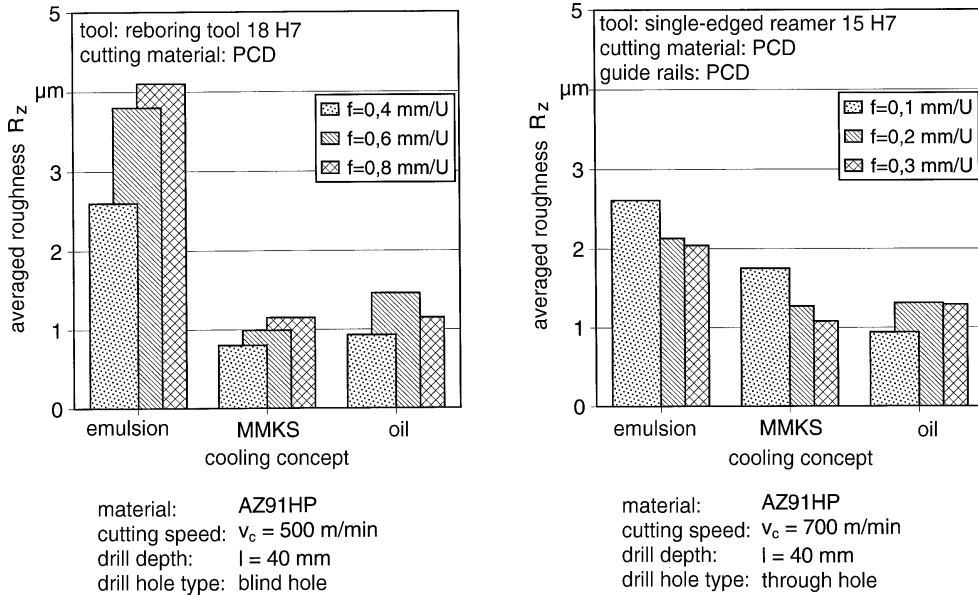


Figure 12: Influence of the cooling system used during precision boring

## 8.6 Machining Magnesium MMCs

Metal matrix composites (MMCs) consist of the matrix alloy, mostly aluminium or magnesium, and a reinforced ceramic phase. Such heterogeneous composites have many advantages, such as higher specific strength, lower thermal expansion, and improved wear resistance. Known applications are as particle-reinforced brake discs, reinforced cylinder barrels, fibre-reinforced diesel engine pistons, and reinforced extrusion profiles [13–18]. These components have hitherto been based on aluminium, but with its low density ( $s_{Mg} = 1.7$  g/cm<sup>3</sup>;  $s_{Al} = 2.6$  g/cm<sup>3</sup>) magnesium will become an interesting substitute. Various processes, such as squeeze-casting, spray-forming, powder metallurgy, and gravity casting, are used to manufacture composites [19–21]. Most moulding processes permit almost final outlines, but many still require a finishing by machining because of the better size and shape accuracy, i.e. defined surface qualities.

The above survey of non-reinforced alloys demonstrated that magnesium has excellent machining abilities and is even amenable to HSC machining. This is evident from the low tool wear and low tool loads, as well as the good surface qualities. However, the machining of composites is a different matter. The main problem with machining composites is of course the high tool wear caused by the hard and abrasive fibres or particles. New and economically viable methods must be developed for a further industrial use of composites.

Polycrystalline diamonds are successfully used for machining composites; they are very hard and thus very abrasion resistant. Two limitations still have to be considered. Multiple tooling with PCDs is difficult and the design of complex tools (e.g. screw taps) is limited. Another problem is the very high costs; a 6 mm drill costs 350 € compared to 35 € for a

corresponding hard metal tool. However, coating technology is advancing, and therefore solid hard metal tools coated with TiAlN or diamond might become established for machining composites.

Knowledge of the correct machining parameters is of vital importance for an optimized machining process. However, since the volume of magnesium composites produced is still small, these parameters are still imperfect. The same is true for the choice of a specific cutting material, i.e. the coating for each composite.

### 8.6.1 Experimental Constraints

Experiments on the machining of magnesium composites have been focused on drilling for several reasons. First of all, drilling has tremendous implications for screw and rivet joints. Furthermore, specific difficulties such as chip transportation through a narrow flute do not arise in the same way as in milling or turning. Additionally, tools with PCD coatings are very costly and complex, hence this area in particular will profit from the development of hard material coatings.

For the experiments, solid hard metal drills of the type HW K10 with a fine grit of  $< 0.7 \mu\text{m}$  (FK), i.e.  $1\text{--}3 \mu\text{m}$  (MK) and a four-sided cut were available. The TiAlN (3400 HV) and diamond coatings (10,000 HV) were segregated with PVD, i.e. CVD, on the fine-grained hard metal tools.

The first magnesium composite studied was a fibre-reinforced AZ91 cast alloy containing 20 vol.%  $\delta\text{-Al}_2\text{O}_3$  short fibres (800 HV) made by squeeze-casting. The second material investigated was a particle-reinforced ZC63 alloy containing 12 vol.% SiC particles (3400 HV,  $D = 10 \mu\text{m}$ ). The latter is a commercially available composite made by traditional melting metallurgy.

### 8.6.2 Tool Wear

The tool wear when machining magnesium composites must be considered fairly early, while for non-reinforced magnesium alloys wear at the cutting edge only occurs after long drill distances (*cf.* Fig. 6). The wear mechanism responsible is abrasion caused by the hard reinforcement fibres or particles (800–3400 HV). During machining, these particles or fibres impinge on the cutting edge and slip on the flank and the face of the tool. In this way, the cutting material is mechanically and thermally stressed, especially under dynamic loads.

Different abrasion mechanisms can be operative depending on the relationship between the cutting material and the reinforced phase of the composite. The hardness, volume fraction, and dimensions of the hard material are especially important (Fig. 13).

Zum Gahr distinguishes between micro-ploughing, micro-fatigue, micro-machining, and micro-cracking [22]. Micro-ploughing occurs when a hard particle enters the material's surface, the cutting material in this case, and causes plastic deformation through the relative movement. If only pure ploughing occurs, no material is removed. If several particles enter the surface, the multiple plastic deformation leads to fatigue and ensuing abrasion. This abrasion mechanism is usually of secondary importance in machining, as the cutting materials are typically very strong and resistant towards plastic deformation. Nevertheless, high stresses at the contact areas between the cutting material and reinforcement

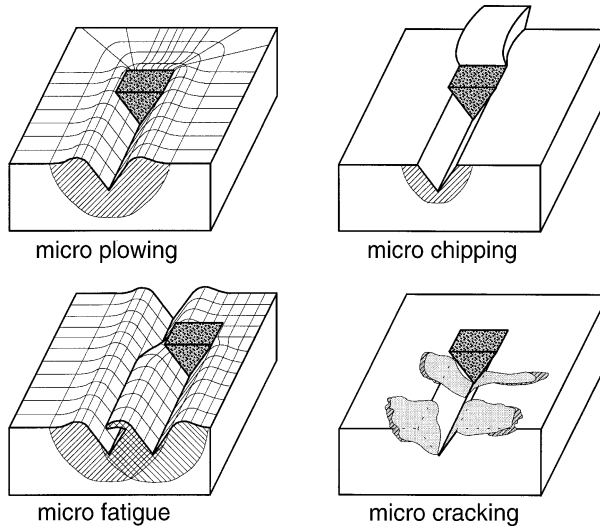


Figure 13: Abrasion wear mechanisms

phase can lead to plastic deformation. In micro-machining, the material is removed as small chips. This mechanism mainly occurs when the cutting material is much weaker than the reinforcements and the grain size of the cutting material is smaller than that of the reinforcement particle or the fibre size. In the case of micro-cracking and fatigue, small cracks are initiated in the cutting material due to the high dynamic loads that occur when the particles or fibres hit the cutting edge surface. Thus, the cutting material needs to be harder than the reinforcements.

Drilling experiments were conducted with a fibre-reinforced magnesium alloy and uncoated hard metal drills. The hardness of the reinforcement phase was fairly small, and hence a constant tool wear was predicted. This assumption was confirmed by experiments in which the cutting speed was varied (Fig. 14).

The tool wear of the drill flanks measured 25 to 45 mm. Higher cutting speeds led to higher tool wear. As a consequence of the contact between the cutting material and the reinforcement fibres, the surface is smoothed, as confirmed by SEM analysis. This behaviour is suggestive of micro-cracking, where micro-cracks are initiated on the tool surface by particles hitting it. Afterwards, particles from the cutting material become loose and smooth the surface by gliding movements comparable to lapping. The increased wear of the flanks with increasing cutting speed is attributable to dynamic stresses, which result in crack formation. Another influencing variable is the higher thermal load on the cutting material, which also increases with increasing cutting speeds.

At the maximum cutting speed,  $v_c = 300$  m/min, i.e. with the highest flank-wear, additional measurements with TiAlN and diamond coatings were carried out. Different results were obtained for these two coatings. The TiAlN coating is much harder than the substrate; it sticks to it very well and has a good wear protection. The flank-wear is much reduced compared to that with the various non-coated hard metals. However, the topography of the active surface is also somewhat smoothed, pointing to micro-cracking as one wear mechanism. With diamond, on the other hand, significant flaking occurs. Two reasons may be proposed for this failure. On the one hand, the problem might be insufficient

coating stability, resulting from non-optimal substrate preparation or errors during the coating. Impact stresses of the fibres at the higher cutting speeds might be another reason. The fracture toughness of the extremely hard diamond coating (10000 HV) is evidently much higher than that of the corresponding TiAlN coating (3400 HV), which might explain the flaking. It is clearly apparent that optimized cutting parameters are required for a successful use of coatings.

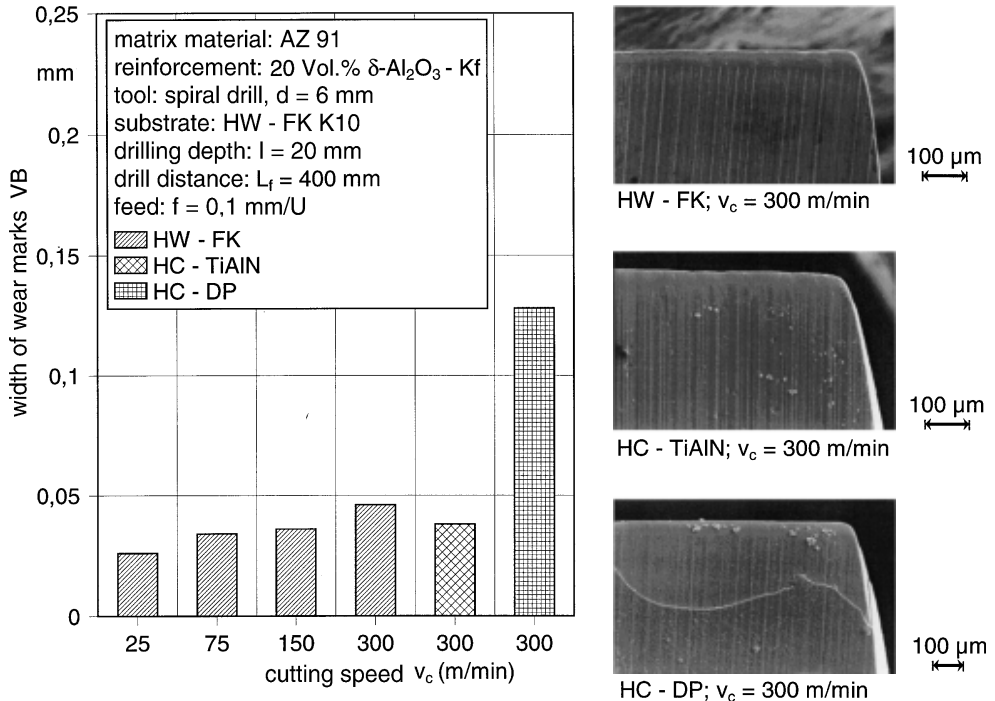


Figure 14: Tool wear when drilling fibre-reinforced magnesium

The influence of the feed on the flank wear was analyzed for fibre-reinforced AZ91 at a cutting speed of  $v_c = 75$  m/min (Fig. 15). Higher feeds were found to lower the wear on the flanks. Increasing the feed directly influences the feed force and therefore the mechanical stress as well. Despite this, higher feeds with equal drill distances have a greater influence because they reduce the contact time between the cuts and the reinforced material. Generally speaking, higher feeds are favourable. When drilling thin structures, however, care must be taken to avoid possible deformations of the components.

Particle reinforcements cause considerably higher tool wear than fibre-reinforced magnesium alloys (Fig. 16).

Using an uncoated hard metal drill, an experiment had to be aborted early after a drill distance of  $L_f = 100$  mm, since wear had already advanced too far. The tool's flanks showed deep ridges, probably caused by micro-machining. In this case, the hard particles are able to ridge the weaker tool material. This can be prevented by means of a diamond coating, but there will be progressive wear as soon as the diamond coating is removed from the



cutting edge. The bonding of the coating is very good in this case, and therefore it is assumed that the failure of the coating is mainly due to a low fracture toughness combined with high dynamic stress.

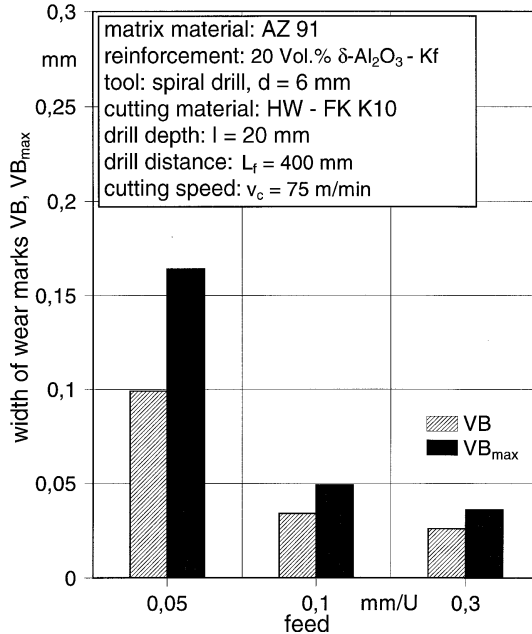


Figure 15: Influence of the feed on the tool wear when drilling fibre-reinforced magnesium

The diamond coating behaved better at a higher feed of  $f = 0.4$  mm/rotation. Only the edges of the cuts showed some coating failures. This means that a diamond coating is more suitable for pressure loads from higher feeds than for dynamic loads as occur with high cutting speeds.

A closer SEM analysis of the diamond-coated cutting edges showed no abrasion ridges like those seen on the hard metal. Flattened active surfaces could be seen instead, again pointing to micro-cracking as a wear mechanism.

The reference for these experiments was a diamond-tipped drill, which showed the least flank wear despite a twofold greater drill distance.

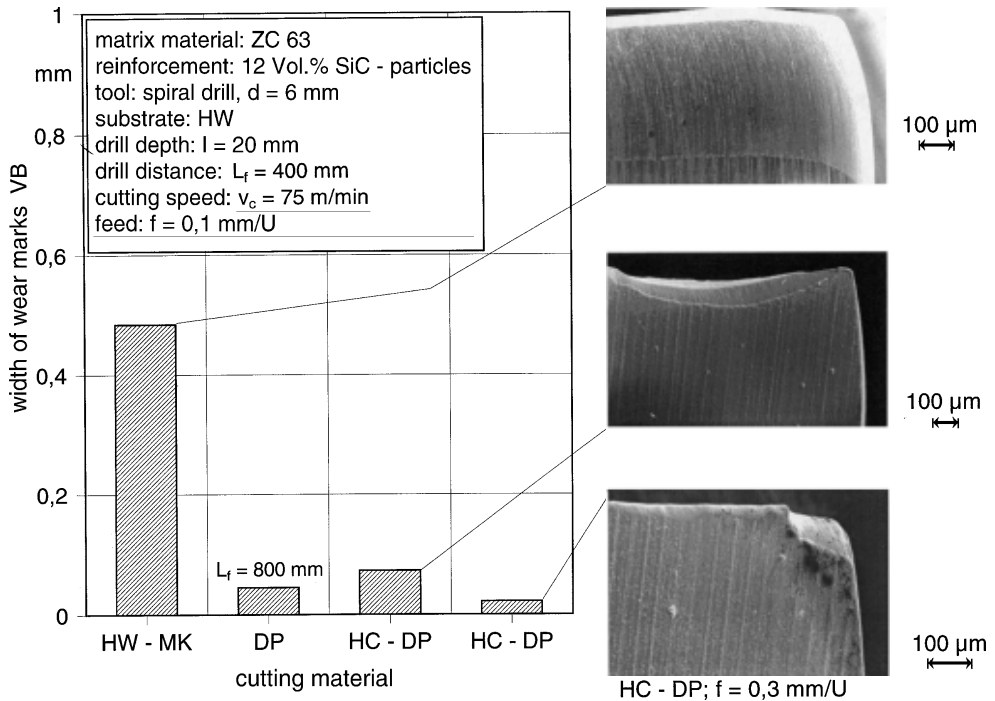


Figure 16: Tool wear when drilling particle-reinforced magnesium

### 8.6.3 Mechanical Tool Load

The force measurements during the drilling of non-reinforced AZ91 showed only small loads on the tools. Comparison between the reinforced and non-reinforced material is supposed to show any change in the tool stress. Figure 17 shows measured feed forces and drill moments during the machining of various magnesium composites.

The comparison refers to very short drill distances, to eliminate influences of the tool wear on the force. As already assumed, the values of the feed force and drill moment are lowest for conventional magnesium. A reinforcement, whether particle or fibre, invariably leads to higher loads. The drill moments are identical despite different matrix alloys and different reinforcements, i.e. volume fractions. However, the feed force shows greater differences. While the feed forces are almost equal among the short-fibre alloys, they are significantly higher for particle-reinforced alloys.

Figure 18 shows how the tool wear acts on the mechanical tool stresses. It displays the feed forces and drill moments for hard metal and polycrystalline diamond (PCD) as a function of the drill distance. Using the hard metal tool for machining, flank wear occurs very quickly in the shape of a rounded cutting and chisel edge. Thus, the contact areas between the material and the cutting material grow, the friction rises, and more chipping occurs. Additionally, the feed force increases from 450 N to 1100 N, whereas the drill moment only increases by 50%. In comparison, the diamond tool is charged with less stress

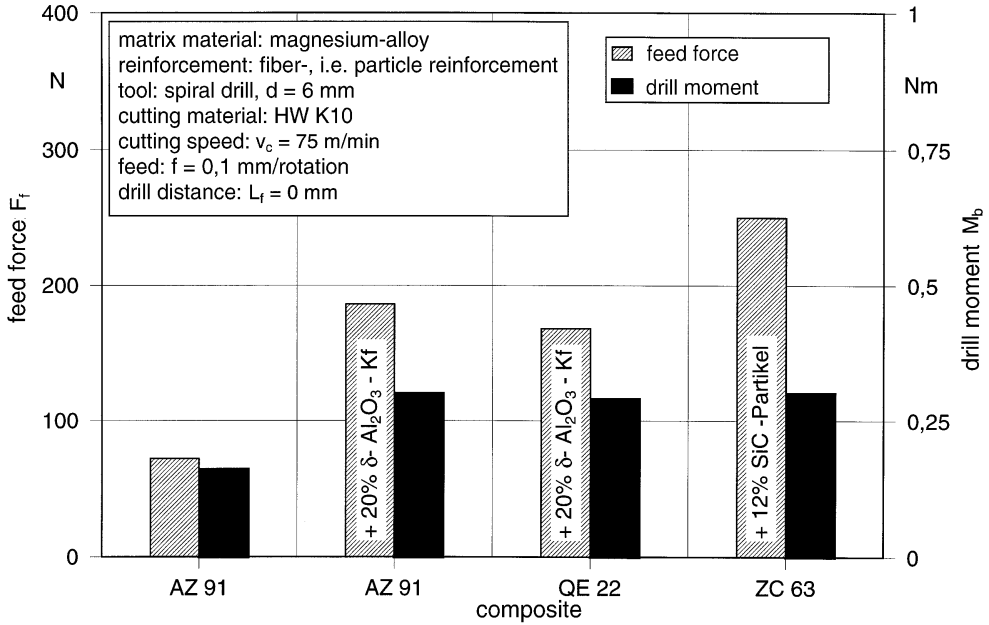


Figure 17: Feed force and drill moment when drilling various magnesium composites

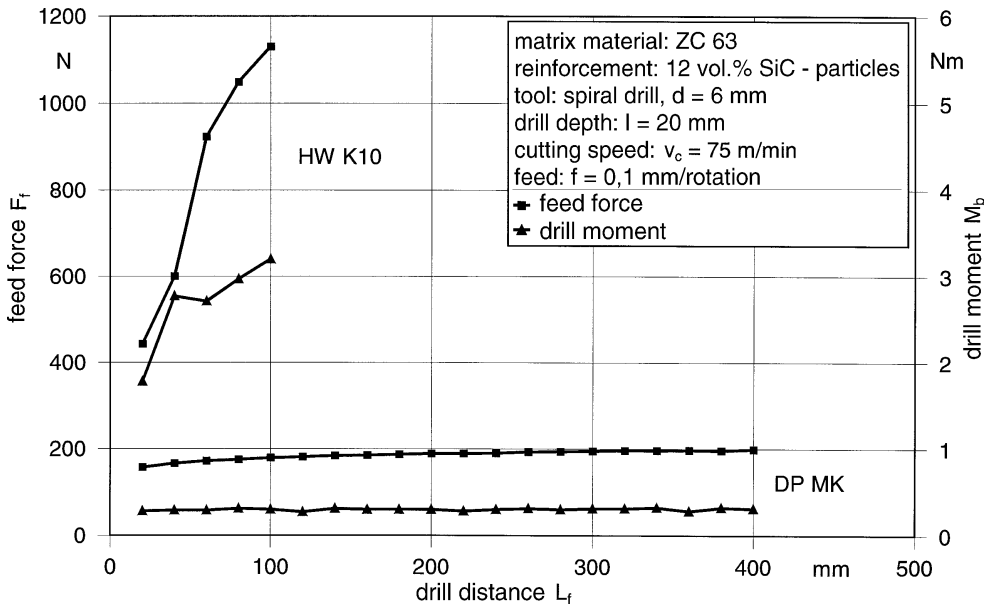


Figure 18: Influence of the tool wear on the feed force and the drill moment when drilling particle-reinforced magnesium

( $F_f = 190 \text{ N}$ ,  $M_b = 0.3 \text{ Nm}$ ), which remains almost constant throughout the whole drill distance. Similar behaviour was observed with a diamond-coated tool (not shown in the figure).

### 8.6.4 Component Quality

The properties of the machined workpiece surface are important criteria for the evaluation of the material machinability because the surface determines the serviceability. The machining directly influences the surface fringe; the physical properties (microstructure, hardness, internal stress) and the geometrical properties (shape deviation, roughness, waviness, and surface damage such as cracks) are especially important. To characterize the surface properties after machining, the surface roughness was examined and the surface was analyzed by SEM. Furthermore, the microstructure was analyzed.

The measured roughnesses following drill-machining of magnesium were rather low. The arithmetic mean average roughness lay between  $R_a = 0.1$  and  $0.7 \mu\text{m}$  for both fibre- and particle-reinforced magnesium composites. The averaged roughness was  $R_z = 0.8$  to 4 microns. The roughness changes during the course of the machining. New tools are very sharp and cause a greater roughness than partly worn and rounded tools that have served a certain drill distance.

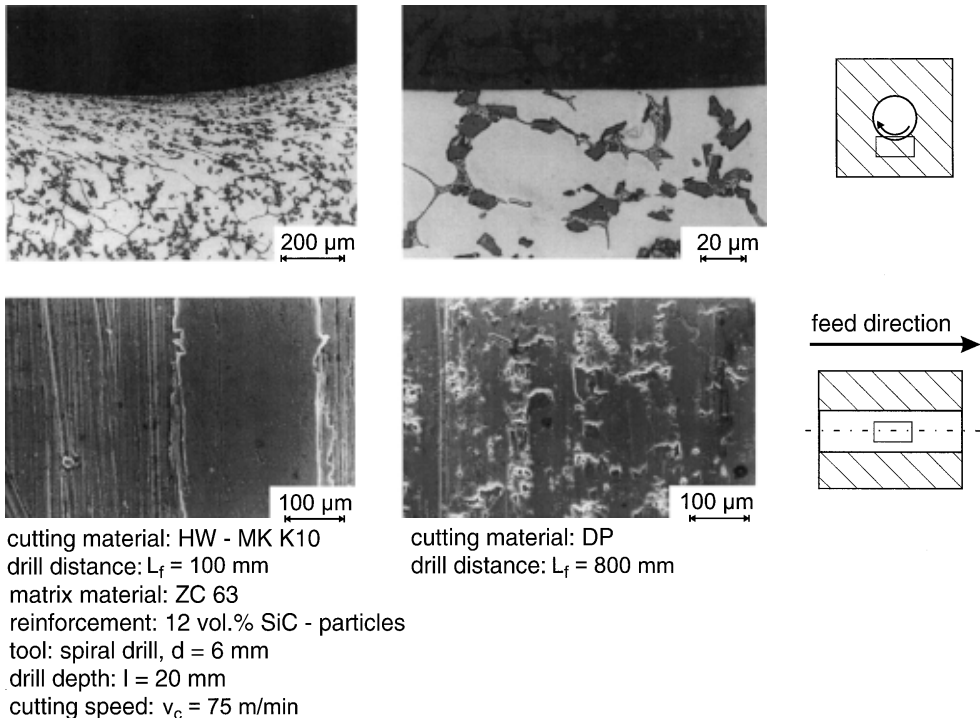


Figure 19: Surface and fringe when drilling particle-reinforced magnesium

The trend in the hole diameters was rather variable, with both undersized as well as oversized holes being measured. Besides thermal expansion of the composite, mechanical yielding of the material itself is another reason for this. Polycrystalline diamond has good heat conductivity, thus the process temperature is low. Therefore, the composite does not expand and this is not the cause of any undersized holes. On the other hand, this effect will arise with hard metal tools, especially at higher cutting speeds.

The influence of the machining on the surface properties is very important for composites, because it may adversely affect the component's function. Broken fibres were detected in the drilling experiments on AZ91. This influence of the fringe area was caused by plastic deformations at the fringe. However, this effect mainly occurs at a higher tool wear and more in the direction of the perimeter than in the longitudinal direction. The influenced zone extends to approximately 20 mm.

Figure 19 shows an extraordinary example of edge-zone influences. With particle-reinforced magnesium composites, the tremendous wear on the hard metal drill causes an extended layer of plastic deformation up to 200  $\mu\text{m}$  deep. The diamond-tipped drill, on the other hand, shows no influence at all after  $L_f = 800$  mm.

There are differences between the surface topologies drilled with hard metal or PCD-coated drills. The plastic deformation forms a very flat surface with the hard metal, and depositions can still be found in some areas. The PCD-drilled surface shows characteristic pores. This occurs because particles lying close to the surface are separated by the hard cutting edge of the tool.

## 8.7 Summary

Magnesium is capable of heavy duty machining; this was shown by the tests concerning the load on tools. The feeds currently used could easily be increased, but it is unreasonable to increase the cutting parameters beyond those used here in experiments on drilling and reaming. No further reduction would be achieved, since the end of the machine's dynamic range would then be reached. It makes more sense to optimize the cutting speeds and especially feeds for complex machining operations. For drilling and precision boring, a high quality is attained, even for increased cutting parameters.

Changing to a minimum amount of lubrication does not reduce the drill quality either. The need to adapt the safety concept toward the MLS still needs to be discussed.

Machining experiments on reinforced magnesium alloys have shown that the tool wear, depending on the reinforced phase, is much higher compared to that with conventional materials. This wear corresponds to the hardness of the reinforcement phase and the hardness of the cutting material. Wear can be reduced using diamond-tipped tools. Hard material coatings based on TiAlN or diamond offer an alternative to PKD tools. Optimization of the cutting parameters and an adjustment of the coating hardness to the reinforcement hardness are fundamental for a successful application. The tool load is increased irrespective of the tool wear through particle- or fibre reinforcement. As regards component quality, i.e. roughness of the machined surfaces, the roughness heights are low. The diameter deviation on drilling ranged from undersize to oversize. Drilling particle-reinforced magnesium with hard metal led to an extensive influence of the fringe area.

## 8.8 Literature

- /1/ Albright, D. L.; Ruden, T.: Magnesium Utilization in the North American Automotive Industry. *Light Metal Age*, April 1994, p. 26-28
- /2/ Bolstad, J.: Magnesium ein überlegener Werkstoff für Bauteile. *Metall* 44 (1990) 6, p. 589-592
- /3/ Bonk, H.: Brand- und Explosionsschutz bei der Magnesiumbearbeitung – Sicherheit im EG-Binnenmarkt. Bohren und Fräsen im modernen Produktionsprozeß. Fachgespräch zwischen Industrie und Hochschule, 21./22. Mai 1997, Dortmund, p. 165-177
- /4/ Friedrich, H.; Schumann, S.: The Use of Magnesium in Cars: Today and in Future. Proc. of the 1st Israeli International Conference on Magnesium Science & Technology, 10.-11. November, Dead Sea, Israel
- /5/ Kaufeld, M.: Hochgeschwindigkeitsfräsen von Leichtmetallguß im Stirnschnitt. *Werkstatt und Betrieb* 123 (1990) 2, p. 143-145
- /6/ Messmann, W.: Automobil-Druckguß läßt Magnesium expandieren. *Metall* 43 (1989) 12, p. 1194-1198
- /7/ Schnier, M.: Fertigungskonzepte zur Magnesiumbearbeitung. Bohren und Fräsen im modernen Produktionsprozeß. Fachgespräch zwischen Industrie und Hochschule, 21./22. Mai 1997, Dortmund, p. 179-191
- /8/ Tokisue, H.; Kato, K.: Turning machinability of magnesium alloy castings for high-temperature structures. *Aluminium* 66 (1990) 5, p. 479-482
- /9/ Tomac, N.; Tønessen, K.; Rasch, F. O.: The Use of Water Based Cutting Fluids in Machining of Magnesium Alloys. International Conference on Innovative Metal Cutting Processes and Materials. P. 107-113, Torino, Italy, 02.-04. Oct. 1991
- /10/ Weinert, K.; Biermann, D.; Schroer, M.; Schulte, K.: Hochgeschwindigkeitsbearbeitung mit Einschneiden-Reibahlen – Bearbeitung von Aluminium-Druckguß und Vergütungsstahl mit unterschiedlichen Kühlschmierstoffkonzepten. VDI-Z Special Werkzeuge August 1997, p. 22-27
- /11/ Weinert, K.; Liedschulte, M.; Opalla, D.; Schroer, M.: Bohren, Reiben und spanendes Gewinden von AZ91HP. Tagungsband zur 1. Plenumsitzung des Projektes Madica, 05./06. März 1998, Aalen
- /12/ Weck, M.; Marpert, M.: Maschinenseitige Anforderungen an die Magnesiumbearbeitung. Tagungsband zur 1. Plenumsitzung des Projektes Madica, 05./06. März 1998, Aalen
- /13/ Beer, S.; Henning, W.; Liedschulte, M.: MMC-Motorenkomponenten: Herstellung und Eigenschaften. In: *Spanende Fertigung*, Hrsg.: K. Weinert, Ausgabe 2, Vulkan-Verlag, Essen, 1997, p. 333-346
- /14/ Essig, G.; Henning, W.; Mielke, S.: Faserverstärkte Serien-Preßgußkolben. *Ingenieur Werkstoffe* 5 (1991) 3, p. 48-50
- /15/ Köhler, E.; Ludescher, F.; Niehues, J.; Peppinghaus, D.: LOKASIL-Zylinderlaufflächen – Integrierte Verbundwerkstofflösung für Aluminium-Zylinderkurbelgehäuse. *ATZ/MTZ-Sonderausgabe Werkstoffe im Automobilbau*, 1996
- /16/ Richter, D.: Bremsscheiben aus keramik-partikelverstärktem Aluminium. *Aluminium* 67 (1991) 9, p. 878-879
- /17/ Tank, E.: Erfahrungen bei der Erprobung von experimentellen Motor-Bauteilen aus faser- und partikelverstärkten Leichtmetallen. *Metall* 10 (1991) 44, p. 988-994

- /18/ Zeuner, T.; Sahm, P.R.: Gegossene, lokal verstärkte Leichtbaubremsscheiben für Hochgeschwindigkeitszüge. *Ingenieur-Werkstoffe* 7 (1998) 1, p. 32-35
- /19/ Degischer, H.-P.: Schmelzmetallurgische Herstellung von Metallmatrix-Verbundwerkstoffen. In: *Metallische Verbundwerkstoffe*, DGM Verlag, Oberursel, 1994, p. 139-168
- /20/ Kainer, K.U.: Herstellung und Eigenschaften von faserverstärkten Magnesiumverbundwerkstoffen. In: *Metallische Verbundwerkstoffe*, DGM Verlag, Oberursel, 1994, p. 219-244
- /21/ King, J.F.; Wilks, T.E.: Development of Lightweight Castable Magnesium Alloy Composites. *Proc. of the 51. IMA-Conf.* 17.04.-19.04.1994, Berlin, p. 26-31
- /22/ Zum Gahr, K.-H.: *Microstructure and Wear of Materials*, Elsevier, Amsterdam-Oxford, 1987

# 9 Joining Magnesium Alloys

*A. Schram, Chr. Kettler, ISAF, Technical University Clausthal*

## 9.1 Introduction

The growing environmental impact of vehicle emissions, scarce resources, and the constraint to save energy have led to extensive research work with the aim of developing extremely light and at the same time recyclable construction materials. With this in mind, magnesium and its alloys are constantly gaining more importance. Besides the development of new alloys with improved properties, it is also necessary to study their joining ability with respect to high performance welding techniques and special joining methods in order to create the basic requirements for specific applications.

Magnesium alloys have become important materials for cast mass products and semi-products in a variety of industrial fields, such as the automobile branch, the computer industry, and in communications and electronics. For a more extensive use of magnesium and its alloys in these industrial areas, there need to be more concepts developed for magnesium alloys with special regard to the mechanical and tribological as well as the physical properties of the materials.

This chapter gives an overview with regard to the joining of magnesium alloys. Besides the development of joining, emphasis is also placed on single joining methods and their special features in relation to the process. The aim is to give an overall impression of the possibilities concerning the joining of magnesium alloys.

## 9.2 The History of Joining Magnesium

Some 116 years ago, in 1886, the first magnesium production through electrolysis started in Hemelingen and introduced a new era for technically usable magnesium. However, it took until 1921 for the production of magnesium to become suitably developed to yield fully operational materials.

The publications on joining referred to gas welding and the optimization of the welding flux and the additives required for welding (G. Michel, 1924). Gas welding is not used anymore; it does not meet the quality standards for either mechanical properties or for corrosion resistance. For brazing, a similar approach as for aluminium was proposed (Magnesium Handbook 1923), but at that time brazing did not play an important role in joining.

The worldwide production of magnesium was 30,000 t at the beginning of World War II, reaching a maximum of 235,000 t in 1943. Within the scope of developments in aeronautics and motor sports, especially racing, magnesium alloys increasingly gained importance. Concomitantly, joining technology was developed, which allowed the use of magnesium as a construction material for the first time. Riveting was used more and more next to welding. The rivets were processed in hot condition, or else aluminium rivets containing 3–5% magnesium were used because these enabled processing at room temperature.

After the war, arc-welding was mainly used. New joining techniques also offered new application possibilities for magnesium, until the interest in magnesium greatly diminished



at the beginning of the 1970s. Recently, magnesium has undergone a renaissance and this has also prompted new interest in economical joining methods.

Today, high-performance arc-welding processes and, to a great extent, beam-welding processes as well, are of great interest because they offer new possibilities when considering the energy infiltration or economic aspects for mass production [1, 2].

## 9.3 The Different Joining Processes

### 9.3.1 Arc-Welding

Two main processes are used, the metal inert gas (MIG) process and the tungsten inert gas process, i.e. inert arc-welding with a non-consumable electrode (TIG; tungsten inert gas welding). Both methods need only little capital expenditure for new facilities or can use already existing ones. Moreover, both processes may be used for manual welding, which is of importance for small unit volumes or repairs. The disadvantages are lower welding speeds, significantly more extensive heat-affected zones, and higher part distortions compared to beam-welding.

#### 9.3.1.1 The TIG process

Usually, alternating current is used for the TIG-welding of magnesium. As with aluminium, the positive pole is needed to break apart the oxide layer, while the negative pole reduces the heat load at the non-consumable electrode. Today's TIG arcs attain 5 mm in length without any disturbance of the process stability. As inert gas, mainly argon mixed with helium is used, the latter having a positive effect on the penetration depth.

Through flexible use of welding additives, in particular the seam's cross-section and the notch effect of the seam's flanks can be minimized. The use of a filler rod as a bar opens the process to a wider spectrum of available magnesium alloys and is cheaper than using a rolled filler rod. However, a mechanized process still requires the more expensive rolled version.

#### 9.3.1.2 The MIG process

In the past, MIG was only used to a limited extent for welding magnesium. Compared to TIG, welding with a consumable electrode leads to some specific problems with the material:

- melted drops explode at the wire's tip during the separation process and cause splattering
- the amount of energy conveyed to melt the base material is limited due to the low thermal and electrical conductivity
- difficulties stemming from a specific drop detachment from the welding wire because of low amperage and magnesium's low density
- the minimum wire diameter is 1.6 mm, which leads to tremendously raised seams for component thicknesses  $< 2$  mm.

Depending on the deposition rate, two different arcs occur in the welding of magnesium. At low wire feeds, a short-circuit arc is used for welding, whereas an impulsion arc is used at medium speeds; these influence the seam geometry in characteristic ways (Fig. 1).

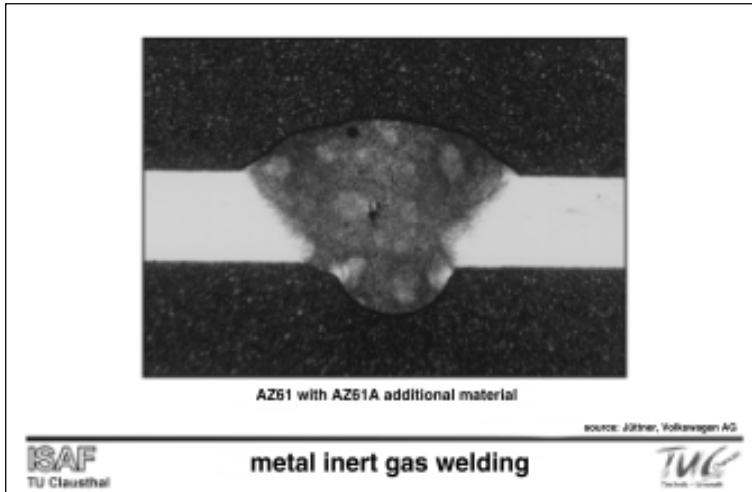


Figure 1: Micrograph of an arc-welded seam

The TIG and MIG processes represent the current state of the art as regards the welding of cast parts in maintenance and production. There is increasing interest in their use in engineering [3, 4].

### 9.3.2 Laser-Beam Welding

With the invention of the first CO<sub>2</sub> and Nd:YAG lasers in the mid-1960s, the application of lasers for material working began. Since then, laser systems have been increasingly used for working with materials, and since the 1980s this has been viewed as a key technology, especially for joining components.

Laser-welding can be divided into two types, which differ from each other in the laser generation and source. On the one hand, there are gas-lasers, their laser source being a resonator filled with a defined gas mixture. Solid-state lasers, on the other hand, have a crystal rod made of neodymium-doped yttrium/aluminium garnet.

The key difference between the two systems lies in the wavelength  $\lambda$  of the emitted light. The wavelength  $\lambda$  of a solid-state laser is 1.06 microns, whereas that of a CO<sub>2</sub> laser is  $\lambda = 10.6$  microns. This difference can have a tremendous influence on the welding speed, depending on the absorption behaviour of different materials. Both systems have specific advantages, justifying a parallel use. A CO<sub>2</sub> laser can have an output power of more than 30 kW and is more efficient than a Nd:YAG laser at 20–30%.

Modern solid-state lasers have a maximum output power of 5 kW, and their efficiency is around 10%. These values approach the limits for their technical use. The big advantage of a solid-state laser is that it is possible to use fibre optics for the beam guidance. This allows a very flexible application of the laser system. In addition, the Nd:YAG laser can work with a pulsating induction of energy, and thus even materials with poor absorption behaviour can be fully penetrated [5].

For all measurements carried out to date, solid-state lasers with 1 to 2.5 kW output power have been used. The sheets welded were between 1.0 and 3.2 mm thick and the

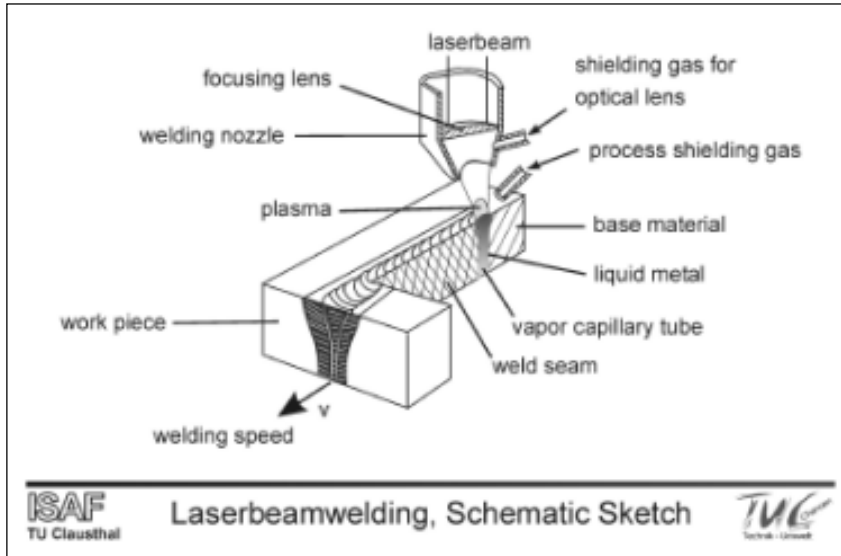


Figure 2: Schematic of the laser-welding process

welding speed ranged from 2.5 m/min up to 9.0 m/min (Fig. 3). The excellent absorption behaviour of magnesium is crucial in this regard. Laser-welded magnesium wrought alloys almost match the base material strength; pores and penetration cuts can be eliminated by suitable adjustment of the parameters [6]. Figure 3 shows a schematic representation of a laser-welding.

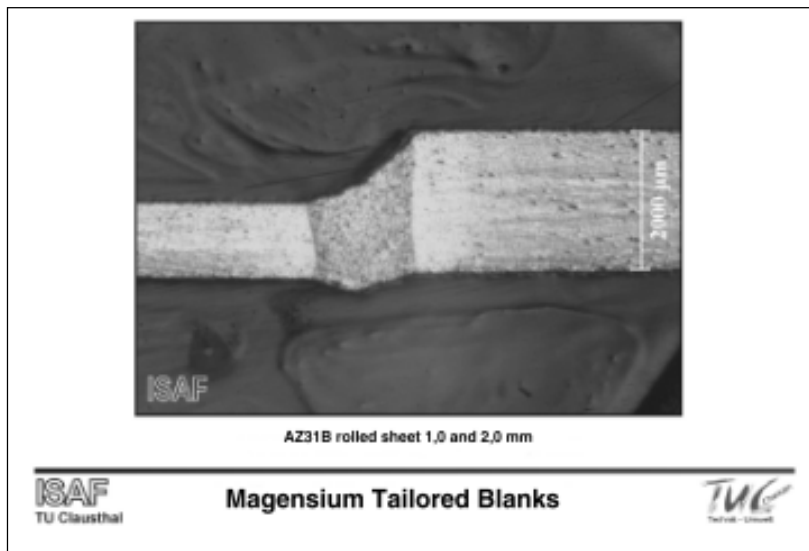


Figure 3: Cross-sectional view of an Nd:YAG laser-welding

The only limitation for welding magnesium alloys is the lack of available welding wires. As yet, only AZ61A and AZ92A are available as addition materials. Besides, wires of less than 1.6 mm in diameter are rare, and below 1.2 mm nothing is available at all. The price of the material is still too high for an economic use due to a complex production process and a low demand. However, the extension of the application field to automated welding should have a positive influence.

### 9.3.3 Electron-Beam Welding

Electron-beam welding under normal atmospheric conditions (NV-EBW) is a key technology that has already become established in some application areas, e.g. in the welding of aluminium and its alloys, especially in the U.S.A. [8]. The process is distinguished by a fast production, improved integration abilities for production lines, and an easier handling than electron-beam welding in vacuo because it obviates the effort of creating a vacuum [9]. The use of additional materials to prevent notches at seam borders and descending seams with thin components, or for the welding of different materials, has become easier as well. Favourable economic factors are the low running costs and a rather high efficiency of the beam generation [10]. Furthermore, the welding plasma is permeable to electrons and does not affect the possible welding speed. Changes in the beam efficiency due to reflection or absorption are negated in this case.

NV-EBW has the following advantages:

- high efficiency
- high process safety and availability
- good coupling of the beam, even in light metals
- low reflection
- metal plasma is permeable to electrons
- high power density
- high process speeds
- high potential for automation
- lower running costs than laser-beam welding

There are some restrictions to its use:

- limited working distance
- X-ray shielding necessary
- high expenditure costs (typical for beam processes)

As in conventional electron-beam welding, the beam for NV-EBW is generated in a vacuum. However, the acceleration voltage usually starts at 150 kV or higher. Afterwards, the beam leaves the vacuum through a special gate set-up, consisting of an array of shutters, and emerges into the atmosphere. From there on, it is led to the workpiece through a small gap of air or inert gas. As soon as the beam enters the atmospheric gas, it interacts with the molecules and gets wider. This effect can be reduced by means of stirring or by using an inert gas (Fig. 4). For more reactive metals, the use of helium is suggested to prevent pore formation. Besides, the heating up of the transferred gas results in a lower density, thus limiting the widening of the beam. The same behaviour can be observed when the beam passes through metal vapour during welding [11].

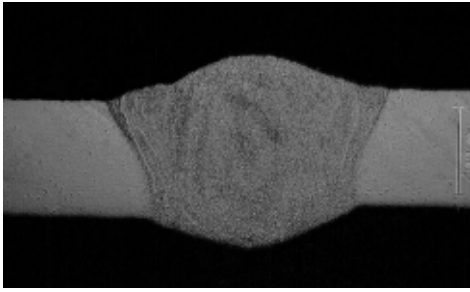
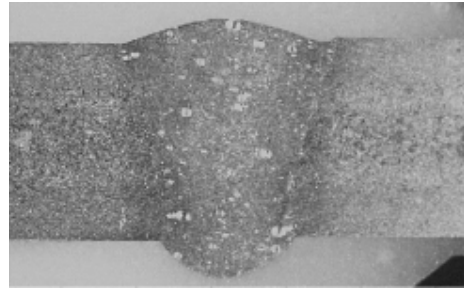
AZ31B / AZ61A,  $s = 1,3$  mmAM50A / AZ61A,  $s = 3$  mm

Figure 4: Seams of NV-electron-beam weldings

### 9.3.4 Friction Welding

The friction welding process belongs to the group of pressure welding. The heat for the welding of the clamped parts is provided by friction. This friction is generated by the relative motion between a clamped and a rotating component. The two parts are then pushed together without any additives. The final welding shows a pad typical for this process. The rotation is stopped after a sufficient heat input. This type of heat input is also the reason for a relatively low joining temperature ( $<T_0$ ). For this reason, friction welding is suitable for material combinations or for materials that are difficult to join [12].

Figure 5 lists the three stages of the friction-welding process. During the first stage, one component is set in rotation and a hydraulic axial feed brings the two surfaces into contact. The friction between the surfaces produces energy in the second stage. The friction energy depends on the rotational speed  $n$  and the friction force  $F_1$ . The friction force  $F_1$  and the gathering force  $F_2$  are increased during the braking in the third stage [13].

Reproducible weldings between similar and dissimilar magnesium alloys have been achieved within the scope of the conducted tests [6]. The aim of ongoing tests is an optimization of the mechanical and technological properties with a homogeneous pad formation for similar and dissimilar alloys (Fig. 6).

Besides this, the process allows the welding of different types of materials since there is no liquid phase that could lead to intermetallic phases. For the combination of steel and aluminium, this method is already applied on a large scale, and has opened a wide field of application for this composite design.

The advantages of friction welding are listed below:

- no additional material
- no inert gas
- high degree of automation
- no fluid phase
- production of composite designs
- minimum influence on the base material

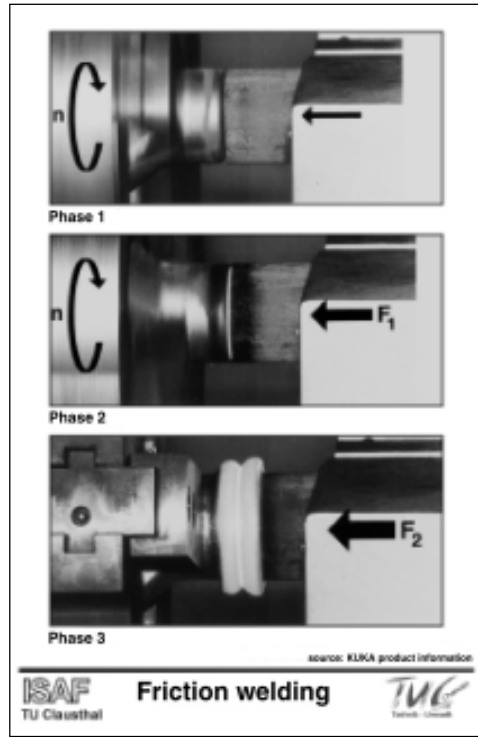


Figure 5: Friction-welding process steps

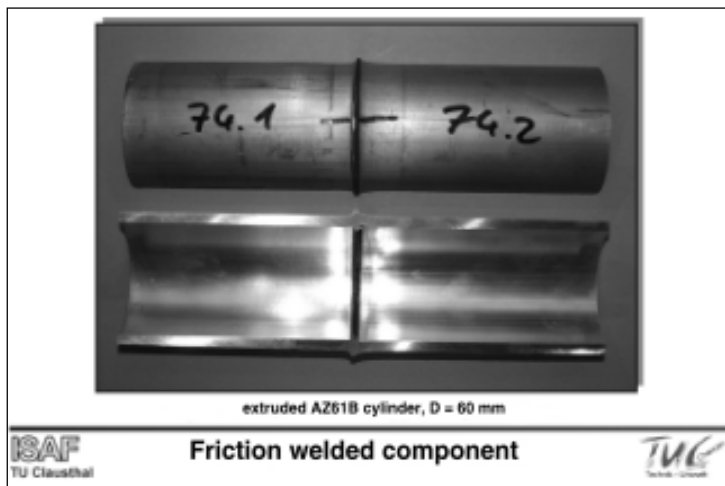


Figure 6: Friction-welded magnesium component

### 9.3.5 Diffusion Bonding

Diffusion plays a key role in superplastic deformation processes that proceed at high deformation temperatures but at very slow speeds. Hence, it is possible to combine superplastic shaping with diffusion bonding in a single process [14]. This might be very interesting for magnesium alloys that otherwise could only be cast because of their limited deformability.

Today, this SPF/DB method is especially used in the aviation industry for titanium alloys, e.g. Ti6Al4V, which are very tough to handle. It has become an established production method. In this way, even complex components can be produced from titanium sheets and profiles, which would never be possible by conventional methods.

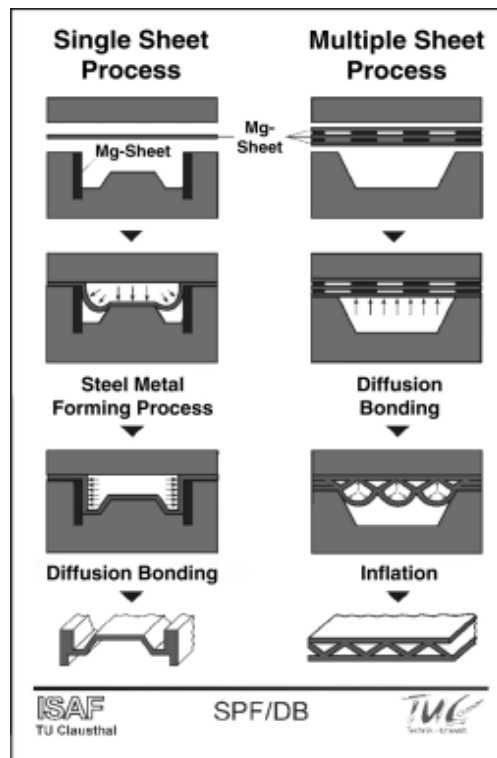


Figure 7: Combined production methods: superplastic metal forming/diffusion bonding

### 9.3.6 Glueing

Glueing is one of the most flexible processes for joining components of similar and dissimilar materials. The intermedium glue layer effectively prevents contact corrosion, which often occurs with screw joints. A great advantage of this layer is that it has good damping behaviour, especially for alternating stresses.

The poor ageing and heat resistance and the low strength are rather bad compared to welding. The main cause of failure, however, is not the poor strength, but an insufficient preparation of the surfaces before glueing. Adhesion, as the working mechanism, is strongly dependent on the surface structure. This needs further study, especially for magnesium components [15].

## 9.4 Weldability of Different Magnesium Alloys

Magnesium alloys can be separated into two groups (Fig. 8):

1. Casting alloys
2. Wrought alloys

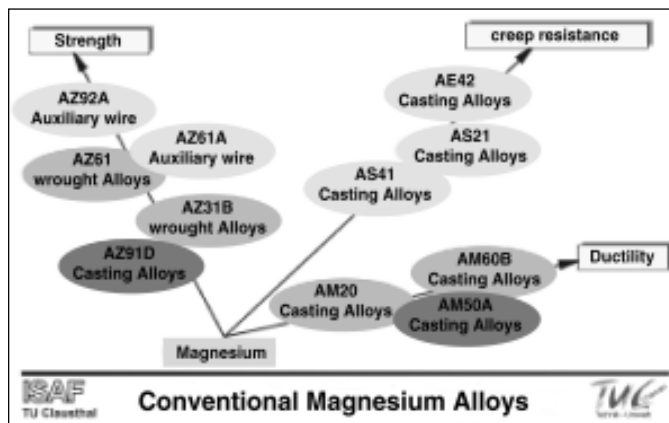


Figure 8: Development of conventional magnesium alloys

The different production methods of the casting alloys influence the weldability of the semi-products. Processing sand or ingot casting is without problems with respect to welding and is often applied in maintenance and production. The first results from welding in engineering have also appeared [6]. Figure 9 shows the weldability of different alloys depending on the alloying elements and their content. It gives a summary of the most widely used alloying elements and their effects on regular magnesium alloys.



alloying elements: <ul style="list-style-type: none"><li>– Al: 2–10% brittleness due to intermetallic phases; increase in strength</li><li>– Zn: &gt;1% tendency towards microporosity; increase of grain refinement</li><li>– Mn: up to 2% improvement of weldability</li><li>– RE: no heat treatments, higher creep resistance</li><li>– Si: reduced corrosion resistance</li></ul> oxidation tendency: surface oxide layer: <ul style="list-style-type: none"><li>– TIG: cathodic cleaning</li><li>– MIG: (+) polarity</li><li>– mechanical processing (brushing)</li><li>– chemical de-oiling</li><li>– etching</li></ul>
--

Figure 9: Parameters of the weldability of magnesium alloys

During the welding of castings, serious problems with pore formation occur in the melting bath. Tests have shown that, as for aluminium, dissolved process gas is released during the melting. Additionally, the pores can grow in the melt because they were first enclosed under high pressure. This growth is unfavourable since the pool becomes foamed and then freezes. Thus, the supporting cross-section of the seam is reduced and this results in unacceptable mechanical properties. This specific behaviour can be combatted in two ways. One possible strategy is to avoid joining methods involving fluid phases; friction welding may be mentioned as one possibility here. The other solution is to suppress pore formation during the casting process, e.g. by using vacuum- or thixo-casting [16]. With developments of this kind, satisfactory weldings can be expected in the future (Fig. 10).

The production method does not influence the weldability of wrought alloys in a negative way. Besides extruded profiles, sheets will become applied more and more in all kinds of areas. This will not only be achieved through improved production methods, but also through the development of suitable joining methods.

The heat input of the welding process influences the base material, as seen for other wrought materials. The extent of the heat-affected zone depends on the welding process. Meltings at grain boundaries, grain growth, and precipitations can be identified in the heat-affected zone. The dissolution or dislocation of fine grains, which can lead to pronounced softening, needs to be considered when the recrystallization temperature is exceeded. With the right joining process and additional material, there will be no effect on the mechanical properties.

In essence, it can be said that wrought alloys are highly weldable.

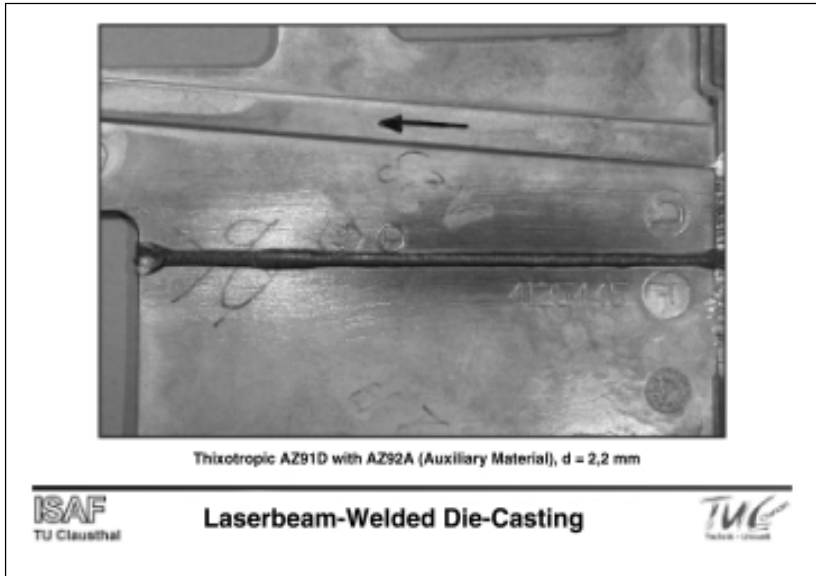


Figure 10: Laser-welded component made of thixotropic magnesium

## 9.5 Summary

Until recently, the welding of magnesium has been limited to the maintenance and production of cast parts. To this end, mainly melting welding methods such as MIG or TIG have been used. Rising requirements in terms of the design and properties of components will necessitate the welding of different casting and wrought alloys in engineering, although there are some limitations to the processing of magnesium alloys.

Magnesium has a great potential for lightweight concepts that are gaining in importance, but some further effort is still necessary in the research and development of joining methods before it can contribute fully to solving problems as a construction material.

The variety of joining processes, with their specific advantages, form the basis of a wide application field. In turn, this demands an equally broad-based development of these processes.

## 9.6 Literature

- /1/ Schichtel, G.: „Magnesium-Taschenbuch“, VEB Verlag Technik Berlin, 1954.
- /2/ Meyer, R.J., et al: „Gmelins Handbuch der anorganischen Chemie: Magnesium“, Verlag Chemie, GmbH, Weinheim/Bergstraße, 8. Auflage, 1952.
- /3/ Danzer, W., Lehner, C.: „Fügen von Magnesium“, Vortrag, Magnesiumabnehmerseminar, Aalen, 8./9.10.1997.

- /4/ Jüttner, S.: „Arc Welding of Magnesium Alloys“, Vortrag, IIW Seminar, Trends in Welding of Lightweight Automotive and Railroad Vehicles, Wels, Austria, 26.-28.2.1997.
- /5/ Beyer, E., et al.: „Laserstrahltechnologien in der Schweißtechnik“, DVS Verlag, Bd. 86, Düsseldorf 1989.
- /6/ Draugelates, U., Schram, A., Kettler, Chr.: „Prozeßführung und Gestaltungskonzepte für das Fügen komplexer Bauteile“, Arbeitsbericht SFB 390, Teilprojekt B3, Clausthal/ Hannover, Feb. 1998.
- /7/ Draugelates, U., Schram, A., Kettler, Chr.: „Laserstahlschweißen und Reibschweißen von Magnesiumlegierungen“, Vortrag, Schweißen und Schneiden '98, DVS-Berichte Band 194, Hamburg, Sep. 1998.
- /8/ Draugelates, U., Bouaifi, B., Bartzsch, J.: „Elektronenstrahlschweißen an Atmosphäre von Bauteilen aus Aluminium und seinen Legierungen“, Innomata '96, Dresden, 7.-9.Mai 1996.
- /9/ Fritz, D.: „Der Elektronenstrahl an freier Atmosphäre – eine wirtschaftliche Wärmequelle für das Schweißen von Massenteilen in der Serienfertigung“, Konferenz Strahltechnik SLV-Halle 1996.
- /10/ Aichele, G.: „Die strahlende Idee. Das Werkzeug Elektronenstrahl“, Schweizer Maschinenmarkt (1995) Heft 19, P. 62-65.
- /11/ Draugelates, U., Bouaifi, B., Bartzsch, J., Ouaisa, B.: „Advanced Technology for Cold Chamber Die Properties of Non Vacuum Electron Beam Welds of Magnesium Alloys“, Vortrag, DGM-Tagung, Magnesium Alloys and their Applications, Wolfsburg, April 1998.
- /12/ „Reibschweißen von metallischen Werkstoffen“, DVS-Merkblatt 2909, Teil 1, 3/1989.
- /13/ „Das schnelle und vielseitige Fügeverfahren: Reibschweißen“, Produktinformation, KUKA-Schweißanlagen + Roboter GmbH, Augsburg, 1996.
- /14/ Draugelates, U., Schram, A., Kedenburg, C.-C.: „Superplastische Eigenschaften und Diffusionsschweißen von Magnesiumwerkstoffen“, Arbeitsbericht SFB 390, Teilprojekt C1, Clausthal/Hannover, Feb. 1998.
- /15/ Budde, L., Bischoff, J., Widder, Th.: „Low-Temperature Joining of Magnesium-Materials in Vehicle Constructions“, DGM-Tagung, Magnesium Alloys and their Applications, Wolfsburg, April 1998.
- /16/ Decker, R.F., Cornahan, R.D., Vining, R.E., Walukas, D.M.: „Thixomolding of Magnesium“ 1<sup>st</sup> Israeli Int. Conf. On Magnesium Science & Technology, Nov. 1997.

# 10 Rapid Solidification and Special Processes for Processing Magnesium Alloys

*T. Ebert, Institute for Materials Research and Technology, Technical University of Clausthal*

*K. U. Kainer, Institute for Materials Research and Technology, Clausthal-Zellerfeld  
GKSS Research Center GmbH, Geesthacht*

## 10.1 Introduction

The rapid solidification process (RSP) produces materials with extraordinary and specific properties in the field of near-net-shape manufacturing. Furthermore, because of the extreme cooling rates, the material freezes far away from the equilibrium, which results in a variety of micro- and macro effects.

The advantages of RSP are well known and have already been studied with new and conventional alloys [1]. An increasingly fast freezing process results in a strong morphological change of the frozen microstructure, of the alloy composition, and ultimately of the crystalline structure.

While classical melting metallurgy allows only limited improvements of the properties, e.g. strength, creep resistance, and corrosion resistance, the RSP opens up more options for developing alloys, and thus for designing new and fine structures. The result is highly improved mechanical and physical properties over a wide temperature range.

Looking at the recent publications and patents dealing with the development of alloys and processes for new alloys with improved properties, there is a noticeable focus on the use of RSP methods. Primarily, these methods are melt-spinning, inert gas sputtering, and spray-forming, together with appropriate consolidation techniques. However, the potential for successful development of new alloys has yet to be fully exploited, even though the possibilities for improving magnesium alloys seem to be very good. One of the main reasons for this is the high reactivity of fine magnesium particles. Nevertheless, the studies carried out to date have indicated excellent possibilities even for these materials. The extended freedom in terms of choosing element concentrations and elements not usually present in conventional alloys opens an enormous but still unexploited margin for development.

## 10.2 Processes for Rapidly Solidifying Microstructures

Different moulding processes and production techniques lead to very different cooling rates in terms of the produced volume. Controlled processes, such as continuous casting, die-casting, or band-casting, allow maximum cooling rates of  $10^3 \text{ K s}^{-1}$ . The volume of powders, foils, thin bands, or even wires is very low, so that very fast cooling rates can be reached according to the cooling conditions. These methods are mainly melt-spinning, gas sputtering, or spray-forming. These technologies allow cooling rates ranging from  $10^3$  to  $10^6 \text{ K s}^{-1}$ . Processes involving laser or electron beams, CVD, or cathodic sputtering can

reach extremely high rates up to  $10^{10} \text{ K s}^{-1}$  when they are used for very thin layers or extremely small material volumes ( $\mu\text{m}^3$  scale).

A rapidly solidifying crystal structure can be quantitatively evaluated with the help of the secondary dendrite spacing  $L$ . If  $L$  is  $< 5 \mu\text{m}$ , one may refer to rapidly solidified microstructures (cooling rate at least  $10^3 \text{ K s}^{-1}$ ).  $L$  depends on the temperature gradient  $G$  ( $\Delta T/\Delta X$ ) and on the speed of the freezing front  $R$  ( $\Delta X/\Delta t$ ), whereby various microstructure morphologies can occur depending on the cooling conditions. A distinction is drawn between planar, cellular, and dendritic structures [3]. The temperature gradient  $G$  and the cooling rate  $R$  are related to the actual cooling rate by the following formula [4]:

$$\dot{T} \left( \frac{\Delta T}{\Delta t} \right) = G * R \quad (10.1)$$

The frozen volume assumes a microstructure that is finer and more homogeneous the higher the product of the temperature and freezing front.

The high cooling rates offer tremendous advantages over “regular” freezing. Among other things, a key feature is the forced solution of a higher amount of alloying elements than is actually possible in the solid state. In systems with limited miscibility, the solubility limit is shifted to higher concentrations for increasing cooling rates. In this way, the alloying elements stay forced in the lattice and contribute to the solid-solution hardening. Another positive effect of an increased cooling rate is the reduction or avoidance of macro-segregation. One usually obtains a fine, crystalline microstructure with a homogeneous distribution of the alloying elements, i.e. phases. The distribution in the solid matches the statistical distribution in the melt because the diffusion in the solid is largely suppressed by the rapid freezing. In general, the microstructure will become finer with faster cooling. Depending on the process used, a microstructure with grain sizes between 0.5 and 10  $\mu\text{m}$  can be obtained. By choosing the appropriate consolidating techniques, this microstructure may be largely preserved and can contribute significantly to grain hardening. In addition to the aforementioned improvements, the modified grain structure is linked with a tremendous improvement of the ductility. Depending on the cooling conditions and the alloy, the most important changes of the properties may be listed as follows [1, 5, 6]:

- fine-grained microstructure with a homogeneous distribution of elements and phases
- reduction or avoidance of macro-segregation
- high oversaturation of the solid-solution crystal and therefore extension of the solubility range
- formation of metastable and quasi-crystalline phases
- modified grain shape

Quite a variety of different methods for rapidly solidifying structures have been established in the past. The basic principle of the process is based on the separation of a melt or a locally molten material. To achieve this, the melt is separated into particles by flowing gases or fluids, ultrasound, or moving parts. The particles are then rapidly frozen in the separation medium or with the help of additional cooling. The greater the energy supplied to the melt, the smaller the particles will be [6].

Most methods are based on simple technology and are therefore conducted on a laboratory scale. Since there is a complex variety of technologies, only the most important will be mentioned here. They also highlight the main points for an evaluation of the characteristics of rapidly solidifying magnesium materials. Other known laboratory techniques do reach remarkable cooling rates (up to  $10^9 \text{ K s}^{-1}$ ), but they are very limited in terms of specimen

design for pilot- or production scales. Besides, the fast cooling rates are more of a phenomenological character. Overviews of the technologies used are given in [3, 6, 7].

Fast cooling rates can be divided into two basic processes, irrespective of the type of production and method used.

In the first method, the molten jet or molten drops are guided to a usually water-cooled metal surface, where they rapidly solidify. This method produces thin bands up to 50 mm wide. Cooling rates of around  $10^6 \text{ K s}^{-1}$  are characteristic for such processes. The best known is melt-spinning, which has been used for numerous investigations on rapidly solidifying magnesium due to its simple set-up (Fig. 1a), *cf.* Chapter 3. In this planar-flow process, melt outlet nozzles are positioned directly above a rapidly spinning cooling cylinder. In this way, rapidly quenched bands up to 300 mm wide and with a thickness of roughly 30 mm can be cast.

The bands thus produced are then crushed to sizes between 100 and 500 mm for further processing, which is usually akin to the conventional powder consolidation techniques. The particles are enclosed, preformed, and then compacted through extrusion or forging.

A second, wholly different method for producing RSP magnesium materials is inert gas sputtering, in which the accelerated convection of inert gases (argon, helium, or mixtures thereof) during the separation of the melt jet within the chamber is used for heat removal.

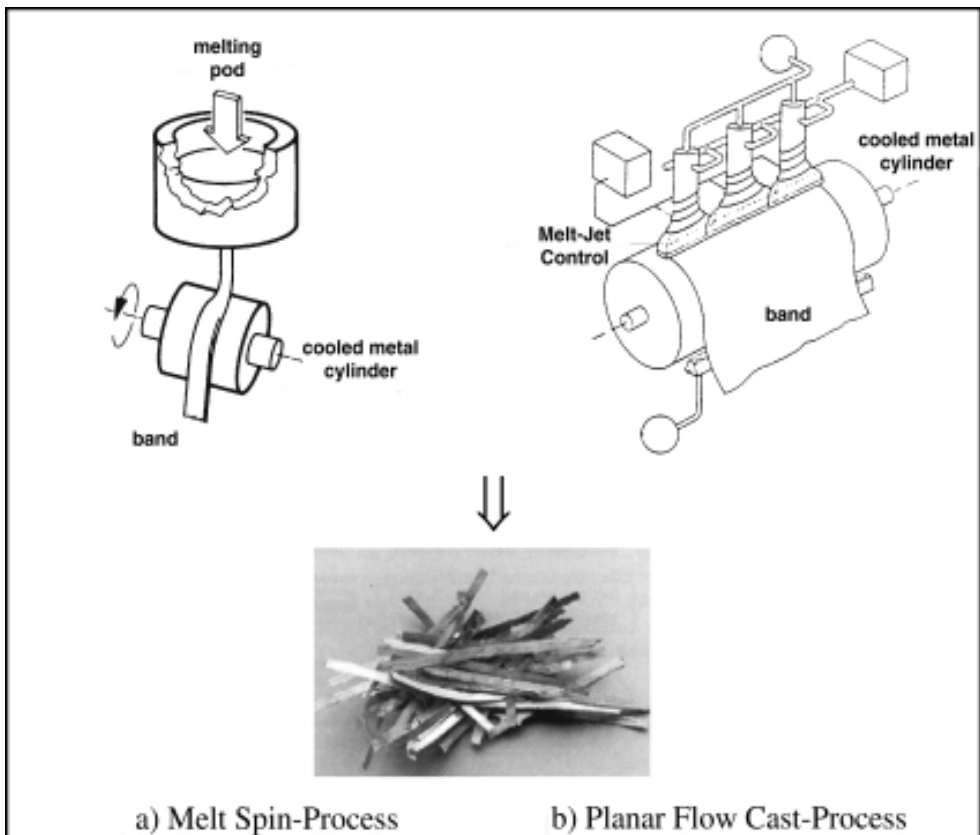


Figure 1:

The particles freeze rapidly within the gas phase and form spherical shapes. They can be post-processed as described above after removal from the chamber (Fig. 2a). The cooling rates are 10 to 100 times lower than in the case of melt spinning. Central to this process are the gas nozzle assembly and the jet control. To separate the jet, so-called Laval nozzles are often used. In a certain section of the nozzle, supersonic speeds are reached (high-pressure sputtering) to improve the separation of the melt and to increase the cooling rate compared to the simple system.

Spray-forming is a technique that has evolved from (inert) gas atomization. It is based on powder production through sputtering of a melt with gas or by centrifugal forces. Most of today's spray-formed products are produced by sputtering. Additionally, the spray can be interrupted by a moveable substrate after a given distance. Under an appropriate liqui-

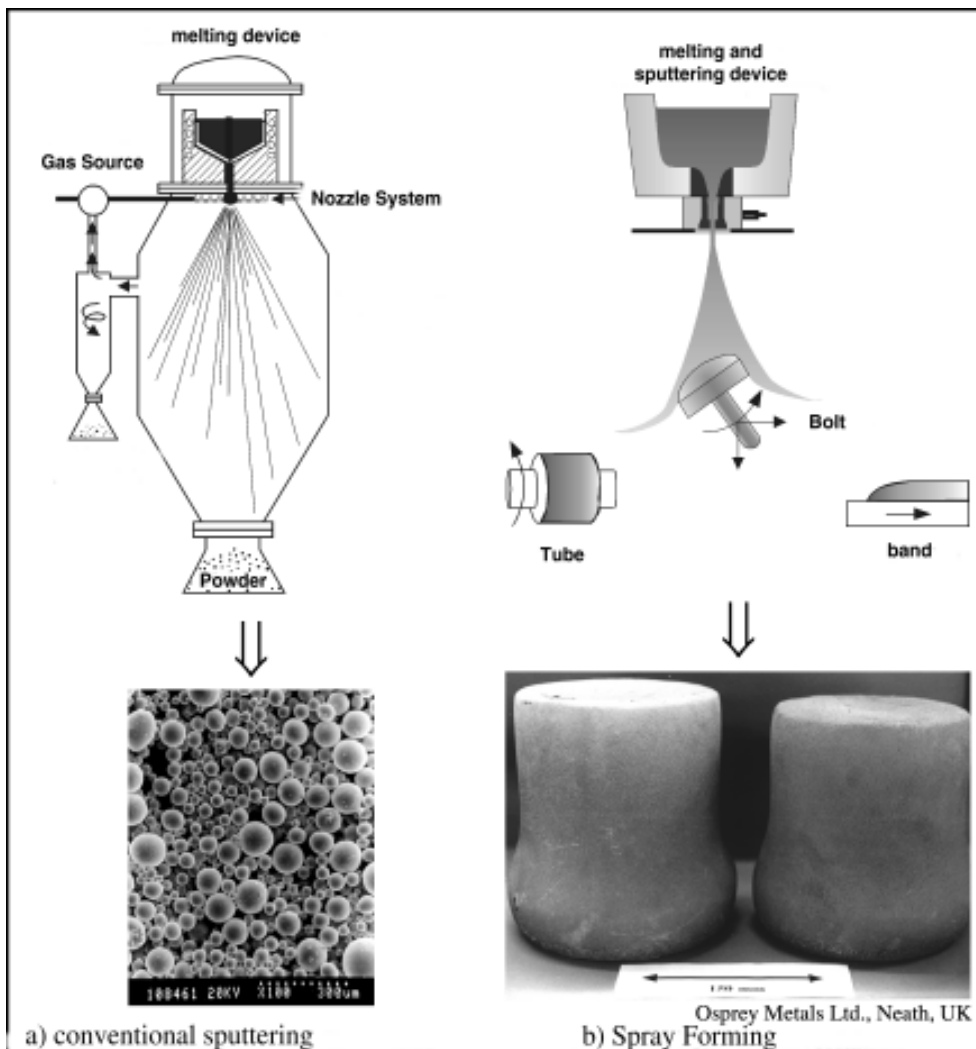


Figure 2: Schematic view of inert gas sputtering and spray-forming

dus/solidus condition, the mixture of liquid, solid, and partly frozen particles separates as a compact semi-product on the substrate. Depending on the process, plate, cylinder, or rotationally symmetrical substrates can be used. Figure 2b shows a schematic of the process. The continuous movement of the substrate in relation to the nozzle, or vice versa, during the spray-forming process allows the creation of semi-products with different geometries. The freezing rates reach rather high values ( $10^3$  to  $10^4$  K s<sup>-1</sup>) compared to conventional melting metallurgical casting methods. Therefore, this method is used for semi-products that show a similar microstructure, and consequently similar material properties, as components made by powder metallurgy methods. At the same time, the length of the process is reduced (*cf.* Section 10.4).

The key feature is that a wide range of characteristic profiles of particles or bands can be achieved with different RSP technologies. The gas flow rate of each assembly and the specific metal determines the cooling rate, which, in turn, determines the particle size and particle-size distribution, and hence the production and energy efficiency of such an assembly as well. The properties of the powder particles (alloy, size distribution, bulk density, flowing ability) depend on their method of production, and influence any subsequent p/m process steps of conventional shaping methods. The process steps need to be critically discussed with respect to aspects of production, although some research results have already shown excellent properties of the rapidly solidified materials. A complex process chain has hitherto inhibited the introduction of this methodology for semi-products or final parts, despite the excellent material properties.

## 10.3 Properties of Rapidly Solidified Magnesium Materials

The production of rapidly solidified magnesium materials with an extended characteristic profile began in 1950 with comprehensive analysis by Busk and Leontis [12]. Gas- and rotational spray-formed powders based on conventional alloys were produced, consolidated by extrusion, and then examined for their microstructures and mechanical properties. Based on these studies, a new series of tests was conducted by researchers at Dow Chemicals USA [13–18] between 1950 and 1960, and later in the 1970s at the U.S. Army Materials and Mechanics Research Center [19, 20].

A breakthrough was the production of a new magnesium base material by a research group at the Allied Signal company in the 1980s. Their studies led to materials with extraordinary properties, which were made by melt-spinning, extrusion, forging, and rolling [21–25]. The potential of these material properties was the starting point for a systematic analysis of the production and consolidation of rapidly solidifying magnesium alloys. The aim was to further develop the mechanical and electrochemical properties of known and new alloy systems to overcome the technological limitations of magnesium. Magnesium is often proposed as a competitor or even as a replacement for aluminium to further reduce weight. The aircraft and space industries, as well as the automotive branch, are mentioned as potential application fields.

Extensive studies of the conversion and corrosion behaviour of melt-spun alloys, as well as the characterization of magnesium alloys with amorphous and semi-amorphous phase components, have contributed to the pace of development regarding the improvement of the properties of rapidly solidifying magnesium materials [2].



Below, some of the most important studies dealing with the improvement of the mechanical and electrochemical properties are briefly outlined. This should give an indication of the property potential that may be realized depending on the production and consolidation method.

### 10.3.1 Sputtered Magnesium Alloys

Busk and Leontis published the first results concerning rapidly solidified magnesium alloy powders in 1950 [12]. Their studies dealt with sputtered alloys based on commercial casting alloys. The inert gas sputtered, mostly spherical particles had sizes between 70 and 400 nm. The preformed green bodies were then extruded into semi-products. Some of the mechanical properties were much improved compared to those of the melting metallurgy materials (Fig. 3).

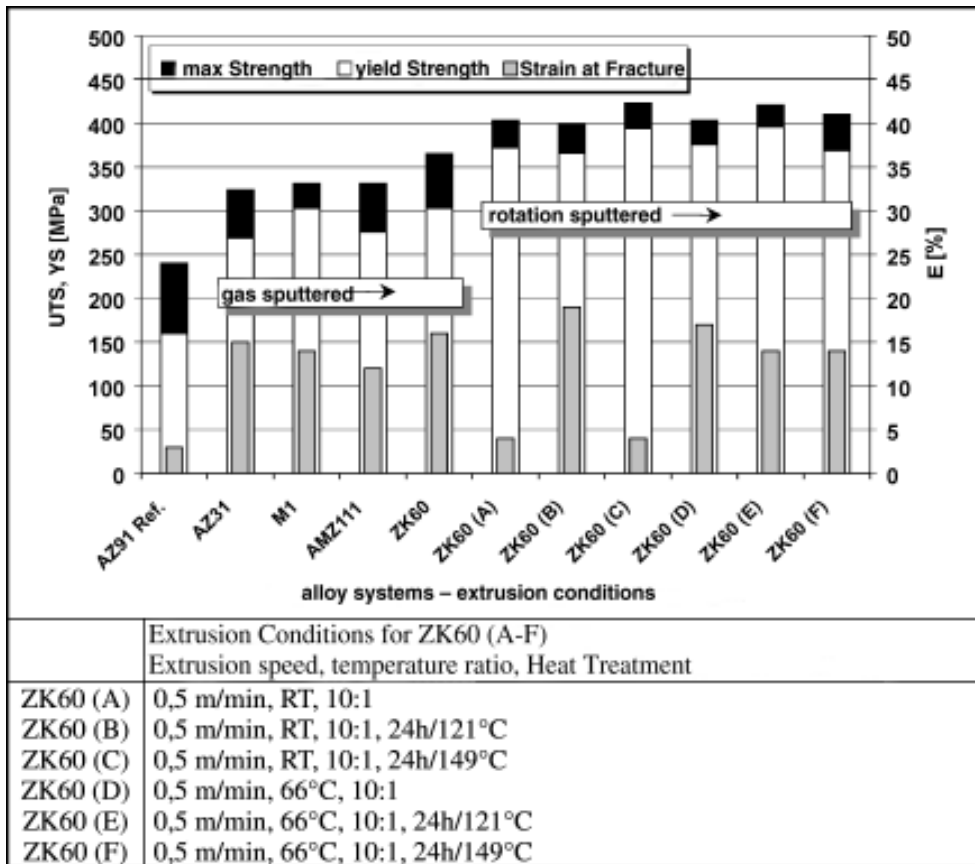


Figure 3: Mechanical properties of rapidly solidified extruded Mg alloys at room temperature [12, 19, 20]; reference alloy AZ91 (die-cast)

Isserow and Rizzitano [19, 20] obtained similar results; they worked with rotation-sputtered ZK60 and examined the influence of different extrusion and heat treatments (Fig. 4). The strength was found to be improved by 50% compared to the cast material. The different ductilities encountered were indicative of a remaining porosity within the extruded semi-products.

Further tests by Krishnamurthy et al. [26] focussed on conventional alloys, as well as new alloy systems of the type Mg/Nd/Zr/Mn and Mg/Li/Al/Si with a view to improving the mechanical and electrochemical properties by rapid solidification processes. The connection between the properties of QE22, ZC63, and AZ91 powders and those of the partly heat-treated semi-products made by extrusion and rolling was addressed by Kainer [28]. The strength was found to be around 400 MPa and is thus much higher than that of comparable, heat-treated, cast materials. The ductility is also increased.

Knoop gathered fundamental knowledge for the production and consolidation of sputtered magnesium powders in his Ph.D. thesis [27]. The main points were the characterization of different technical and experimental alloy powders, the description of the microstructure, and the evaluation of the mechanical properties through extrusion or hot pressing of the consolidated materials.

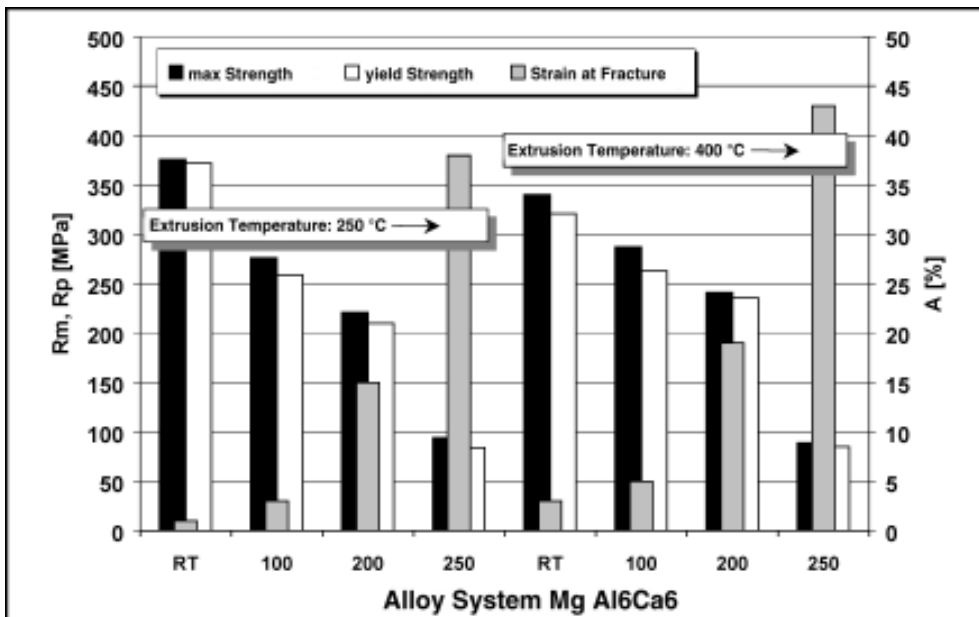


Figure 4: Mechanical properties of sputtered and extruded Mg alloys at room temperature [27]

For the system Mg/Al/Ca, property improvements at room temperature and above were realized by increasing the contents of the alloying elements (Fig. 4). Knoop states that the influence of the extrusion parameters is very important with regard to improving the properties. In his opinion, there is much potential for an improvement of rapidly solidifying, powder metallurgical processed magnesium alloys.

### 10.3.2 Properties of Melt-Spun Magnesium Alloys

Since melt-spinning assemblies are very simple to build and allow high cooling rates, they were employed for many studies during the 1980s. These studies showed some remarkable profiles of RSP magnesium alloys, thereby proving their potential. The possibility of choosing alloys and of setting new states of equilibrium was used as an opportunity by several research institutes and companies to direct specific alloy development towards improving the thermal stability and corrosion resistance. Information about these alloy groups is given in [21, 29, 30]. Below, two comprehensive research works are discussed briefly, which are representative of the characteristic profile of magnesium alloys produced this way.

In this connection, the research group of Chang and Das [21–25] at Allied Signal Inc. contributed fundamental studies between 1985 and 1992. They processed different alloy systems by the planar flow cast method and characterized them with regard to their mechanical properties and corrosion resistance. The variations of the so-called EA/RS alloys are taken as examples from the wide variety of examined alloys (Table 1):

Table 1: Overview of selected melt-spinning alloys

alloy	treatment condition	chemical composition in weight %, Rest Mg					
		Al	Zn	Y	Si	Nd	Pr
EA55A-RS(1)	extruded 1:18	5,1	4,9		1,1		5,3
EA55A-RS(2)	extruded 1:14	5,1	4,9		1,1		5,3
EA55A-RS(3)	extruded 1:14, 30 min 300/350°C, water cooling	5,1	4,9		1,1		5,3
EA55A-RS(4)	extruded 1:14, rolled	5,1	4,9		1,1		5,3
EA55A-RS(5)	extruded 1:14, rolled 2 h 325°C	5,1	4,9		1,1		5,3
EA55B-RS	extruded 1:18	5,1	4,9			5,0	
EA65A-RS	extruded 1:18	5,1	4,9	6,7			

The 20–30 mm thick and 25 mm long bands were ground, enclosed in sleeves, and vacuum degassed, i.e. vacuum heat pressed. The extrusion pivot was then consolidated to produce semi-products on both a laboratory-scale press and a prototype press.

Besides the standard alloying elements Al and Zn, which contribute to strength improvements at room temperature by solid-solution hardening ( $Mg_{17}Al_{12}$ ,  $Mg_2Zn$ ), different rare earth elements and silicon were also alloyed. Averaged densities were given as approximately 1.94 g/cm<sup>3</sup>. The high-melting intermetallic phases such as  $Mg_2Si$ , as well as  $Al_2Y$  and  $Al_2RE$ , were verified, and, together with Mg/RE dispersoids, these contribute significantly to the strengthening at room temperature and above (Fig. 5). The authors are of the opinion that the formation of the aforementioned intermetallic phases stabilizes a very fine microstructure, which persists after extrusion and is responsible for the very good deformability and fatigue strength.

The alloy EA65A-RS stands out for excellent strength and very good corrosion resistance. The best combination of strength, ductility, and castability is obtained with the alloy EA55B-RS, which also gives the best results for fracture toughness with 15 to 20 MPa m<sup>-1/2</sup>.

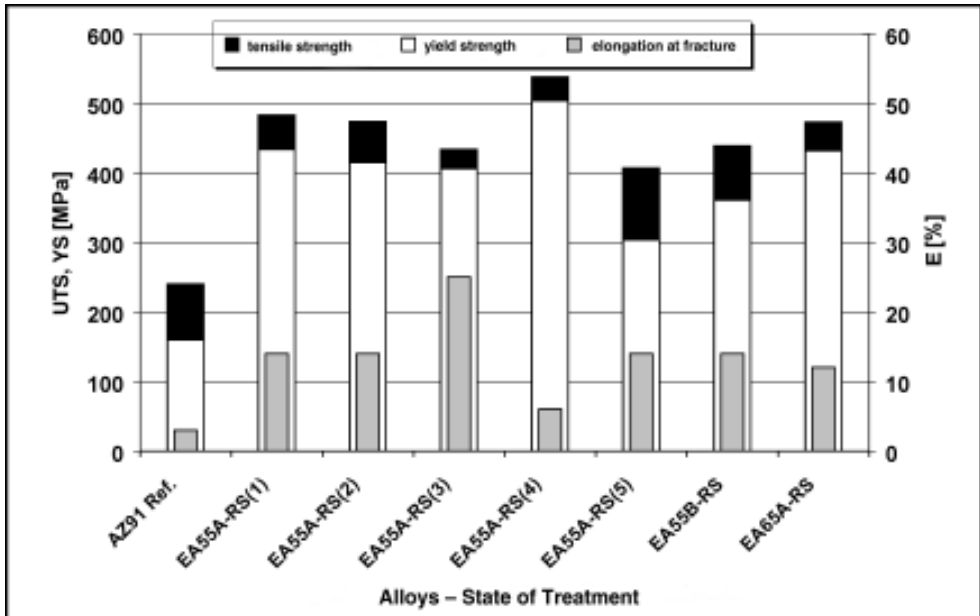


Figure 5: Characteristics of melt-spun and consolidated Mg alloys at room temperature [21–25]; reference alloy AZ91 (die-cast)

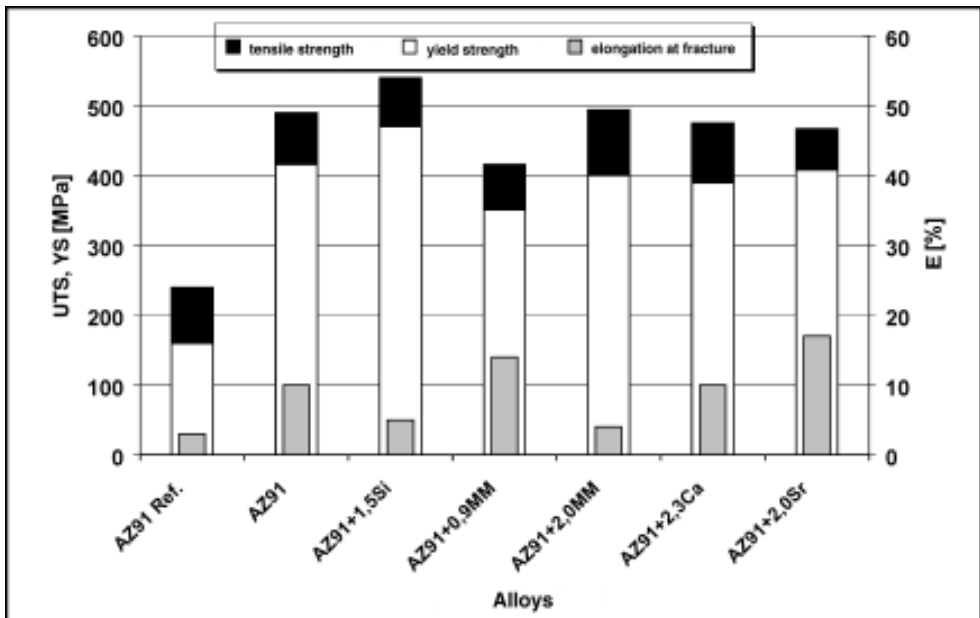


Figure 6: Characteristics of melt-spun and consolidated Mg alloys [31–33]; reference alloy AZ91 (die-cast)

Again, the choice of correct consolidation parameters for a specific adjustment and improvement of the properties is the main consideration. With increasing extrusion temperatures the strength decreases, but at the same time, ductility and fracture toughness improve. Further property improvements were noted following heat treatments. The different strengths in the longitudinal and transversal directions stem from the different degrees of deformation.

Creep resistance is quoted as being low, since the microstructure is very fine.

Similar research work was carried out in a cooperative project between Norsk Hydro and Pechiney, and published between 1989 and 1991 [31–33]. The studies were focussed on the modification of the Allied Signal EA-RS alloys based on AZ91. Mainly Si, Ca, and Sr were used as alloying elements (Fig. 6)

The AZ91 bands made by melt-spinning or planar flow casting had very fine microstructures with grain sizes between 1.5 and 5  $\mu\text{m}$ . Under identical consolidation conditions, differently produced bands gave the same results. Their corrosion and creep behaviour was extensively researched and discussed. The corrosion rate of the rapidly solidified materials was found to be one-quarter of the measured values for the reference material. The effect of Ca as an alloying element has been particularly well-studied; besides having a positive influence on the mechanical properties, it also improves the rather poor creep resistance of the RS-AZ91 alloy.

Compared to conventional AZ91, the microcrystalline RS-AZ91 shows a 100-fold higher creep rate. In the author's opinion, adding 2% Ca leads to the formation of calciferous precipitations at the grain boundaries, which despite the even finer microstructures [Tab. 2], will serve to impede the creep mechanisms. The results are similar to those for Al/Si alloys [2,33].

Table 2: Secondary creep rates of selected magnesium alloys at 150 °C [2]

alloy	stress [MPa]	secondary creep rate [ $\text{s}^{-1}$ ]	grain size [ $\mu\text{m}$ ]
RS AZ91	50	$5,1 * 10^{-6}$	1,5
I/M AZ91	50	$5,9 * 10^{-8}$	11
RS AZ91 + 2%Ca	50	$1,1 * 10^{-8}$	0,7
RS MgAl5Ca5Zn0,7	50	$5,0 * 10^{-9}$	0,7
RS ZK60 + 3% MM	50	$1,2 * 10^{-9}$	0,6
I/M ZE41 T5*	100	$3,5 * 10^{-9}$	> 60
RS ZK60 + 3% MM	120	$2,3 * 10^{-9}$	0,6
I/M QE22 T6**	125	$0,6 * 10^{-9}$	50
* 4 h 215°C			
** 16 h 410°C / quenching / 4 Std. 215°C			

## 10.4 Spray-Forming

### 10.4.1 Potential of Spray-Formed Magnesium Alloys

With this method, new, interesting and unique perspectives and possibilities are opened for magnesium-based alloys and particle-reinforced composites.

This technology is already successfully applied in industry, not only for aluminium and copper, but also for nickel-based alloys and steels. It has contributed to the progress in materials design in terms of more freedom in choosing alloying elements and their concentrations [36, 39–46].

When ceramic materials such as oxides, nitrides, borides and powders are introduced into the spray cone by means of the sputter or transport gas, discontinuous MMCs with a specific profile can be produced. The conditions for the spray-forming may be configured to be inert or reactive, so that the in situ formation of dispersoids or the storage of reaction products is enabled.

There have been only a few tests on the spray-forming of magnesium, even though a lot of improvement is predicted for magnesium-based alloys. Nevertheless, earlier work has proved the excellent possibilities for these metals (Fig. 7).

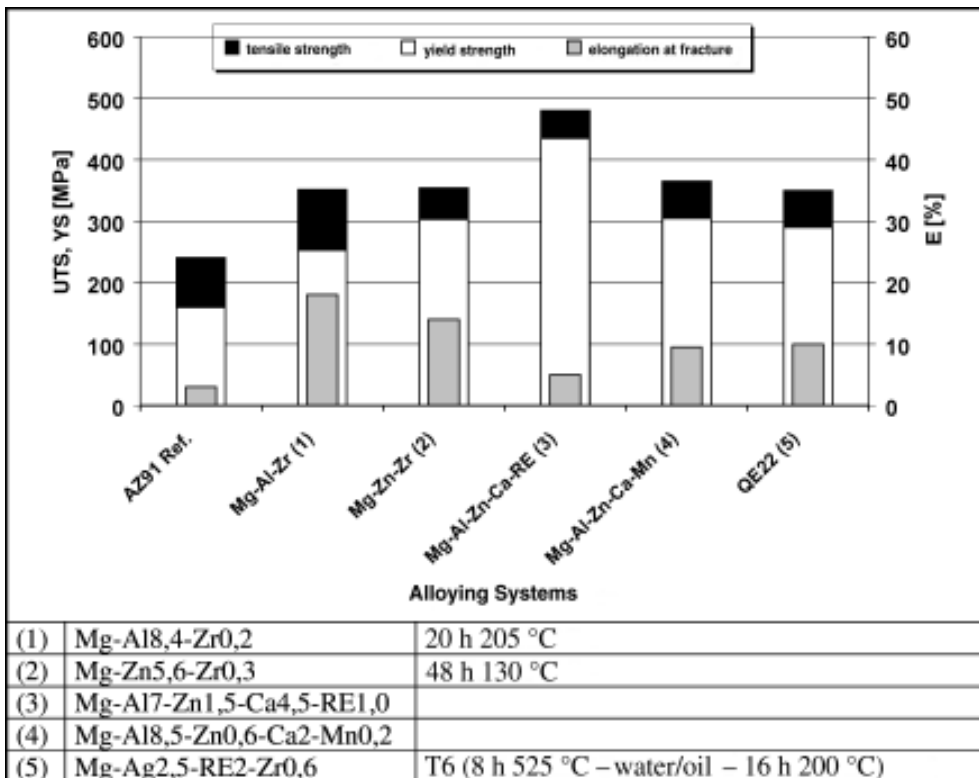


Figure 7: Characteristics of melt-spun and consolidated Mg alloys [2, 37, 48, 49]; reference alloy AZ91 (die-cast)

The first tests on spray-formed and extruded Mg-based alloys were conducted by Lavernia and Grant [48]. They examined the mechanical properties of higher alloyed alloys of the type Mg/Al/Zn/X with different contents of Mn, Ca, and rare earth elements. At higher temperatures, and compared to conventional alloys, these materials show an increase in strength with a simultaneous improvement of ductility. Similar results concerning the alloy systems Mg/Zn/Zr and Mg/Al/Zr were published in a U.S. patent [49].

In situ alloying with spray-forming was exploited by Elias et al. [50], who injected Al powder, i.e. AlSi40 powder, into two manganese-containing Mg alloys. First, one Mg/Mn1 alloy was spray-formed and injected with Al powder (56  $\mu\text{m}$ ) during compacting. Peaks deviating from the base material were found by thermoanalysis (DSC) and ascribed to potential  $\text{Al}_x\text{Mn}_x$  formation, although this was not actually proved. In another experiment, AlSi40 alloy powder (56  $\mu\text{m}$ ) was introduced into an Mg/Mn4 alloy during spray-forming. Optical and electron microscopy revealed very fine precipitations (on a micron scale), which were not believed to be  $\text{Mg}_{17}\text{Al}_{12}$  or  $\text{Mg}_2\text{Si}$  dispersions. The authors justify the formation of the intermetallic phase in terms of added particles that dissolve during co-deposition and reprecipitate in the solid aggregate. Further DSC measurements pointed to the formation of a eutectic Mg/Al/Si alloy. The results obtained for these dispersion-hardened magnesium alloys should pave the way for additional research on other alloy systems and reactants.

The first results of tests on spray-formed magnesium composites produced by co-deposition of SiC particles during spray-forming were presented by Schröder et al. [38] and by Vervoort and Duszczyk [37] in 1993.

The subject matter of the work of Schröder et al. was the influence of the reinforcing components ( $\text{Al}_2\text{O}_3$ ; SiC) in terms of their nature, content, size, and shape on the mechanical properties of the inert gas sputtered and extruded alloy powders AZ91 and QE22. The results were compared with those for a 15% SiC-reinforced, spray-formed QE22 alloy. The improvement of the mechanical properties, especially the Young's moduli, the abrasive behaviour, and the reduced thermal expansion coefficients for this group of alloys was clearly proven for both methods. Since spray-forming has a shorter process chain, it is more beneficial than regular powder metallurgical methods. Both authors emphasized that spray-formed and particle-reinforced composites have definite advantages by virtue of an evenly distributed reinforcement component and less boundary reactivity as a result of short interaction durations with the melt.

The studies of Vervoort and Duszczyk focussed on the heat- and creep-resistant sand-casting alloy QE22. The alloy was studied in spray-formed condition with and without a reinforcing component and was compared with the I/M material. Microstructure, strength, and corrosion behaviour were studied as a function of the extrusion parameters. Even though a good integration of the injected SiC particles, with a homogeneous distribution in the matrix was achieved, the remaining porosity of nearly 20% was due to the process and is less than satisfactory. The remaining porosity was reduced to 4% in the spray-formed, non-reinforced version. Despite rather poor deposition qualities, the non-reinforced and extruded materials showed very good strengths. The strain at fracture of around 12%, as compared to 2% for conventional cast alloys, is worth mentioning.

## **10.4.2 Studies of the Production and Properties of Spray-formed Magnesium within German SFB 390**

Within the scope of the German special research field 390 “Magnesium Technology”, investigations into the production, processing, and properties of spray-formed magnesium materials have been conducted since 1995.

One conceptual focus on spray-formed Mg alloys has been that of the material basis of the influence of alloying elements and process-influenced freezing on the material’s behaviour and the associated correlation between the microstructure and the mechanical properties.

The spray-formed materials are produced on an inert gas sputtering machine at the Institute for Materials Research and Materials Technology of the TU-Clausthal. The material is induction-melted in a pure steel crucible with a capacity of 2.5 to 3 kg.

The key feature of the machine is its induction-heated guide pipe, which transports the superheated melt in precise doses to the nozzle. The process gas hits the melt jet shortly after leaving the Laval nozzle (10–15 mm). It has a diameter of 2–3 mm.

The better productivity and momentum transmission compared to an unguided nozzle assembly is due to this special arrangement of the nozzles. Pressurizing the melting chamber allows the support of gravity during sputtering and ensures a definite and constant melt flow rate.

The mechanical properties of the consolidated material are directly affected by the alloy composition. In this connection, the particle size distribution was measured to ensure reproducibility and reliability of the process. The sputtering temperature and pressure were also varied. The sputtered particles hit a substrate, which was positioned at an axial distance of 400 mm from the fragmentation of the spray-cone. In this way, cone-shaped deposits were made. An argon/oxygen mixture containing 1% oxygen was used as sputtering gas, which was shown to prevent spontaneous reaction when removing powder from the chamber and exposing it to regular atmosphere. The formation of an oxide layer on the particles during fragmentation significantly lowers their reactivity. To ensure a safe handling of the overspray during removal, a further passivation is applied after spray-forming. The alloy powders and deposits were enclosed in AZ31 shells and finally extruded into round bars at different temperatures. With a squeeze ratio of 25:1 and plunger speeds of 3.5 to 4.5 mm s<sup>-1</sup>, extrusion speeds of approximately 3.5 to 7.2 m min<sup>-1</sup> were reached.

## **10.4.3 Choice of Alloying Elements**

A closer look was taken at the testing of ternary systems with rare earth elements, aluminium, calcium, and silicon. The spray-forming experiments have focussed not only on conventional alloys such as WE54 (highly heat-resistant wrought alloy, application temperature up to 300 °C), QE22 (creep-resistant sand-casting alloy), AS21 (die-casting alloy), and AE42 (die-casting alloy with improved high-temperature properties), but also on new ternary Mg/Al/Ca alloys with different proportions of Al and Ca. These commercial alloys were chosen to verify the sputter behaviour of the alloy components and to compare the properties with those achieved by conventional production methods. The new Mg/Al/Ca alloys and the Ca-modified AE42 and AS21 alloys were used to examine the influence of Ca in more detail. Table 3 lists the chemical compositions of the alloys, quantified by means of EDS and X-ray fluorescence analysis:



Table 3: Compositions of the studied alloys in weight %

alloys		alloying elements							
		Ag	Al	Ca	Mn	SE*	Si	Y	Zr
conventional	WE54	-	-	-	-	4,0	-	5,1	0,5
	QE22	2,2	-	-	-	1,8	-	-	0,3
	AE42	-	4,2	-	-	1,5	-	-	-
	AS21	-	2,9	-	0,25	0	1,0	-	-
new or modified	AE42 + Ca	-	4,0	5,6	-	1,3	-	-	-
	AS21 + Ca	-	3,2	4,4	-	-	0,9	-	-
	MgAl9Ca4Si1	-	9,5	4,3	-	-	1,1	-	-
	MgAl3Ca4	-	3,4	4,3	-	-	-	-	-
	MgAl6Ca6	-	6,5	5,9	-	-	-	-	-
	MgAl9Ca6	-	9,4	6,2	-	-	-	-	-

\* SE = Nd-rich rare Earth elements or mixed metal

## 10.4.4 Properties of the Spray-Formed Materials

### 10.4.4.1 Microstructure and porosity in as-sputtered condition

The optical micrographs of WE54 display the microstructure in relation to the axial distance in the sputtered condition (Fig. 8).

The microstructure is homogeneous and equiaxially disposed from the middle to the upper areas of the deposit. The average grain size is 20  $\mu\text{m}$ ; the smallest grains are 10  $\mu\text{m}$

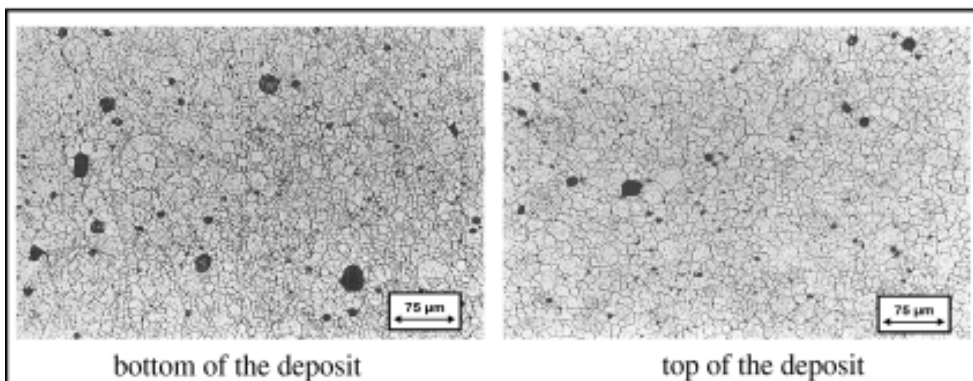


Figure 8: Microstructure of WE54 in the sputtered state

across, the biggest about 30  $\mu\text{m}$ . The boundary area (substrate plate deposit) also shows separate particles due to the rapid solidification, as well as irregular shaped and, on average, bigger pores compared to the upper portion. An average porosity of 2–4% in the deposit cannot be avoided under these conditions, since the gas is entrapped in the particles, and hence in the deposit too. Additionally, turbulences are caused in the preform surface by the sputtering gas. Nevertheless, under these simple sputtering conditions, the final density is sufficient for an almost dense microstructure after consolidation as long as the optimum parameters are used.

#### 10.4.4.2 Microstructure in extruded condition

Different phases were identified in the extruded specimen by means of X-ray diffraction analysis. The identification of the phases for all specimens was made difficult by a superposition of reflections with a characteristic peak widening and an intensity loss. The main interference lines of the phases are often overlaid by the diffraction lines of the magnesium lattice, thereby making a unequivocal identification impossible. The preferred texture

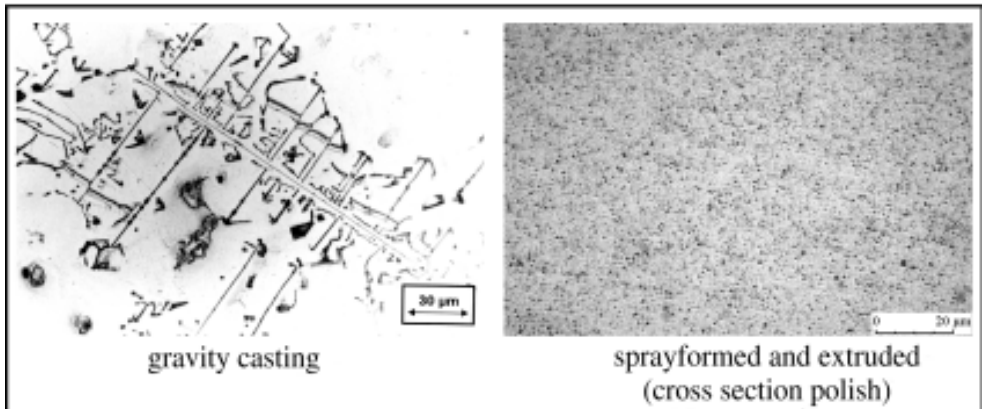


Figure 9: Microstructure of AS21

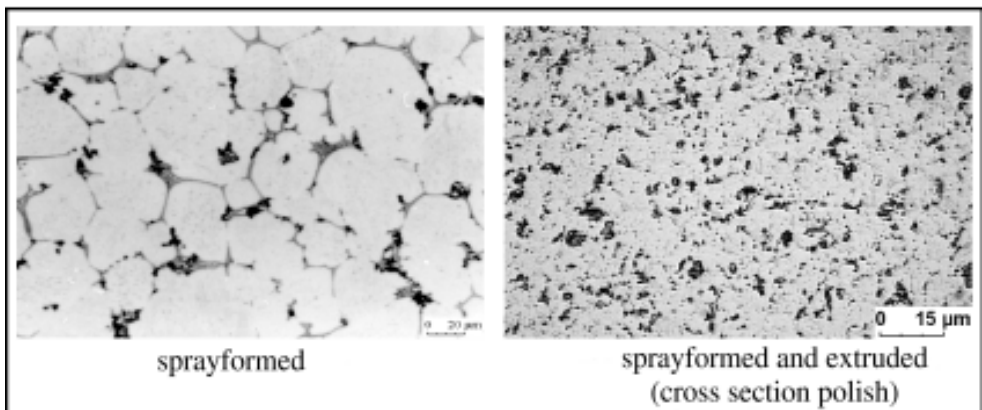


Figure 10: Microstructure of MgAl<sub>3</sub>Ca<sub>4</sub>

orientation following extrusion causes some additional intensities. The phases  $MgO$ ,  $Al_2Ca$ , and  $Mg_{17}Al_{12}$  were identified in the ternary  $Mg/Al/Ca$  alloys. Among the rare earth containing alloys,  $Mg_{12}Nd$  was identified. An unequivocal statement regarding the probable existence of  $Mg_2Ca$  phases and binary  $Al/rare\ earth$  type phases is not possible due to low peak intensities and peak overlays. Figures 9 and 10 show some optical micrographs of spray-formed and extruded magnesium materials.

The spray-formed, conventional alloys show very finely dispersed phases.

Adding Ca to the alloys AS21 and AE42 leads to grain refinement and a multi-dispersive microstructure. The extruded  $Mg/Al/Ca$  alloys are characterized by a distinctive line-type phase composition instead. The whole microstructure appears to be less inhomogeneous and more coarse with increasing alloy content, which stems from the precipitation kinetics of the ternary system  $Mg/Al/Ca$  during sputtering.

#### 10.4.4.3 Mechanical properties

All examined mechanical properties of the produced materials are compared to those of their melting metallurgical counterparts in Figs. 11 and 12:

The spray-formed materials are superior to their melting metallurgy counterparts in terms of their strengths at ambient and higher temperatures. The spray-formed alloys show much improved ductility compared to those produced by all other production methods. Compared to casting alloys, AE42 and AE21 showed higher ductilities at room temperature and higher temperatures, but the fine-grained microstructure led to a drop in ductility beyond 180 °C. The calcium-containing AE42 alloy has excellent strength and emphasizes the potential of rapid solidification on the one hand, and the positive influence of Ca as an alloying element on the other. For the ternary  $Mg/Al/Ca$  alloys, maximum strength values of around 300 MPa were measured.

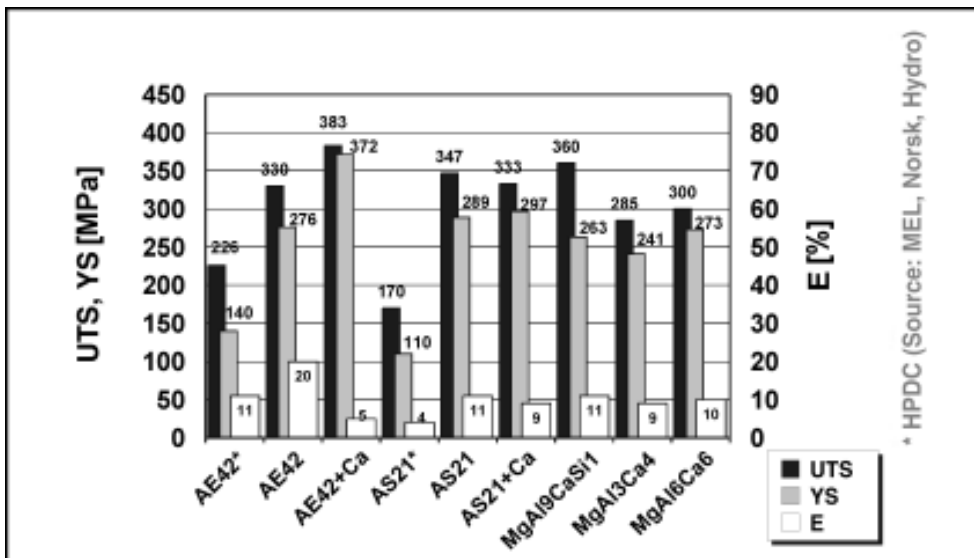


Figure 11: Mechanical properties (tensile strength, yield strength, elongation at fracture) at room temperature

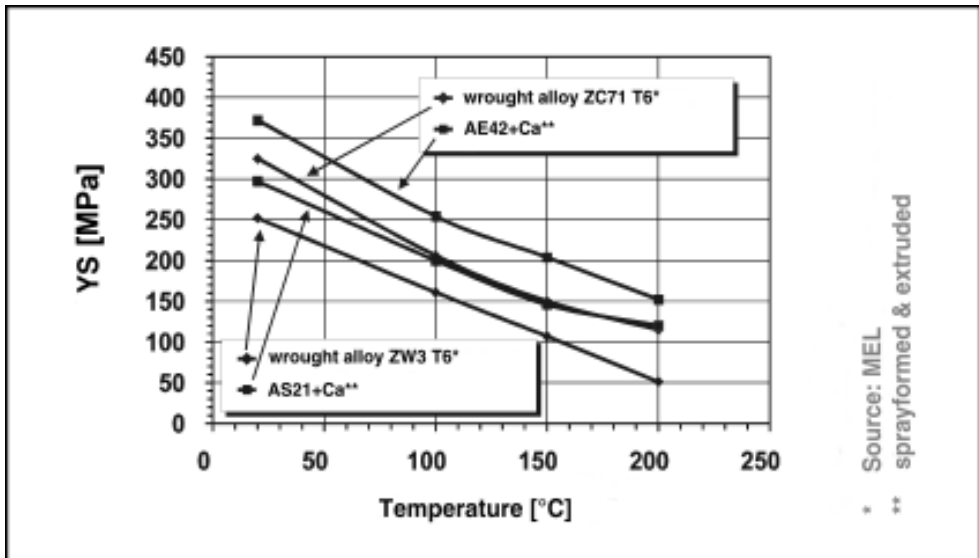


Figure 12: Yielding as a function of temperature

## 10.5 Summary and Conclusion

After much activity in the field of alloy development in the 1930s and 1950s, it has again become a focal point in research. Other main goals are increasing the creep resistance of magnesium alloys, a further reduction in density, and better corrosion resistance. Moreover, the development of alloys with higher ductility and toughness and extraordinary wrought alloys will help to speed up the growth of the magnesium market [35].

Central to the research is the development of new alloys together with the optimization of existing and the development of new processing technologies.

Recent studies on rapidly solidifying magnesium materials prove the excellent possibilities for these metals. Extended degrees of freedom for alloying in terms of higher element concentrations and the choice of additions that are unusual or even impossible for conventional alloys open a wide and presently unexploited scope for development. Materials that contain unusual alloying compositions and elements offer the possibility of producing magnesium alloys with higher proportions of intermetallic phases and finely dispersed dispersoids that stand out for higher strengths at room temperature and above, improved corrosion resistance, and better deformability. Previous results on spray-formed Mg alloys may be described as very promising and await further property improvements through process optimization. A major requirement for this will be an improved characteristic profile along with the development of more productive and economic production and processing methods.

The potential for the extended application of novel and more powerful magnesium materials can be seen in the aircraft and space industries, the automotive industry, and in transport systems, including the production of high quality mass products.

## 10.6 Literature

- /1/ Jones, H.: Rapid solidification of metals and alloys Monograph 8, The Institution of Metallurgists, London 1982.
- /2/ Cahn, R.W. et al.: Materials Science and Technology – Vol. 8: Structure and properties of nonferrous alloys VCH, Weinheim, 1996.
- /3/ Cahn, R.W., Haasen, P.; Kramer, E.J.: Materials Science and Technology – Vol. 15: Processing of metals and alloys, VCH, Weinheim, 1991.
- /4/ Cohen, M., Kear, B.H., Mehrabian, R.: Rapid Solidification Processing – An Outlook in Rapid Solidification Processing I, Claitors, Baton Rouge, 1978.
- /5/ Cahn, R.W., Haasen, P.: Physical Metallurgy., 3. Überarbeitete und erweiterte Ausgabe, Elsevier Science Publishers B.V., Amsterdam, 1983.
- /6/ Schatt, W., Wieters, K.-P.: Pulvermetallurgie – Technologien und Werkstoffe, VDI-Verlag, Düsseldorf, 1994.
- /7/ Lawley, A.: Atomization – The production of metal powders, Monographs in P/M Series No.1, MPIF, Princeton, 1992.
- /8/ Jenkins, I., Wood, J.V.: Powder Metallurgy – An Overview, Institute of Metals, London, 1991.
- /9/ Steeb, S.: Glasartige Metalle: Eigenschaften, Struktur und Anwendungen, Expert Verlag, Ehningen, 1990.
- /10/ Ashbrook, R.L.: Rapid Solidification Technology, ASM, Ohio, 1983.
- /11/ Juchmann, P.: Beitrag zur technologischen Eigenschaftserweiterung von Magnesiumwerkstoffen durch Lithium, VDI Verlag, Fortschrittsberichte VDI Reihe 5 Nr. 554, Düsseldorf, 1999.
- /12/ Busk, R.S., Leontis, T.E.: The extrusion of powder magnesium alloys, Trans. AIME, 1950, 188, 297-306.
- /13/ Chisholm, D.S.; Dow Chemical Co.: Atomizing magnesium and its alloys, US Patent 2676359, 27 April 1954.
- /14/ Chisholm, D.S.; Hershey, G.F.; Dow Chemical Co.: Apparatus for atomizing (Mg) metal, US Patent 2752196, 26 Juni 1956.
- /15/ Busk, R.S., Leontis, T.E.; Dow Chemical Co.: Improvement in making alloy extruded forms by powder metallurgy, US Patent 2657796, 3 November 1953.
- /16/ Foerster, G.S.: Method of extrusion and extrusion billet thereof, US Patent 3219490, 23 November 1965.
- /17/ Colby, N.R., Hershey, G.F.; Dow Chemical Co.: Method of forming non-spherical atomized particles of magnesium and its alloys, US Patent 2934787, 3 Mai 1960.
- /18/ Foerster, G.S.: Dispersion hardening of magnesium, Metals Eng. Quart., 1972, 12 (1), 22-27.
- /19/ Isserow, S.: Investigation of microquenched Mg ZK60A alloy, AD 780799, AM-MRC TR-74-7, April 1974.
- /20/ Isserow, S., Rizzitano, F.J.: Microquenched magnesium ZK60A alloy, Int. J. Powder Metallurgy, 1974 (19), 217-227.
- /21/ Das, S.K., Chang, C.F.: High strength magnesium alloys by rapid solidification processing, In: Das/kear (Ed.): Rapidly Solidified Crystalline Alloys. The Metallurgy Society, Warrendale, Pa., 1985, 137-156.
- /22/ Das, S.K., Chang, C.F.; Raybould, D.: Rapidly solidified Mg-Al-Zn-Rare earth alloys, In: Rapidly Solidified Materials. ASM, Metals Park, Ohio, 1986, 129-135.

- /23/ Das, S.K., Chang, C.F.; Raybould, D.: The effect of heat treatment on the properties of Rapidly solidified Mg-Al-Zn-RE-alloys, In: Processing of Structural Metals by Rapid Solidification. ASM, Metals Park, Ohio, 1987, 409-415.
- /24/ Das, S.K., Chang, C.F.: Rapidly solidified high strength corrosion resistant magnesium base metal alloys, US Patent 4765954, 23 August 1988.
- /25/ Das, S.K., Davis, L.A.: High performance aerospace alloys via rapid solidification processing, Mater. Sci. Eng., 1988 (98), 8-12.
- /26/ Krishnamurthy, S. et. al., Development of light alloys by rapid solidification processing, Int. Journal of Powder Metallurgy, 1990 (26) No.2, 117-129.
- /27/ Knoop, F.-M.: Erzeugung, Konsolidierung und Untersuchung gasverdünster Magnesiumlegierungen, Dissertation, Institut für Werkstoffkunde und Werkstofftechnik, TU Clausthal, 1994.
- /28/ Kainer, K.U., Properties of consolidated magnesium alloy powder, Metall Powder Report 1990 (45), 684-687.
- /29/ Lewis, R.E.; Joshi, A.; Jones, H.: Rapidly solidified magnesium alloys for high performance structural applications: a review, In: Froes/Savage (Ed.): Processing of structural metals by rapid solidification, Orlando, 6.-9. Okt. 1986. ASM International, Ohio, 1987, 367.
- /30/ Hehmann, F.: Developments in magnesium alloys by rapid solidification processing – An Update, In: Cahn/Effenberg (Ed.): Advanced aluminium and magnesium alloys, Proc. of the Int. Conf. on Light Metals, Amsterdam, 20.-22.6.1990. ASM International, Ohio, 1990, 781.
- /31/ Nussbaum, G., Gjestland, H., Regazzoni, G.: Rapid solidification of magnesium alloys, In: 45<sup>th</sup> annual world magnesium conference, Washington, USA, 1.-4.5.1988, IMA, Virginia, 1988, 19.
- /32/ Nussbaum, G., Regazzoni, G.: Rapid solidification reveals an enormous potential, In: Cahn/Effenberg (Ed.): Advanced aluminium and magnesium alloys, Proc. of the Int. Conf. on Light Metals, Amsterdam, 20.-22.6.1990. ASM International, Ohio, 1990, 789.
- /33/ Gjestland, H., Nussbaum, G., Regazzoni, G., Lohne, O., Bauger, O.: Stress-relaxation and creep behavior of some rapidly solidified magnesium alloys, Materials Science and Engineering, A134, 1991, 1197-1200.
- /34/ Li, Y., Jones, H.: Structure and mechanical properties of rapidly solidified magnesium based Mg-Al-Zn-RE alloys consolidated by extrusion, Materials Science and Technology, 1996 (12), 981-989.
- /35/ Ebert, T., von Buch, F., Kainer, K.U.: Sprühkompaktieren von Magnesiumlegierungen im Rahmen des SFB 390 „Magnesiumtechnologie“, Kolloquium des SFB 372, Band 3, Universität Bremen, 1998, 9-30.
- /36/ Grant, N.J.: Spray Forming in: Progress in Material Science, 1995, 39, 497-545.
- /37/ Vervoort, P.J., Duszczyk, J.: Extrusion of spray deposited magnesium alloy and composites, In: Proceedings of the Second International Conference on Spray Forming, John V. Wood ed., Woodhead Publishing Ltd., Cambridge, 1993, 409-425.
- /38/ Schröder, J., Kainer, K.U.: Charakterization of P/M Magnesium-SiCp-Composites processed by Spray Forming, Powder Forging and Extrusion of Composite Powder Mixtures, In: Aldinger, F. (Hrsg.) – Materials by Powder Technology, PTM, '93, DGM-Informationsgesellschaft, Oberursel, 1993, 739.
- /39/ Tokizane, N., Ohkubo, Y., Shibue, K.: Recent progress in spray forming of aluminium alloys, Proceedings of the Third International Conference on Spray Forming, Cardiff UK, 1996, 37-44.

- /40/ Shifan, T. et al.: The spray atomized and deposited superalloys, Proceedings of the Third International Conference on Spray Forming, Cardiff UK, 1996, 61-70.
- /41/ Shaw, L.H., Spiegelhauer, C.: Spray forming and evaluation of large diameter billets in special steels, Proceedings of the Third International Conference on Spray Forming 1996, Cardiff UK, 1996, 101-114.
- /42/ Madden C.: Management of large spray forming plant design and construction, Proceedings of the Third International Conference on Spray Forming, Cardiff UK, 1996, 147-150.
- /43/ Lavernia, E.J.: Spray atomization and deposition of metal matrix composites, Baukhage, K. Uhlenwinkel, V. (Hrsg.): Kolloquium des SFB 372: Sprühkompaktieren-Sprayforming, Band 1, Universität Bremen, 1996, 63-122.
- /44/ Singer, A.R.E.: Recent developments and opportunities in spray forming, Baukhage, K. Uhlenwinkel, V. (Hrsg.): Kolloquium des SFB 372: Sprühkompaktieren-Sprayforming, Band 1, Universität Bremen, 1996, 123-140.
- /45/ Reichelt, W.: Stand der industriellen Anwendung des Sprühkompaktierens, Baukhage, K., Uhlenwinkel, V. (Hrsg.): Kolloquium des SFB 372: Sprühkompaktieren-Sprayforming, Band 1, Universität Bremen, 1996, 189-198.
- /46/ Hummert, K.: Sprühkompaktieren von Aluminiumwerkstoffen im industriellen Maßstab, Baukhage, K. Uhlenwinkel, V. (Hrsg.): Kolloquium des SFB 372: Sprühkompaktieren-Sprayforming, Band 1, Universität Bremen, 1996, 199-215.
- /47/ Kaneko J. et al.: Spray forming of SiCp/Mg-Ce and Mg-Ca Composites, Proceedings of the Third International Conference on Spray Forming, Cardiff UK, 1996, 187-192.
- /48/ Laverina, E.J., Grant, N.J.: Spray deposition of metals: a review, Material Science and Engineering, 1988 (98), 381.
- /49/ Faure, J.-F., Nussbaum, G., Regazzoni, G.: Process for obtaining magnesium alloys by spray deposition, US Patent 5073207, 17. Dezember 1991.
- /50/ Elias, L.G., Duszczyc, J., Hehmann, F.: In-situ alloying of high temperature Mg-alloys by spray forming technology, In: Mordike/Hehmann (Hrsg.): Magnesium alloys and their applications. Garmisch-Partenkirchen, 8.-10. April 1992, DGM Informationsgesellschaft, 1992, 343.
- /51/ Kainer, K.U., Moll, F.: Microstructure and properties of Magnesium-SiCp-Composites influenced by production techniques and particle shapes, In: Roller, D. ed., Proc. Int. Symp. Automotive Technology and Automation, Florence, Italy, 3rd-6th June 1996, Automotive Automation Ltd., 1996, 363-369.

# 11 Fibre-Reinforced Magnesium Composites

Ch. Fritze, BMW Group, München

## 11.1 Introduction

Besides reducing overall vehicle weight, the reduction of oscillating and rotating masses in the engine, such as piston, connecting rod, or valve gear is a major goal in development. Besides simple engineering improvements, the automobile industry also envisages the application of light construction materials such as aluminium and magnesium. Currently, aluminium is preferred, but due to its even lower density, magnesium is gaining importance as an engineering material.

The requirements for engine applications in terms of strength and heat resistance are currently only met by expensive magnesium alloys. However, by reinforcing the matrix with particles or fibres (short and long), the following property changes can be achieved:

- Increase of the maximum strength
- Increase of the yield strength
- Increase of the Young's modulus
- Increase of the heat resistance
- Improvement of the creep resistance
- Reduction of the thermal expansion coefficient

With these kinds of reinforcements, the fibres largely absorb any load applied to the material. The production and properties of fibre-reinforced magnesium composites are presented hereafter by means of several examples.

## 11.2 Basics of Fibre-Reinforcement

### 11.2.1 Calculated Evaluation of the Composite

The properties of composites can be evaluated with the help of linear and inverse rules of mixture. For stresses parallel to the fibre orientation, with unidirectional fibres, the linear rule of mixture is valid, which assumes that the elongations of the composite, fibres, and matrix are equal ( $\epsilon_C = \epsilon_F = \epsilon_M$ ).

The composite stress is given by:

$$\sigma_C = \sigma_F \cdot \Phi + \sigma_M \cdot (1 - \Phi) \quad (11.1)$$

where  $\sigma_C$  = composite stress

$\sigma_F$  = fibre stress

$\sigma_M$  = matrix stress

$\Phi_F$  = volume fraction of fibre

The Young's modulus of the composite is then given by:

$$E_C = E_F \cdot \Phi + E_M \cdot (1 - \Phi) \quad (11.2)$$



With stresses perpendicular to the fibre orientation, the composite's properties can be evaluated with the inverse rule of mixture ( $\sigma_C = \sigma_F = \sigma_M$ ):

$$\varepsilon_C = \varepsilon_F \cdot \Phi + \varepsilon_M \cdot (1 - \Phi) \quad (11.3)$$

The Young's modulus is then calculated by:

$$E_C = \frac{E_F \cdot E_M}{E_M \cdot V_F + E_F \cdot (1 - \Phi)} \quad (11.4)$$

With a short fibre reinforcement, the properties of the fibres and the matrix, as well as of the boundary surface, need to be considered.

For a reinforcement effect, the fibres need to have a certain minimum length; fibres below that length cannot contribute to a full reinforcement. The critical fibre length is given by:

$$l_C = \frac{\sigma_F \cdot d_F}{2\tau} \quad (11.5)$$

The calculated composite strength depends on the fibre length  $l$  according to Eqs. 11.6 to 11.8. The fibre orientation is indicated by the factor  $C$ .  $C$  is equal to 1 for short aligned fibres, and is 1/5 to 3/8 for randomly distributed fibres [2-4]. Furthermore, the yield strength is used for the calculation of  $\sigma_M^*$ . For  $l < l_C$ , the following is valid:

$$\sigma_C = C \cdot \sigma_M \cdot \Phi \cdot \frac{l}{2d_F} + \sigma_M^* (1 - \Phi) \quad (11.6)$$

For a fibre length  $l = l_C$ :

$$\sigma_C = C \cdot 0.5 \cdot \sigma_F \cdot \Phi + \sigma_M^* (1 - \Phi) \quad (11.7)$$

For a fibre length  $l > l_{oc}$ :

$$\sigma_C = C \cdot \sigma_F \cdot \Phi \cdot \left(1 - \frac{l_c}{2l}\right) + \sigma_M^* (1 - \Phi) \quad (11.8)$$

In the above equations,  $C = 1$  for orientated short fibres,  $C = 1/5$  for randomly distributed fibres, and  $C = 3/8$  for a planar isotropic distribution. The properties of the composites can be evaluated on the basis of these equations. The values for carbon-reinforced AZ91 are shown in Fig. 1 as a function of the fibre orientation.

More detailed calculations on discontinuously and continuously reinforced aluminium and magnesium were made by Karg [5] and the results were compared with experimental data. Partial and hybrid reinforcements were considered as well [5].

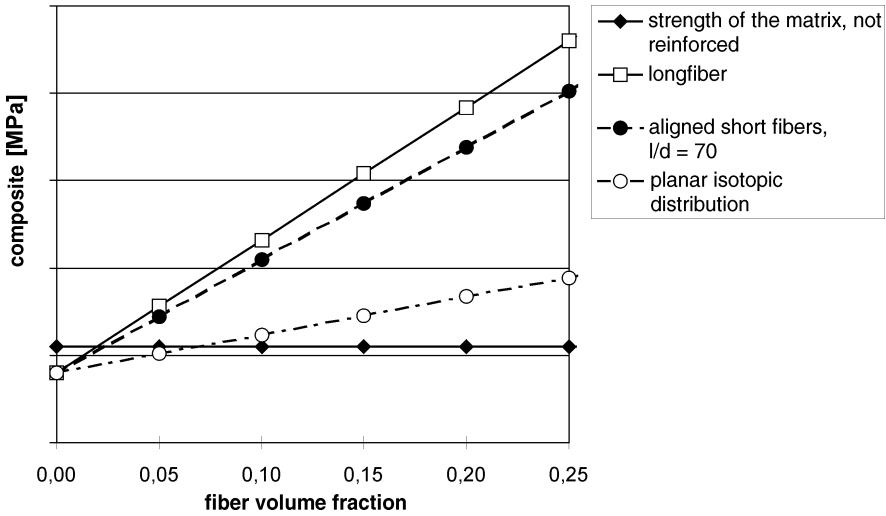


Figure 1: Estimation of the composite strengths of AZ91 ( $R_m \approx 200$  MPa,  $R_{p0.2} \approx 160$  MPa) and Sigrafil C-fibres ( $R_m \approx 3200$  MPa) according to Eqs. 11.6 to 11.8

## 11.2.2 Influence of Wetting on the Components

Wetting is a main factor for producing MMCs since it influences infiltration and the bonding between the fibre and matrix. The wetting of a ceramic phase with a metallic melt is determined by the surface energies of the liquid phase  $\gamma_{la}$  and the solid phase  $\gamma_{sa}$ , and the interfacial energy  $\gamma_{ls}$  between the liquid and solid phases. The total energy of the system is decreased by the formation of a common boundary surface.

Each system tries to bring all forces to equilibrium and to minimize the free energy. The surface and boundary surface stresses and the set angle of wetting are related by Young's equation  $\gamma_{sa} - \gamma_{sl} = \gamma_{la} \cos \Theta$  [6]. With  $\Theta = 180^\circ$ , the substrate is not wetted, whereas full wetting is obtained with  $\Theta = 0^\circ$ . Sufficient wetting occurs for angles smaller than  $90^\circ$ , whereas the wetting is insufficient when the angle is greater than  $90^\circ$ . Chemically reacting systems (e.g.  $Mg + Al_2O_3$ ) show good wetting behaviour, whereas non-reacting systems show poor wetting behaviour. Another very important factor for the process of infiltration is the role of the preform binder, because it contributes greatly to the reaction between the melt and fibres, that is to say, between the melt and binder [7].

In a wettable system, the metal first flows into regions with a high specific surface activity; these are the areas of the preform rich in fibres, i.e. narrow capillaries. In a non-wetting system, the bigger channels are flooded first before the melt reaches the small fibre capillaries. In the case of poor wetting, in theory an unlimited pressure would be necessary to fully infiltrate a fibre gap with mutually touching fibres. Since infiltration of a non-wetting system is not spontaneous, the pressure needed to fully infiltrate the niches between the fibres will steadily increase, the smaller the distance of the melt face from the contact point of the fibres. Hence, there are always defects in a non-wetting system, which act as starting points for cracks.

## 11.3 Components for Magnesium Composites

### 11.3.1 Matrix Materials

In the past years, mainly cast alloys of the Mg/Al system have been used as matrix materials for magnesium composites. There has been an emphasis on the production of composites with AZ91 as the matrix. Other matrix materials used have been AS and AM alloys, and a few studies have been undertaken using ZC71, WE43, and QE22.

### 11.3.2 Reinforcement Components

A discontinuous reinforcement of magnesium is usually realized using fibre preforms. For particle-reinforced materials, the reinforcement component is simply stirred into the melt of the matrix metal, or else the material is produced by powder metallurgy [8]. For discontinuous fibre reinforcements, on the other hand, a fibre solid (preform) is used, which is infiltrated by the matrix metal in a suitable process. The preform is prepared by dispersing the fibres in water, and then adding a binder to fix them [9]. This so-called slurry is then fashioned by a tool; the water is drawn off, the remaining material is pressed, and the resulting plate is then dried. The fibres are planar-isotropically distributed due to the method of production (Fig. 2), and their volume fraction is 15–20%.

A continuous reinforcement with fibres can be realized by producing coiled solids. Their fibre volume fraction is much higher than the usual volume fractions of short fibre preforms and can be as much as 60%. The most commonly used and tested fibres for discontinuous fibre-reinforced magnesium are supplied by ICI and consist of aluminium oxide. Interest in carbon fibres for both continuous and discontinuous fibre reinforcement has increased over the past years due their low density and good strength and toughness properties. The most commonly used reinforcement materials for magnesium matrices are summarized in Table 1.

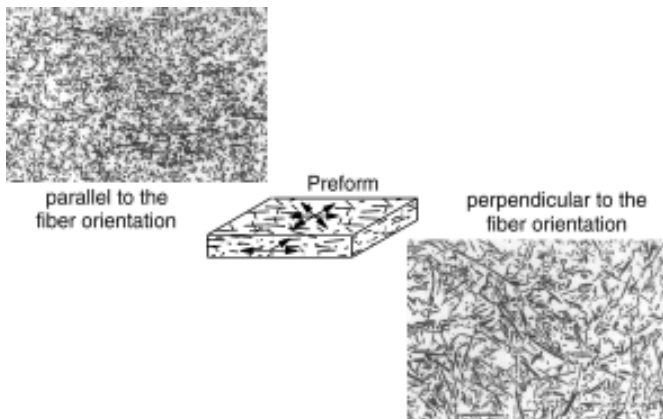


Figure 2: Preform with planar isotropic fibre distribution (schematic)

## 11.4 Production Methods

### 11.4.1 Powder Metallurgy

To produce magnesium composites by powder metallurgy, a mixture of metal powders, particles, or fibres is consolidated by hot pressing, forging, or extrusion. Whereas composites made by melting metallurgy have a planar isotropic distribution of fibres, p/m methods result in oriented fibres after consolidation by extrusion. Although the fibres are somewhat damaged during extrusion, the strengthening effect and orientation of the fibres has a positive influence on the properties of the material [10].

Table 1: Summary of commonly used fibres for the continuous and discontinuous reinforcement of magnesium alloys

type of fiber	manufacturer	density [g/cm <sup>3</sup> ]	strength [MPa]	youngs modulus [GPa]	diameter [μm]
oxide ceramic fibers					
Saffil RF δ-Al <sub>2</sub> O <sub>3</sub>	ICI	3,3	2000	300	3
Altex 15% SiO <sub>2</sub> /85% Al <sub>2</sub> O <sub>3</sub>	Sumitomo	3,30	1800	210	10
carbon fibers					
Sigrafil C	SGL Carbon GmbH	1,8	3200	210	7
Tenax 5331 HTA	Akzo		3950	238	7
M40 J	Toray	1,77	4680	379	5
T300 J	Toray	1,79	4267	233	7

### 11.4.2 Melting Metallurgy

The infiltration of a preform with fluid metal can only occur if there is a pressure gradient between the melt and the preform [11, 12]. This pressure gradient arises from the pressure loss due to the wetting of the reinforcement material by the melt. Squeeze-casting is an example of infiltration; the pressure of the metal melt can be as high as 300 MPa [13]. Using gas-pressure infiltration, the pressure amounts to 5 to 50 MPa after evacuation [14].

#### 11.4.2.1 Squeeze-casting

Squeeze-casting is very suitable for the series production of components. In this methodology, a plunger presses the melt into the preform [8, 13, 15, 16]. In doing so, the preform is pre-heated and is fashioned by a likewise pre-heated tool. This method stands out for its short processing time and good infiltration qualities, but it requires much investment in equipment and cost-intensive dies (Fig. 3):

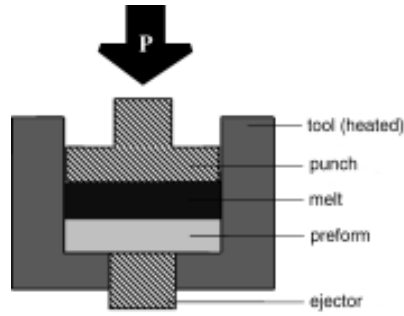


Figure 3: Squeeze-casting process (schematic)

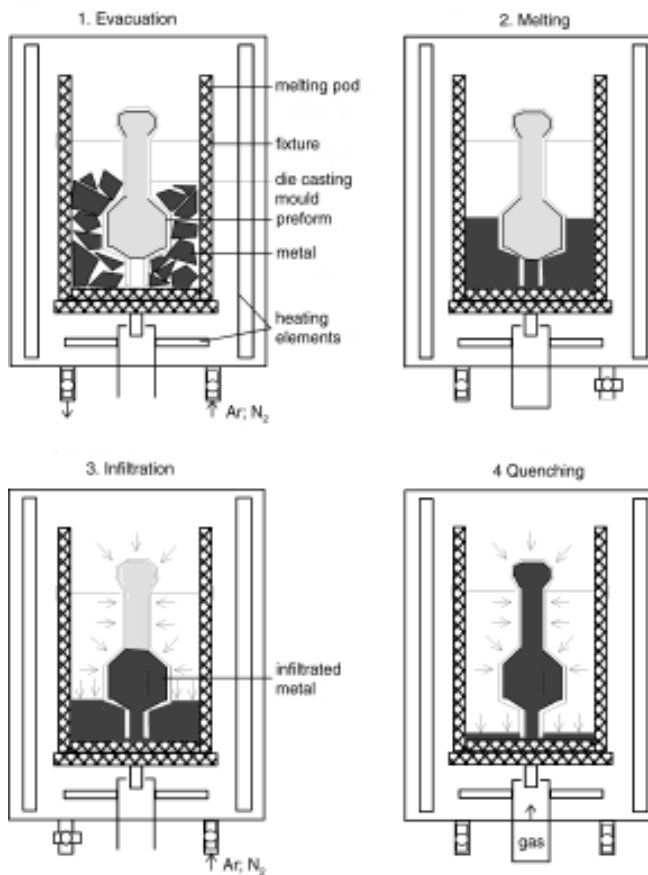


Figure 4: Gas-pressure infiltration according to [14] (schematic)

### 11.4.2.2 *Gas-pressure infiltration*

A more flexible production of prototype parts with less post-processing effort can be achieved by gas-pressure infiltration [8, 14]. However, this process requires an autoclave and has a long cycle time. The cooling rates of the melt after infiltration are also very long, which can lead to reduced strength with some fibre/matrix systems as the fibres are attacked. Nevertheless, for basic studies of fibre/matrix eligibility and exploratory estimations of component and material properties, this process is quite adequate.

## 11.5 Properties of Magnesium Composites

### 11.5.1 Strength and Young's Modulus

#### 11.5.1.1 *Continuously reinforced composites*

Continuously reinforced magnesium composites are characterized by a tremendously increased strength in the preferred fibre orientation. As shown in the calculation models, this is dependent on the fibre volume fraction and the fibre strength. The strength perpendicular to the fibre orientation is expected to be low.

With a volume fraction of 63% of carbon fibres with a high Young's modulus (M40J) in an AZ91 matrix, a maximum strength of more than 1000 MPa is reached; with CP-Mg as the matrix, the strength even exceeds 1500 MPa. The high-strength C-fibre T300J gives slightly lower values. The bending strength varies in a similar manner to the tensile strength [17]. However, as mentioned above, little strength is expected perpendicular to the fibre orientation. Indeed, Tenax fibre T5331 HTA reinforced magnesium composites showed tensile strengths of only 5–20 MPa in this direction [18]. Thus, the properties of continuously reinforced materials are highly anisotropic and limit the application field.

#### 11.5.1.2 *Discontinuously reinforced magnesium composites made by powder metallurgy*

Discontinuously reinforced light metals made by powder metallurgy have higher yield strengths and tensile strengths at room temperatures than the corresponding non-reinforced alloys. The strengthening effect stems mainly from the strength increase during extrusion and from texture influences. Beyond 200 °C, the strength decreases to values below those of composites made by melting metallurgy [19].

#### 11.5.1.3 *Discontinuously reinforced magnesium composites made by melting metallurgy*

Most strength tests have been conducted on fibre-reinforced magnesium composites made by melting metallurgy. In the case of discontinuous reinforcement, the properties of the final magnesium composites depend strongly on the fibre orientation. Most common pre-forms have a planar isotropic fibre distribution, and hence the properties are likewise planar isotropic.

Since the process limits the fibre volume fraction to 25%, the room temperature strength is rather poor. Nevertheless, the mostly homogeneous properties in each layer are advantageous. Only the strength perpendicular to the planar isotropic distribution of the fibres is

expected to be low. The Young's modulus, heat resistance, and creep resistance vary in the same way as tensile strength.

The increase in strength is much greater at higher temperatures. The fibres take over the strength absorption, and therefore the heat- and creep resistance can increase compared to those of the non-reinforced material. Figure 5 shows the change in maximum strength as a function of temperature for reinforced AZ91 + Ca (1 weight % Ca) and AS41 compared to QE22 and a KS1275 aluminium piston alloy. While at room temperature the fibre-reinforced standard magnesium alloys show lower strengths than the aluminium alloy, it can be seen that acceptable heat resistance is reached at higher temperatures.

Moreover, these composites are characterized by good bending strength at elevated temperatures as well [21]. The fibre-reinforced alloy AZ91 + Ca withstood  $0.58\text{--}4.2 \times 10^6$  load cycles at  $250\text{ }^\circ\text{C}$  and a load of 60 MPa. The large variation in the results can mainly be attributed to an inhomogeneous distribution of the fibres due to method of manufacture. No values for non-reinforced alloys are available for comparison purposes, but considering the temperature and load these would surely fail after a few cycles.

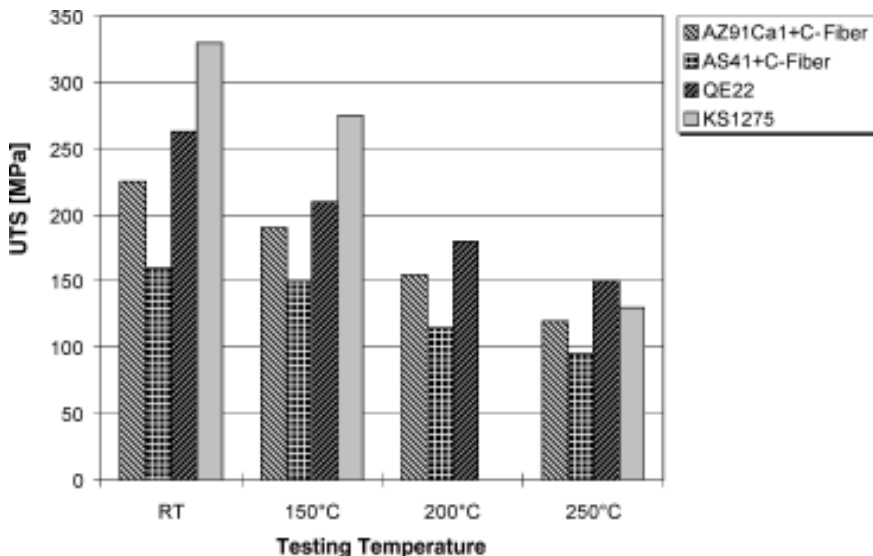


Figure 5: Tensile strengths of discontinuously C-fibre-reinforced magnesium compared to magnesium and aluminium alloys [20]

The creep behaviour could be markedly improved with reinforcements [21]. Compared to typical creep curves for monolithic materials, which show primary, secondary, and tertiary creep, fibre-reinforced magnesium shows a steadily declining creep rate until fracture [21]. This indicates that a continuous strengthening occurs in the material during the creep test. A weakening of the matrix could not be verified. Furthermore, these tests highlight the great influence of the matrix alloy on the creep behaviour of the components. The creep rate of the AS41 alloy is about one order of magnitude lower than that of AZ91 + Ca. This is due to heat-stable precipitations in the AS41 matrix [20,22]. Changes in the temperature and load also lead to a great change in the creep rate. For carbon fibre

reinforced AS41, increasing the temperature from 225 °C to 250 °C under constant load will lead to an increase in the creep rate by one order of magnitude [23].

Finally, it can be stated that by using an a priori creep-resistant matrix and a short fibre reinforcement, a significant decrease in the creep rate will be obtained.

## 11.6 Boundary Surfaces of Magnesium Composites

A good fibre/matrix bonding can only be accomplished with a boundary surface that allows a good transmission of the force from the matrix to the fibre. The formation of coarse and brittle reaction products should be avoided since this weakens the bonding. Furthermore, the more the alloying elements add to the boundary surface, the less prevalent they are within the matrix, thus leading to a decrease in strength.

Tests on Saffil<sup>®</sup>-reinforced CP-magnesium showed mostly MgO, and with AZ91 as matrix some additional Mg<sub>17</sub>Al<sub>12</sub> at the boundary surface [16, 24]. The boundary surfaces of CP-Mg and Mg/Al alloys, and of QE22 reinforced with T300J and M40J fibres, were characterized by Öttinger [17]. While in the case of CP-magnesium and T300J fibres, magnesium is absorbed by the fibres, the M40J fibres show no such behaviour. No reaction occurs between the alloy and the fibres. When using Mg/Al alloys, zones of reaction, Mg<sub>17</sub>Al<sub>12</sub> particles, as well as AlMn-loaded particles were found at the surface boundaries. Both types of fibres add Zr and Nd at the boundary surface with QE22 as the matrix [17]. Similar results were obtained using Tenax fibres, which, especially with Mg/Al alloys, show a strong reaction with aluminium, forming Al/Mg solid-solution carbides (Al<sub>2</sub>MgC<sub>2</sub>) and needle-shaped aluminium carbides (Al<sub>4</sub>C<sub>3</sub>) [18].

TEM observations of typical fibre/matrix boundary surfaces of Sigrafil C-fibre reinforced AZ91 showed a thin layer of polycrystalline MgO and Mg<sub>17</sub>Al<sub>12</sub> precipitates. They also revealed the addition of Zn to the Mg<sub>17</sub>Al<sub>12</sub> phase, leading to a depletion of Zn in the matrix. All specimens showed a very good bonding between fibre and matrix, which points to good strength of the composite. Reinforced AS41 creep specimens were investigated by TEM, which revealed micro-cracking in the polycrystalline boundary surface layer that lies between the fibres and the matrix. Thus, cracking begins at the fibre/matrix boundary surface (Fig. 7).

Different coating systems were tested for their use with carbon fibres. The coating acts as a barrier for reactions and diffusion, supports wetting and bonding, and prevents oxidation of the fibres. Modern coatings mainly consist of pyrolytic carbon (pyC), SiC, and TiN [18]. In the studies, long carbon fibres served as substrates. In contrast to uncoated Tenax fibres, these coatings lead to an increase in bending strength as well as in transverse tensile strength. A further increase of the already high strength in the fibre direction can be achieved by applying a coating. The magnitude of this increase in strength is mainly determined by the Al-content of the matrix alloy. As yet, coatings have only been tested with long fibres. Whether coated short fibres have a positive effect on the bonding between the fibre and matrix is a matter for ongoing research.



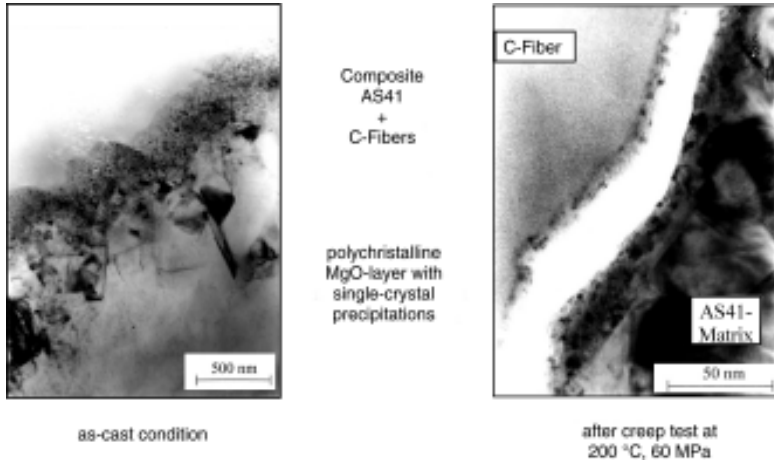


Figure 7: Surface boundaries of C-fibre-reinforced AS41 in as-cast condition and after a creep test.

### 11.6.1 Recycling Ability of Discontinuously Reinforced Magnesium

Different recycling concepts are assessed in terms of their ability to process magnesium composites with short fibre reinforcements. In this way, Saffil<sup>®</sup>-reinforced magnesium has been processed to give a new composite under pressure-casting conditions. However, the composites thus produced showed an inhomogeneous distribution of the fibres, which led to brittleness of the matrix at low temperatures.

Another possibility allowing further use of short-fibre magnesium composites is the separation of the fibres and the matrix under flux. The fibres are bound to a salt and the melt is separated; the latter is of good quality and so it can be used again [24].

## 11.7 Applications of Fibre-Reinforced Magnesium and Outlook

The improvement of the properties of magnesium by reinforcement enables the use of these materials under high stresses. One example of a likely application is in pistons [21].

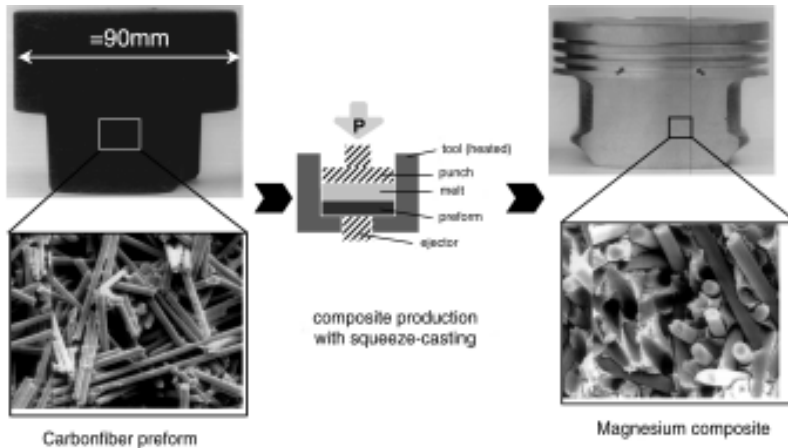


Figure 8: Carbon fibre preform and fibre-reinforced magnesium piston [21]

Table 2 summarizes the relevant material properties in relation to those of the piston alloy KS1275. It is clear that the required properties can be almost fully met with fibre-reinforced magnesium alloys. A low bending strength and Young's modulus need to be taken into consideration for the component engineering.

Table 2: Properties of fibre-reinforced magnesium compared to those of the carbon alloy KS1275 [21]

properties	unit	KS1275 (AlSi12CuMgNi heat treated)	20 Vol.-% C-fibers + AS41	20 Vol.-% C-fibers + AZ91Ca1
density	g/cm <sup>3</sup>	2,7	1,8	1,9
yield strength R <sub>p0.2</sub> (RT)	MPa	275-335	149-160	200-240
max. strength R <sub>m</sub> (RT)	MPa	295-360	175-196	225-260
yield strength R <sub>p0.2</sub> (250°C)	MPa	90-120	85-91	101-115
max. strength R <sub>m</sub> (250°C)	MPa	110-165	95-102	112-122
strain at fracture	%	1~3	~0,5	~0,5
bending strength (200°C)	MPa	85	50	60
youngs modulus	GPa	79,5	55-60	55-60
heat conductivity	W/mK	155	n.e.	~140
thermal expansion coefficient	10 <sup>-6</sup> K <sup>-1</sup>	20	19,7-19,3	19-19,8
creep rates (150°C 70MPa)	10 <sup>-9</sup> s <sup>-1</sup>	n.e.	1,3-2,9	13

n.a. - values not available

According to the load on the parts, the properties of composites can be modified by adjusting the variables of fibre, matrix, and process.

## 11.8 Summary

The application of fibre-reinforced magnesium can only be realized with a cost-efficient method of production and good, reproducible material properties. Therefore, the following may be identified as areas of research for the advancement of magnesium composites:

1. Development work in the field of preform technology.  
The ultimate goal must be the final-shape production of preforms, so as to limit post-processing and enable series production.  
Another aim is to further improve the homogeneity of the fibre distribution to obtain uniform and reproducible material properties.
2. Partial reinforcement of magnesium components for more highly stressed component areas.  
The process technology for producing such components is still insufficiently developed. An advancement in this field will yield additional, potential applications for magnesium composites.
3. Mass production suited and cost-efficient production of magnesium composites.  
Cost-efficient manufacturing methods need to be developed for a series production of magnesium composites. A main focus lies in the area of production by die-casting.

The extended application of fibre-reinforced light metals, especially of reinforced magnesium, can clearly be anticipated once these problems are solved.

## 11.9 Literature

- /1/ Ibe, G.: Grundlagen der Verstärkung in Metallmatrix-Verbundwerkstoffen, in: „Metallische Verbundwerkstoffe“, Kainer, K.U. (Hrsg.), DGM Informationsgesellschaft Oberursel (1994), 3-41.
- /2/ Kelly, A.: Strong Solids., Oxford University Press, London (1973).
- /3/ Kelly, A., Davies, G.J.: The principles of the fibre reinforcement of metals, *Met. Reviews* 10 (1965), 1-78.
- /4/ Friend, C.M.: The Effect of Matrix Properties Reinforcement in Short Alumina Fibre-Aluminium Metal Matrix Composites, *J. Mater. Sci.* 22 (1987), 3005-3010.
- /5/ Karg, J.: Teil- und Hybridverstärkung von Bauteilen aus Leichtmetalllegierungen, Dissertation TU Darmstadt, Darmstadt 1997.
- /6/ Young, R.M.K.: A liquid metal infiltration model of unidirectional fibre preforms in inert atmospheres, *Matrix. Squeeze-Casting. Eng. A 135A* (1991) ½, 19-22.
- /7/ Fritze, C.: Infiltration keramischer Faserformkörper mit Hilfe des Verfahrens des selbstgenerierenden Vakuums (SGV); Dissertation, TU Clausthal (1997).
- /8/ Degischer, H.P.: Schmelzmetallurgische Herstellung von Metallmatrix-Verbundwerkstoffen, in: „Metallische Verbundwerkstoffe“, K.U. Kainer (Hrsg.), DGM Informationsgesellschaft Oberursel (1994), 139-168.
- /9/ Hegeler, H., Buschmann, R., Elstner, I.: Herstellung, Eigenschaften und Anwendungen von Kurz- und Langfaserpreforms, in: „Metallische Verbundwerkstoffe“, Kainer, K.U. (Hrsg.), DGM Informationsgesellschaft Oberursel (1994), 101-116.
- /10/ Kainer, K.U.: Strangpressen von kurzfaserverstärkten Magnesium-Verbundwerkstoffen, *Umformtechnik* 27 (1993) 2, 116-121.

- /11/ Mortensen, A., Masur, L.J., Cornie, J.A., Flemings, M.C.: Infiltration of fibrous preforms by a pure metal: Part I. Theory; *Met. Trans. A* 20A (1989) 11, 2535-2547.
- /12/ Mortensen, A., Michaud, V.: Infiltration of fiber preforms by a binary alloy. Part. I: Theory; *Met. Trans. A* 21A (1990) 7, 2059-2072.
- /13/ Chadwick, G. A.: Squeeze-casting of magnesium alloys and magnesium based metal matrix composites, *Magnesium Technology, Proc. London Conf. 3-4 Nov. 1986*, The Institute of Metals (1987) 75-82.
- /14/ Öttinger, O., Singer, R.F.: An advanced melt infiltration process for the net shape production of metal matrix composites, *Z. Metallkd.* 84 (1993) 12, 827-831.
- /15/ Chadwick, G.A.: Squeeze-casting of metal matrix composites using short fibre preforms; *Matrix. Sci. Eng. A* 135 A (1991) ½, 23-28.
- /16/ Kainer, K.U.; Mordike, B.L.: Herstellung und Eigenschaften von kurzfaserverstärkten Magnesiumlegierungen: *Metall* 44 (1990) 5, 438-443.
- /17/ Öttinger, O.: Herstellung, Mikrostruktur und Eigenschaften von Kohlenstoff-langfaserverstärkten Magnesiumlegierungen, Dissertation, Universität Erlangen (1996).
- /18/ Wurm, D.: Einfluß einer Faserbeschichtung auf die Eigenschaften von Kohlenstoff-langfaserverstärkten Magnesiumlegierungen, Dissertation, Universität Erlangen (1998).
- /19/ Kainer, K.U.: Strangpressen von kurzfaserverstärkten Magnesium-Verbundwerkstoffen, *Umformtechnik* 27 (1993) 2, 116-121.
- /20/ Kainer, K.U., Berek, H., Fritze, C., Mielke, S., Wielage, B.: Charakterisierung und Herstellung von langfaserverstärkten Magnesiumlegierungen, *Werkstoffwoche 96 Symposium 2 Werkstoff für die Verkehrstechnik*, Hrsg. Koch, U., DGM Informationsgesellschaft mbH, Frankfurt (1997), 73-78.
- /21/ Fritze, C., Berek, H., Kainer, K.U., Mielke, S., Wielage, B.: Faserverstärktes Magnesium für die Anwendung als Kolbenwerkstoff im Motorenbau, in: *Werkstoffe für die Verkehrstechnik/Werkstoffwoche 98, Symposium 2, Bd. 2*, R. Stauber, C., Liesner, R., Bütje, M., Bannasch (Hrsg.), Wiley-VCH (1999), 23-28.
- /22/ Kainer, K.U.: Herstellung und Charakterisierung von langfaserverstärkten Magnesiumlegierungen, Abschlussbericht der TU Clausthal, BMBF-Verbundprojekt, Förderkennzeichen 03M3061D.
- /23/ Sommer, B., Kainer, K.U., Berek, H.: Kriecheigenschaften der Kohlenstoff-faserverstärkten Magnesiumlegierungen AS41 und AZ91; *Verbundwerkstoffe und Werkstoffverbunde*, Friedrich, K. (Hrsg.), DGM Informationsgesellschaft, Frankfurt (1997), 513-518.
- /24/ Kiehn, J., Buch, F. von, Ditze, A., Kainer, K.U.: „Weiterverwertung von Altschrott und Kreislaufmaterial aus der Produktion kurzfaserverstärkter Magnesiumlegierungen“, Tagungsband „Verbundwerkstoffe und Werkstoffverbunde“, Friedrich, K. (Hrsg.), DGM Informationsgesellschaft, Frankfurt (1997), 577-582.

# 12 Particle-Reinforced Magnesium Alloys

*F. Moll, Institute for Materials Research and Technology, Technical University of Clausthal*

*K. U. Kainer, Institute for Materials Research, GKSS Research Center Geesthacht GmbH, Geesthacht*

## 12.1 Introduction

The steadily growing requirements for engine components and engineering parts with a high mechanical and thermal stability, together with the restraint to save natural resources, has resulted in a demand for new materials that meet the current requirements. The expedite goal is to replace conventional materials with novel, lightweight ones without losing any technical potential. With this in mind, magnesium has become more and more interesting as an engineering material in recent years. Nevertheless, the application of magnesium remains limited due to its insufficient strength, its low Young's modulus, and the rather poor creep and abrasion resistance. These kinds of disadvantages can, however, be partly or even completely overcome by a reinforcement of the matrix with an additional phase such as particles or fibres.

For local acting component reinforcements with high strengths and Young's moduli, the application of long fibres is beneficial. A more cost-effective solution and a much lower anisotropy can be realized by using short fibres or particles as reinforcement components. Compared to fibre reinforcements, particles have the advantages of high availability, low price, economic production, amenability to deforming post-processes, as well as a great variety of adjustable material properties.

## 12.2 Particle-Reinforced Matrix Alloys

For the reinforcement of magnesium and its alloys, many different types of particles, or particle shapes made of ceramics such as oxides, nitrides, or carbides, can be used. The particle contents vary between 5 and 30 vol.% depending on the production method needed for the composites. The shapes range from spherical and solid to flake-like and needle-shaped particles. The particles usually have dimensions between 1 and 60  $\mu\text{m}$ . Figure 1 shows different types of SiC particles.

When looking at composites, especially when they are produced by melting metallurgy methods, the resistance of the particles towards the matrix is very important. For this reason, as well as economic aspects, mainly particles made of carbide ceramics, such as silicon carbide, boron carbide, and titanium carbide, have become established as reinforcement materials.

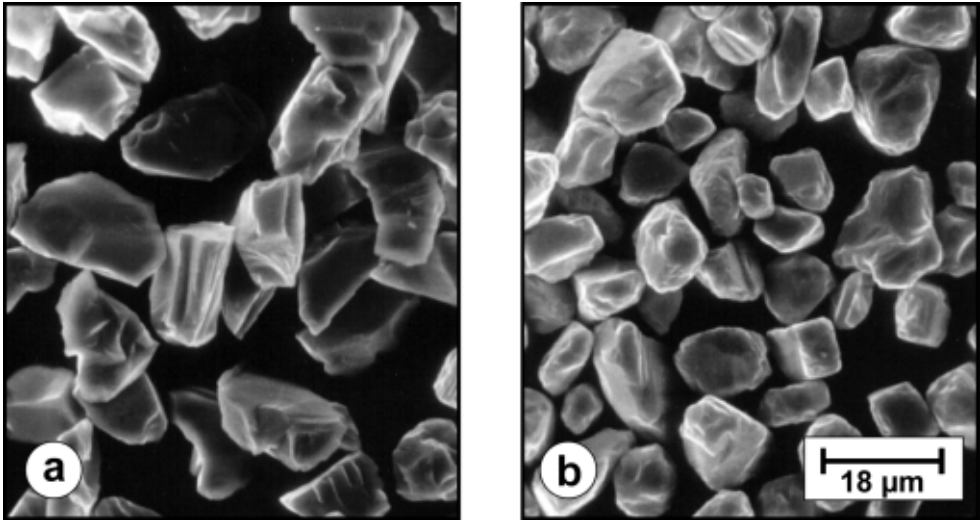


Figure 1: Ceramic SiC particles for the reinforcement of light metals, a) block-shaped geometry, b) spherical geometry [12]

The use of aluminium oxide particles remains limited to powder metallurgical processing. In a melting metallurgical method, with longer contact durations between the fluid metal and the ceramics, significant chemical reactions would occur, leading to various products such as magnesium oxide and spinel, which cause permanent damage to both composite components. Nitrides, on the other hand, represent suitable reinforcement materials, but they are less resistant than carbides and dissolve at lower temperatures [1]. Table 1 gives an overview of some particle materials and their mechanical and physical properties.

Table 1: Mechanical and physical properties of particle materials

Material	Crystal Structure	Melting Point [°C]	Density (RT) [g/cm <sup>3</sup> ]	Expansion Coefficient [10 <sup>-6</sup> K]	Young's Modulus (RT) [GPa]	Heat Conductivity (RT) [W/(mK)]
Carbides	B <sub>4</sub> C	2450	2,52	6,00	450	29
	SiC	2300	3,21	5,00	480	59
	TiC	3140	4,93	7,40	320	29
	ZrC	3420	6,60	6,70	390	19
Nitrides	BN	3000	2,25	3,80	90	25
	AlN	2300	3,25	6,00	350	10
	TiN	2950	5,40	9,40	260	38
	ZrN	2980	7,30	6,50	k.A.	19
Borides	TiB <sub>2</sub>	2900	4,50	7,40	370	27
	ZrB <sub>2</sub>	2990	6,10	6,80	350	23
Oxides	Al <sub>2</sub> O <sub>3</sub>	2050	3,99	8,30	410	25

Hard material particles are produced by standard methods according to the chemical composition of the ceramics. SiC is made by the Acheson process from silica sand and coke between 2000 and 2300 °C according to Eq. 12.1 [1]:



SiC occurs as a cubic, low-temperature phase ( $\beta$ -SiC) and a hexagonal high-temperature phase ( $\alpha$ -SiC), with a transformation temperature of roughly 2100 °C. The phase change from  $\alpha$ -SiC to  $\beta$ -SiC proceeds very slowly, so that commercially available silicon carbide predominantly consists of hexagonal  $\alpha$ -SiC [1].

Aluminium oxide is usually obtained from bauxite (a mixture of different aluminium hydrates) by the Bayer method, and then melted and cleaned in an arc furnace. Next, the oxides and carbides produced are broken apart, ground to a powder, and finally fractionated by filtering, sintering, or sedimentation according to the desired particle size. As a measure of the particle size, the so-called median or  $d_{50}$  value is often mentioned, which describes the average particle size distribution with the help of a distribution curve and does not necessarily match the arithmetic mean of the particle sizes [2, 3]. The  $d_{50}$  value has become an important index with respect to powder metallurgical processes, and this will be described in more detail later on.

Basically, all commercially available magnesium alloys that are amenable to powder- or melting metallurgical processing can be used for the composite matrix. We will not discuss further the mechanical properties of these alloys at this stage. Studies on the influence of a particle reinforcement, especially in terms of mechanical properties, have been conducted with pure magnesium (CP-Mg) and alloys of the AZ, AS, QE, WE, ZE, ZC, and ZCM series [4–13]. When employing the most commonly used particle materials, i.e. silicon carbide and aluminium oxide, the following boundary surface reactions between magnesium and the reinforcement component are conceivable:



Moreover, direct or indirect reactions between alloying elements and particles may also occur, for example, a reaction between aluminium of an AZ or AS alloy and silicon carbide or free carbon forming a stable  $\text{Al}_4\text{C}_3$  aluminium carbide. In the case of composites based on ZC alloys, no chemical interaction between the matrix and reinforcement components could be verified [6]. Thus, the extent and nature of possible boundary surface reactions is strongly dependent on the chosen material combination and the production method. Therefore, no universally valid statement can be made concerning any specific particle–matrix reactions within different composites. It has been repeatedly observed that a particle-reinforced matrix shows mostly accelerated precipitation behaviour compared to a regular matrix, which is attributable to a higher dislocation density in the immediate vicinity of the particles [5, 14].

This and possible boundary surface reactions that lead to a depletion of the alloying element in the matrix usually result in a different microstructure from that in the non-reinforced aggregate. Other effects that change the microstructure, such as grain refinement, have been described in relation to particle reinforcements. In this context, Holden et al. [8] examined a ZC63 alloy reinforced with 12% SiC particles in a post-casting state.

They found small equiaxial grains rather than a coarse dendrite casting structure. The particles mainly added at the grain boundaries and were linked by eutectic bridges.

## 12.3 Basics of Particle Reinforcement

Usually, the Young's modulus is most affected by reinforcement, but it should be kept in mind that the measuring method as well as the chosen stress may have an effect on the Young's modulus and the strength properties. Thus, the toughness is usually found to be slightly greater when measured by dynamic rather than static methods, which are based on regular, stress-strain curves with the elastic part being used for the determination. The static strength, on the other hand, may change under a tensile or compression load. Internal thermal stresses are deemed responsible for this behaviour, which arise during the processing due to a temperature difference between the matrix and particles. Depending on the polarity of the stress overlaying an applied external stress, the yield strength under tension or compression shifts to lower or higher values, respectively. These relationships are made even more complex by inhomogeneities in the particle distribution, leading to an uneven stress distribution and thus to local plasticity.

A theoretical estimate of the Young's modulus of a long-fibre composite (continuous reinforcement) can be made on the basis of the linear rule of mixture:

$$E_c = V_p E_p + V_m E_m \quad (12.5)$$

where

$E_c$  = Young's modulus of the component

$E_p$  = Young's modulus of the reinforcement phase

$E_m$  = Young's modulus of the matrix

$V_p$  = volume fraction of the reinforcement phase

$V_m$  = volume fraction of the matrix

However, when applied to particle-reinforced composites, this approach yields (IMR) values for the Young's moduli that are too high. On the contrary, the inverse rule of mixture, which describes the behaviour of laminate structures, yields values that are too low. An extension of the inverse rule proposed by Halpin and Tsai [16] allows an acceptable calculation of the Young's modulus, as was verified for some particle-reinforced aluminium and magnesium matrix composites [13–15].

With the Tsai–Halpin model, the Young's modulus of a particle-reinforced composite is calculated as follows:

$$E_c = \frac{E_m(1 + 2sqV_p)}{(1 - qV_p)} \quad (12.6)$$

with

$$q = \frac{\frac{E_p}{E_m}}{\frac{E_p}{E_m} + 2s} \quad s = \text{geometry factor } 1/d$$



Figure 2 shows the influence of the particle volume fraction on the theoretically calculated and experimentally measured values of the Young's modulus of a particle-reinforced magnesium composite.

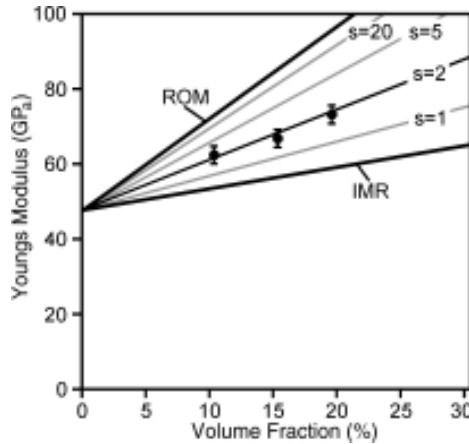


Figure 2: Comparison between calculated and experimentally measured values of the Young's modulus (according to [15])

From this figure, it can clearly be seen that the values estimated by means of the mixture rules differ significantly from the actual measured values, while the Tsai–Halpin equation, with its geometry correction, gives almost the correct result [15].

The effect of particles on the strength properties is largely based on four distinct mechanisms, which act on the properties of the composite very differently in terms of process, composition, and particle size. They are

- the Orowan mechanism, i.e. the interaction between dislocations and particles
- hardening through a decrease, and therefore stabilization, of the grain and sub-grain size
- increase of the dislocation density around the particles and the formation of internal thermal stresses due to different thermal expansion behaviours of the particles and matrix
- hardening of the matrix because of differential elongation behaviour of the two composite parts [14].

The strength properties of particle-reinforced composites have been modelled and described with the help of finite-element methods [17–22]. Continuum mechanical approaches, such as the shear-lag model [23] do not include the aforementioned influences of the particles on micro-mechanical mechanisms. Hence, for composites with small geometry factors, the strength values that they yield are too low [14].

Humphreys et al. [18, 19] have developed a model based on metal physics that allows an estimation of hardening by the different mechanisms of particle reinforcement. Accordingly, the increase in the yield strength  $\Delta R_{pC}$  is the sum of all single increases in strength

$$\Delta R_{pC} = s_v + s_k + s_{sk} + s_{kf} \quad (12.7)$$

The terms on the right-hand side are explained as follows:

$\sigma_v$  (contribution of stress from mandatory geometrical dislocations and internal thermal stresses)

Since the matrix and particles have different thermal expansion coefficients, they are subject to different contractions on cooling, which leads to severe thermal stresses in the matrix. These can be cleared by diffusion processes or by the formation of relieving geometrical dislocations. Despite this relaxation, the remaining stresses expose the matrix to tensile stress and the particles to compression stresses. The magnitude of the thermal stresses and of the dislocation density is a function of the particle size  $d$ , the particle volume fraction  $V_p$ , the difference of the thermal expansion coefficients  $\Delta C$ , and the temperature gradient  $\Delta T$ , so that the contribution of stress  $s_v$  can be estimated from:

$$s_v = \alpha G b \rho^{1/2} \quad (12.8)$$

where  $\rho = [(12\Delta T\Delta C)/bd]$ ,  $\alpha = \text{const.} = 0.5-1$ ,  $G = \text{shear modulus}$ ,  $b = \text{Burger's vector}$

The distribution of all geometrically necessary dislocations within the matrix can be quite different. Tests on particle-reinforced materials made of pure aluminium and aluminium alloys showed evenly distributed dislocations for the pure material, while with the alloys the dislocations mainly formed at the boundary surface between the matrix and the particles. The thermal stresses influence the flow stress in such a way that they form a hydrostatic tensile stress state with equiaxial particles. This condition leaves the yield strength untouched, while the maximum strength is influenced by shear stresses close to the particles.

$\sigma_k$  and  $\sigma_{sk}$  (contribution of stresses determined by the grain and sub-grain size)

Due to thermal and mechanical treatment such as the annealing of a deformed composite, recrystallization of the composite's microstructure can occur. In this case, the particles act as recrystallization nuclei even though they are usually larger than 1  $\mu\text{m}$  in these types of materials. The resulting grain size  $D$  is a function of the number of particles per volume fraction, i.e. directly proportional to the particle size. The grain size of the recrystallized composite is normally between 1 and 10  $\mu\text{m}$ , and is therefore much smaller than the corresponding grain size of non-reinforced material, such that a hardening effect analogous to the Hall-Petch relationship can be described by:

$$\sigma_k = k \cdot D^{-1/2} \quad (12.9)$$

with  $k = \text{const.} \approx 0.1 \text{ MNm}^{-3/2}$

If no recrystallization occurs due to the volume fraction and particle size, e.g. in the case of mechanically alloyed materials with a high content of fine dispersoids, a sub-grain structure remains in the annealed material, which can also contribute to hardening through the Hall-Petch effect. Sub-grains can also form when the necessary geometrical dislocations are redistributed by thermally activated recovery processes. This works as a hardening effect as well. In terms of hardening by sub-grains and the term  $\sigma_{sk}$ , the constant  $k$  of the Hall-Petch relationship can be replaced by a much lower value of about  $0.05 \text{ MNm}^{-3/2}$ .

$\sigma_{kf}$  (contribution of stress by strain hardening)

The initial rate of hardening is often much higher with particle-reinforced composites than with the non-reinforced matrix, since the particles and matrix exhibit different strains. Up to a certain total elongation, the matrix will deform plastically while the particles still behave elastically. Extensive stress fields, which cause great composite hardening, are

built-up by non-relaxed strains in the matrix due to dislocations adding to the particles. The contribution that this makes to the stress is given by [18, 19]:

$$\sigma_{KF} = \alpha \cdot G \cdot V_p \cdot \sqrt{\frac{2b}{d}} \cdot \sqrt{\varepsilon} \tag{12.10}$$

where  $\varepsilon$  = total elongation

Figure 3 summarizes the effect of the individual stress contributions on composites with different sized particles according to the micro-mechanical model described above. The figure shows that the particle size and volume fraction are the main parameters, which, within the different mechanisms, deliver the characteristic contribution.

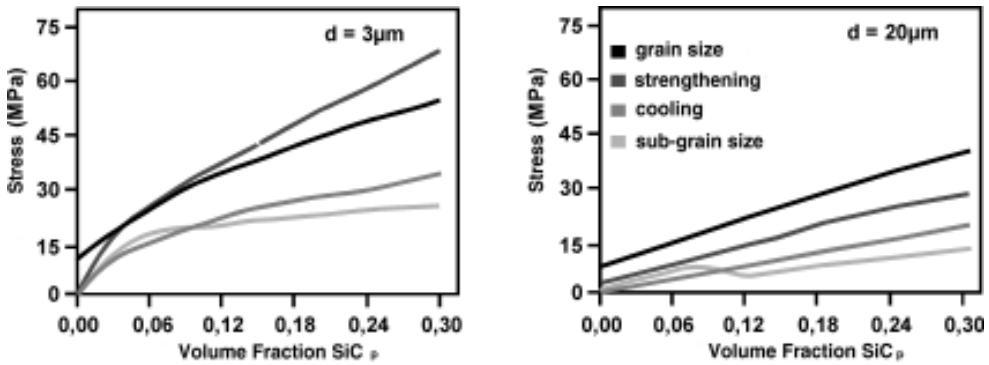


Figure 3: Stress contributions of different mechanisms to the yield point due to particles of various sizes, according to [25]

In general, the model tends to calculate higher amounts of hardening for smaller particle diameters than for coarse particles. With small particles, the strain hardening contributes most to the increase in tensile strength [15].

The Orowan mechanism mentioned above enables gliding dislocations to pass barriers in such a way that they bulge in between the obstacles. The bulge forming is very extensive, so that a part of the dislocation remains as a ring around the obstacle, while the dislocation proceeds on its gliding layer. For particle-reinforced composites with particles of a few microns in diameter, this mechanism is of minor importance. For materials with precipitation and dispersion hardening, however, or even for reinforcements by nanoscale particles, it is of great importance.

## 12.4 Production Methods

### 12.4.1 Melting Metallurgical Processes

The melting metallurgical production of particle-reinforced magnesium matrix composites includes three major processes: the stirring of particles into the fluid metal, the infiltration of porous particle and hybrid solids (preforms) with melt under high pressure, and finally spray-forming. The basic requirement for a melting metallurgical production is a sufficient wetting of the reinforcement phase by the melt and a good bonding between them. Methods

not involving any pressure fulfil these requirements by the material combination itself or by prior treatment of the reinforcement phase (annealing, coating). Infiltration methods, such as the infiltration of preforms by squeeze-casting, overcome barriers such as insufficient wetting or inadequate capillary pressures through the application of an external force, which enforces good bonding between both components of the composite.

Particles can be added with stirring to the fluid or half-frozen melt either in powder form or in the form of pellets or briquettes. The actual mixing process is then performed with the help of a mechanical stirrer, ultrasonic excitation, electromagnetic stirring, sand-casting or pressure-casting. The most important parameters for stir-casting are the stirring speed; the atmosphere; the size, shape, prior treatment, and volume fraction of the particles; the melt temperature, and finally the holding time and any degassing steps that might be necessary [24,25]. In the case of mechanical stirring, the geometry and size of the propeller as well as its position within the crucible are further important parameters.

The correct selection of these parameters is crucial with regard to the quality of the final composite. Thus, very fine particles show a much greater tendency towards agglomeration and rinsing with rising voids than coarse particles, which show instead segregation by sedimentation or floating. The temperature of the melt is important since serious propeller wear and excessive chemical attack of the particles by the molten matrix material can occur, together with an increased gas absorption by the melt. On the other hand, the angle of wetting becomes smaller with increasing temperature so that the boundary surface bonding between matrix and particles is improved. Moreover, a multitude of problems concerning the particle distribution and the castability of the molten composite material arise when the temperature is too low.

Laurent et al. [26] examined the influence of different production and material parameters, such as the stirring position inside the crucible, the temperature control during stirring,

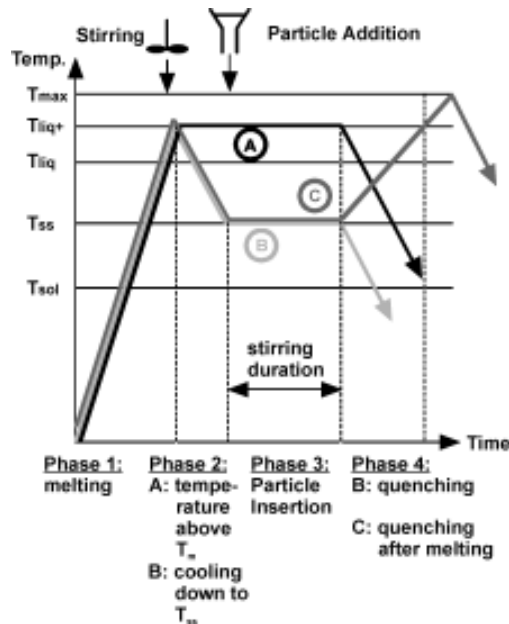


Figure 4: Temperature control when compo-casting, according to [26]

and the particle size on the structure and properties of an SiC-reinforced AZ91 alloy. The different temperature profiles, which differ in the temperature during the stirring, proved to be of primary importance. Figure 4 shows a schematic of the profiles.

In the case of profile “A”, the particles were stirred at temperatures above the liquidus line, while the stirring took place in the solid-liquid two-phase area for profiles “B” and “C” (compo-casting). The composite melts of the profiles “A” and “B” were quickly cooled to room temperature immediately after the stirring; only in the case of profile “C” was the melt again heated well beyond the liquidus temperature before cooling. Through macroscopic and microstructure observations, it was found that stirring of the particles into the half-frozen material resulted in the most homogeneous particle distribution and lowest porosity, especially for profile “C”. This effect was stronger for coarse particles with an average size of 54  $\mu\text{m}$  than for medium-sized particles of 12  $\mu\text{m}$ . Moreover, the distribution of the coarse particles could be greatly influenced by a change in the stirring position. The particles accumulated in the lower part of the crucible when the agitator was lifted by about 10% of the melt height. This effect was not seen with the very fine particles.

Luo [9,27] made identical observations on studying the distribution of SiC particles that had been stirred into technical pure magnesium and into the alloys AZ91 and AS41. Micrographs of the pure magnesium-based composites showed that the particles were completely dispersed on the grain boundaries, indicating that they were not wetted by the melt but rather pushed forward with the melt front to ultimately reside in the portion of the melt that was last to freeze. The alloy AZ91 gave the most homogeneous particle distribution; particles were found at the grain boundaries as well as within grains, which gives clear evidence for a sufficient wetting of the particles by the melt. The particle distribution was only slightly less even for AS41, in which more particle aggregates were found than in the AZ91 composites. None of the examined composites showed the intermetallic phase  $\text{Al}_4\text{C}_3$ , which is predicted on the basis of the reaction kinetics. Nevertheless,  $\text{Mg}_2\text{Si}$  precipitates were detected in the two aluminium-containing alloys, as reported by Laurent et al. Reaction products on the particles were interpreted as the ternary phase of aluminium, carbon, and oxygen. In contrast, Wilks et al. [6] described the formation of  $\text{Al}_4\text{C}_3$  when SiC particles were heated at 725 °C for two hours within a melt of AZ91.

The reinforcement components for the production of particle and hybrid preforms by squeeze-casting or gas-pressure infiltration are fixed with the help of inorganic  $\text{SiO}_2$  or  $\text{Al}_2\text{O}_3$  as binders, which ensure the preform stability during infiltration. In this way, many different volume fractions can be accommodated. However, the size and volume fraction of particles is limited for pure particle preforms, because an uncomplicated infiltration of the solids is no longer guaranteed with high volume fractions or with too small particle sizes. Taking this into consideration, the use of hybrid preforms, e.g. mixtures of particles and fibres, has definite advantages since the fibres only act as supporting structures, whereas the particles are embedded, thus leaving enough porosity for infiltration. The fibres arrange themselves randomly in layers inside the preform. This is called planar-isotropic distribution [18, 29].

Squeeze-casting offers the advantages of high productivity and easy shaping together with the production of high quality, non-porous materials [30]. Complex parts can be realized with cores or male cores. The heat transfer between the mould and the melt/cast part is greatly improved by the high pressure of squeeze-casting. A supercooling of the melt may be thermodynamically achieved through judicious choice of the casting temperature. As a result, the melting point shifts to higher temperatures. The freezing is accelerated as a consequence and the microstructure turns out to be finely dispersed [30–32].

The infiltration of particle- and hybrid preforms has been described and characterized, among others by Kainer et al. [13, 33, 34]. The infiltration of pure particle preforms was indeed achieved, but led to some non-reinforced zones and fracture, as well as to particle delaminations due to insufficient preform strength [13]. Hybrid reinforced magnesium matrix composites, on the other hand, showed complete infiltration and a homogeneous distribution of the ceramic particles since the bridging – which connects the particles to the fibres – dissolved during infiltration. The particles are embedded within the matrix. Tests on the orientation dependence of various material properties revealed a higher isotropy for hybrid composites based on different magnesium alloys compared to single-fibre composites. This can be explained in terms of the low fibre content of the hybrid reinforcements.

Spray-forming is an alternative and new technology for producing final-shaped components and semi-products. Spray-forming, in principle, allows the direct manufacture of tubes, plates, rods, or sheets in one processing step. It can be categorized between powder metallurgical processes and near-net-shape casting and is especially suitable for processing alloys with poor castability and discontinuously reinforced metal matrix composites. The method is characterized by a microstructure with a homogeneous dispersion of elements and phases along with few segregations and high purity, which improves mechanical and physical properties and the corrosion resistance.

Sputtering a metal melt and the deposition of the resulting drops on a substrate produces the material. Sputtering works in such a way that a melt-jet leaves the crucible and is impinged with a high-pressure inert gas from the side. After a short falling distance, the molten drops fall on the substrate as either fluid, half-solid, or solid aggregate according to their size. As the process time increases, the spray forms a solid, also called a deposit. The substrate plate is constantly lowered and concurrently rotated during the deposition sequence to ensure a constant deposit growth. In this way, the deposit reaches 95–98% of the theoretical density and is later completely consolidated by forging or extrusion. The sputtered material that does not contribute to the deposit building falls down as overspray and can be recycled. This combination of powder metallurgical production and consolidation makes the production of metallic composites very easy. When ceramic particles are added to the spray, they are distributed even more homogeneously in the material than would be possible by melting metallurgy. The clearly faster cooling rates lower possible boundary surface reactions between the non-metal phase and the melt so that the damage to the reinforcement material can be eliminated almost completely.

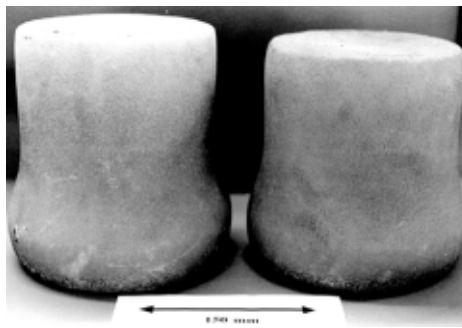


Figure 5: Spray-formed, particle-reinforced magnesium matrix composite (Osprey Metals Ltd., Neath, U.K.)

By comparing the analyses of spray-formed and powder metallurgical magnesium composites based on QE22, it was verified [35–37] that spray-forming is advantageous over conventional methods in terms of the process steps required and the technological properties of the produced materials. Figure 5 shows such spray-formed solids of a QE22/20% SiCp composite. The microstructure of the spray-formed material after sputtering is porous at first, and interstratified with particle clusters. However, as with other production methods, extrusion leads to a superb and even particle distribution and a reduction in the porosity from 20% to 0.5%. The greatest maximum elongation and tensile strength was seen for spray-formed composites and the overspray in extruded and heat-treated condition.

## 12.4.2 Powder Metallurgical Methods

Metallic powders are usually produced by mechanical methods such as chipping or machining of a solid metal, or by sputtering or spraying of metallic melts with fluids or gases, respectively. Other methods, such as electrochemical processes or condensation processes, are also applied, although mainly with noble or heavy metals. Besides mechanical chipping, gas sputtering is the most important process for producing magnesium powders. The working principle of sputtering has already been explained in Section 12.4.1 in relation to spray-forming. The only difference here is that the sputtered drops are not captured by a substrate, but are instead completely frozen during their fall through the chamber, thus forming a loose powder swell.

Figure 6 shows powders of two magnesium alloys, which were made mechanically (a) and by sputtering (b). Particles generated by gas sputtering are usually more spherical and have a higher bulk density than the corresponding particles made by machining or by water sputtering. For the sputtering of magnesium, an argon/oxygen mixture containing 1–2% O<sub>2</sub> is usually used as the sputter medium, whereby a specific phlegmatization of the reactive metal powder is achieved and a non-hazardous handling becomes possible [38].

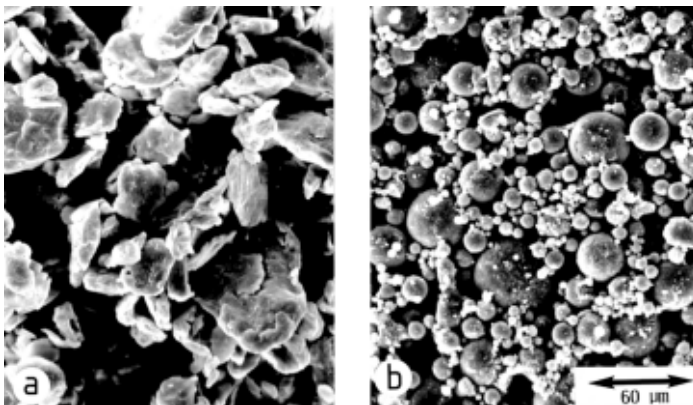


Figure 6: Magnesium alloy powder, a) AZ91, produced by mechanical breaking, b) QE22, produced by gas-sputtering [55]

Besides liquid-phase sintering, the powder metallurgical production of metal matrix composites has the advantage of a low process temperature, so that excessive reactions at the boundary surfaces between the composite components do not occur. In this way, it is possible to produce composites that would cause problems in melting metallurgical processes through intense reactivity at the boundary surfaces or by a lack of wetting of the reinforcement by the melt. The process also enables very high reinforcement volume fractions of up to 50% [12].

For the preparation of a powder metallurgical magnesium matrix composite with particle reinforcement, a two-step process has been established, whereby the metallic powder is thoroughly mixed with ceramic particles and then milled, e.g. in a ball mill [39].

A homogeneous particle distribution in the latter composite requires the metal powder and ceramic particles to have a certain mutual size relationship with the aforementioned  $d_{50}$  value as an orientation value. According to [39], the ratio between the average size distribution of the metal powder and that of the reinforcement component should be around 5:1 to avoid agglomeration or separation. Therefore, it is important to classify particles in terms of their size before starting the actual mixing process. The milling, which follows the mixing, serves to mechanically fix the ceramic particles to the metal powder particles and increases the homogeneity. The final consolidation is accomplished by extrusion [12, 37, 39] or forging [40].

For extrusion, pre-pressed and pre-sintered green bodies, as well as loose swells in complying bins or shells, can be handled. These powders are then forced under high pressure at high temperature through the nozzle, and the powder mixture is deformed and thoroughly welded together, so that the resulting solid metal has a density close to the theoretical maximum. As can be seen in Fig. 7, the reinforcement phase is very evenly distributed.

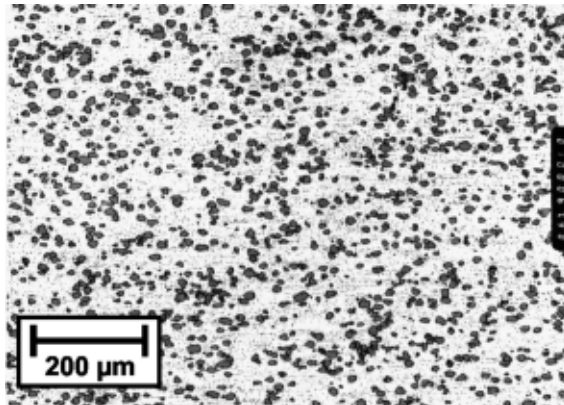


Figure 7: Microstructure of a p/m-QE22/SiC<sub>p</sub> composite parallel to the extrusion direction

These processes are very suitable for metals such as aluminium and magnesium, which form an oxide layer on exposed surfaces. The oxide films are broken apart during extrusion due to the high deformation rates, exposing more metallic contact faces than a simple hot



pressing [3]. Particle reinforcements have become most prominently established for the powder metallurgical formation of metallic composites since their geometry prevents any disintegration or cracking during the deformation.

## 12.5 Mechanical Properties and Creep Behaviour

### 12.5.1 Mechanical Properties

The mechanical properties of particle-reinforced magnesium matrix composites have been well-studied, with an emphasis on composites made by stirring, especially those based on AZ91 [26,27,42,43]. Compo-cast AZ91/15% SiC<sub>p</sub> composites, as reported in [26], showed a significantly increased yield strength of about 40 MPa compared to that of the non-reinforced alloy. The maximum strength was slightly less than that of the matrix; the Young's modulus was measured as about 65 GPa, which is roughly 20 GPa higher than that of the regular material. As observed for all the composites, the ductility also decreased due to the reinforcement. The strain at fracture fell from 10% for the non-reinforced material to about one-tenth of this value following the addition of the particles. Rozak et al. [42] produced AZ91 composites with 20 vol.% SiC particles by various methods. First they stirred particles into the melt, and then the composite was post-processed by squeeze-casting, sand- or gravity-casting. The squeeze-cast materials were further extruded. The yield strength and tensile strength had the same values of 210 and 295 MPa, respectively, for each differently cast material. Only the extrusion of the pressure-cast material, including the subsequent heat treatment, resulted in a significant increase in strength; the yield strength and tensile strength then amounted to 310 and 430 MPa.

Luo [27] and Moll et al. [43] observed the mechanical behaviour of AZ91 with a 10% SiC particle reinforcement. Particles with an average size of 7 μm, as used in [27], led to an increase in the yield strength and to reduced ductility and tensile strength, similar to that seen in [26]. However, the low particle content did not lead to a higher Young's modulus. In

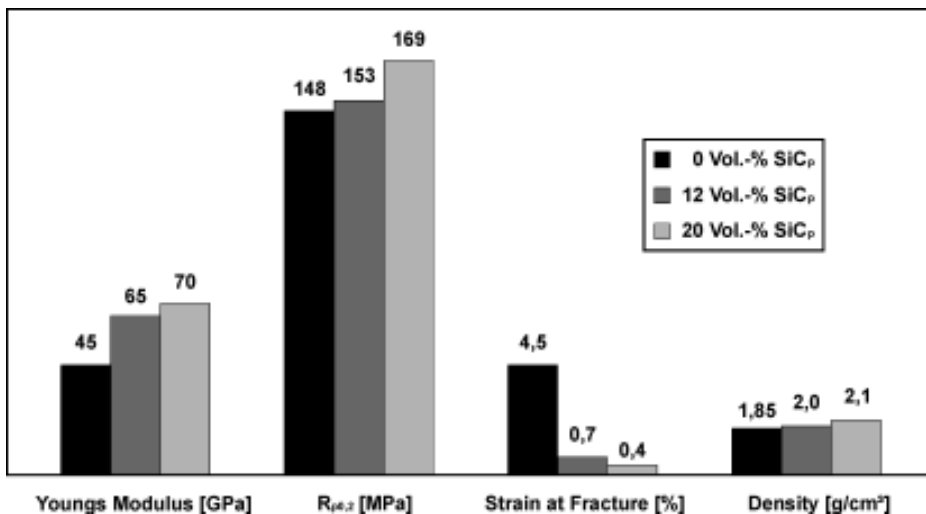


Figure 8: Mechanical properties of the alloy ZE41 with particle reinforcements [41]

[43], the mechanical strength at room temperature and at elevated temperatures was analysed; the average particle size distributions were found to be 17  $\mu\text{m}$  and 9  $\mu\text{m}$ , respectively, in these cases. As in the results described above, the maximum strength at room temperature was lowered in the squeeze-cast condition due to the presence of the particles, while an increase of the tensile strength of 20–25 MPa took place in the temperature range 150–200  $^{\circ}\text{C}$  with both types of particles. Hu described an increase in the Young's modulus of AZ91 from 45 GPa to 176 GPa for a 40 vol.% SiC particle reinforcement of material made using a squeeze-cast infiltrated particle preform. The increase in the tensile strength from 255 to 302 MPa was rather low in this case.

Other magnesium alloys taken from the AS, ZC, ZM, or ZE alloy series have also been used as matrix materials for particle-reinforced composites and tested with regard to their mechanical properties. Figure 8 lists the mechanical properties of the 12 vol.% SiC-reinforced ZE41 alloy [41]. As can be seen from the figure, the Young's modulus was improved most with this alloy, while the other properties were only slightly improved.

Holden et al.'s [8] studies concentrated on the strength and creep behaviour of the ZC63 alloy, again with 12 vol.% SiC particles. The results for the composite's Young's modulus deviate a lot, especially at higher temperatures up to 150  $^{\circ}\text{C}$ , but on average they are still below the corresponding values for the non-reinforced matrix. All values for the strength properties are summarized in Table 2.

Table 2: Strength properties of a ZC63 and a ZC63/SiC<sub>p</sub> composite [8]

Temperature [ $^{\circ}\text{C}$ ]	Youngs Modulus [GPa]	Yield Strength [MPa]	max. Strength [MPa]	Strain at Fracture
ZC63 non-reinforced				
20	39,8	138	244	8,5
100	38,5	122	198	4,6
150	37,2	121	167	4,7
ZC63/SiC <sub>p</sub> -composite				
20	65,0	148	197	0,7
100	44,6	136	184	2,0
150	69,9	123	148	1,4

Mikucki et al. [45] listed various mechanical property data for a variety of powder- and melting-metallurgically produced magnesium matrix composites with particle reinforcements. The wrought alloy AZ31 and the binary alloy Z6 were produced by stirring 20% SiC particles of sizes 10  $\mu\text{m}$  and 16  $\mu\text{m}$  into the melt. The alloys were cast as bolts, which were then extruded. Since the formability of AZ31 is very good, the extrusion ability was, as expected, better than that for the Z6 composite. Z6, on the other hand, showed a very high yield strength of up to 413 MPa and a tensile strength of 469 MPa, which represents the maximum strength currently available on the commercial market.

Besides their own data, Mikucki et al. [45] also provided an overview of the literature on various powder metallurgical produced magnesium particle composites for comparison purposes (Table 3). Clark and Garret [47] extended this information with observations concerning a ZK60A alloy, which was reinforced with 30 vol.% B<sub>4</sub>C particles by a powder-

metallurgical process. This alloy showed even higher values of yield strength and tensile strength of 455 and 510 MPa; the Young's modulus was as much as 94 GPa.

Table 3: Strength properties of various (p/m)-Mg/particle-reinforced materials [45]

Material	Youngs Modulus /GPa/	Yield Strength /MPa/
AZ61A+15 Vol.% B <sub>4</sub> C	61	229
AZ61A+20 Vol.% B <sub>4</sub> C	64	254
AZ61A+25 Vol.% B <sub>4</sub> C	78	258
AZ90+25 Vol.% B <sub>4</sub> C	91	460
ZK60A+15 Vol.% B <sub>4</sub> C	73	388
ZK60A+20 Vol.% B <sub>4</sub> C	78	393
ZK60A+25 Vol.% B <sub>4</sub> C	86	418
Mg+10 Vol.% B <sub>4</sub> C	57	260
Mg+20 Vol.% B <sub>4</sub> C	59	273
AZ31B+20 Vol.% SiC	102	466
Mg+15 Vol.% SiC (1 $\mu$ m)	62	422
Mg+17 Vol.% SiC (3 $\mu$ m)	68	409
Mg+18 Vol.% SiC (4 $\mu$ m)	69	382
Mg+20 Vol.% SiC (3 $\mu$ m)	72	386
Mg+20 Vol.% SiC (4 $\mu$ m)	70	368
ZK60A+15 Vol.% SiC	78	399
ZK60A+20 Vol.% SiC	84	428

Lee et al. [46] examined the mechanical properties and the microstructures of various AZ91/10 vol.% SiC<sub>p</sub> composites, produced by p/m and extrusion, and varying in their particle size (8, 30, 50  $\mu$ m). They characterized the material properties as a function of extrusion parameters such as extrusion ratio or extrusion temperature. The non-reinforced matrix as well as the composites showed very small equiaxial grains of sizes between 10 and 17  $\mu$ m after extrusion, which formed due to dynamic recrystallization during extrusion. The strength values for the materials increased with increasing extrusion ratio, with the strength of the composites always being higher than that of the non-reinforced matrix. The highest yield strength of 271 MPa was accomplished with an 8  $\mu$ m SiC particle reinforcement. In [46], the results concerning strength were rationalized in terms of the Hall–Petch relationship by considering the small grains and the high strength of the composite as a grain growth limiting effect of the particles. Solution annealing after extrusion resulted in a loss of tensile strength in all cases, but this was less pronounced for the composites than for the matrix material.

A dependence of the mechanical properties on the particle size and shape was also found by Moll et al. [12], who studied the properties of a p/m QE22/15 vol.% SiC<sub>p</sub> composite in extruded condition, as well as following a T6 heat treatment. The results of these measurements are listed in Fig. 9. Silicon carbide particles of average size 9, 12 and 30  $\mu$ m were introduced into the matrix, whereupon there was a distinction between a spherical and square-weave shape for the latter two particle sizes. When 30  $\mu$ m particles were used for reinforcement, the values for tensile and yield strength decreased, whereas 9 and 12  $\mu$ m sized particles contributed to a significant increase in strength. This gain in strength was slightly higher for square-weaved particles than for spherical ones. In general,

both the non-reinforced matrix and the composites exhibited a loss in strength following heat treatment, in accordance with the results in [46]. The strengthening effect of small particles could not be verified beyond 200 °C; the good high-temperature properties of silver- and rare earth containing alloys were largely lost due to the particles.

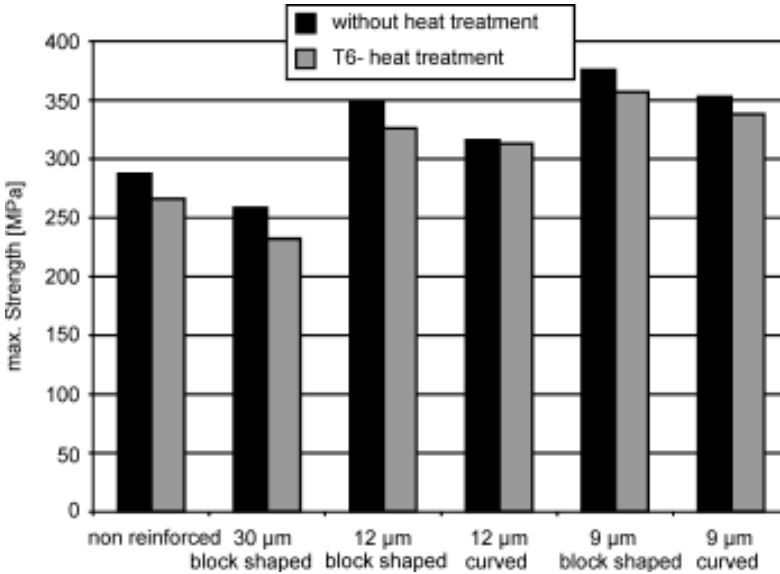


Figure 9: Tensile strengths of the alloy QE22 (p/m) and QE22/15 vol.% SiC<sub>p</sub> composite (p/m) at room temperature

Moreover, if one compares the mechanical behaviour of these composites with that of other composites based on QE22, as shown in Fig. 10, it can be seen that the powder metallurgical version has room temperature strength properties which are far superior to those of pressure-cast hybrid or short-fibre reinforced composites. At higher temperatures, however, the fibre-reinforced materials are much stronger.

Kainer et al. analysed magnesium matrix composites with hybrid reinforcements of 10 vol.% Saffil short fibres/15 vol.% SiC particles and 5 vol.% Saffil short fibres/20 vol.% SiC particles. Both composites showed significantly improved mechanical properties compared to the non-reinforced matrix, QE22 in this case. Thus, the Young's modulus could be increased to approximately 75 GPa for both materials, and the yield and tensile strengths were 80 to 100 MPa higher than the corresponding matrix values. The reinforcement mixture with the higher fibre content always exhibited a greater increase in strength.

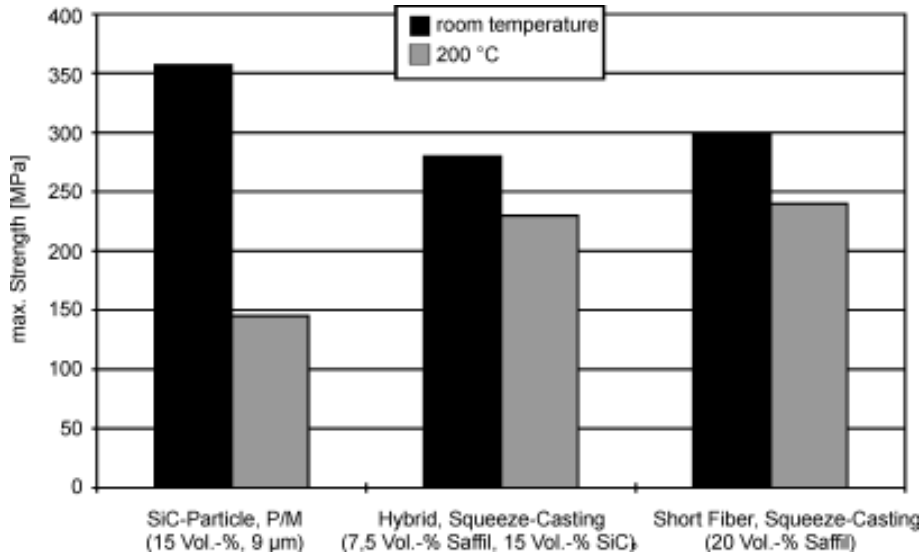


Figure 10: Tensile strengths of various QE22 composites

## 12.5.2 Creep Behaviour

The creep behaviour of particle-reinforced magnesium alloys has been relatively little studied and divergent results have been reported. The matrix seems to have the main influence on the creep resistance. Wilks and King [4] worked on a ZC71-based composite with a reinforcement of 10 µm SiC particles, which were stirred into the fluid matrix melt. Creep tests proved that the composite required double the load at 150 °C to reach equal strains within the same time as compared to the pure matrix material. The difference became especially obvious in long-term tests run for up to 1000 h.

Using ZC63 as the base material, with all process parameters and particle properties remaining constant, the composite is less creep-resistant than the matrix [8]. At temperatures up to 150 °C and loads of up to 100 MPa, the composite materials showed creep rates that were faster by one order of magnitude for almost all temperature and load steps.

Moll et al. [12, 13, 43, 48] looked at the creep behaviour of various powder and melting metallurgically produced particle-reinforced magnesium matrix composites based on AZ91 and QE22, which were reinforced with SiC particles of different sizes and shapes. The creep tests were carried out at stresses between 35 and 70 MPa at temperatures of 150 and 200 °C. As an example, Fig. 11 shows the creep results at 200 °C and 35 MPa for p/m QE22/15 vol.% SiCp-T6 composites. It can clearly be seen that the creep resistance decreases tremendously when the particles are incorporated. The most influential parameter regarding this effect is the particle size; the bigger the particles, the higher the creep rates. The rates increased by at least four orders of magnitude. At 200 °C, no significant secondary creep could be observed, which is consistent with a literature report [49]. The fracture times shorten from over 2000 h for the non-reinforced matrix to 7–8 h for composites with particle sizes between 9 and 12 µm.

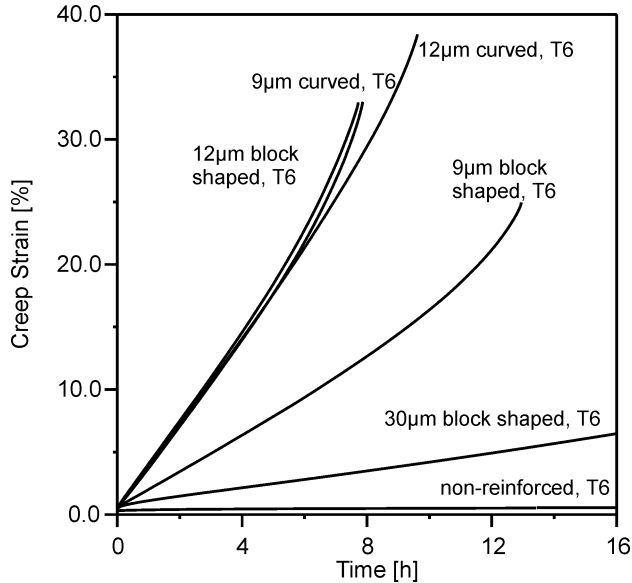


Figure 11: Creep behaviour of (p/m)-QE22/SiC<sub>p</sub> composites at 200 °C and 35 MPa [48]

Creep tests on a melting metallurgically produced composite with an AZ91 matrix and 17 µm SiC particles showed that the effect of temperature and stress on the creep behaviour is irregular. The particle reinforcement reduced the minimum creep rate to roughly  $3\text{--}4 \times 10^{-10} \text{ s}^{-1}$  in areas of low stress and temperature (35 MPa, 150 °C). Increasing the temperature by 50 °C led to almost identical secondary creep rates of  $1 \times 10^{-8} \text{ s}^{-1}$  and  $3 \times 10^{-8} \text{ s}^{-1}$  for the matrix and the composite, respectively. The same creep rates of  $3 \times 10^{-8} \text{ s}^{-1}$  were measured for a doubled load of 70 MPa (150 °C). At 200 °C, the creep rate of the composite ( $1 \times 10^{-6} \text{ s}^{-1}$ ) was about one order of magnitude higher than that for the matrix alloy ( $2 \times 10^{-7} \text{ s}^{-1}$ ). A significant tertiary creep was observed only for materials under high loads at high temperatures. At 150 °C, the matrix alloys and composites failed suddenly in the secondary creep stage.

Wolfenstine et al. [50] studied the high-temperature behaviour of the cubic-centered alloy MgLi14 reinforced with 3–5 µm particles of elemental boron. The composite was produced from extruded powders. This material showed improved creep resistance between 230 and 280 °C with increasing particle contents of 10, 20, and 30 vol.%. The composite with 30 vol.% of particles withstood eight times the load of the regular matrix at a constant creep rate. Even though the ultra-light magnesium/lithium alloys have a high specific strength, their creep resistance is still far below that of the pure hexagonal magnesium. In [50], it is stated that the creep rate of pure Mg is five times higher than that of Mg/Li alloys, which is attributed to the much greater lattice diffusion coefficient of the cubic-centered Mg/Li structure.

## 12.6 Summary

The mechanical properties of particle-reinforced magnesium composites described herein clearly demonstrate that these materials offer interesting perspectives whenever there is a demand for a light material with a high Young's modulus. With a suitable choice of material compositions and production methods, strengths and Young's moduli can be achieved that match or even surpass those of aluminium materials. At this point, the improved wear resistance should be mentioned, as well as the reduction of the thermal expansion coefficient, both of which are achieved with ceramic particle reinforced light metals [51]. The main focus of research and development in magnesium composites has hitherto been on fibre reinforcements, although these are still not used to any great extent. The high prices of the fibres and the complex production are the main reasons for this stagnation. Herein, we have mentioned the advantages that particle reinforcements have to offer. Commercial production of these materials has already begun; some potential semi-products and parts such as tubes or cylinder sleeves are available on the market [52]. There is also interest in these materials in the aviation and space industries. The devolvement of particle-reinforced magnesium alloys still needs more detailed research work. For example, only a few results have been reported pertaining to fatigue tests and high-temperature properties [53, 54]. High-temperature and creep tests demonstrated a dependence of each composite on the production method. This leaves some research work still to do, namely to evaluate the application of particle-reinforced magnesium matrix composites at higher temperatures and loads and to create a complete performance profile.

## 12.7 Literature

- /1/ Salmang, H., Scholze, H.: *Keramik, Teil 1: Allgemeine Grundlagen und wichtige Eigenschaften*, 6. Aufl., Springer, 1982.
- /2/ Kainer, K.U.: in *Metallische Verbundwerkstoffe* (Hrsg.: Kainer, K.U.), DGM-Informationsgesellschaft, Oberursel, 1994, p. 43.
- /3/ Schatt, W.: *Pulvermetallurgie – Sinter- und Verbundwerkstoffe*, 3. Aufl., Dt. Verlag für Grundstoffindustrie, Leipzig, 1988.
- /4/ Wilks, T.E., King, J.F.: in *Magnesium Alloys and Their Applications* (Hrsg.: B.L. Mordike, F. Hehmann), DGM-Informationsgesellschaft, Oberursel, 1992, p. 431.
- /5/ Inem, B.: in *Magnesium Alloys and Their Applications* (Hrsg.: Mordike, B.L., Hehmann, F.), DGM-Informationsgesellschaft, Oberursel, 1992, p. 439.
- /6/ Wilks, T.E., King, J.F., Warlow, G.D.: in *Proc. 3<sup>rd</sup> Int. Magnesium Conf.* (Hrsg.: G.W. Lorimer), The Institute of Materials, London, 1997, p. 585.
- /7/ Gopalakrishna, V., Krishnadas Nair, C.G., Krishnadev, M.R.: in *Proc. 3<sup>rd</sup> Int. Magnesium Conf.* (Hrsg.: Lorimer, G.W.), The Institute of Materials, London, 1997, p. 575.
- /8/ Holden, P.E., Pilkington, R., Lorimer, G.W., King, J.F., Wilks, T.E.: in *Proc. 3<sup>rd</sup> Int. Magnesium Conf.* (Hrsg.: Lorimer, G.W.), The Institute of Materials, London, 1997, p. 647.
- /9/ Luo, A.: in *Proc. 10<sup>th</sup> Int. Conf. on Composite Materials (ICCM 10)* (Hrsg.: A. Poursartip), Woodhead Publishing Ltd., 1995, p. II-287.
- /10/ Schröder, J., Kainer, K.U., Mordike, B.L.: in *Proc. 3<sup>rd</sup> European Conf. on Composite Materials (ECCM 3)*, EACM und Elsevier Applied Science, 1989, p. 171.

- /11/ Roos, U., Kainer, K.U., Mordike, B.L.: in Proc. 1994 Powder Metallurgy World Congress, Société Française de Métallurgie et de Matériaux, Les Editions de Physiques Les Ullis, 1994, p. 2249.
- /12/ Moll, F., Kainer, K.U.: in *Verbundwerkstoffe und Werkstoffverbunde* (Hrsg.: Friedrich, K.), DGM Informationsgesellschaft, Frankfurt, 1997, p. 619.
- /13/ Moll, F., Kainer, K.U.: in Proc. 11<sup>th</sup> Int. Conf. on Composite Materials (ICCM 11) (Hrsg.: Scott, M.L.), Woodhead Publishing Ltd., 1997, p. III-287.
- /14/ Lloyd, D.J.: *International Materials Reviews*, 1994, 39, 1-23.
- /15/ Kainer, K.U.: *Mitteilungsblatt der TU Clausthal*, 1997, 82, 36-44.
- /16/ Halpin, J.C., Tsai, S.W.: *Air Force Materials Laboratory*, 1967, AFML-TR-67-423.
- /17/ Lloyd, D.J.: in Proc. 12<sup>th</sup> Risø Int. Symp. on Metallurgy and Materials Science (Hrsg.: Hansen, N. et al.), Risø Nat. Laboratory, Roskilde, 1991, p. 81.
- /18/ Humphreys, F.J.: in Proc. 9<sup>th</sup> Risø Int. Symp. on Metallurgy and Materials Science (Hrsg.: Anderson, S.I. et al.), Risø Nat. Laboratory, Roskilde, 1988, p. 51.
- /19/ Humphreys, F.J., Basu, H., Djazeb, M.R.: in Proc. 12<sup>th</sup> Risø Int. Symp. on Metallurgy and Materials Science (Hrsg.: Hansen, N. et al.), Risø Nat. Laboratory, Roskilde, 1991, p. 51.
- /20/ Christman, T., Needleman, A., Suresh, S., *Acta Metall.*, 1989, 37, 3029-3050.
- /21/ Tvergaard, V.: in Proc. 12<sup>th</sup> Risø Int. Symp. on Metallurgy and Materials Science (Hrsg.: N. Hansen et al.), Risø Nat. Laboratory, Roskilde, 1991, p. 173.
- /22/ Levy, A., Papazian, J.M. in Proc. 12<sup>th</sup> Risø Int. Symp. on Metallurgy and Materials Science (Hrsg.: Hansen, N. et al.), Risø Nat. Laboratory, Roskilde, 1991, p. 475.
- /23/ Piggott, M.R.: *Load Bearing Fibre Composites*, Pergamon Press, Oxford, 1980
- /24/ Rohatgi, P.: *Modern Castings*, 1988, 47-50.
- /25/ Asthana, R.: *J. Mat. Synthesis and Processing*, 1997, 5, 251-277.
- /26/ Laurent, V., Jarry, P., Regazzoni, G., Apelian, D.: *J. Mat. Sci.*, 1992, 27,4447-4459.
- /27/ Luo, A.: *Met. Mat. Transactions A*, 1995, 26A, 2445-2455.
- /28/ Kainer, K.U.: in *Metallische Verbundwerkstoffe* (Hrsg.: K.U. Kainer), DGM-Informationsgesellschaft, Oberursel, 1994, p. 219.
- /29/ Hegeler, H., Buschmann, R., Elstner, I.: in *Metallische Verbundwerkstoffe* (Hrsg.: Kainer, K.U.), DGM-Informationsgesellschaft, Oberursel, 1994, p. 101.
- /30/ Chadwick, G.A.: in *Magnesium Technology – Proc. London Conf. 1986*, The Institute of Metals, 1987, p. 75.
- /31/ Kaczmar, J.W., Kainer, K.U.: in Proc. 12<sup>th</sup> Risø Int. Symp. on Metallurgy and Materials Science (Hrsg.: Hansen, N. et al.), Risø Nat. Laboratory, Roskilde, 1991, p. 423.
- /32/ Kaczmar, J.W., Kainer, K.U.: in Proc. Int. Conf. Advances in Materials and Processing Technologies (Hrsg.: Hashmi, M.S.J.), Dublin City University, Dublin, 1993 1993, p. 2069.
- /33/ Schröder, J., Kainer, K.U.: *Mat. Sci. Eng.*, 1991, A135, 33-36.
- /34/ Kainer K.U.: in Proc. Int. Conf. Advances in Composites 93 (Hrsg.: Chandra, T., Dhingra, A.K.), TMS, 1993, p. 1213.
- /35/ Schröder, J., Kainer, K.U.: in Proc. Int. Conf. on Materials by Powder Technology PTM '93 (Hrsg.: F. Aldinger), DGM-Informationsgesellschaft, Oberursel, 1993, p. 739.
- /36/ Schröder, J., Kainer, K.U.: in Proc. 9<sup>th</sup> Int. Conf. on Composite Materials (ICCM 9) (Hrsg.: A. Miravete), University of Zaragoza und Woodhead Pub. Ltd, 1993, p. 340.



- /37/ Kainer, K.U., Schröder, J., Mordike, B.L.: in Proc. Int. Conf. Advances in Composites 93 (Hrsg.: Chandra, T., Dhingra, A.K.), TMS, 1993, p. 1061.
- /38/ Knoop, F.M., Kainer, K.U.: Metall, 1994, 6, 461-465.
- /39/ Schröder, J.: Untersuchungen zum Aufbau und zu den mechanischen Eigenschaften von partikelverstärkten Magnesium-SiC-Verbundwerkstoffen, Dissertation, Technische Universität Clausthal, 1991.
- /40/ Schröder, J., Kainer, K.U. in Magnesium Alloys and Their Applications (Hrsg.: Mordike, B.L., Hehmann, F.), DGM-Informationsgesellschaft, Oberursel, 1992, p. 469.
- /41/ N.N.: Firmenschrift Magnesium Elektron Ltd., Manchester, UK.
- /42/ Rozak, G.A., Lewandowski, J.J., Altmisoglu, A., Wallace, J.F.: SAE Technical Paper, 1993, 930180, 1-10.
- /43/ Moll, F., Kainer, K.U.: in Tagungsband Werkstoffwoche 1998 (Hrsg.: Kopp, R., Herfurth, K., Böhme, D., Bormann, R., Arzt, E., Riedel, H.), Bd. VI – Metalle, Simulation Metalle, Wiley-VCH, 1998, p. 477.
- /44/ Hu, H.: J. Mat. Sci, 1998, 33, 1579-1589.
- /45/ Mikucki, B.A., Mercer II, W.E., Green, W.G.: SAE Transactions, 1990, 900533, 597-605.
- /46/ Lee, D.M., Suh, B.K., Kim, B.G., Lee, J.S., Lee, C.H.: Mat. Sci. Tech., 1997, 13, 590-595.
- /47/ Clark, J.B., Garrett, R.K.: in Proc. Symp. on 1991 PM in Aerospace and Defense Technologies, Metal Powder Industries Federation, p. 129.
- /48/ Moll, F., Kainer, K.U., Mordike, B.L.: in Proc. Int. Conf. on Magnesium Alloys and Their Applications (Hrsg.: Mordike, B.L., Kainer, K.U.), Werkstoffinformationsgesellschaft, Frankfurt, 1998, p. 647.
- /49/ Taya, M., Dunn, M., Lilholt, H.: in Proc. 12<sup>th</sup> Risø Int. Symp. on Metallurgy and Materials Science (Hrsg.: Hansen, N. et al.), Risø Nat. Laboratory, Roskilde, 1991, p. 149.
- /50/ Wolfenstine, J., Gonzáles-Doncel, G., Sherby, O.D.: J. Mater. Res., 1990, 5, 1359-1362.
- /51/ Schröder, J., Kainer, K.U.: in Proc. Int. Conf. on Powder Metallurgy 90 (PM 90), The Institute of Metals, London, 1990, p. 304.
- /52/ N.N.: Elektron Database 2.2, Magnesium Elektron Ltd., Manchester, UK, 1996.
- /53/ Vaidya, A.R., Lewandowski, J.J.: Mat. Sci. Eng., 1996, A220, 85-92.
- /54/ Nunez-Lopez, C.A., Skledon, P., Thompson, G.E., Lyon, P., Karimzadeh, H., Wilks, T.E.: Corrosion Science, 1995, 37, 689-708.
- /55/ Schröder J.: in Metallische Verbundwerkstoffe (Hrsg.: Kainer, K.U.), DGM-Informationsgesellschaft, Oberursel, 1994, p. 193.

# 13 Corrosion and Corrosion Protection of Magnesium

*P. Kurze, AHC-Oberflächentechnik GmbH & Co. OHG, Kerpen*

## 13.1 Introduction

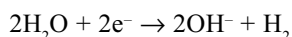
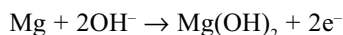
Magnesium is very ignoble (normal potential  $-2.34$  volts). It forms thin passive layers in air and water.

## 13.2 Corrosion Types

All corrosion types affecting magnesium alloys can be reduced to electrochemical processes. A high corrosion trend is predicted due to the high electron negative potential of Mg.

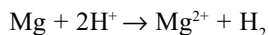
### 13.2.1 Passivation Behaviour

In pure or alkaline water, Mg forms passivating crystalline films of  $\text{Mg}(\text{OH})_2$  on the surface [1]. The following chemical reaction will then take place:



This passive layer is not stable in aqueous solutions with  $\text{pH} < 10$ . This is because there are high compression stresses within the layer (geometrical mismatches with respect to the Mg lattice), which cause cracks. Thus, the magnesium is exposed and corrosion begins. The hydrogen liberated during corrosion then causes a further detachment of the passivating layer. The layer is very stable in pure alkaline aqueous solutions with  $\text{pH} > 10.5$  (striking difference compared to aluminium), since the cracks are sealed with  $\text{Mg}(\text{OH})_2$  (curing).

In aqueous solutions containing chloride, sulfide, or carbonate ions, among others (except fluoride ions), the passivating layer of  $\text{Mg}(\text{OH})_2$  is destroyed and magnesium goes into solution:



Unprotected magnesium is often exposed to this type of corrosion, e.g. by exhaust gases, acid rain, salts, etc.

The corrosion attacks the whole passivating layer equally. The corrosion rate of magnesium is two orders of magnitude greater in solutions containing chloride or sulfide ions than in pure distilled water. Hydrogen formation is the main cathodic reaction in this corrosion mechanism.

Passive layers can also be specifically generated in aqueous solutions. Chromate films are well-known in this regard since they act in a self-curing manner on magnesium and

form a good bonding basis for organic coatings, although they are physiologically questionable. Systematic electrochemical tests with regard to replacing chromate led to dilute aqueous solutions containing cerium permanganate or -vanadate, but not the phosphate and fluoride ions described in the literature.

### 13.2.2 Pitting Corrosion

The origin of pitting lies in inhomogeneous crystal structures such as  $Mg_{17}Al_{12}$  precipitations. They show a higher standard voltage (more noble) and form an electrolysis junction with the surrounding matrix. This galvanic corrosion generates hole-like corrosion prints and is therefore not pitting corrosion in the common sense (no potential for pitting in passive area).

### 13.2.3 Stress Corrosion Cracking

With magnesium alloys, stress corrosion cracking occurs when inner or outer tensile stresses are combined with a corrosive medium (chloride-, sulfide-, chlorate-containing solutions). This leads to brittleness at the tip of the crack, because the hydrogen evolved during the corrosion process is absorbed.

### 13.2.4 Galvanic Corrosion

The basic requirements for galvanic corrosion are the formation of a galvanic element. This corrosion mode is very frequently encountered for two reasons:

- a) The Mg alloys always contain more noble components, such as heavy metals, especially Fe, Cu, Ni
- b) There is hardly any technical application in which magnesium does not come into contact with other more noble metals, often steel.

As regards point a)

Galvanic corrosion becomes very excessive with magnesium alloys containing noble metals (alloying components or impurities) such as heavy metals, especially iron, copper, or nickel, which thus have an electrical contact with the matrix. When aqueous media affect the alloys, hydrogen is formed with a slight overpotential. The whole process is supported by specific anions (e.g. chloride, sulfide). High-purity Mg alloys were developed to prevent this process. They are much more corrosion-resistant in chloride-containing aqueous media than the "older versions" with high contents of Fe, Cu, and Ni. HP alloys contain minimal amounts of these heavy metals. Table 1 summarizes the compositions of the most common ET alloys.

Table 1: Compositions of magnesium die-castings

Alloy	% Al	% Mn	% Zn (max)	% Si (max)	% Cu (max)	% Ni (max)	% Fe (max)	% RE	Others each max %
AZ91D <sup>1)</sup>	8.5-9.5	0.17-0.40	0.45-0.9	0.05	0.025	0.001	0.004		0.01
AM60B <sup>1)</sup>	5.6-6.4	0.26-0.50	0.20	0.05	0.008	0.001	0.004		0.01
AM50A <sup>1)</sup>	4.5-5.3	0.28-0.50	0.20	0.05	0.008	0.001	0.004		0.01
AM20 <sup>2)</sup>	1.7-2.5	min.0.20	max.0.20	0.05	0.008	0.001	0.004		0.01
AS41B <sup>1)</sup>	3.7-4.8	0.35-0.6	0.10	0.60-1.4	0.015	0.001	0.0035		0.01
AS21 <sup>2)</sup>	1.9-2.5	min.0.2	0.15-0.25	0.7-1.2	0.008	0.001	0.004		0.01
AE42 <sup>2)</sup>	3.6-4.4	min.0.1	max.0.20		0.04	0.001	0.004	2.0-3.0	0.01

<sup>1)</sup> ASTM B93-94a. <sup>2)</sup> Hydro Magnesium Specifications

#### Die Cast Parts

AZ91D <sup>1)</sup>	8.3-9.7	0.15-0.50	0.35-1.0	0.10	0.030	0.002	0.005		0.02
AM60B <sup>1)</sup>	5.5-6.5	0.24-0.6	0.22	0.10	0.010	0.002	0.005		0.02
AM50A <sup>1)</sup>	4.4-5.4	0.26-0.6	0.22	0.10	0.010	0.002	0.004		0.02
AS41B <sup>1)</sup>	3.5-5.0	0.35-0.7	0.12	0.50-1.5	0.02	0.002	0.0035		0.02

<sup>1)</sup> ASTM B94-94

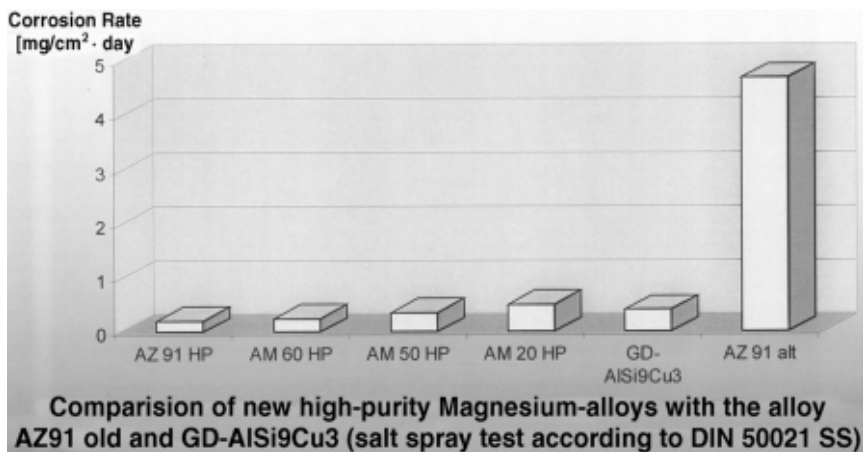


Figure 1: Corrosion tests on magnesium die-casting alloys

Figure 1 lists some corrosion tests (comparison of old/new, comparison with GD-AISi9Cu3) carried out on magnesium cast alloys in a salt spray (DIN 50021-SS) [2].

As can be seen from the figure, the corrosion rate of AZ91 (old version), for example, is 19 times faster in the salt-spray test than that of AZ91 HP.

As regards point b)

The two metals in electrical contact with each other have different potentials. The higher the difference, the more the ignoble metal Mg (anode) will dissolve. It will dissolve in the electrolyte accumulated at the contact point.

The following precautionary measures logically stem from the model for galvanic corrosion:

In a dry atmosphere, no galvanic protection is necessary for magnesium (no electrolyte)

When there is high corrosion potential (electrolyte at the contact point), the following measures are proposed:

- The electrical contact between magnesium and other metallic materials should be prevented by insulation. There can be no direct contact to copper, nickel, iron, or stainless steel.
- Al/Mg alloys (AlMg2.5, AlMg4.5Mn, AlMgSi1), or those containing zinc, tin, or cadmium, exhibit only little galvanic corrosion of magnesium. Contact corrosion when using steel and aluminum screws can easily be prevented by using HART-COAT<sup>®</sup> covered washers. HART-COAT<sup>®</sup> coated aluminum screws are also serviceable (insulation).
- Avoidance of accumulations of electrolyte at the contact areas

## 13.3 Corrosion Protection Measures

Currently, three main protection measures are in use:

### 13.3.1 Improving the Purity of Mg Alloys

The aim here is to prevent galvanic corrosion. Section 13.2 gives more information on this. The heavy metal content needs to be lowered even further.

### 13.3.2 Addition of Specific Alloying Elements

The addition of special alloying elements is intended to prevent galvanic processes on a micro-scale and to form a superior cover coating.

The classic alloying elements – except for Al – can hardly improve magnesium's corrosion resistance. At up to 10%, Al has no effect on the Mg matrix.

A specific addition of rare earth elements such as Nd, La, and Ce has a positive influence on the corrosion behaviour of the corresponding magnesium alloy. The electrochemical standard potentials of rare earths are, without exception, close to that of magnesium. In this way, galvanic corrosion is prevented. An example of such a material is WE54 (5% Y, 3.5% Nd and other RE, 0.5% Zr), which is heat resistant up to 300 °C and shows excellent corrosion resistance (in Cl-containing aqueous solution) [3].

An improvement should be seen if the Mg alloy attains a higher level of homogeneity by suitable freezing. In that way, additional passivation effects will occur, which lower the corrosion current density by two to three orders of magnitude. The synergistic effects with multiply alloyed Mg materials have hardly been studied, even though they are of tremendous potential.

### 13.3.3 Surface Treatment of Magnesium

Some important preliminary remarks need to be made for this part:

1. Even the best surface protection is useless for a non-HP quality material.
2. The casting skin of Mg die-castings is the closest packed area.

Removing the skin by acid cleaning or mechanical treatment, and then applying a surface protection results in much worse corrosion rates than with the untouched casting skin.

3. The surface protection is less effective on a porous casting than on a dense one.
4. The surface cannot be compacted by abrasive blasting (glass pearls, corundum particles) as with aluminum, as it would be rendered impure by the blasting medium.

Figure 2 shows possible methods for a surface treatment of magnesium materials.

Methods for the surface pre-treatment	mechanically: grinding, polishing, brushing, blasting		
	cleaning: use of organic solvents and/or alkaline cleaners		
methods for inorganic coatings on the Mg surface	chemical treatment	electrochemical treatment	physical methods
	bondering	anodizing (HAE, DOW, UBE, TAGNITE, MAGOXID)	PVD
	chromating	galvanizing (Zn, Cu, Ni, Cr, etc.)	flame-spraying plasma-spraying
		electroless segregation such as chemical nickel-plating	
methods for organic coatings on the Mg surface, i.e. on the inorganic coating		painting	
		wet paint	
		powder lacquer	
		textured paint	
		dip paint	
		sliding lacquer	

Figure 2: Possible methods for a surface treatment of magnesium materials

Anodic treatment is a widely used process for magnesium. Table 2 lists the most common methods for the anodic oxidation of magnesium.

The MAGOXID-COAT® process was developed by the AHC company [4] and is described in more detail in [5–8]. The surface is covered with a ceramic layer by a plasmatic reaction of the electrolyte; the whole process is run by partial anodes. It is a gas–solid reaction in the electrolyte.

Table 2: Processes for the anodic oxidation of magnesium and its alloys

Process	Electrolyte Components	Current Density [A/dm <sup>2</sup> ]	Type of Current	Electrolyte Temperature [°C]	Layer Color
HAE	Potassium fluoride Sodium phosphate Potassium hydroxide Aluminium hydroxide Potassium permanganate	1,5–2,5	AC or DC	27	brown
DOW 17	Ammonium difluoride Sodium dichromate o-phosphoric acid	0,5–5,0	DC	70–80	green
AHC Magoxid-Coat®	Mineral acid (fluoric, phosphoric, boracic acids) organic matters	1–5	Special types of signals with plasma- chemical reaction	15–20	white

Figure 3 shows the reaction mechanism of the MAGOXID-COAT® coating, which is separated into four constituent parts.

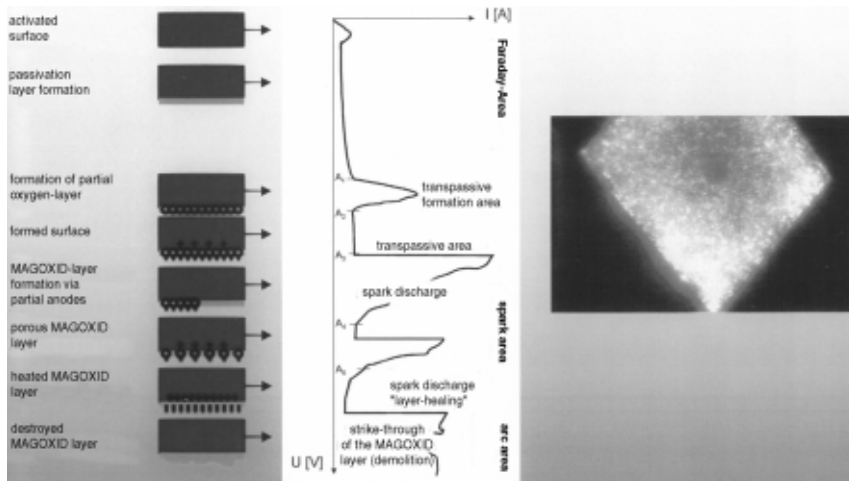


Figure 3: Reaction mechanism of the MAGOXID-COAT® coating

The layers formed by the MAGOXID-COAT® process are of an oxidizing nature; they are ceramic-like, white layers, which contain a large amount of highly resistant spinels, e.g.  $\text{MgAl}_2\text{O}_4$ . Colored MAGOXID-COAT® layers are also available, e.g. black. Figure 4 shows a schematic of a MAGOXID-COAT® layer. It should be mentioned that the layer consists of two parts, a pore-free and a porous oxide ceramic layer. The pore-free layer prevents corrosion, while the porous layer serves as a basis for painting or proofing, e.g. with PTFE.

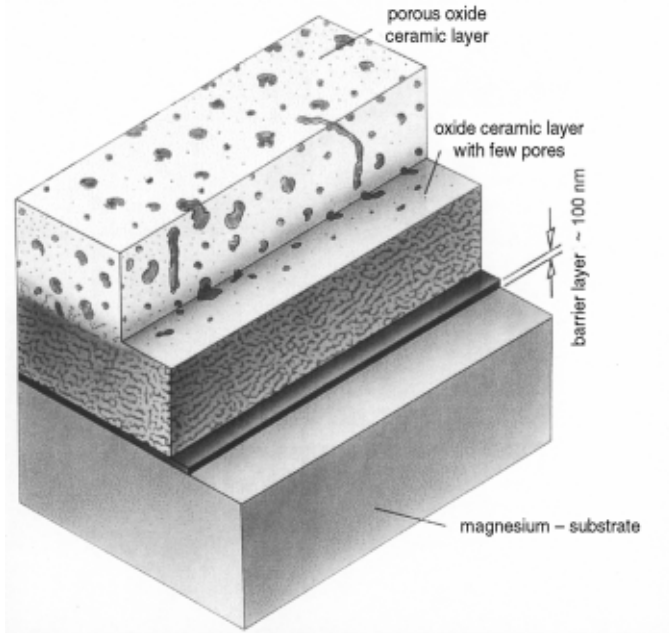


Figure 4: Schematic model of the set-up of a MAGOXID-COAT® layer

Table 3 lists the properties of MAGOXID-COAT® layers.

Table 3: Properties of MAGOXID-COAT® layers (thickness 25  $\mu\text{m}$ )

Corrosion resistance	600 h salt-spray test according to DIN 50021SS
Wear resistance, Taber abraser, load 10 N, grinding roll	6.9 mg abrasion per 1000 rotations
Bonding strength	> 30 MPa
Dielectric strength	13 V/ $\mu\text{m}$
Layer thickness	up to 50 $\mu\text{m}$
Accuracy to guage	layer grows into base material on one side; no edge effect; even coating at edges and cavities

The corrosion resistance of the MAGOXID-COAT® layer can be further improved for special applications. Special processes, reaching a corrosion resistance of up to 3000 h, additionally seal the layer. Table 4 lists potential fields of application for a MAGOXID-COAT® layer.



Table 4: Applications of MAGOXID-COAT® layers

<ul style="list-style-type: none"><li>- Automotive production</li><li>- Installation engineering</li><li>- Aerospace</li><li>- Electronics</li><li>- Adhesion for organic coatings</li></ul>
--

## 13.4 Literature

- /1/ Ferrando, W.A.: „Review of Corrosion and Corrosion Control of Magnesium Alloys and Composites“, J. Mat. Eng. 11 (1989), 299-313.
- /2/ Olsen, A.L.: „Oberflächenbehandlung und Korrosionsschutz von Magnesiumgußteilen“, Hydro Magnesium, Norwegen, 1993.
- /3/ Frazier, E.W. et al.: „Advanced Lightweight Alloys for Aerospace Applications“, JOM May 1989, 22-26.
- /4/ EP 8 910 423.
- /5/ Olbertz, B., Haug, A.T.: „Oberflächenschutz für Magnesiumwerkstoffe“, Metalloberfl., 43 (1989) 4, 174-178.
- /6/ Kurze, P.: „Electrochemical Coatings of Magnesium Alloys“, Tagungsmaterial der DGM „Magnesium Alloys and Their Applications“, Garmisch-Partenkirchen, April 1992.
- /7/ Kurze, P.: „Magnesiumlegierungen elektrochemisch beschichten“, Metalloberfl. 48 (1994) 2, 104-105.
- /8/ Kurze, P., Banerjee, D.: „Eine neue anodische Beschichtung zur Verbesserung der Korrosions- und Verschleißbeständigkeit von Magnesiumwerkstoffen“, Gießerei-Praxis 11/12 (1996), 211-217.

# 14 Magnesium Corrosion – Processes, Protection of Anode and Cathode

*H. Haferkamp<sup>1</sup>, Fr.-W. Bach<sup>2</sup>, V. Kaese<sup>1</sup>, K. Möhwald<sup>2</sup>, M. Niemeyer<sup>1</sup>,  
H. Schreckenberger<sup>3</sup>, Phan-tan Tai<sup>1</sup>*

*1 Institute for Materials Research, Technical University of Hannover*

*2 Chair of Materials Technology, Dortmund University*

*3 Volkswagen AG, Central Lab Wolfsburg*

## 14.1 Introduction

The renaissance of magnesium alloys has led to a doubling of the supply in Europe in the last few years [1]. This has been accompanied by some improvement of the metallurgical properties. Alloy development [2] is mainly focused on the improvement of mechanical properties, such as ductility [3] and creep resistance [4]. Improving corrosion resistance is also a subject of current alloy research [5, 6]. Unless an active corrosion protection is available, the anode and cathode must be carefully separated. From the technical point of view, it makes sense to coat the cathode of low stressed Mg components since the magnesium substrate, with its bad anode-to-cathode ratio, would rapidly dissolve in the event of non-curing damage of the coating. Since this is not always realizable, both the anode and cathode are coated.

## 14.2 Corrosion Processes

The casting process can already influence the corrosion resistance. The use of high-purity alloys with strictly limited amounts of corrosion-supporting elements represents the state of the art [7]. Impurities that support corrosion can be avoided by ensuring that corrosion promoters such as nickel are absent from the crucible or armature materials. Figure 1 shows a formula that demonstrates the principle of proportionality between alloying elements and the corrosion rate [8]. Manganese precipitates iron in the melting bath through forming an Al/Mn/Fe composition, while aluminium and zinc lower the corrosion rate by contributing to the protection layer [9]. In this case, a discussion about the influence of alloying elements cannot be based, e.g., on the interdependence of the elements or various boundary conditions such as the limit of solubility or the formation of intermetallic phases, *cf.* [10]. The casting method itself can influence corrosion resistance. The heterogeneous cross-section of die-cast, thin-walled parts becomes corrosion-critical if the more noble outer shell is pierced. An electrolyte may then form a local element with the underlying material. The corrosion rate is also influenced during further processes such as machining or deformation [11].

Corrosion Rate

$$\approx (0.04 \cdot Mg - 0.54 \cdot Al - 0.16 \cdot Zn - 2.06 \cdot Mn + 0.24 \cdot Si + 28 \cdot Fe + 121.5 \cdot Ni + 11.7 \cdot Cu)$$

Figure 1: Formula for the corrosion resistance as a function of the mass fraction of the alloying components [8]

The corrosion resistance is also influenced by construction design that avoids accumulations of electrolyte and includes drain holes [12, 13], *cf.* Section 14.4.3.4.

Magnesium has a very good corrosion resistance under standard atmospheric conditions [16]; it is also one of the most resistant metals in sulfurous gases or hydrogen fluoride [17]. However, significant corrosion attack is observed with aggressive electrolytes at medium pH values, e.g. sea water. Magnesium alloys are not resistant towards chloride-, sulfide-, or nitrate-containing electrolytes since these anions form soluble salts with Mg [18]. Magnesium alloys are only able to form coatings beyond a pH value of 11.5, and so there is no protective coating for a typical application pH range of 4.5–8.5, which represents the range of stability for aluminium protective layers [6, 19]. Furthermore, 70% of the dissolution process may consist of intermetallic corrosion, leaving a cathodic corrosion protection ineffective [20]. This intermetallic corrosion, also known as abnormal self-dissolution or negative difference effect [21], arises from the electrochemical corrosion and proceeds concomitantly without any external current (Fig. 2); it needs to be considered for experiments. Magnesium’s normal potential lies at –2.375 V and magnesium parts are known to have the lowest free corrosion potential of all construction metals; thus, they behave as an anode for contact corrosion (Fig. 3).

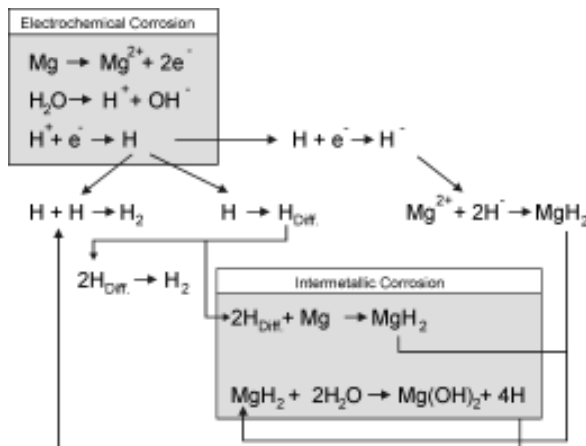


Figure 2: Intermetallic corrosion [20]

The corrosion attack can begin as selective corrosion for alloys containing a high proportion of aluminium; hence, a notch effect will additionally load the component. E. F.

Emley noted that there is no intercrystalline corrosion with magnesium [22]. However, intercrystalline corrosion has been observed with a complex load of atmospheric corrosion and wetting, as noticed for a water vapour atmosphere at 96 °C [6]. Pitting corrosion lowers the fatigue strength, as was verified in sea salt spray tests [23].

metal	potential [V <sub>SCE</sub> ]	metal	potential [V <sub>SCE</sub> ]
magnesium	-1,73	galvanized steel	-1,14
<b>Mg-alloys</b>	<b>-1,67</b>	cadmium plated steel	-0,86
AlSi12	-0,83	steel	-0,78
brass (60/40)	-0,33	cast iron	-0,78
copper	-0,22	chrome steel, active	-0,43
nickel	-0,14	chrome steel, passive	-0,13

Figure 3: Free corrosion potentials in 3–6% NaCl solution [13]

### 14.3 Anode Corrosion Protection

Magnesium parts are coated to protect against corrosion within the visual range or to ensure their function. This protection is realized by the separation of the galvanic couple, either against a cathode or on the magnesium surface itself, to prevent corrosion, e.g. on a visible surface. New coating technologies allow further layer functions, such as a local increase in the substrate strength or a controlled emission of infrared light as required, e.g. for satellites [24]. There is a whole variety of coating systems available for the protection of magnesium parts [10]. Wax coatings are used for transportation [23]. The anodic processes are also applied as pre-treatments for painting or for wear protection, although the DOW-17 and HAE [25] processes have only become established in special areas. The hard anodic oxidation MAGOXID-COAT® layer is akin to nickel-plating, and is the topic of other authors (Fig. 4). Thermal spray coatings are likewise a topic in their own right; these have the same high potential as polymer coatings [27–29]. Organic protections, such as coating powder on a KTL agent, are usually applied in specific designs.

This chapter focusses on laser technology, PVD, and the ANOMAG process.

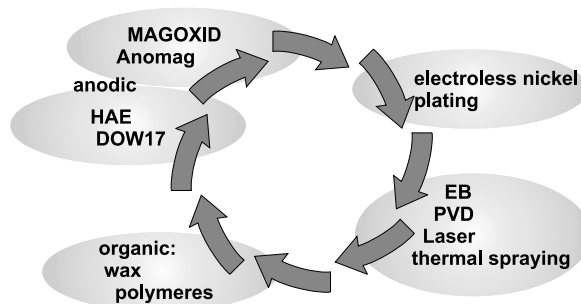


Figure 4: Corrosion-protective coatings for Mg substrates

### 14.3.1 Laser Surface Treatment

There are three known fields of development relating to the surface modification of liquid phases of magnesium. Besides laser treatment, electron-beam [30] and TIG coating technologies have been developed. Since its boundary conditions are very favourable, the laser definitely has the greatest potential for development. Laser technology has become established in the very innovative automotive industry, and it can be variously used for processing magnesium: welding, cutting, remelting, dispersion, or alloying processes, as well as heat treatments are possible. Moreover, it allows local modifications of magnesium parts without changing the component's geometry, which is important for alloys with a high thermal expansion. Other advantages are that it obviates the need for a surface pre-treatment and offers the possibility of alloying gases as well as solids. In contrast to electron-beam technology, which partly applies a sandwich construction of substrate, intermetallic interlayer, and coating [30], the laser-treated surfaces show a gradient set-up, which is thermal-shock resistant.

Of all alloying elements, i.e. Al, Ca, Cu, Mo, Ni, Si, W, Al+Cu, Al+Mo, Al+Ni, or Al+Si, Al is most effective in increasing the corrosion resistance; *cf.* [31]. The corrosion resistance reaches a maximum with respect to the aluminium content for magnesium-based alloys. Beyond the maximum solubility of aluminium, the corrosion resistance may increase again due to the corrosion protective  $Mg_{17}Al_{12}$  phase, which then becomes more prevalent [9]. High cooling rates lead to an increased precipitation of  $Mg_{17}Al_{12}$  [32] and the grains are refined (Fig. 5), *cf.* [33]. Excimer lasers, for example, can reach cooling rates of  $1000\text{ K s}^{-1}$ . This grain refinement lowers the corrosion rate because the cathodic areas shrink [43]. The corrosion potential of a laser-welded and therefore grain refined, extruded ZK60 alloys is shifted upwards by 300 mV compared to that of the non-treated base material [34]. This increase in corrosion resistance can be further enhanced by Al, which forms  $MgAl_2O_4$  spinels. The more aluminium the alloy contains, the greater the corrosion resistance and the greater the hardness as well, thus the wear resistance is also improved, *cf.* [30].

The process gas may also influence the corrosion resistance. Surface-treated ZK60/SiC-MMC shows increased corrosion resistance under standard atmospheric conditions because the laser energy cleaves the  $O_2$  and  $N_2$  molecules and  $Mg_3N_2$  forms due to the Gibbs free energies.  $Mg_3N_2$  is much more corrosion-resistant than the base material, but it leads to grey opacity. Laser surface modifications under Ar atmosphere do not show this colouring behaviour [35].

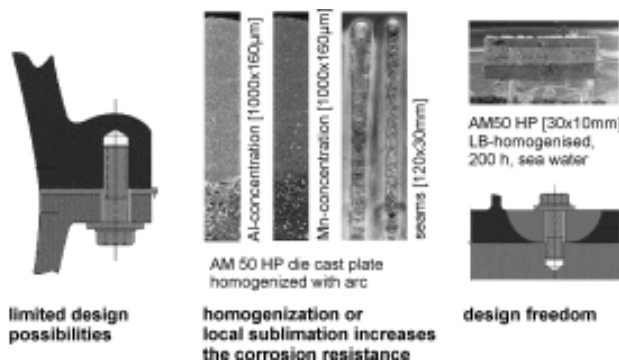


Figure 5: ESMA mapping and diving test in synthetic seawater of an LB homogenized AM50 die-cast plate

Laser surface treatment, as part of a hybrid process, would seem to be useful for envisaged, large-area magnesium parts. Alloying components that lower wear and corrosion – which also includes particle reinforcements – can be alloyed by a two-step process using preforms. A large-area process may lead to cracking [31], and therefore the laser modification needs to be limited to local areas such as tapped blind holes or gliding surfaces. A polymer or a conversion layer overlapping the laser modification can protect the remaining surface. A low porosity is absolutely essential for the treatment of cast components to prevent foaming of the material. Application of the process parameters to sheet materials is difficult due to the different geometry.

### **14.3.2 PVD**

Surface conditioning by physical vapour deposition is subject to the same two critical magnesium characteristics as seen with the laser technology, namely poor corrosion and wear resistance. Layer growth rates of 20 mm/h can be achieved at a process temperature of 300 °C. Modern developments use Al, Cr, Mn, V, and Ti layer technologies [36, 37]. Since Cr has a good connection to the substrate, it is used as a bonding agent on AM50 and AZ91. The wear resistance of the Cr layer is further improved by using N<sub>2</sub> as the process gas, which results in a CrN coating [38]. The corrosion resistance can be improved by three mechanisms: 1. if the applied elements increase the potential; 2. if they form sacrificial anodes; 3. through the corrosion resistance of the coating itself. As on untreated surfaces, spinels are corrosion protective [37].

Generating a PVD coating on Mg substrates assumes an oxide-free substrate surface. To guarantee this, the surface preparation and coating should take place in a permanently evacuated receptacle. For coating preparation, the substrate surface is cleaned, deoxidized, and activated through an ionic etching process by means of high-energy argon and metal ions. Afterwards, the substrate surface is conditioned by thermochemical enrichment or alloying, e.g. with titanium; the vacuum chamber is not flooded in between the processing steps. This results in an improvement of the surface hardness and aids support of the PVD layer. The process of implanting ions allows a specific adjustment and optimization of the bonding, layer structure, and layer composition. With a forced but controlled oxidation by glow discharge (Fig. 6), dense and stable protective coatings are possible. They are arranged as passivating layers between a PVD hard coating and the Mg substrate. The oxidative surface finish is achieved with vacuum glow discharge plasma on a surface activated by ionic etching. In this way, passive layers on an Mg mixed oxide basis are developed. The process control allows influence of the composition, structure, and morphology of the passivating layer. The PVD coating is applied directly after the surface treatment, again without a temporary flooding of the vacuum chamber. The process steps are thus:

- Cleaning, deoxidation, activation
- Thermochemical enrichment/alloying
- Oxidative surface finish
- PVD coating

Without temporary flooding, a 10 kW Mod pulser of the Metaplas type was added to give the arc PVD facility “20-Metaplas-Ionon” (Fig. 6).

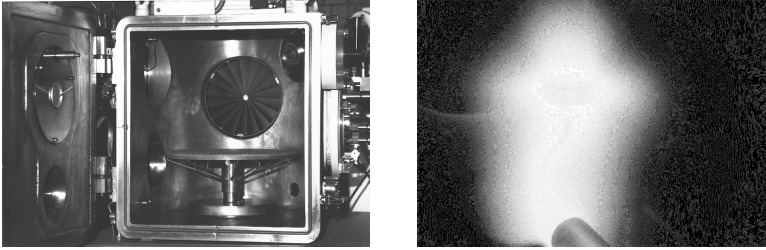


Figure 6: Arc PVD receptacle (left) and plasma-glow discharge on an AZ91 surface, specimen diameter 40 mm

First tests with a substrate conditioning proved that the pulsed high-voltage supply of the substrate enables an effective plasma cleaning, and thus native oxide layers and organic impurities can be completely removed at low substrate temperatures. The substrate surface is left highly activated and can therefore be subjected to pulsed thermochemical plasma oxidation, which leads directly to passivating oxide layers as a result of the substrate potential and the pulsing frequency. The final layer has a dense microstructure and a well-defined stoichiometry. The use of several evaporators and a movable component enables a multi-sided deposition, despite the directionality of the process.

### 14.3.3 ANOMAG

Anodic layers and conversion layers are much less effective on magnesium than on aluminium substrates; they can even reduce fatigue strength [10]; *cf.* Section 13.3.3 about MAGOXID-COAT®.

The ANOMAG method is an anodic coating that has been developed at the CSIRO in New Zealand since 1992. Its aim is to produce a magnesium coating that is comparable to aluminium coatings in terms of corrosion and wear resistance. Three classes of layers (3–8  $\mu\text{m}$ , 10–15  $\mu\text{m}$ , and 20–25  $\mu\text{m}$ ) can be applied with a gentle sparkleless plasma discharge on the substrate. The ANOMAG layers are not only characterized by a good corrosion resistance, but also by a good wear resistance. The good galvanic separation can be attributed to the high breakdown voltage of 600 V. This was verified in a salt-spray test according to ASTM B117 and in outdoor exposure tests according to ASTM D1654. Colouration is favoured by the good colour adhesion for subsequent dry and wet processes, but it can also occur during the actual process with colour steps of yellow, cyan, or red, as well as blue, grey, or black being available (Fig. 7). Other advantages are the adequate coating of complex parts, a low influence of the anodic coating on the fatigue behaviour, low costs, and environmental friendliness [39]. The first European ANOMAG line has been erected at the Franz Oberflächentechnik GmbH & Co. KG.

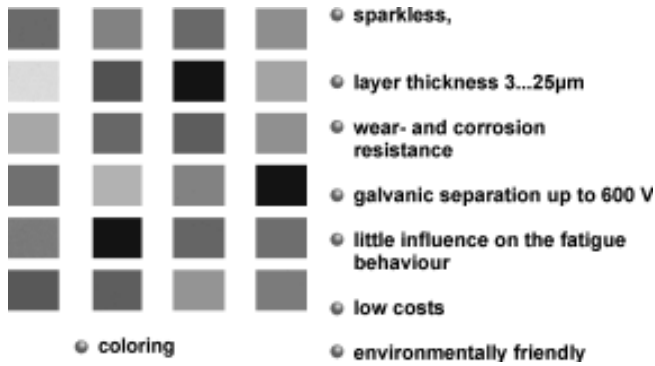


Figure 7: ANOMAG process: characteristics and colour scheme [40]

## 14.4 Corrosion Protection Layers on the Cathode

In operation, a magnesium gearbox housing suffers a material loss that is gravimetrically comparable to G-AlSi9Cu3. Connection points, e.g. bolted joints, however, are significantly corroded, which can lead to component failure.

### 14.4.1 Influences on Contact Corrosion

The actuating variables of contact corrosion can be described by a formula with the help of the Ohm's law, *cf.* DIN 50919. To lower the element current  $I_e$ , the numerator must be as low as possible and/or the denominator must be as high as possible (Fig. 8). According to the Faraday law, the corrosion current is proportional to the mass of the metal dissolved by corrosion.

$$I_e = \frac{U_{R,K} - U_{R,A}}{R_A + R_K + R_M}$$

where:

- $I_e$  element current
- $U_{R,K}$  equilibrium rest potential of cathode
- $U_{R,A}$  equilibrium rest potential of anode
- $R_A$  electrical resistance of anode
- $R_K$  electrical resistance of cathode
- $R_M$  electrical resistance of medium

Figure 8: Calculation of the element current of a contact corrosion cell; a homogeneous current distribution is assumed according to DIN 50919



The numerator is constituted by the difference in the equilibrium rest potentials of the metals in contact, which can be drawn approximately from the electromotive chain [23]. The aim is to keep this difference as low as possible with a suitable combination. However, one needs to bear in mind that the electromotive chain does not include external currents, and therefore polarization effects such as the hydrogen overpotential at the real element are not taken into account. A corrosion-favourable contact partner for magnesium should contribute to a lowering of the potential difference and show a hydrogen overpotential as high as possible to prevent the hydrogen evolution as the cathodic reaction.

The denominator is made up of the sum of the electrical resistances of the metals in contact and the medium. The electrical resistance of the metals is rather low and may only be increased by an insulating organic or inorganic coating. The electrolyte and its conductivity are of extraordinary importance. In an ideal case, such as in an electrolyte-free vehicle interior, the denominator will become infinitely high and no contact corrosion protection will be necessary. Besides the specific ionic conductivity of the electrolyte, its conductivity is influenced by the cross-sectional area. If it is high, a greater galvanic current can flow than for a pure film-like wetting. Flat washers extend the electrolyte distance between the Mg component and the screw head, and can therefore lower the contact corrosion with a higher electrolyte resistance depending on the material.

On transferring this theory to a corrosion protection system for screwed joints with magnesium components, it becomes obvious that possible actions are essentially restricted to the influence of the equilibrium rest potential and the electrical resistance of the screw surface. The equilibrium rest potential, together with a possibly high hydrogen overpotential, are mainly determined by a usually galvanically deposited, metallic surface coating of the screw. In addition, this layer needs to protect the base material from self-corrosion, which limits the choice. The electrical resistance of the screw surface may be increased by a final inorganic sealing or by applying an organic top-coat.

## 14.4.2 Classification of Verified Protection Systems

The Volkswagen Group currently coats bolted joints used with magnesium with the c687 surface according to TL194. A glossy zinc coating is deposited from a slightly AcOH-acidified electrolyte; layer thickness  $> 15 \mu\text{m}$ . This layer is then sealed by Gelbchromatierung and naß-in-naß (wet-in-wet) sealing using a slightly alkaline, aqueous siliceous solution (JS500 from MacDermid). A subsequent lubricant treatment adjusts the desired friction coefficient. Areas that are extremely prone to corrosion stress, such as the lower bolt joints of gearbox housings, are additionally protected with hard-coated flat washers [40].

Zinc lamellar coatings, such as Delta Tone or Dacromet, offer a good protection against base metal corrosion of the screw [43]. These layers have proved effective with aluminium constructions as well [40]. However, such zinc lamellar coatings cannot be applied to magnesium parts since they cause serious contact corrosion [41] *cf.* also [23].

Figure 9 lists the possible combinations between the metallic surface coating and the resulting inorganic or organic insulation layer and assigns the 32 tested systems. The group standard c687 serves as a reference.

metallic coatings			
zinc layers	zinc alloy layers	aluminium layers and base materials	other layers
insulating layers, additionally applied			
inorganic sealing e.g. JS 500, Deltacoll 80	organic top-coats e.g. KTL, Gliss-Coat, Delta-Seal		
organic top-coats	inorganic sealing	duplex systems	

Figure 9: Overview and set-up of the tested surface coatings

### 14.4.3 Experiments and Results

The corrosion behaviour of magnesium parts with connector elements was assessed by means of block experiments in the laboratory. The actual part was emulated with a block ( $160 \times 40 \times 35$  mm), which was milled from an AZ91 ingot and then provided with four tapped holes, cf. Fig. 10a. As connection elements, differently coated collar screws, M8x18, from the ABC Company and cut Al screws from the Knipping Company were used. They were tightened to 10 Nm with a moment wrench. The test was performed over 120 h in a salt-spray according to DIN 50021SS.

The Mg blocks were cleaned in an isopropanol ultrasonic bath and weighed dry before the testing. The lateral planes could not be directly affected by contact corrosion; they were covered with a strip varnish (Foliflex from Spies und Hecker) and finally coated with hot wax, which is also used for cavity sealing.

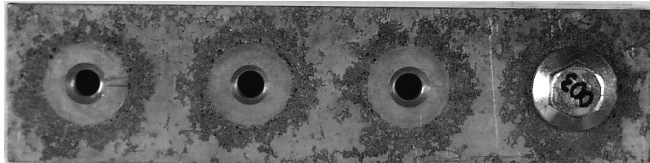


Figure 10a: Mg block,  $160 \times 40$  mm with bolted joint c687 after 120 h load according to DIN 50021SS



Figure 10b: Mg gearbox housing after 12 cycles of dynamic corrosion testing (EK3); with the bolted joint "zinc plus olive-chromated plus KTL"

Only the loss in mass by contact corrosion is of importance, and therefore the blind values for the determinations of self-corrosion are evaluated with PTFE screws. The corrosion products are then removed by dipping in chromic acid (180 g  $\text{CrO}_3$  in 1 dm<sup>3</sup> aqueous solution, 85 °C). The measured loss in mass is then given by the mass difference between the beginning and the end of the experiment, minus the blind value [42].

#### 14.4.3.1 Zinc systems

The Mg-suitable surface protection c687 belongs to the zinc systems, *cf.* Section 14.4.2. According to Fig. 11, the mass losses with two coatings of c687 show deviations as expected from their series scatter and the inherent scatter of the testing. Therefore, a gradation is impossible. The mass loss with the unsealed zinc-olive-chromated systems is more than twice that with c687, emphasizing the effectiveness of the latter siliceous sealing. A subsequent aluminium flake coating will not improve the corrosion behaviour; in fact, it makes it rather worse. The siliceous sealing Deltacoll 80 offers similar protection to c687.

The protective effect of c687 is even seen with certain duplex systems. Additional cathodic dip coatings, gloss coating, or a combination of Delta Seal and Deltacoll can totally prevent contact corrosion in this short-term experiment. These coatings provide insulation and prevent contact corrosion by stopping hydrogen formation. The screws are not dip-coated in the usual drum; instead, they are coated after separation on a conveyor belt.

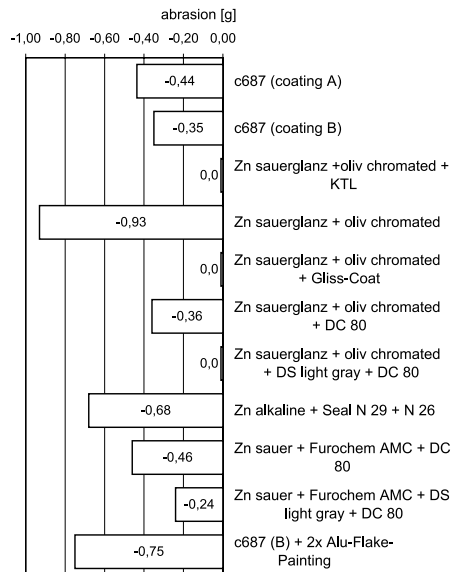


Figure 11: Metal removal through contact corrosion after 120 h for zinc systems, according to DIN 50021SS

Later experiments verified the effectiveness of the duplex system zinc plus dip-coating. Indeed, it is even better than the currently used company standard c687, and so the duplex system “zinc (15  $\mu\text{m}$ ) plus olive-chromated plus KTL (10  $\mu\text{m}$  dip-coating) is becoming increasingly used for magnesium. Figure 10 shows an Mg gear box housing with a zinc-plus-KTL coated bolted joint after 12 cycles of a dynamic corrosion driving test EK3, which is equivalent to 4 to 6 years of actual outdoor duty. The connecting surface shows distinctive contact corrosion, and therefore it is still necessary to apply additional hard-coated Al washers in areas of heavy corrosion attack. A systematic optimization of the duplex system in collaboration with the coating company Hillebrand-Galvanotechnik is aimed at producing joints that do not require the expensive, hard-coated Al washers.

#### 14.4.3.2 Zinc alloying systems

With steel screws, zinc alloying systems offer good protection against base metal corrosion; they are much better than common zinc layers [43]. Zinc alloy coatings are also recommended for screws obstructed with aluminium to avoid contact corrosion [40]. The use of zinc coatings with magnesium parts shows a totally different result in terms of mass loss (Fig. 12). The mass loss is much greater compared to that with unprotected steel screws. Even slight impurities of nickel in magnesium cause significant self-corrosion, so that for AZ91, for example, the tolerable level is set at 10 ppm. None of the different sealings and top coatings are capable of suppressing the negative effects of nickel as an alloying component.

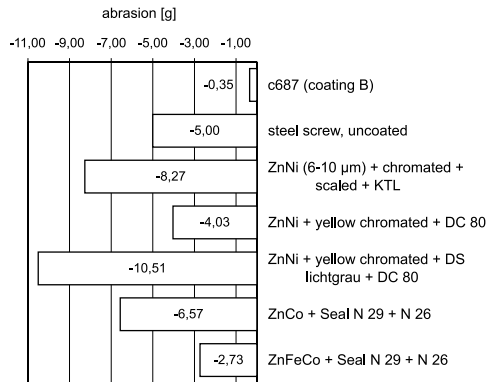


Figure 12: Metal removal through contact corrosion after 120 h for zinc systems, according to DIN 50021SS

The mass loss of an untreated steel screw (5 g) is roughly 14 times higher compared to that of a corresponding screw coated with c687. An unprotected screw would not be used with magnesium. It is clear, however, just how fast contact corrosion increases in the case of base metal corrosion with steel screws. This may occur if the coating corrodes or is damaged during tightening.

### 14.4.3.3 Aluminium systems: screw materials and galvanic coatings

It is often proposed that aluminium screws should be used with magnesium. Aluminium has a similar thermal expansion coefficient as magnesium, which avoids additional stresses when heating, as is seen when using steel screws [44]. The contact corrosion is assumed to be lower due to the electrochemical potential, which is close to that of magnesium. In this study, the alloy AlMgSi1 showed exceptionally good properties. It is used as screw material for the additionally yellow-chromated oil drain plug of an Mg gear box housing B80 and its efficacy has been verified in several long-term tests.

The aluminium alloy 6013 offers better contact corrosion protection than the group standard c687 (Fig. 13) and this protection exceeds that of the Al alloy 7075. The 7075 alloy is a high strength, copper-containing material with a tendency for corrosion cracking through incorrect heat treatment, which limits its application in corrosive surroundings. Experimental results from the corrosion test EK3 additionally affirmed the utility of Al 6013 screws. After 120 cycles, there was only slight contact corrosion of the bolted joints of an Mg supporting unit.

The coatings Al, Alcoat 1, and Alcoat 2 were segregated from a non-aqueous electrolyte on collar screws. Only Alcoat 2 seemed to offer effective protection against contact corrosion, but this is offset by the low protection against base metal corrosion.

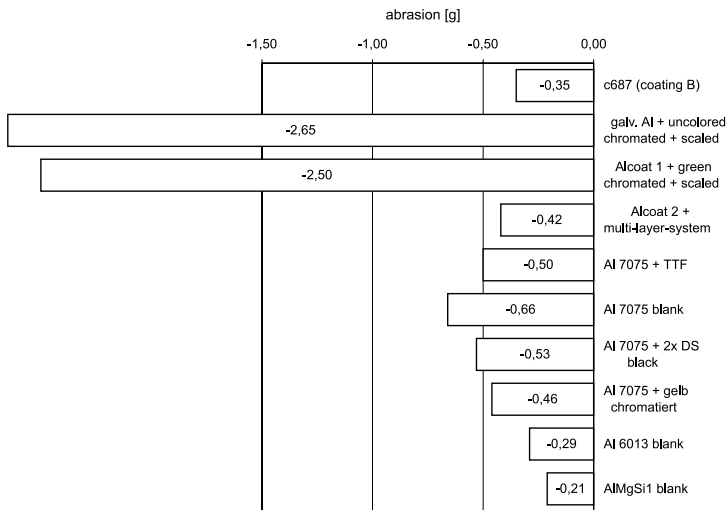


Figure 13: Metal removal through contact corrosion after 120 h for aluminium materials, according to DIN 50021SS

### 14.4.3.4 Additional coatings and structural actions

The improved corrosion protection offered by the use of hard-coated aluminium washers has been proven experimentally (Fig. 14). There is no detectable contact corrosion after 120 hours of testing. Uncoated washers made of AlMg3 increase the corrosion protection compared to c687. Screw heads encapsulated by plastics extend the electrolyte distance, thus also having a positive effect; cf. Section 14.2. Tinned screws protect less effectively

than c687, but they are employed when good electrical conductivity is fundamental to the required application (magnesium parts serve as electrical conductors for the Massestrom) [41].

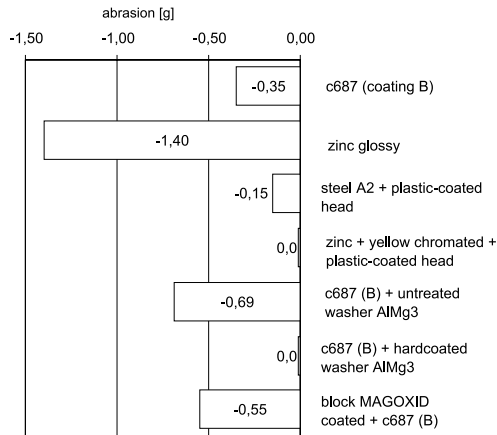


Figure 14: Metal removal through contact corrosion after 120 h for further coatings, according to DIN 50021SS

MAGOXID® is an anodic coating for magnesium components and offers suitable protection against self-corrosion. Several MAGOXID®-coated blocks have been tested together with c687-coated screws. PTFE screws again provided a blind reference value, since there may be different abrasion values for chemical stripping with chromic acid. MAGOXID® does not protect against contact corrosion in this test; the mass loss is even a little higher than that with the uncoated blocks. The corrosion morphology also differs from the other cases. The corrosion attack surrounding the screw head is less homogeneous and is centred more on discrete areas with heavy corrosion pitting. Depending on the coating, additional hard-coated Al washers should be applied to bolted joints with MAGOXID®.

## 14.5 Summary

A technically sufficient corrosion protection of magnesium alloys can be achieved through the coating of the anode or cathode, respectively.

The anode coatings cover a great variety of processes, whereas technologies for special applications are being developed alongside the existing anodic oxidation coatings and organic coatings.

Cathodic connection elements require additional protection against base metal corrosion, as well as a sufficient compatibility of the meeting parts. Zinc alloy coatings and lamellar zinc coatings, which serve well in other respects, should not be applied to magnesium components. The current Volkswagen Group standard c687 can be recommended as a protection against contact corrosion. The duplex system zinc plus KTL is equivalent to

c687 and can be used down to medium corrosive stresses. Significant corrosion attack requires hard-coated Al washers. Al 6013 screws also protect against contact corrosion.

The additive coatings of the anode and cathode point to a composite design. The milestone of an active, self-healing protection has not yet been realized.

This work was supported by the Deutsche Forschungsarbeit as part of the “Sonderforschungsbereich 390 – Magnesiumtechnologie”.

Special thanks are due to Mr. Michael Niemeyer, now at AUDI AG, for carrying out the laser-coating experiments.

## 14.6 Literature

- /1/ <http://www2.hydro.com/mag/eng/>; URL vom 15.02.99; Norsk Hydro, Norwegen.
- /2/ N.N.: Magnesium bevor the breakthrough, Aluminium 74 (1998) 7/8, p. 530-533.
- /3/ Juchmann, P.: Beitrag zur technologischen Eigenschaftserweiterung von Magnesium-Werkstoffen durch Lithium, Dissertation, Universität Hannover, 1999.
- /4/ Buch, F. von, Mordike, B.L.: Microstructure, Mechanical Properties and Creep Resistance of Binary and More Complex Magnesium Scandium Alloys, Magnesium Alloys and Their Applications, DGM, Frankfurt, 1998.
- /5/ Kaese, V., Niemeyer, M., Tai, Phan-tan, Röttger, J.: Korrosionsschützendes Legieren von Magnesiumbasiswerkstoffen, Teil I: Dynamische Alkalisierung der Grenzschicht – Tertiäre Legierungssysteme; Materials and Corrosion 50 (1999) 4.
- /6/ Haferkamp, H., Kaese, V., Niemeyer, M., Tai, Phan-tan: Corrosion of Al- or Ca-Alloyed MgLi-Alloys in Gaseous and Aqueous Media, Magnesium Alloys and Their Applications, DGM, Frankfurt, 1998.
- /7/ King, J.F.: Development of Magnesium Diecasting Alloys; Magnesium Alloys and Their Applications, DGM, Frankfurt, 1998.
- /8/ Aghion, E., Bronfin, B.: The Correlation Between the Microstructure and Properties of Structural Magnesium Alloys in Ingot Form; Third International Magnesium Conference, Institute of Materials, London, 1997.
- /9/ Lunder, O., Lein, J.E., Aune, T.Kr., Nisancioglu, K.: The Role of Mg<sub>17</sub>Al<sub>12</sub> Phase in the Corrosion Behaviour of Mg Alloy AZ91; Corrosion 45 (1989) 9 p. 741-748.
- /10/ Bommer, H.: Korrosion und Korrosionsschutz von Magnesiumlegierungen, DGM-Fortbildungsseminar Magnesium 1997, DGM, Frankfurt, 1997.
- /11/ Eliezer, A., Abramov, E., Gutman, E.M.: Mechanochemical Behaviour and Plasticity of Mg-Al-Alloys; First Israeli Int. Conference on Magnesium Science & Technology; MRI, Beer Sheva, Israel, 1998.
- /12/ N.N.; Korrosionsbeständige Magnesiumdruckgußteile; Firmenschrift 4961M; Norsk Hydro, Norwegen.
- /14/ Olsen, A.L.: Designing Galvanic Corrosion Out of Magnesium Drivetrain Components; SAE Technical Paper 870364, Warrendale, USA, 1987.
- /15/ N.N.: Schutz gegen Kontaktkorrosion von Magnesiumbauteilen; Norsk Hydro und Rapolid Thiel GmbH, Selbstverlag, Lüdenscheid.
- /16/ Beck, A. Hrsg.: Magnesium und seine Legierungen; Springer, Berlin, 1939.
- /17/ Makar, G.L.: Corrosion of Magnesium, Int. Materials Reviews 38 (1993) 3, p. 138-153.
- /18/ Mitrovic-Scepanovic, V.: Localised Corrosion Initiation on Magnesium Alloys, Corrosion 48 (1992) 9.

- /19/ Pourbaix, M.: Atlas of Electrochemical Equilibria in Aqueous Solutions, Second English Edition, NACE National Association of Corrosion Engineers, Houston, 1974.
- /20/ Wang, Y.: Beitrag zur Verbesserung korrosiver Eigenschaften superleichter Magnesium-Lithium-Basislegierungen, Dissertation, Universität Hannover, 1997.
- /21/ Nazarov, A.: Anodic Dissolution and Autodissolution of Magnesium in the Presence of Depassivator Ions, *Protection of Metals*, 29 (1993) 3.
- /22/ Emley, E.F.: Principles of Magnesium Technology, Pergamon Press, Oxford, 1966
- /23/ Busk, R.S.: Magnesium Products Design; Marcel Dekker, New York and Basel, 1987.
- /23/ Mayer, H., Papakyriacou, M., Stanzl-Tschegg, S., Tschegg, E., Zettl, B., Lopowsky, H., Rösch, R., Stich, A.: Korrosionsermüdung von Aluminium- und Magnesium-Gußlegierungen, *Materials and Corrosion* 50 (1999) 2, p.81-89.
- /24/ Sharma, A.K., Uma Rani, R., Malek, A., Acharya, K.S.N., Muddu, M., Kumar, S.: Black Anodising of a Magnesium Lithium Alloy, *Metal Finishing*, (1996) 4.
- /25/ Schreck, K.: Corrosion Prevention of Structure Parts Produced from Mg-Alloys and the Experience by Use in Aircraft, *Magnesium Alloys and Their Applications*, DGM, Oberursel, 1992.
- /26/ Lenz, U., Weisheit, A., Mordike, B.L.: Thermal Spraying on the Magnesium Alloy AZ91, *Magnesium Alloys and Their Applications*, DGM, Frankfurt, 1998.
- /27/ M. Koppers: Grenzflächenreaktionen zur molekularen Haftvermittlung und zum Korrosionsschutz in Schichtverbunden mit Magnesiumlegierungen, Dissertation, TU Clausthal, 1999.
- /28/ Hawke, D., Gaw, K.: Effects of Chemical Surface Treatments on the Performance of an Automotive Paint System on Die Cast Magnesium, SAE Technical Paper 920074, SAE, Warrendale, USA, 1992.
- /29/ Robinson, A.I.: Evaluation of Various Magnesium Finishing Systems, 42<sup>nd</sup> Annual World Conference, International Magnesium Association, New York, 1985.
- /30/ Wielage, B., Fleischer, K., Zenker, R., Schlammer, S.: Electron Beam Alloying of Magnesium Materials; *Magnesium Alloys and Their Applications*, DGM, Frankfurt, 1998.
- /31/ Galun, R., Weisheit, A., Mordike, B.L.: Properties of Laser Alloyed Surface Layers on Magnesium Base Alloys; *Magnesium Alloys and Their Applications*, DGM, Frankfurt, 1998.
- /32/ Luo, A.: Understanding the Solidification of Magnesium Alloys; Third International Magnesium Conference, Institute of Materials, London, 1997.
- /33/ Niemyer, M.: Strahl-Stoff-Wechselwirkung und resultierende Verbindungseigenschaften beim Laserstrahlschweißen von Magnesiumlegierungen; Dissertation, Universität Hannover, 1999.
- /34/ Lübbert, K., Kopp, J., Wendler-Kalsch, E.: Korrosionseigenschaften laserstrahlgeschweißter Aluminium und Magnesium Automobilwerkstoffe; *Materials and Corrosion* 50 (1999) 2, p. 65-72.
- /35/ Yue, T.M., Wang, A.H., Man, H.C.: Improvement of the Corrosion Resistance of Magnesium ZK60/SiC Composite by Excimer Laser Surface Treatment; *Scripta Materialia* 38 (1998) 2, p.191-198.
- /36/ Diplas, S., Tsakirooulos, P., Brydson, R.M.D., Dodd, S., Gardiner, R.W.: Characterisation of Physical Vapour Deposited Mg-V-Alloys; Third International Magnesium Conference, Institute of Materials, London, 1997.



- /37/ Baliga, C.B., Tsakirooulos, P., Dodd, S.B., Gardiner, R.W.: Physical Vapour deposited Mg-Ti-Alloys; Third International Magnesium Conference, Institute of Materials, London, 1997.
- /38/ Senf, J., Berg, G., Friedrich, C., Broszeit, E., Berger, C.: Wear Behaviour and Wear Protection of Magnesium Alloys using PVD Coatings; Magnesium Alloys and Their Applications, DGM, Frankfurt, 1998.
- /39/ <http://www.magnesium.co.nz/Magnesium/german.asp>; URL vom 15.02.99; Magnesium Technology Licensed Ltd., Neuseeland.
- /40/ Reinhold, B., Kopp, J., Klose, S.G.: Korrosionsschutz bei Leichtmetallverschraubungen, Tagungsband DVM Bauteil '98.
- /41/ König, F., Papke, M.: Kontaktkorrosion an Al/Stahl – und Mg/Stahlverbindungen; 20. Ulmer Gespräche 1998.
- /42/ Haferkamp, H., Kaese, V., Niemeyer, M., Tai, Phan-tan, Laudien, G., Koeppen, H.-J., Schreckenberger, H., Lehnhus, D.: Oberflächenschutzsysteme für die Verschraubung von Magnesiumbauteilen; 6. Magnesiumguß Abnehmerseminar & Automotive Seminar 1998; FH Aalen, Selbstverlag, 1998.
- /43/ Schreckenberger, H., Koeppen, H.J., Laudien, G.: Bewertung von Oberflächenschutzsystemen für Schrauben II, Journal für Oberflächentechnik, München, 9/1998.
- /44/ Gugau, M., Berger, C.: Korrosionsschutz von Mg im Kontakt mit anderen Werkstoffen; Eurokarosserie 1999 Bad Nauheim; DVM, 1999.

# 15 Nickel-Phosphor Alloy Coatings for Magnesium without External Current

F. Leyendecker, AHC-Oberflächentechnik GmbH & Co. OHG

## 15.1 General Notes

The search for materials with a low specific weight often ends with the use of magnesium or its alloys. Fortunately, in this regard, magnesium is an almost inexhaustible resource.

Besides the many advantages of magnesium alloys as engineering materials, there are also limitations, e.g. low fatigue strength, wear, and corrosion resistance. The so-called high purity alloys do show better corrosion resistance, although additional surface protection is usually necessary.

## 15.2 Surface Processes

Mechanical, physical, and chemical/electrochemical processes are available for the surface treatment of magnesium. Mechanical machining includes chipping processes, milling, turning, abrasive blasting, and slide grinding. Painting, as well as PVD (physical vapour deposition) flame and plasma-flame spraying, are the major physical methods. In these processes, the deposition temperature needs to be carefully controlled to avoid damage of the base material.

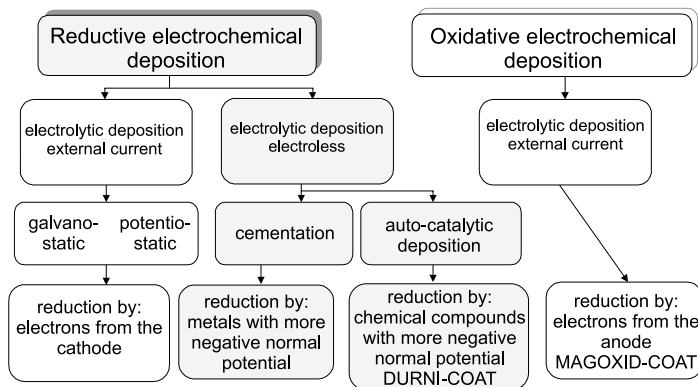


Figure 1: Classification of electrochemical coating methods

If, besides corrosion resistance, there is also a demand for metal-like properties such as electrical conductivity, good thermal diffusivity, gloss, reflection, good shielding, or solderability, then galvanic or electrochemical methods are the first choice. The classification

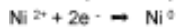
of all the processes is listed in Fig. 1. They can be separated into reductive and oxidative depositions, which can be further split into processes with and without an external current. The present chapter focuses on the autocatalytic deposition of nickel/phosphor alloy coatings.

## 15.3 Autocatalytic Deposition Processes

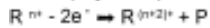
Chemical nickel-plating without an external current is one possible means of autocatalytic deposition. In this process, no external electrons are added; instead, the whole energy – electromotive force – is supplied by the electrolyte itself. Figure 2 shows the two reactions at the main electrodes. The deposition mechanism is shown schematically.

main-electrode reactions:

cathode (reduction)



anode (oxydation)



R<sup>n+</sup> = reducing agent  
(here: NaH<sub>2</sub>PO<sub>2</sub>)

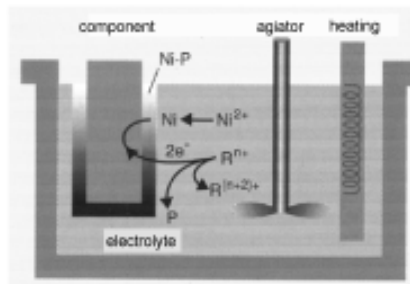


Figure 2: Schematic of the electroless nickel/phosphor alloy deposition

## 15.4 Process Steps for Magnesium Coatings

The base materials of magnesium alloys are chemically highly active (*cf.* Fig. 3) due to magnesium being very ignoble. Therefore, such materials need an initial pre-treatment before the coating process.

Figure 4 shows typical processing steps for the electroless nickel-plating of magnesium materials. The processes on the left-hand side are standardized coating steps. That on the right-hand side is AHC's special coating method [1].

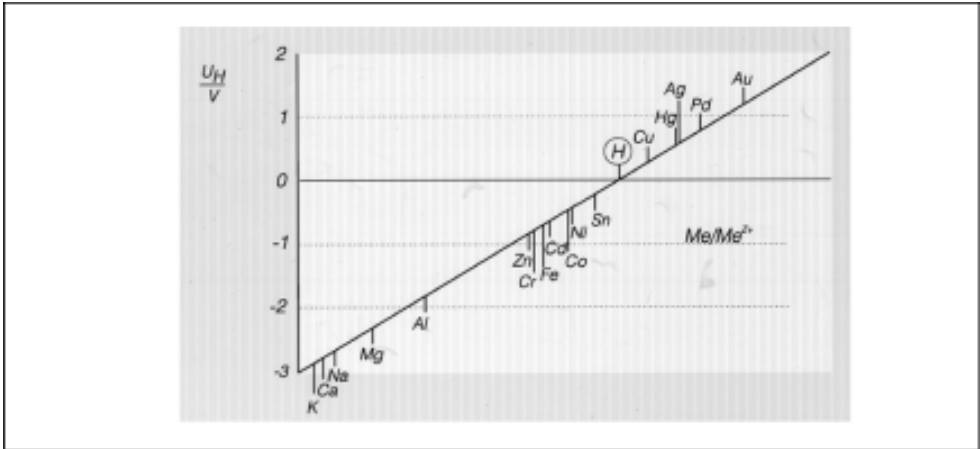


Figure 3: Electromotive order of the elements in aqueous solution (25 °C, 1 bar, referenced to the standard hydrogen electrode)

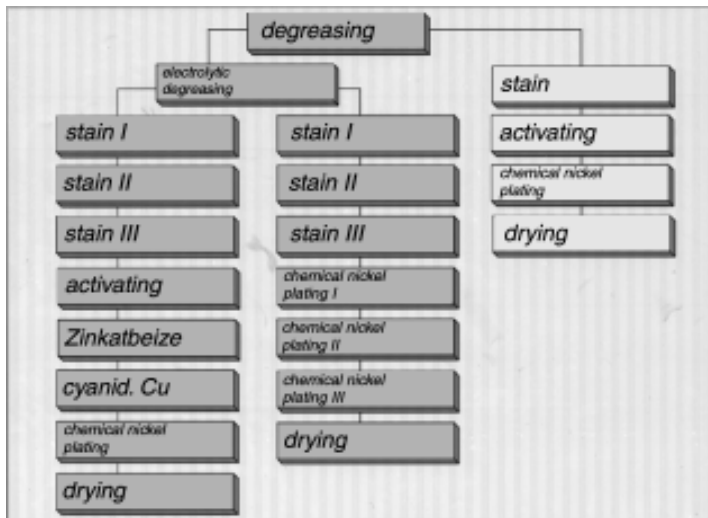


Figure 4: Overview of the conventional and AHC-specific process steps for electroless nickel plating

## 15.5 Standard Processes

All regular metal-coating processes start with a surface cleaning step. The release agent from the casting process is removed by degreasing. The casting surface also contains many errors, and therefore ultrasound is used to supplement the degreasing by boiling. The composition of the degreasing medium must be such that it attacks the base material only

slightly. Therefore, only mildly alkaline solutions are used, which contain suitable inhibitors. To achieve a strong adherence of the coating, the oxidation products and the casting skin need to be removed in a second step. The stain is usually applied in several processing steps. Both acids and alkaline solutions are suitable for this. Phosphoric acid, chromic acid, nitric acid, and hydrofluoric acid have all been applied for this purpose. However, their handling and effect on the environment are rather problematic. They also attack the surface very extensively, which leads to a high degree of roughness or even dissolution.

The third process step is the activation or conditioning, in which the surface is neutralized. In particular, the remaining stain chemicals are removed from the surface defects.

In the standard procedure, the surface is treated with a so-called zincate stain shortly before the actual coating. Its purpose is to plate the surface with a homogeneous, thin zincate layer. Finally, the surface is nickel-plated.

## 15.6 AHC Process

Of key importance for the reliability of the production process and the quality standard is the number of steps and their control. Additionally, a future-oriented process must be environmentally friendly, which needs to be considered when choosing the treatment chemicals. The latter criterion also determines the economic efficiency, since only a positive answer to this will open up new fields of application.

This is the reason why AHC developed a method requiring only three pre-treatment steps. The first step, that of surface cleaning, is conducted analogously to the processes mentioned above by boiling off. For the second step, it is important to use mildly alkaline stain media, which will attack the surface in a one-step process. The third step is an activation process that conditions the surface for direct nickel-plating. Finally, magnesium can be directly coated with a specially developed electrolyte.

The exact sequence of steps for this direct, non-external current/chemical nickel-plating by AHC is given in Fig. 5.

process step	working temperature	treatment duration	remarks
degreasing (boiling)	60 °C	5–10 min	
stain	RT	5–7 min	alkali-based
activation	RT	1–2 min	slightly acidic
nickel plating	85–92 °C	1–2 h	approx. 15–25 µm
drying	100 °C	10 min	

Figure 5: Process steps for the direct electroless nickel-plating of magnesium materials

Metallographic cross-section polishes show an interesting, black intermediate layer (2) underneath the nickel/phosphor alloy layer (1) (Fig. 6). Analyses have shown that this layer contains only very little phosphor, indicating an exchange reaction between magnesium and nickel.

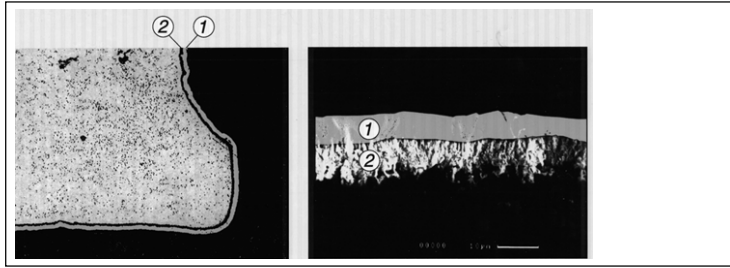


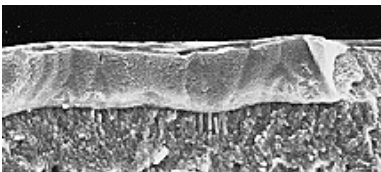
Figure 6: Low-in-phosphor intermediate layer between the nickel/phosphor layer and the base material

### 15.6.1 Layer Properties

Looking directly at the nickel/phosphor alloy layer deposited on magnesium, some advantageous layer properties become apparent.

Physical properties:

- Mostly 15–25  $\mu\text{m}$  layer thickness, whereas up to 100  $\mu\text{m}$  might be of technical interest
- 4–6% phosphor
- 500–600 HV 0.025
- approx. 0.5% elongation
- scratching test and heat shock test (180  $^{\circ}\text{C}$ , cooling in cold water) confirmed the adherence strength (Fig. 7)
- electrical conductivity (especially important for the connection of electronic components)
- can be painted
- solderable



← Chemical nickel/phosphor alloy layer

← Magnesium base metal

Figure 7: REM micrograph of a good bonding

## 15.6.2 Distribution of Layer Thickness

These layers can be deposited in a narrow tolerance range because the layer thickness is homogeneously distributed. Even the most complex structures can be reproduced in a net-shape (Fig. 8). The parts should have a suitable component part fixture for a coating. Furthermore, component geometries that allow air inclusions must be avoided. The surface needs to be free of cracks, voids, material doublings, and enclosures (Fig. 9). The use of agents and pulling aids should be minimized. There must not be any silicon-containing agents on the surface.

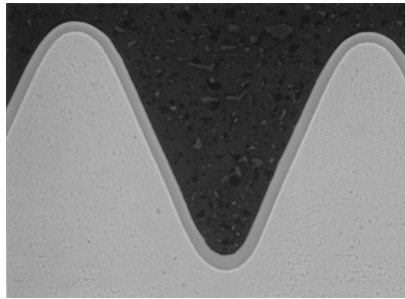


Figure 8: Homogeneous layer-thickness distribution, illustrated for an M4 screw

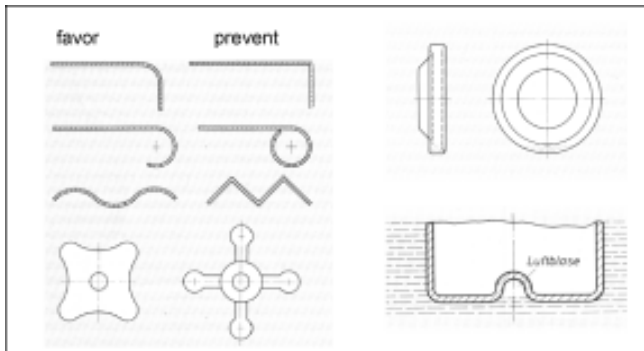


Figure 9: Examples of galvanometric-friendly design

## 15.7 Corrosion Resistance

Good corrosion resistance requires an all-sided, thick, and dense coating. Since magnesium is very ignoble, this layer is necessary to prevent pitting corrosion. A dense coating also means low porosity; Fig. 10 shows the influence of the surface roughness on the coating.

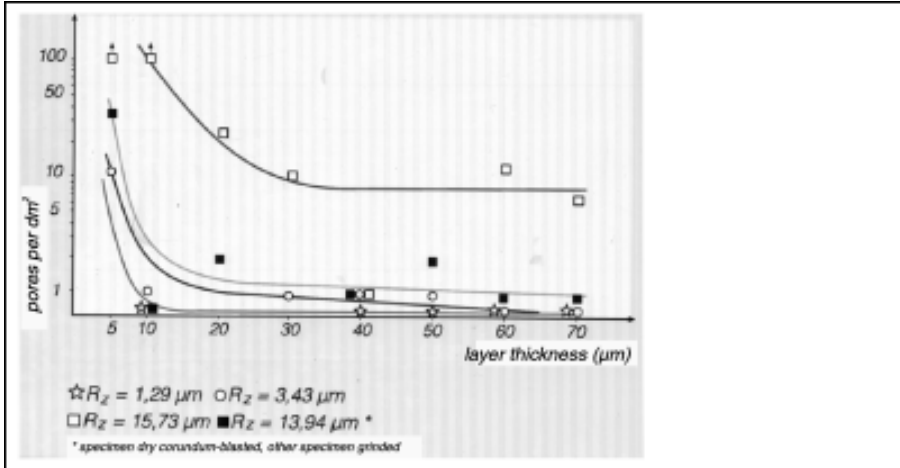


Figure 10: Influence of the surface roughness on the coating

In practice, three corrosion test cycles were required. One test is the “condensate-alternating climate test”, conducted according to DIN 50017 (8 h, 40 °C; 16 h, room temperature). All layers passed this test. Another fast corrosion test is the salt-spray test according to DIN 50021SS. The first corrosion products were observed after five days [2].

## 15.8 Thermal Stability

Chemical nickel/phosphor alloy coatings are often employed at high temperatures. For this use, no defects are allowed. For this reason, a test was carried out, in which plate specimens were loaded with  $1.3 \times 10^{-3}$  Pa in a vacuum furnace at 250 °C over a period of 48 hours. After the test, none of the specimen showed any coating defects [2].

## 15.9 Thermal Cycling Tests

The ductility and adherence under a repeated load was examined by means of a so-called thermal cycling test. Specimens were first stressed for 5 min at -50 °C, then for 15 min at room temperature, and finally for 5 min at 100 °C. After 100 cycles, no visual changes could be detected [2].



## 15.10 Abrasion Measures

All tests of abrasion are based on a tribologic system. The abrasion values are therefore highly dependent on the base body, the other body, and the adjusted parameters of the testing facility. Generally, the abrasion resistance increases with decreasing phosphor content. A subsequent heat treatment at 400 °C/1 h has a positive effect.

The abrasion and adhesive wear were measured by the pen-disc method. In this method, a pen rotates with a defined force over a coated ring-shaped body. The abrasion and the friction coefficient  $m$  make up the values, which are listed in Fig. 11.

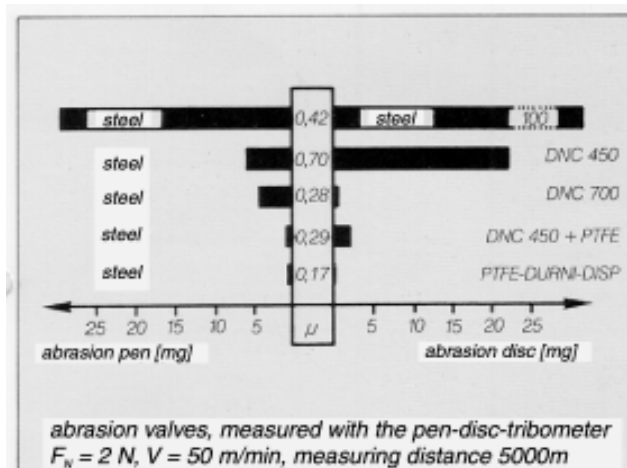


Figure 11: Pen-disc measurements of various surfaces. DNC 450 denotes a high-phosphor-containing (approx. 10–14% P) and DNC 700 denotes a low-phosphor-containing (approx. 3–7% P) nickel/phosphor layer

## 15.11 Coating Systems

Coating systems are applied in cases where a single layer can no longer meet the requirements. However, the costs need to be reasonable in relation to the benefit. There are numerous possible coating systems. One example might be the application of additional nickel/phosphor alloy coatings with different phosphor contents (e.g. low-phosphor DURNI-COAT® DNC-700, medium-phosphor DURNI-COAT® DNC-520, high-phosphor DURNI-COAT® DNC-450). Each layer has its own corrosion- and wear-resistance depending on the phosphor content. Furthermore, nickel/phosphor dispersion layers could be deposited. These contain hard particles such as SiC or diamond for better wear resistance or PTFE-dispersion particles to reduce friction or to impart anti-adhesion properties (*cf.* Fig. 12).

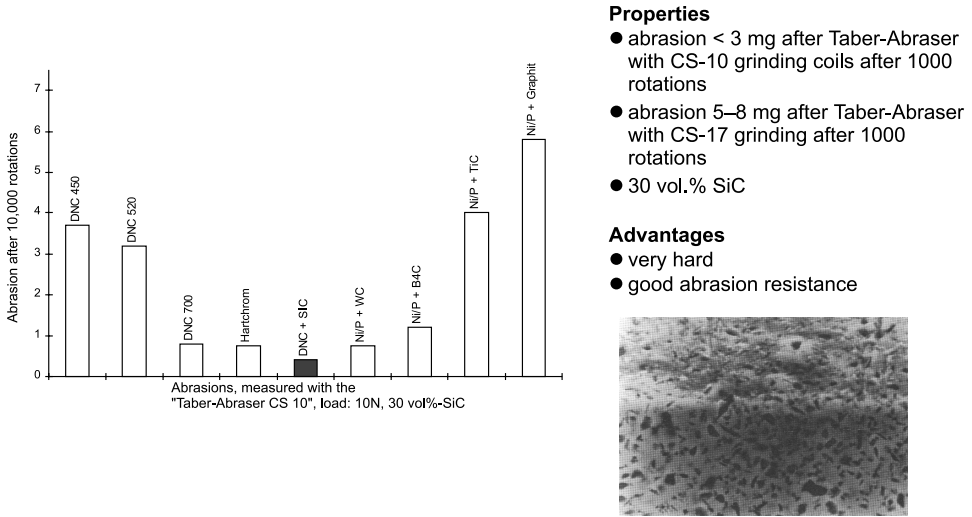


Figure 12: Abrasion values of dispersion layers compared to other layers, measured according to Taber abraser

Electrolytic coating systems are also very interesting. They are mostly used for decorative reasons and are applied to nickel/phosphor alloy coatings without an external current (e.g. copper, nickel, chrome).

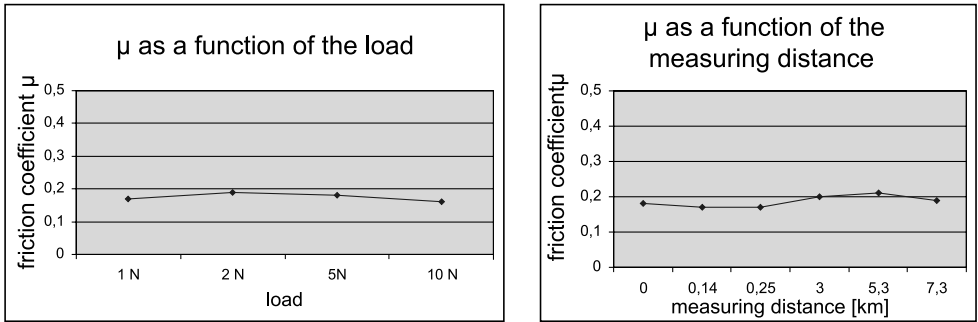
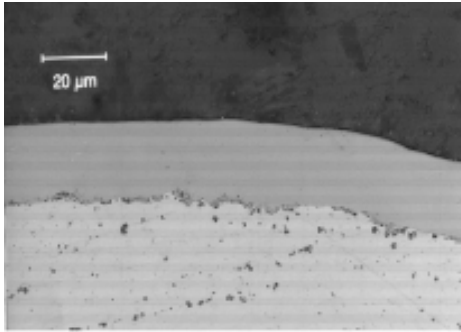


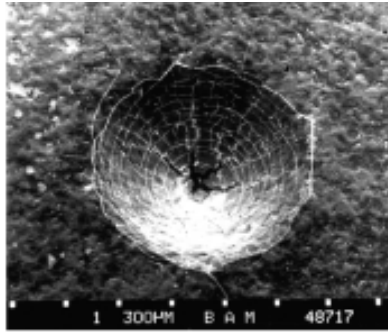
Figure 13: Low abrasion of PTFE-nickel/phosphor dispersion layer as a function of load and measuring length

Recently, combinations of plasma-physical layers (e.g. PVD-TiN, Ti(C,N), CrN) have been used in instances where a very hard surface together with good corrosion resistance is required.

The cross-section polish in Fig. 14 shows such a combination, consisting of a chemical nickel/phosphor alloy layer and a PVD-TiN layer. The homogeneous notching of the base material can clearly be seen, which indicates a good adherence. An additional Rockwell test validated this.



cross-sectional polish  
25 μm CD-Ni/P + 0,8 μm PVD-TiN



Rockwell-print of a combination-layer  
25 μm CD-Ni/P + 0,8 μm PVD-TiN

Figure 14: Combined chemical nickel/phosphor alloy layer and PVD-TiN layer [3]

The performance of the combined coatings in terms of the increase in strength is shown in Fig. 15.

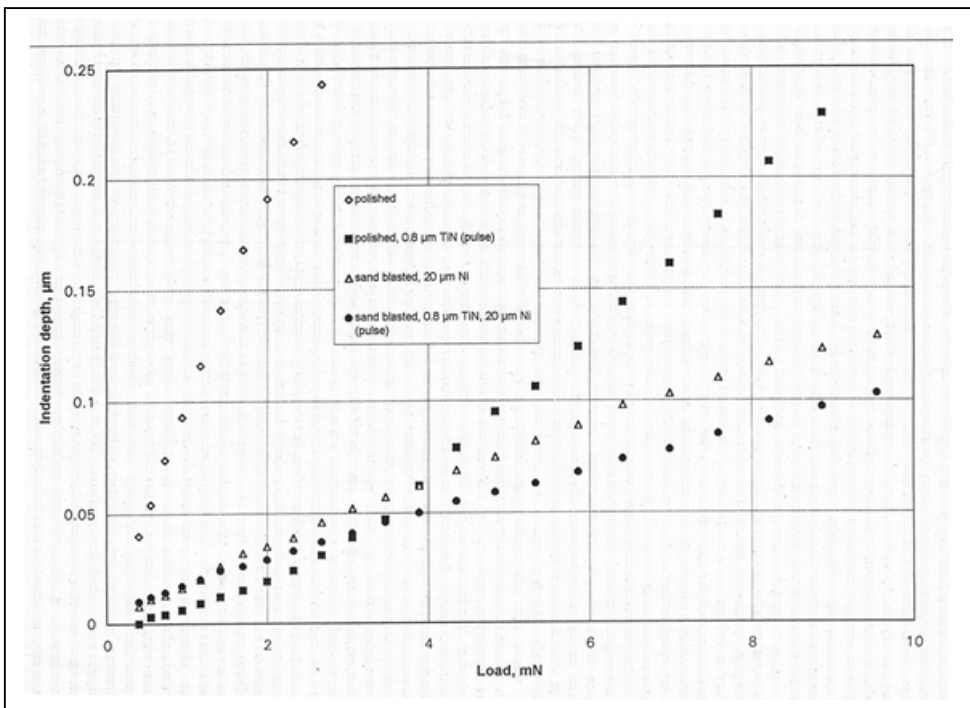


Figure 15: Hardness of different coatings

## 15.12 Magnesium Alloys that can be Coated

Currently, all technical magnesium alloys, such as AZ91 HP, AZ61, AZ31, AM50, and AM20, can be coated with a chemical nickel/phosphor alloy coating. However, prior tests are necessary for alloys containing rare earth metals.

## 15.13 Application Examples



<p>DGM-Fortbildungsseminar „Magnesium“ Clausthal-Zellerfeld Parts for hard disk</p>	
<p>requirements: - corrosion resistance   (6h in neutral salt-spray test) - low contact resistance</p> <p>layer thickness: 25 µm DNC</p> <p>base material: AZ31B</p>	

Figure 16: Application example 1, electronics


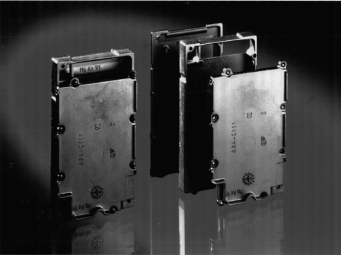
<p>DGM-Fortbildungsseminar „Magnesium“ Clausthal-Zellerfeld Mobile-phone case</p>	
<p>requirements: - suitability for mass production - good shielding over the whole frequency range - conductive surface for proper contact behaviour when combining multiple parts - paintability - good corrosion resistance - good adhesion</p> <p>layer thickness: 20 µm DNC-Mg</p> <p>base material: AZ 91</p>	

Figure 17: Application example 2, electronics

DGM-Fortbildungsseminar „Magnesium“ Clausthal-Zellerfeld  
Laptop case



requirements:

- suitability for mass production
- good shielding over the whole frequency range
- conductive surface for proper contact behaviour when combining multiple parts
- paintability
- corrosion resistance
- good adhesion

layer thickness: 20  $\mu\text{m}$  DNC-Mg

base material: AZ91



Figure 18: Application example 3, electronics

## 15.14 Literature

- /1/ Holländer, A.: Chemische Vernickelung von Magnesium. In: Metalloberfläche 49 (1995)4, p. 265-267.
- /2/ Sharma, A.K., Suresh, M.R., Bhojraj, H., Narayanamurthy, H., Sahu, R.P.: electroless nickel plating on magnesium alloy. In: metall finish (1998)3, p. 10-18.
- /3/ Reiners, G., Griepentrog, M.: hard coatings on magnesium alloys by sputter deposition using pulsed DC bias voltage. ICMCTF-Tagung San Diego 1995.

# 16 Recycling of Magnesium Alloys

*Ditze, C. Scharf, Institute for Metallurgy, Technical University Clausthal, Clausthal-Zellerfeld*

## 16.1 Introduction

The world's primary magnesium production was 360,000 t/a in 1990 [1], with a similar figure for 1997 [2]. For 1995, 299,000 t/a without China is quoted in ref. [27], while ref. [39] describes a primary demand of 295,400 t for 1996. According to ref. [3], the primary magnesium capacity actually amounts to 447,000 t/a, while the figure is 390,000 t/a in ref. [27]. The ratio of primary to secondary magnesium has remained at 5:1 in the last years. An increase in the use of structural magnesium and aluminium alloys, as well as in the process of desulfurization, is predicted.

Compared to other metals, such as aluminium, recycling of magnesium is not very widespread. This is mainly because of magnesium's high reactivity towards oxygen and nitrogen, impurities in the scrap metal such as copper and nickel, and because it already has uses. Thus, magnesium is used for the desulfurization of steel and iron, for producing cast iron, for thermal reductions, or as a sacrificial anode. When used for these processes, the magnesium is lost for recycling. However, magnesium used as an alloying element for aluminium is partly recycled. For this reason, mostly structural magnesium is available for recycling; around 100,000 t is predicted for 2005. Other predictions quote about twice this value. The usage of magnesium in percentage terms is given in Table 1 (taken, in part, from [39]).

The main incentive for the recycling of magnesium is the energy saving. Instead of 35 kWh/kg (minimum) for primary production, only 3 kWh/kg or less is necessary for remelting new scrap metal. Recycling currently means the remelting of new scrap metal and its delivery to the aluminium, iron, and steel producers. Scrap with big surfaces or deposits with low magnesium content, such as crucible sludge or dross, are usually discarded. A still unsolved problem is the recycling of old scrap [34] to use it again as structural magnesium.

Table 1: Usage of magnesium.

Alloying metal for aluminium	50 %
Demand for die-casting	24 %
cast iron and desulphurisation	19 %
corrosion protection	3 %
Metallurgical process	2 %
Others	2 %

## 16.2 Raw Materials

Cast alloys, especially rejects from production, i.e. new scrap, are the common raw materials for magnesium recycling. The casting alloys, such as the well-known die-casting alloy AZ91, contain up to 10% Al, up to 3.5% Zn, up to 0.5% Mn, up to 1% Si, and traces of Cu, Ni, and Fe. Special alloys contain rare earth elements up to 4%, silver up to 3%, and zirconium up to 1%. Recently developed alloys (SFB, Magnesium Technology TU-Clausthal, University of Hannover) contain up to 10% or even more rare earth elements and have high contents of lithium.

Wrought alloys contain up to 10% Al, up to 2% Mn, up to 1.5% Zn, a small amount of silicon around 0.1%, and traces of Cu, Ni, and Fe.

The average composition of magnesium scrap can include 4–13% Al, 0.1–0.3% Mn, up to 5% Zn, up to 0.4% Cu, and up to 1.5% Si. This reflects the composition of a typical magnesium casting alloy. Copper and nickel cause problems; they get into the scrap through contamination by aluminium alloys or through magnesium surface treatments (coating of phone and computer components with copper and nickel).

Secondary raw material magnesium can be classified as follows:

1. New scrap/old scrap
  - No. 1 scrap: high-quality, clean scrap
  - No. 2 scrap: reject parts, primed with adherences (steel/Al inclusions, without copper or brass impurities)
  - No. 3 scrap: dirty, oily, wet, contains sand, copper, nickel
2. Scrap with big surfaces
  - No. 4 scrap: chips, metal-rich dross (sometimes separated into wet/oily and clean/dry)
  - No. 5 scrap: low-metal dross, sludge from machining parts, crucible sludge
  - No. 6 scrap: scrap-containing agent, used refining salt

Figure 1 lists the amount and type of scrap that results from the production of die-casting alloys. Considering the 70,000 t of magnesium used for die-casting in 1997, about 28,000 t returns as clean scrap (no. 1), which can be used again directly by the foundry. On the other hand, the scraps nos. 2 to 6 go to specialized, external processors or they are directly deposited. Altogether, between 30 and 50% of new scrap originates from die-casting.

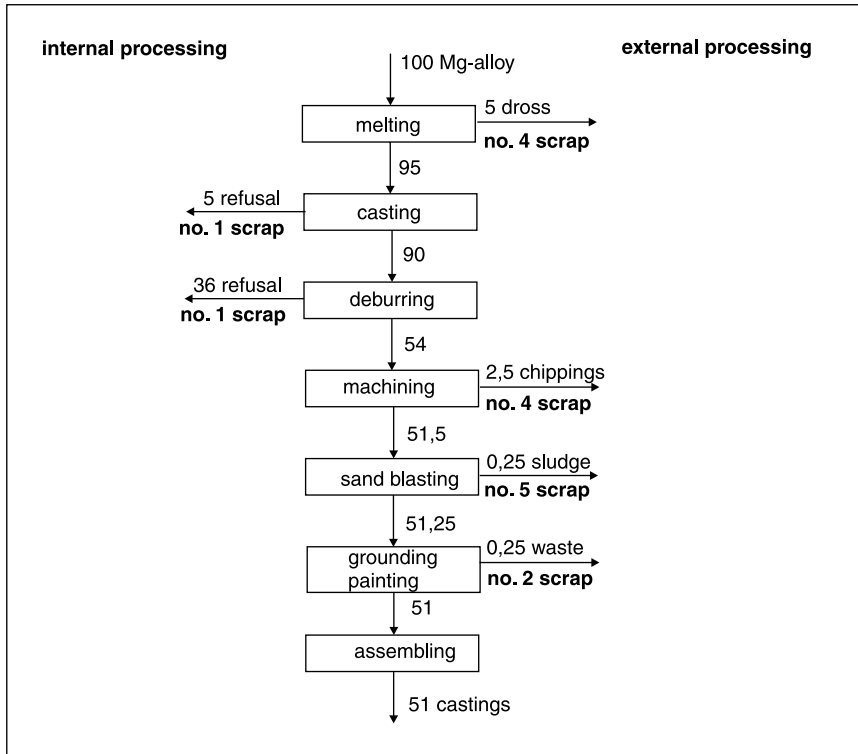


Figure 1: Accumulation of scrap when producing die-cast parts

## 16.3 Recycling

The basic requirement for reasonable recycling is the collection and preparation of the scrap metal in order to recover an enriched product with precise knowledge of its composition. The composition should be guaranteed for new scrap metal. The preparation methods for old scrap metals are mainly sorting by hand, automatic sorting after crushing, and the removal of iron with magnets and floatation. The problem with old scrap is that even the smallest amounts of copper and nickel will render the magnesium useless for structural purposes. The limits for HP quality are 10 ppm Fe, 150 ppm Cu, and 10 ppm Ni. This is one reason for the lack of secondary recycling, as is carried out for other metals. Currently, there is no preparation available which reaches the required purity for structural magnesium. The other reason is the use of magnesium itself. From this stage, there are three simplified recycling scenarios, which are outlined in Figs. 2–4. The total consumption is set at 360,000 t/a.

1. All new and old scrap is used for alloying aluminium, or for iron and steel, since the demand in these fields is greater than that for pure structural magnesium (Fig. 2)



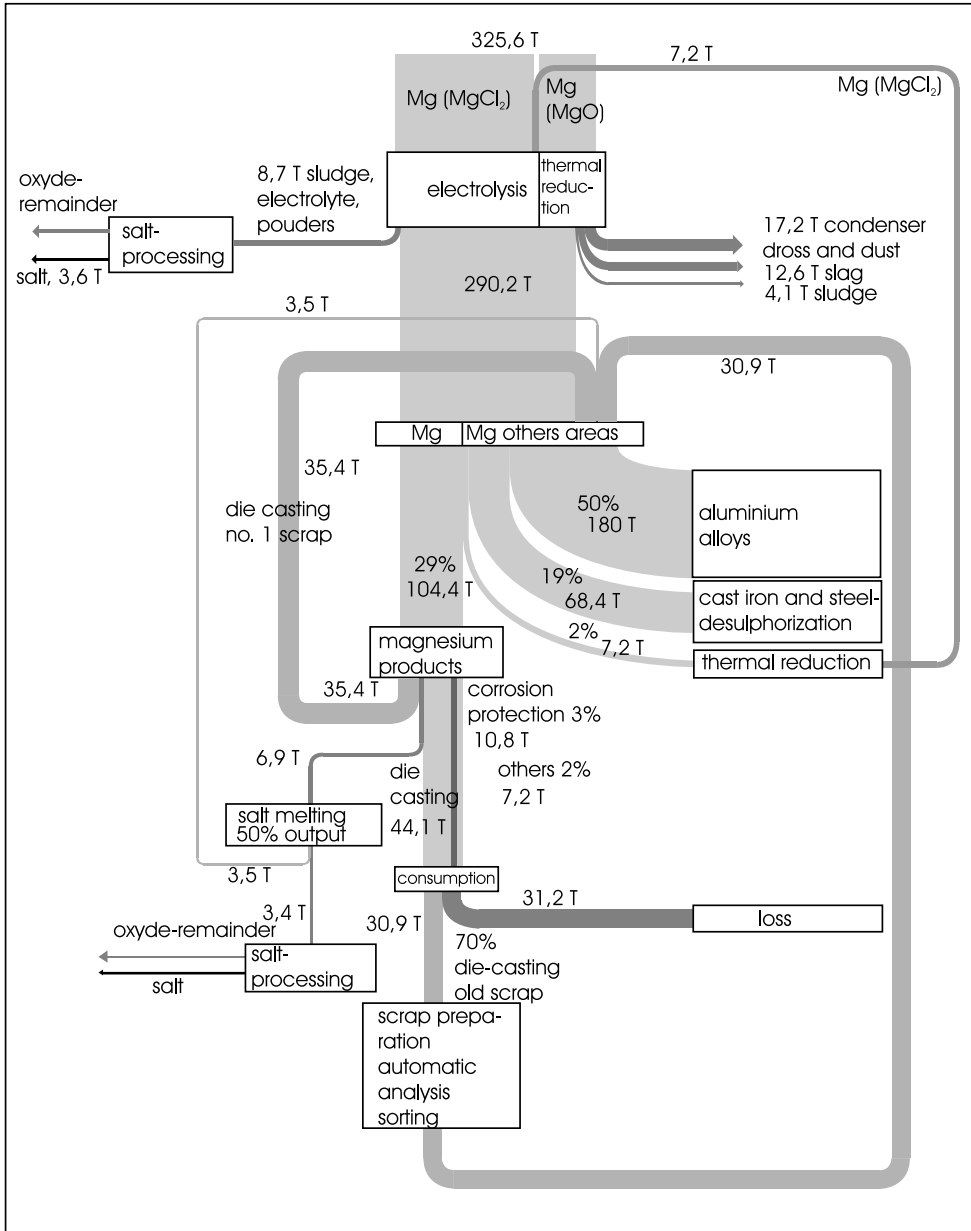


Figure 2: Recycling of magnesium, version 1: all scrap used in aluminium, cast-iron, and steel.  $T = 1000/t/a$  [43,45]

2. Only old scrap is used for aluminium, iron, and steel. The new scrap no. 1 is entirely recycled at the foundry (Fig. 3).
3. The new scrap is recycled by the foundry; one-third of the old scrap is suitable for remelting to produce structural magnesium, one-third goes into aluminium, steel, and

iron production, and one-third is used as an additive for thermal reduction processes to remove copper and nickel impurities (Fig. 4).

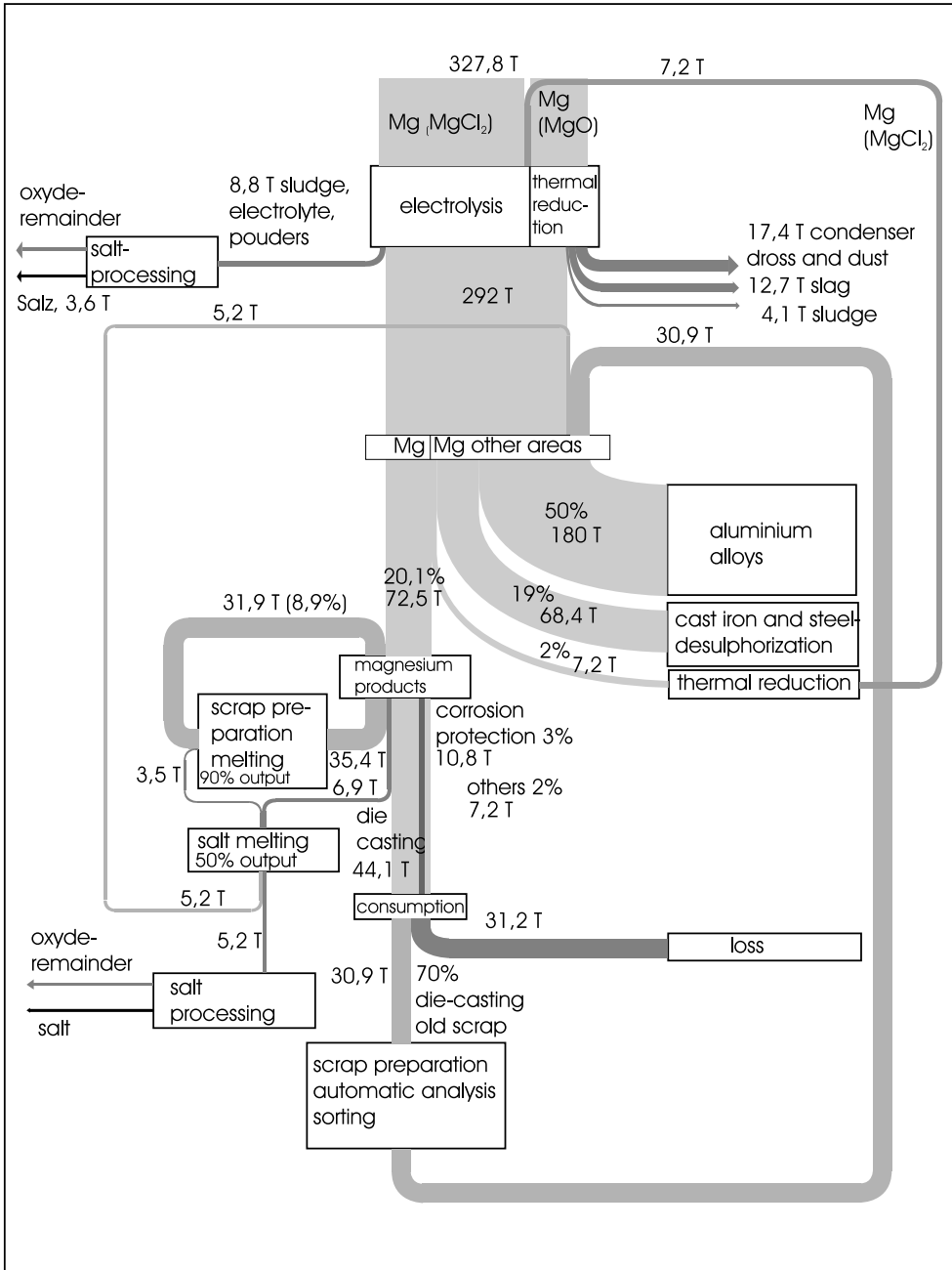


Figure 3: Recycling of magnesium, version 2: new scrap is recycled at the die-caster. T = 1000/t/a [43, 45]



As long as aluminium, cast iron, and steel are able to take all the returning structural magnesium, version 1 will be globally seen as the most economic and ecological solution. The least primary magnesium is used and the amount of remaining waste is also the lowest. This alternative is the main one used nowadays. The second alternative, in which all new scrap is remelted directly at the foundry, needs only little additional primary magnesium. Therefore, it is comparable to alternative 1 in terms of economic and ecological aspects. With this method, scrap transportation is not necessary, but a reversive melting process is needed instead, which again generates waste. The last recycling alternative includes remelting of new scrap as well as remelting of old scrap and involves the steps of preparation, automatic analysis, sorting, and melting. Only one-third of the old scrap is predicted to meet the requirements for structural magnesium. The remaining two-thirds will be in such a contaminated condition that refining by distillation will be mandatory. This type of recycling will only become efficient in the case of a great demand for structural magnesium. The diagrams in Figs. 2–4 are very simplified. The production of powdery magnesium, e.g. for desulfurization, also generates waste through the milling and melting process or simply by milling. Additionally, zinc-containing alloys are not very desirable [42].

A general schematic for the recycling of materials with high magnesium content and low-order materials with low magnesium content, including old scrap, is given in Fig. 5. As already mentioned, the majority of magnesium is used for the production of aluminium, cast iron, and steel. This kind of recycling is referred to as a “dry process”. After cleaning, the magnesium parts are milled to a powder. Dross can be directly fractioned by milling and screening, and can be sold without any melting. No. 1 scrap can also be directly used as alloying material for aluminium or in the desulfurization of steel.

The basic requirement for recycling old scrap, as well as parts of new scrap, to produce structural magnesium, is a sorted registration. This requires engineering directed towards efficient disassembly, a disclaimer of coatings if possible (gear-box housings, use of HP alloys), and a standardized identification system of the components. The application of automatic analysis methods and their associated sorting techniques allows a partial use of old scrap, but it is also necessary for new scrap to prevent frequent off-specification batches when remelting.

An interesting experiment with regard to the automated sorting of automobile scrap is given in Fig. 6. After classification, the parts of sizes in the range 15–16 mm go through a step in which iron, wires, and non-metals are removed. They are then arranged in a chain-like fashion, stimulated by a laser, and finally analyzed on-line by AES. A pick-up then separates the parts, according to the analysis, into different metals and even alloys. The output rate of the unit is 3–5 t/h of non-ferrous metals.

A metal-sorting machine is available from the Aumund Company. At the heart of the machine is an energy dispersive X-ray fluorescence analyser for a continuous determination of the shredded metal parts [28]. The facility consists of the feeding zone (oscillating conveyor, magnetic separator, separation of parts), the analysis zone (detector, X-ray fluorescence source), and the dropping zone, in which the parts are dropped pneumatically according to their composition. Up to 12 different alloys can be sorted; the range of grain sizes is 30–120 mm.

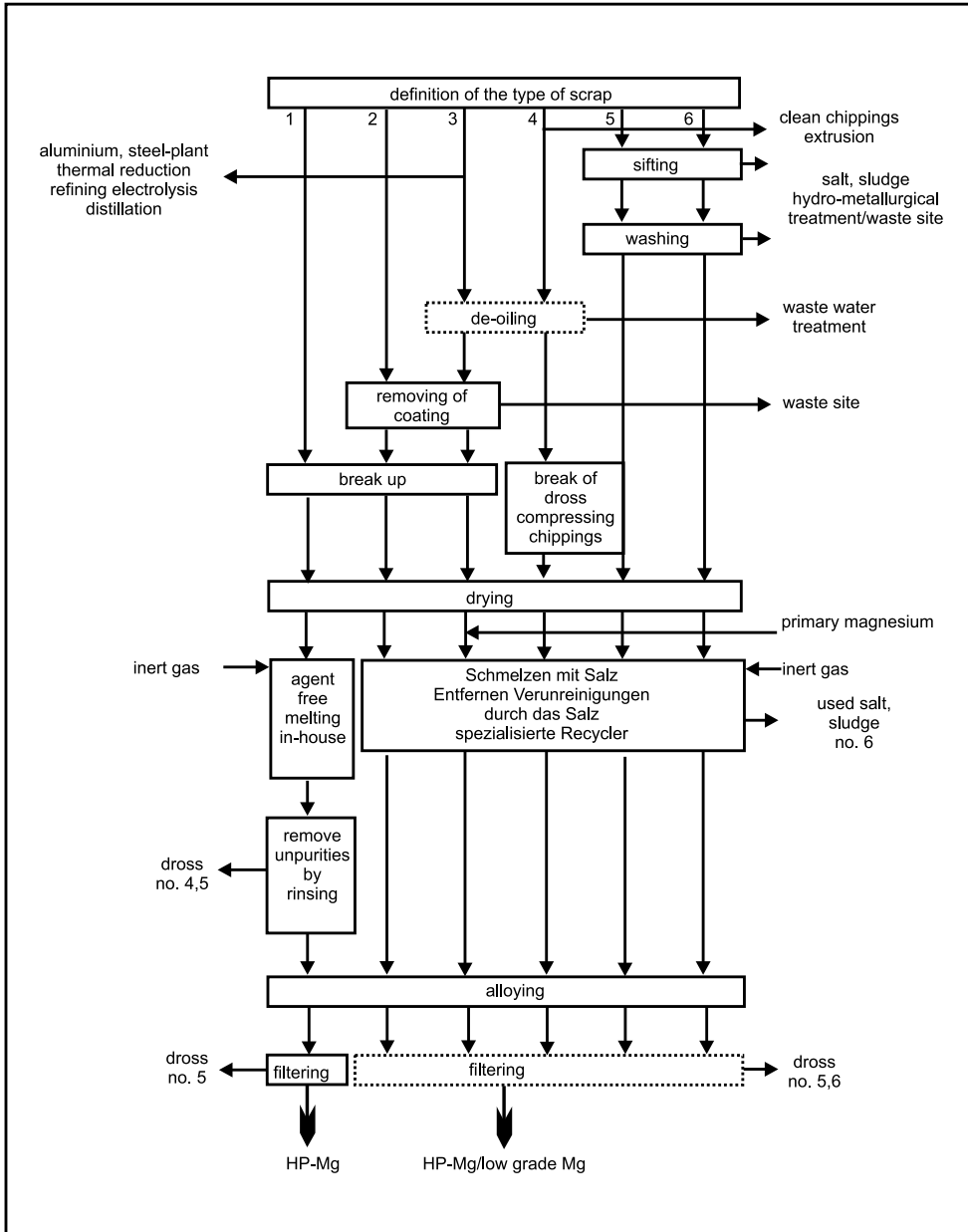


Figure 5: Schematic of magnesium recycling [33]

Depending on the size, the output lies in the range 400–800 kg/h (30–50 mm) and 800–1000 kg/h (60–90 mm). The machine has a power of approximately 13.5 kW. There are, however, also restrictions, e.g. the direct determination of aluminium is not possible. This must be deduced from secondary features, e.g. the copper content in specific alloys (Fig. 7).

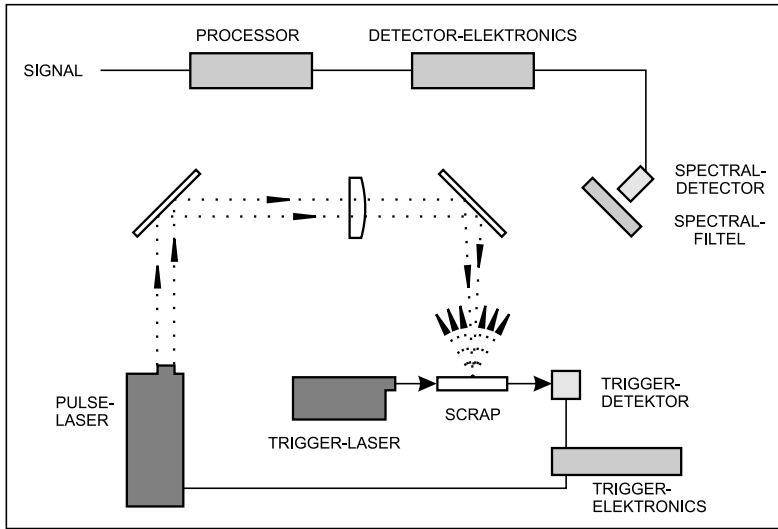


Figure 6: Schematic of an automatic scrap analysis [6]

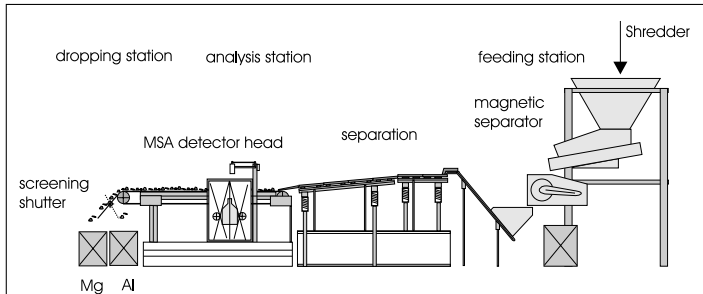


Figure 7: Metal-sorting facility (Aumund Company) [28]

## 16.4 Melting Processes; Special Features

### 16.4.1 Particles

One of the main problems associated with recycling magnesium is the presence of inclusions in the melt [4]. Therefore, the type and amount of inclusions must be exactly defined in comparing the recycled magnesium with primary magnesium. Table 2 lists all particles that occur in the materials.

They can be classified as big ( $> 1$  mm), medium-sized (0.1–1 mm), and small (0.001–0.01 mm). Intermetallic phases rich in iron are between 0.5 and 15 mm. The oxide film measures 0.1–1 mm and the particles are between 10 and 150 mm long.

Table 2: Particles in magnesium melts.

non-ferrous enclosures	intermetallic compounds
magnesium oxide, magnesium nitride	iron-rich intermetallic compounds
Na, Ca, K, and Mg chlorides	manganese/aluminium compounds
aluminium- and calcium carbides	magnesium/aluminium compounds
magnesium sulfide, and -sulfate	
magnesium fluoride	

Below are listed the methods for the determination of the particles and for the testing of the materials:

- Ultrasound
- LiMCA (liquid metal cleanliness analyzer) [4], based on a conductivity measurement of the melt
- Vacuum and pressure filtration
- Microscopic examination, counting of the particles
- Detection of salt enclosures by humidity

## 16.4.2 Reactivity of Magnesium

The protection of the melts against oxidation is very important for the highly reactive magnesium. For the protection, refining salt, sulfur, beryllium (5–15 ppm), and the gases  $\text{SO}_2$ ,  $\text{SF}_6$ ,  $\text{CO}_2$ ,  $\text{N}_2$ , and Ar with some dry air can be used. An overview can be found in [47]. The refining salts usually consist of a mixture of chlorides of magnesium, calcium, or sodium. Moreover, calcium fluoride and magnesium oxide can be included as well. The final composition is similar to that of the electrolyte used for fused salt electrolysis.

Table 3: Common refining salts.

	%CaCl <sub>2</sub>	%NaCl	%KCl	%MgCl <sub>2</sub>	%CaF <sub>2</sub>	%MgO	%BaCl <sub>2</sub>	
Melting	40	30	20	10				[10]
Melting and Refining	20	10	10	35	15	10		[10]
Melting and Refining	55	30	5	3,5	3,5			[7]
Melting and Refining		10-15	50	25		5	5-10	[8, 9]
Melting	15	10	10	35	20	10		[10]

The salts are usually heavier than magnesium, but because of the surface tension they form a protective layer on the melt and they can only sink when the layer is disrupted. The minimum difference in density for the agents aimed for is 0.15–0.20 g/cm<sup>3</sup>. Thickening agents (refining salts) contain MgO, CaF<sub>2</sub>, and MgF<sub>2</sub>. Their function is to bind the particles

and to remove them by sinking to the bottom of the crucible. The difference in density for refining salts should be between 0.5 and 0.8 g/cm<sup>3</sup>.

Sulfur reacts with air to form SO<sub>2</sub> and it is mainly used for protection during transportation as well as during casting. SO<sub>2</sub> forms a protective film on the surface, consisting mainly of MgO with a small fraction of MgS. The gas mixtures contain roughly 0.5% SO<sub>2</sub> but it has only little effect above 700 °C. SF<sub>6</sub> also forms a protective layer on the melt, i.e. MgO, and with SF<sub>6</sub> contents of around 1%, some MgF<sub>2</sub> is found. The mixtures used contain 0.1–0.5% SF<sub>6</sub>, 15–50% CO<sub>2</sub>, and the rest is air. Steel corrodes in the presence of more than 1% SF<sub>6</sub>. All gases for the protection of magnesium contain sulfur as a common element. Since elemental sulfur is also used to protect the melt, sulfur-containing layers might conceivably be responsible for the protection when SF<sub>6</sub> is applied. However, in [30,47] no sulfur was found in the layer, the analyses showing instead MgO and a little MgF<sub>2</sub> at higher SF<sub>6</sub> contents. The use of SF<sub>6</sub> as a protection gas is viewed critically because it has a much higher potential for atmospheric warming (GWP) than CO<sub>2</sub> (1 kg SF<sub>6</sub> = 24,000 kg CO<sub>2</sub>). Although the amounts of SF<sub>6</sub> used are low compared to those of CO<sub>2</sub>, the life cycle of SF<sub>6</sub> is quoted as 3200 years [15], and thus a concentration of the atmosphere is expected. The proportion of the 5000–8000 t of SF<sub>6</sub> produced in 1995 that escaped into the atmosphere is estimated to be 50%. For this reason, there should be a trend away from the use of SF<sub>6</sub>, and a reduction in a specific application would represent progress in this regard. A data sheet from Hydro Magnesium [29] compares the use of SF<sub>6</sub> and SO<sub>2</sub> for a 1 kg die-cast part with respect to the GWP. In this respect, SO<sub>2</sub> is advantageous. The replacement with SO<sub>2</sub> requires the registration and cleaning of the exhaust gases. The use of gas-tight, closed melting units with locks and partial recirculation of the SF<sub>6</sub>-containing gas can also contribute to a lower emission. There is no need for gases containing sulfur in the case of completely gas-tight melting units. In [31], such a melting and die-casting process is described, in which only argon is used. However, the vaporization of magnesium is not suppressed when argon or nitrogen is used. In essence, the degree of protection offered by SO<sub>2</sub>-containing gases is worse than that of gases containing SF<sub>6</sub>. This affects the ability to extinguish an incipient magnesium fire, and indeed SO<sub>2</sub> will subsequently support the fire. Since all dense and thin protection layers consist mainly of MgO, it is said that the gases SF<sub>6</sub>, SO<sub>2</sub>, and CO<sub>2</sub> need to have some sort of absorption mechanism. Hence, oxygen must be present for the formation of such a layer that prevents the vaporization and burning of magnesium. Therefore, mixtures of argon and nitrogen with SF<sub>6</sub> are not really suitable. Nevertheless, since some air invariably enters a technical process, some oxygen will also be present.

Several melting tests on 6–10 kg batches of AZ91 in a cauldron with different gas mixtures resulted in the following observations:



Table 4 Behavior of an AZ91 melt with different protective gases

Protective gas	Temperature/°C	Protective layer	Observations
0.5 SO <sub>2</sub> /Ar	675–705	thin	no burning
	715	thick	burning
	720–750	thick	burning; smoking of melt
0.2 SO <sub>2</sub> /Ar	680–725	thin	no burning
	740	thick	no burning
Ar	680–715	thick	burning; smoking of melt
CO <sub>2</sub>	680–750	thin	no burning

Especially at melt temperatures above 700 °C, the SF<sub>6</sub>-containing gas was found to behave more favourably than SO<sub>2</sub>-containing gases or CO<sub>2</sub>. Argon is not suitable at all because the melt reacts directly with the oxygen entering and no dense protective layer is formed. Pure CO<sub>2</sub> resulted in a good protection of the melt, the layer was thin, and no burning took place. However, small defects in the layer resulted in selective burns, especially when humidity could enter. Similar behaviour was reported in [47], where a detailed overview of the effect of different gases was given. The use of CO<sub>2</sub> is ecologically neutral; the net GWP is zero when the emitted CO<sub>2</sub> comes from suitable sources, such as air or process carbon dioxide. Logging of the exhaust gas is necessary, since a small portion is turned into CO<sub>2</sub>. The best protection is provided by SF<sub>6</sub>-containing gas, which avoids burning even in open bins and during uncovered casting.

### 16.4.3 Metallurgical Cleaning Methods

The ignoble magnesium also limits the refining of the melts. The frequently occurring impurities Fe, Cu, Ni, Mn, Zn, Al, Si, Ca, and Na can be removed to a certain extent by metallurgical refining methods. The solubility of iron in magnesium increases with the temperature (0.04–0.05% at 700 °C), but it can be removed with Mn, Zn, Be, or TiCl<sub>4</sub> [10]. Magnesium reduces the chlorides, forming intermetallic compounds or solid-solution crystals, which precipitate from the melt and are absorbed by the salt. Silicon can be removed with ZnCl<sub>2</sub> or CoCl<sub>2</sub>, while sodium and calcium can be converted with MgCl<sub>2</sub> [10]. Hydrogen is eliminated by treatment with chlorine at 725–750 °C; nitrogen is removed with the help of argon and helium at 650–680 °C. The contents of copper and nickel, which strongly influence the corrosion behaviour, may be adjusted by dilution with primary magnesium. One solution might be distillation in vacuo or at normal pressure with an inert gas, considering magnesium's low melting point. It should be possible to add scrap to the thermal reduction process. Aluminium does not interfere because it supports the reduction of magnesium oxide.

### 16.4.4 Materials

The high affinity of magnesium for oxygen does not allow the common use of standard refractory materials. Iron oxides, silicon oxides, and refractory linings with high silicon contents are out of the question. The interior linings of the melting units consist of unalloyed steel, e.g. ST37 or mild steel 1020. The parts outside the melt are plated (e.g. with stainless steel 430) and must be nickel-free. The exterior of the crucible is also often plated to prevent corrosion. The crucible interior may be plated with chromate steel. The economical limit for a steel crucible is 1–5 t capacity according to the foundries. The linings that accommodate the crucibles should consist of material with a high  $\text{Al}_2\text{O}_3$  content. The materials need to be microporous because molten magnesium has a low viscosity of 1.1 MPa s (melting point), which is close to that of water (1.0). Material with the following composition is proposed [18]: 90.5%  $\text{Al}_2\text{O}_3$ , 1.4%  $\text{SiO}_2$ , 0.2%  $\text{Fe}_2\text{O}_3$ , 1.7%  $\text{TiO}_2$ , 4%  $\text{MgO}$ , 0.2%  $\text{CaO}$ , and 2% others as tamping clay. The maximum application temperature is quoted as 1080 °C. Refractory linings of pure magnesium oxide or aluminium oxide are also possible.

### 16.4.5 Transportation of Liquid Magnesium

The low melting point allows the transportation of liquid magnesium by means of pumps and lifters. Some possibilities are outlined in Fig. 8.

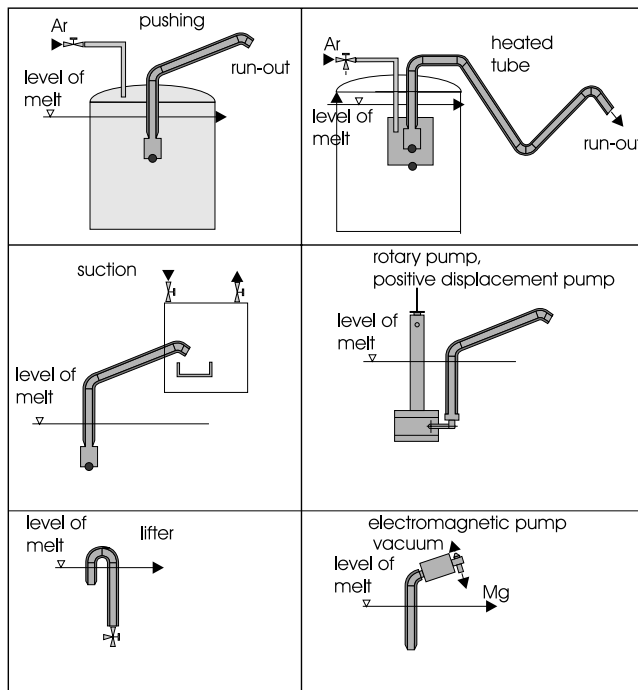


Figure 8: Transportation of liquid magnesium

## 16.5 Melting Metallurgical Recycling

Induction furnaces, resistance furnaces, as well as oil- and gas-heated furnaces are used as melting furnaces. The processes can be divided into agent-free melting, melting with little agent, and melting with much agent [33]. In principle, there is no difference between the methods for primary magnesium and scrap. The more contaminated the scrap and the bigger the surface is, the more agent is used. For melting metallurgical recycling, the scrap is crushed, pre-heated, and melted. As is common practice in metallurgy, it is appropriate to carry out the metallurgical work in separate units. This results in several connected individual melting units or in multi-chamber furnaces in which the chambers are connected. The two-chamber system is the most common one. The first chamber is for melting; dross and sludge emerge from here. Therefore, it is important to optimize this chamber in terms of cleaning abilities. In the second chamber, the melt is prepared for casting.

### 16.5.1 Melting Without Agent

Melting without agent uses inert gas and stirring gas, sometimes together with filtering. It is used for new scrap and has following advantages [12]:

- removal of dissolved gases from the melt (hydrogen) by dispersion of an inert gas
- reduced metal loss due to less dross
- elements with an affinity for chromate (rare earths) stay in the melt
- easy removal of floating particles from the melt surface

Figure 9 shows a two-chamber furnace method for remelting magnesium. The inert gas is, for example, a mixture of 20% CO<sub>2</sub>, 0.2% SF<sub>6</sub>, and dry air. The new scrap is melted in a 500 kg resistance furnace made of steel. A perforated steel plate separates the melting chamber from the rest of the crucible. A heated lifter then transports the melt into the casting furnace. Both furnaces are covered and the gas mixture protects the surface of the melt. The average working temperature inside the furnace is kept at 660 °C. Some 92% of the dross collects on the surface of the melting furnace, 2–3% is sludge on the crucible floor, and about 5% of the dross appears in the casting furnace. Dross collects on the melt as soon as the return flow is added. When the return flow amounts to 100%, dross also appears in the casting furnace.

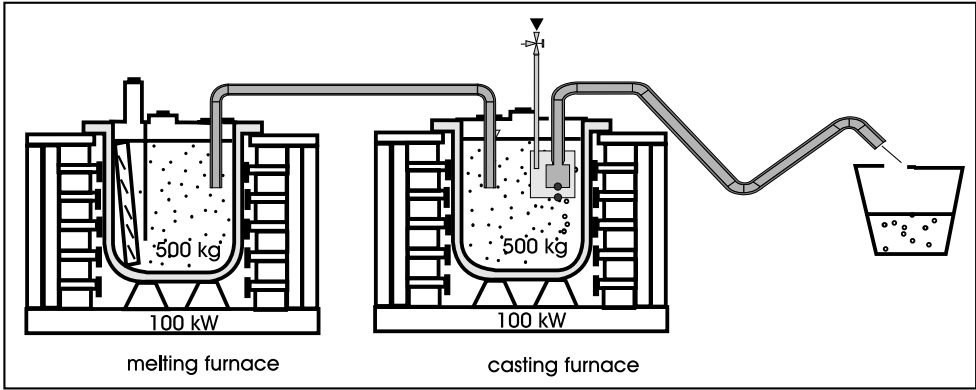


Figure 9: System for melting new scrap, Norsk Hydro [13]

The alloy AZ91 thus produced complies with the required composition. The dross is 97–98% metallic, while 82–87% of the sludge is metallic.

This system is used by Husqvarna die casting for 100% return flow; the melting furnace has a capacity of 1500 kg (180 kW), and the casting furnace has a capacity of 500 kg (90 kW). Small amounts of agents are supplied to the melting furnace. A constant temperature and a constant melt level are important to minimize the amount of dross.

The Dow Chemical Co. introduced an agent-free concept [25]. The process is discontinuous for one crucible and continuous for two crucibles. The steps of the agent-free processing are de-oiling, crushing, pre-heating to at least 150 °C (better 300 °C as then hydroxides are also dissolved), and melting at 680–720 °C under an atmosphere containing 0.3–0.5% SF<sub>6</sub>. Stirring argon into the melt with a mixer makes the particles float on the surface, whereupon they can be removed as dross. Crucible sludge forms here as well. A filter, connected to a pump tube, is submerged in the melt. The filter is cylindrical in shape and has outlets. It is made of 410SS, the outlets are 1 mm in diameter, the open area amounts to 31%, and the total surface area is 0.44 m<sup>2</sup>.

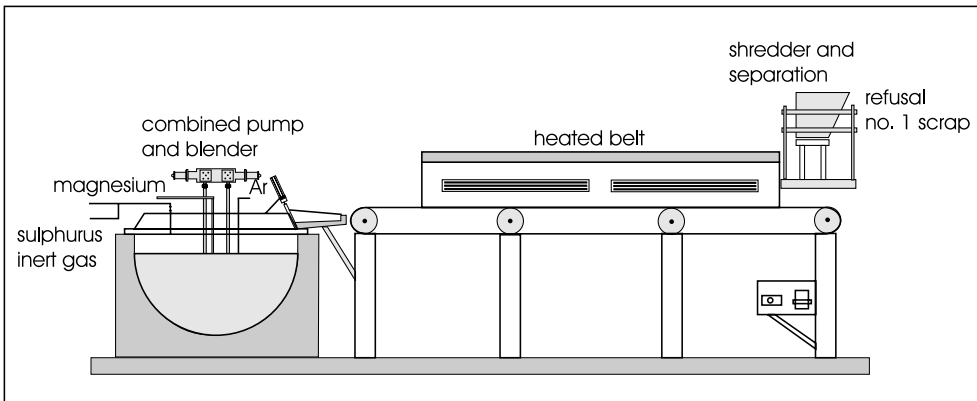


Figure 10: Study of the agent-free melting of magnesium die-casting scrap [25], Dow Chemical Co.

Cleaning is accomplished by means of a flame, by immersing in water or acid, or by sandblasting [14]. A process for no. 1 scrap is described in [40].

Another example of an in-house recycling system is the multi-chamber furnace used by Schmitz and Apelt LOI [26, 35] (Figs. 11 and 12).

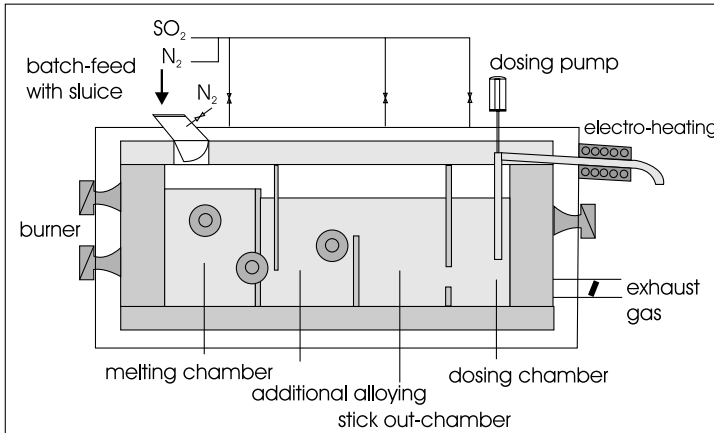


Figure 11: Multi-chamber furnace for recycling type I scrap [26,35,41]. Contents approx. 10 t, melting performance 1.5 t Mg/h. Schmitz & Apelt LOI/Rauch

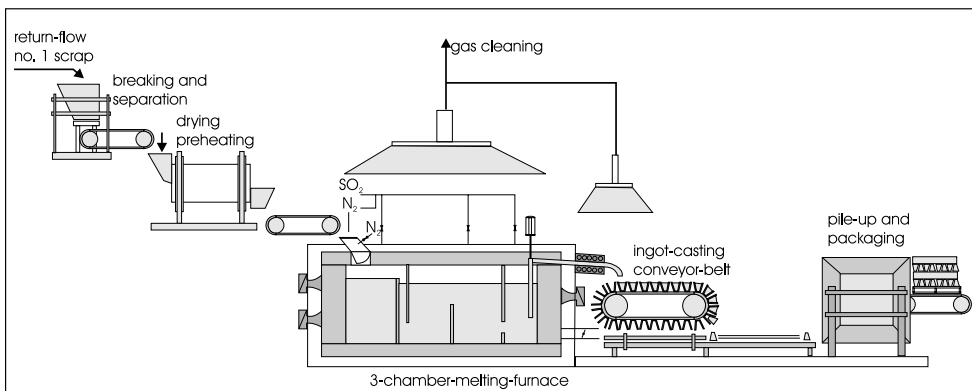


Figure 12: Recycling system for type I scrap, Schmitz & Apelt LOI/Rauch [26,35]

### 16.5.2 Melting and Refining with Little Agent

Steel crucibles and steel cauldrons are wetted from the inside with melting agent. The agent is introduced in liquid form after the crucible has been heated to 700 °C; the magnesium is melted with or without an inert gas. Possible oily adherences are removed under cold

conditions and then the scrap is heated up to 150 °C to remove water and to char organic impurities. The gases are afterglowed. The direct addition of cold scrap is possible as well, i.e. without a separate pre-heating. The amount of agent required is 1% of the amount of magnesium; for refuse it is 3% of the amount of metal. All refuse must always be refined because of the particles. The metal is heated to 700–730 °C, the surface is skimmed, and the agent is stirred into the melt in several portions. The surface is covered with a thin agent layer and the metal is allowed to stand for 10–15 min. Filtering may be necessary to achieve good casting qualities. The disadvantages are:

- release of corrosive  $\text{Cl}_2$  and  $\text{HCl}$  gases
- metal enclosures in the sludge
- problem of depositing the sludge
- agent enclosures in the metal lead to increased corrosion

### 16.5.3 Melting with Much Agent

A continuous refining method developed by Norsk Hydro for small foundries is depicted in Fig. 13.

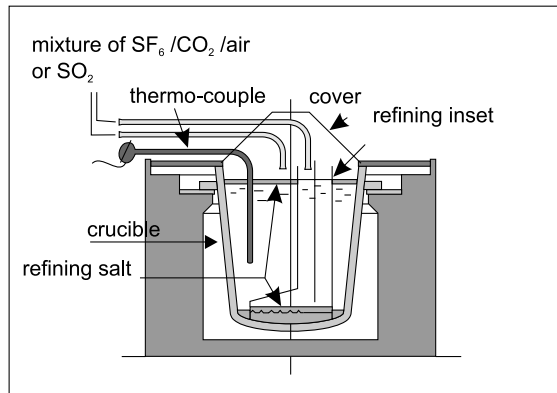


Figure 13: Furnace for the treatment of refuse; Hydro Magnesium data manual

The liquid agent at the bottom serves as a plug. The metal fed in from the outside must go through the salt and can be skimmed from within. The outer crucible is covered with agent, and  $\text{SF}_6$ - or  $\text{SO}_2$ -containing gas mixtures protect the whole crucible.

A recycling concept for the die-casting production of AZ91 from primary magnesium and AZ91 scrap no. 1 is shown in Fig. 14.

The scrap is melted in a multi-chamber furnace with the agent, the metal is fed to an induction furnace, and finally refined in another multi-chamber furnace with the agent prior to casting.

The two agent-melting furnaces are similar in their design. The quality must be adjusted inside the refining and casting furnaces. The particles in the fused salt need to be restrained. The desired casting temperature is adjusted by the electrodes in the fused salt. At

the same time, the furnace is used as a metal reservoir between alloying and casting [11, 16, 17].

The Norsk Hydro patent [7] describes a quasi-continuous multi-chamber furnace for melting scrap, which is depicted in Fig. 15.

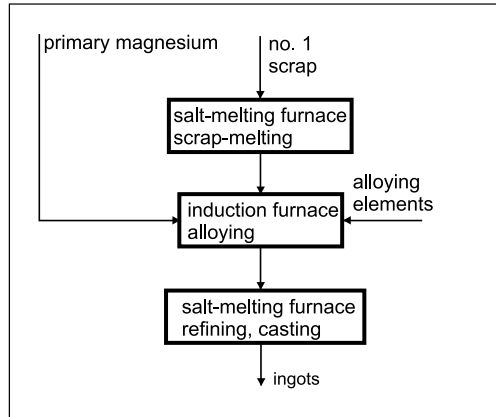


Figure 14: Schematic for the processing of cast scrap

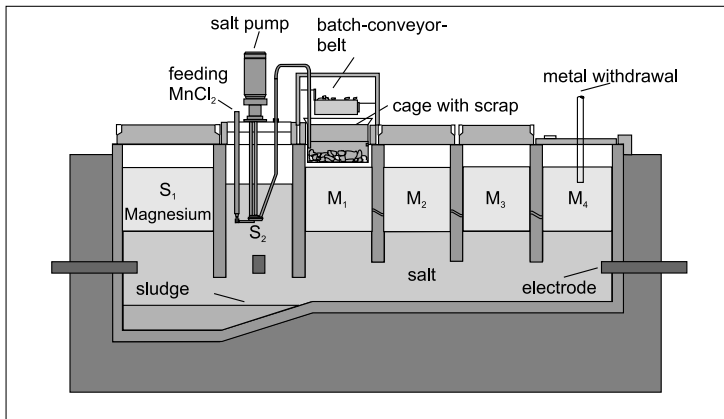


Figure 15: Multi-chamber furnace for melting magnesium scrap and cuttings , Norsk Hydro [7]

The schematic shows a furnace with four metal-collecting chambers and two agent-melting chambers. S1 is twice the size of S2 and serves as a large magnesium reservoir. The metal-collecting chambers are separated by refractory partition walls with gaps. The agent-melting chamber S1 is separated by a wall without an outlet. The whole furnace is closed with a top cover. The number of chambers is optional and depends on the objective. At least two regular remelting chambers and three chambers for the processing of scrap of

unknown composition are required. The agent is heated up with electrodes; the electrodes in chamber S2 serve to overheat the agent.

The metal or scrap is melted by the hot molten salt that is poured over the metal inside a cage. This is very effective in preventing oxidation. The difference in density between the molten salt and magnesium is 0.2–0.3 g/cm<sup>3</sup>. The circulation of the salt amounts to 13 t per t of magnesium, and the melting performance is 2–3 t/h. This process can also be employed to process chips and dross with a high metal content. Dampness of the metal is no problem since the water does not come into contact with the liquid metal. Oily adherences, e.g. from turning chips, burn and are finally afterglowed. The temperature of the liquid metal is only slightly above its melting point, so that intermetallic phases can be absorbed by the salt. Sludge collects at the bottom of the furnace. Solid components containing nickel, copper, or iron remain in the cage and can be removed. Similar furnaces are described in [8, 9]. The salt is refreshed when it is consumed. The consumed salt goes to a hydrometallurgical salt preparation.

## 16.6 Processing Chips

Before a remelting of chips containing oil, the majority of the oil should be removed by pressing or centrifugation. The chips can then be directly melted with the salt [7] or the oil is distilled off at 300–400 °C as described in [46] before the remelting starts.

## 16.7 Processing Extraordinary Scrap

Scrap that contains valuable alloying elements (rare earth elements, lithium) can be treated like dross containing those elements using complex procedures [36]. In this case, the goal is not the recycling of the magnesium, but rather the recovery of the alloying elements. Distillation and melting electrolysis or hydrometallurgical methods are some examples. For very ignoble alloying elements such as lithium and fractions of rare earth elements, however, the common melting process with salt cannot be applied. Instead, special salts, such as KCl/LiCl mixtures, are necessary to keep the lithium in the metal phase. Figure 16 shows a schematic of the processing of this type of scrap.



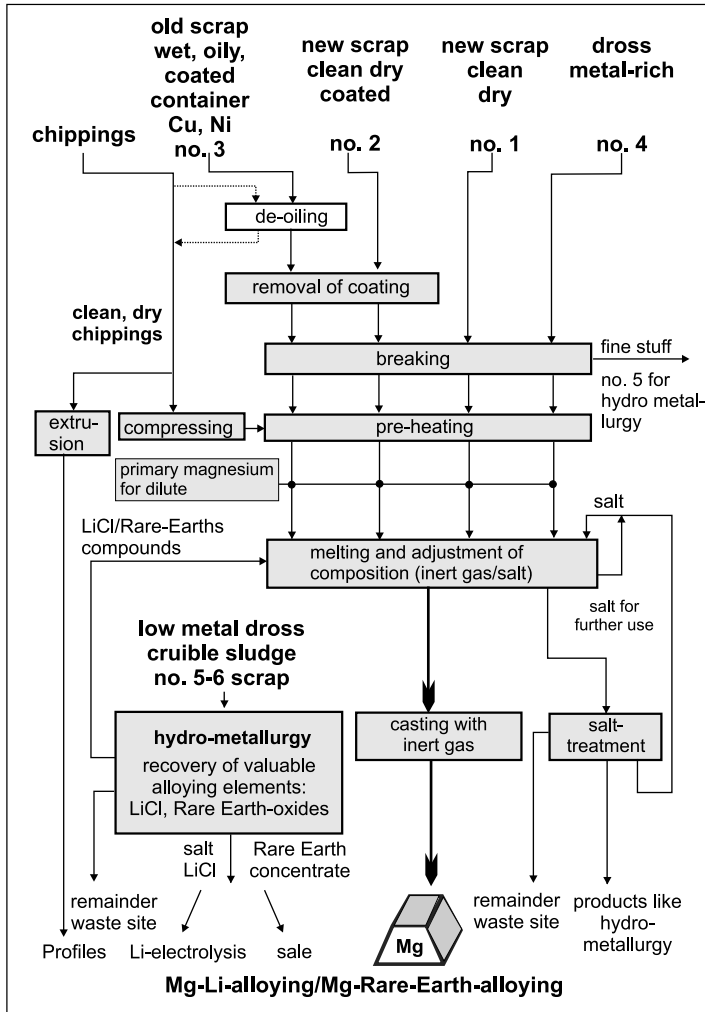


Figure 16: Recycling of special magnesium scrap

As an example, Fig. 17 shows the process for the hydrometallurgical recovery of scandium [19, 36, 37, 44] from dross collected from the melting of Mg/Sc alloys. Dross and remainders from the production of conventional magnesium alloys can also be processed by hydrometallurgical methods [38].

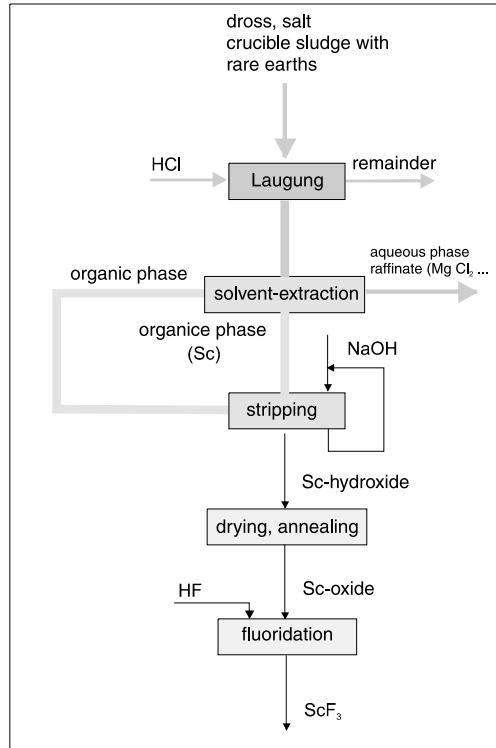


Figure 17: Processing of dross, chips, crucible sludge, and salt from the production of special magnesium alloys, for instance those containing scandium

## 16.8 Recycling of Composite Materials

Composite materials can be broadly divided into fibre- and particle-reinforced materials and laminar structures. A basic recycling set-up, which corresponds with [20] and [21] is given in Fig. 18.

With fibre composites, typically containing  $\text{Al}_2\text{O}_3$  or carbon fibres, the orientation of the fibres is important. Recycling cannot produce materials with similar or even comparable properties to the original. For this reason, a separation of fibres and metal must be accomplished through the use of refining salts [21, 24].

Hydrometallurgical methods may also be used to recover the valuable fibres from the dross.

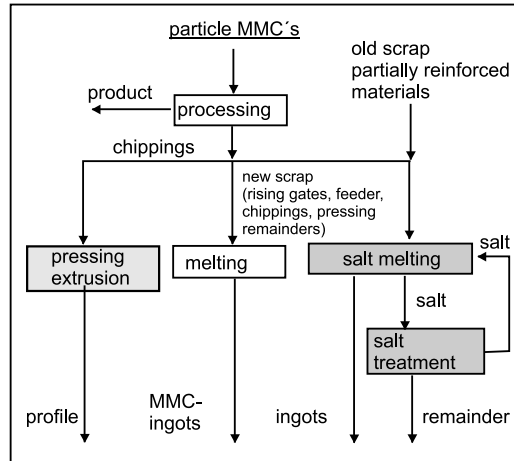


Figure 18: Recycling of particle-reinforced magnesium composites

On the contrary, the remelting of no. 1 new scrap consisting of SiC particle reinforced materials is possible without applying a salt. Salt meltings of old scrap, however, separate the particles and metal. Other solutions are the extrusion of chips, the separation of fibres <10 mm with filters, and the crushing and feeding of partially reinforced components to a melt for the production of homogeneously reinforced parts. Machining will also result in a homogeneous distribution of fibres and particles.

## 16.9 Summary

Recycling of magnesium currently focuses on the processing of no. 1 scrap due to the main use of magnesium in producing aluminium, cast iron, and steel. In the future, when the use of structural magnesium is more prevalent, old scrap will need to be recycled as well. This requires an optimized scrap preparation, so that the recycling yields high quality products. A significant premise is material identification and a pro-recycling engineering that allows for easy disassembly.

The protection of the melt with sulfurous gases is increasingly being performed with  $\text{SO}_2$  instead of  $\text{SF}_6$ . The collection and cleaning of exhaust gases then becomes necessary. The use of pure  $\text{CO}_2$  offers an interesting alternative to sulfur-containing gases. The use of a melting salt is environmentally friendly when applied correctly, but it produces more waste.

## 16.10 Literature

- /1/ Clow, B.B., Garber, F.: Metall 45 (1991), p. 599-601.
- /2/ NN: Metall 48 (1994), p. 442.
- /3/ Mordike, B.L., Hehmann, F.: Magnesium Alloys and Their Applications, Garmisch-Partenkirchen 1992, DGM, ISBN 3-88355-184-8.

- /4/ Hu, H., Luo, A.: Inclusions in Molten Magnesium and Potential Assessment Techniques, JOM Oct. (1996) pp. 47-51.
- /5/ King, J.F., Hopkins, A., Thistlethwaite, S.: Recycling of By-Products from Magnesium Diecasting, in Lorimer, G.W. (ed.) Proc. of the Third International Magnesium Conference 1996 ISBN 1 86125 013 4, pp. 51-61.
- /6/ Sattler, H.P., Yoshida, T.: Recycling of Magnesium from Consumer Goods after Use, in Mordike, B.L. a. F.Hehmann (Hrsg.) Magnesium Alloys and their Applications, Garmisch-Partenkirchen, DGM 1992 ISBN 3-88355-184-8, pp. 29-36.
- /7/ Wallevik, O., Ronhaug, J.B.: Method and Apparatus for Remelting and Refining of Magnesium and Magnesium Alloys, U.S. Patent 5,167,700 (1992).
- /8/ Kulinskii, A.I., Gribov, V.I., Belkin, N.A., Rudnitskii, M.L., Belkin, M.I.: Optimizing Liquid Bath Composition and Processing Technology of Magnesium and Magnesium Alloys, Scrap and Rejects, Tsvetnye Metally (Russian Journal of Non-Ferrous Metals) 12 (1987) pp. 56-58.
- /9/ Gribov, V.I., Belkin, N.A., Shaibakov, T.I., Belkin, M.I.: Material Balance for the Processing of Magnesium Scrap and Waste in a Liquid Salt Bath, Tsvetnye Metally (Russian Journal of Non-Ferrous Metals) 3 (1988) pp. 63-65.
- /10/ Hfy-Petersen, N. u.a.: in Ullmann's Encyclopedia of Industrial Chemistry. VCH Verlagsges. Weinheim 1990, pp. 559-953.
- /11/ Riopelle, L.: The Recycling of Magnesium Makes ¢ents. JOM Oct. (1996) pp. 44-46.
- /12/ Dow Chemical Company: Fluxless Refining of Magnesium Diecasting Scrap 1994.
- /13/ Øymo, D., Holta, O., Hustoft, O.-M., Henriksson, J.: Magnesium recycling in the die casting shop, Metall 46 (1992) pp. 898-902.
- /14/ Petrovich, V.W., Waltrip, J.S.: Flux-Free Refining of Magnesium Die Cast Scrap, Light Metals 1989 pp. 749-755.
- /15/ Gjestland, H., Westengen, H., Plathe, S.: Use of SF<sub>6</sub> in the Magnesium Industry: an Environmental Challenge, in Lorimer, G.W. (ed.) Proc. of the Third International Magnesium Conference 1996 ISBN 1 86125 013 4, pp. 33-41.
- /16/ Albright, D.L.: Technology Paths to Magnesium Alloy Recycling, Die Casting Management Dec. (1993) pp. 24-28.
- /17/ Pinfold, P.M.D., Øymo, D.: An Evaluation of Refined, Recycled AZ91D Alloy, 930420 Warrendale, PA: Society of Automotive Engineers, March 1993, pp. 65-70.
- /18/ Granitzki, K.-E.: Feuerfeste Werkstoffe in Aluminium- und Magnesiumgießereien, Aluminium 73 (1997) p.31-33.
- /19/ Ditze, A., Kongolo, K.: Recovery of scandium from magnesium, aluminium and iron scrap, Hydrometallurgy 44 (1997) pp. 179-184.
- /20/ Kainer, K.U.: Konzepte zum Recycling von Metallmatrix-Verbundwerkstoffen, in Leonhardt, G. u. B.Wielage (Hrsg.) Recycling von Verbundwerkstoffen und Werkstoffverbunden, DGM 1997 ISBN 3-88355-244-5, p. 39-44.
- /21/ Kiehn, J., Oldörp, F., Kainer, K.U., Böhm, E.: Wiederverwertung von Kreislaufmaterial aus kurzfaserverstärkten Magnesiumlegierungen, in Leonhardt, G., Wielage, B. (Hrsg.) Recycling von Verbundwerkstoffen und Werkstoffverbunden, DGM 1997 ISBN 3-88355-244-5, p. 51-56.
- /22/ Agarwal, J.C., Frydenlund, A.R., Katrak, F.E.: Economics of Recycling Magnesium, Proc. of the Met. Soc. of Can. Inst. Min. Met. 19 (1990), pp. 301-306.

- /23/ Kramer, D.A.: Magnesium and Magnesium Compounds, Minerals Yearbook 1989, Vol.I: Metals and Materials, US Dep. of the Interior, Washington, 1991, ISBN 0-16-035820-5, pp. 675-689.
- /24/ Kiehn, J., Buch, F. von, Ditze, A., Kainer, K.U.: Weiterverwertung von Altschrott und Kreislaufmaterial aus der Produktion kurzfaserverstärkter Magnesiumlegierungen, in Friedrich, K. (Hrsg.) Verbundwerkstoffe und Werkstoffverbunde, DGM 1997 ISBN 3-88355-250-X, p.577-582.
- /25/ Dow Chemical Company: Fluxless refining of magnesium die casting scrap, 1994.
- /26/ Schmitz + Apelt LOI: Firmeninformation 1998
- /27/ Rienäß, G.: Gießerei 85 (1998) p.116-126.
- /28/ Aumund Fördertechnik GmbH&Co: Firmeninformation 1998.
- /29/ Hydro Magnesium: Life Cycle Environmental Data for Production of Magnesium Diecastings, Nr. 22564, 04.98.
- /30/ Cashion, S., Ricketts, N., Hayes, P.: Cover Gas Protection for Magnesium – New Perspectives. In: Magnesium Alloys and their Applications. Mordike, B.L., Kainer, K.U. (Ed.) 1998, ISBN 3-88355-255-0, pp. 471-475.
- /31/ Kahn, D., Sahm, P.R., Kluge, S., Becker, H.-H., Carli, S.: Innovative Manufacturing Technology for Melting and Casting Magnesium Alloys. In: Mordike, B.L., Kainer, K.U. (Ed.) 1998, ISBN 3-88355-255-0, pp. 471-475.
- /32/ Haferkamp, H., Bach, Fr.-W., Niemeyer, M., Lindner, P., Holzkamp, U.: Advanced Technology for Cold Chamber Die Casting of Magnesium Alloys. In: Mordike, B.L., Kainer, K.U. (Ed.) 1998, ISBN 3-88355-255-0, pp. 501-506.
- /33/ Scharf, C., Ditze, A.: Present State of Recycling of Magnesium and its Alloys. In: Mordike, B.L., Kainer, K.U. (Ed.) Magnesium Alloys and their Applications, Wolfsburg April 28-30, 1998, ISBN 3-88355-255-0, pp. 685-690.
- /34/ Wardlow, G.D., Thistlethwaite, S., King, J.F., Martin, T., Walton, S.: Feedback Analysis and Statistical Process Control in Recycling Magnesium Alloys: The Integral Link in Component Manufacture. In: Mordike, B.L., Kainer, K.U. (Ed.) 1998, ISBN 3-88355-255-0, pp. 691-696.
- /35/ Leyendecker, T., Rauch, M.: Economical Process for the In-house Remelting in Magnesium Diecasting Shops. In: Mordike, B.L., Kainer, K.U. (Ed.) Magnesium Alloys and their Applications, Wolfsburg April 28-30, 1998, ISBN 3-88355-255-0, pp. 703-707.
- /36/ Ditze, A., Schwerdtfeger, K.: Concepts for Recycling of New Magnesium Alloys. In: Mordike, B.L., Kainer, K.U. (Ed.) Magnesium Alloys and their Applications, Wolfsburg April 28-30, 1998, ISBN 3-88355-255-0, pp. 709-714.
- /37/ Ditze, A.: Verarbeitung von Reststoffen aus der Produktion von Magnesium – Seltene Erden – Legierungen durch Laugung und Solventextraktion. In: Agst, J. (Ed.) Achte Duisburger Recycling Tage Informationsschrift 53, 1998, ISBN 3-926875-29-1, p. 188-201.
- /38/ Rohmann, M., Scherzberg, H.: Verfahren zur Aufarbeitung von aus der Magnesiumherstellung anfallenden Schlacken oder Krätzen, EP 0693563 (1996).
- /39/ Fleteren, R. van: Magnesium Supply and Demand in IMA Proc. 54, June 8-10, 1997, Toronto pp. 1-5.
- /40/ Grebetz, J.C., Day, Haerle, A.G.: Qualification of Recycled Magnesium Type 1 Die Casting... In: Proc. IMA Annual World Magnesium Conference 1998 pp. 8-15.

- /41/ Leyendecker, T., Schroder, D.: Economical Process for the In-House Remelting in Magnesium Diecasting Shops. In: Proc. IMA Annual World Magnesium Conference 1998 pp. 16-18.
- /42/ Zebrowski, G.R.: A Love Affair with Sulfur. In: Proc. IMA Annual World Magnesium Conference 1998 pp. 52-15.
- /43/ Ditze, A.: Stoffkreislauf von Magnesium. Aluminium Nr. 3 1999.
- /44/ Ditze, A., Scharf, C., Kader, H., Saoudi, A.: Extraktion von Scandium, Yttrium und Neodym aus chloridischen Lösungen. In: Schriftenreihe der GDMB, Fortschritte in der Hydrometallurgie, Heft 82, 1998, ISSN 0720-1877, ISBN 3-9805924-5-6, p. 207-220.
- /45/ Ditze, A.: Grundlagen und Technik der Magnesium-Schmelzflußelektrolyse. In: Schriftenreihe der GDMB, Elektrolyseverfahren in der Metallurgie, Heft 81, 1997, ISSN 0720-1877, ISBN 3-9805924-2-1, p. 269-282.
- /46/ US Patent 5338335, 1994.
- /47/ Fruehling, J.W.: Protective Atmospheres for molten Magnesium. University of Michigan Ph.D., 1970.
- /48/ Hanawalt, J.D.: 8<sup>th</sup> SDCE Int. Die Casting Expo. A. Congr., Paper No. G-T75-111, Detroit 1975.

# Register

## A

Abnormal self-dissolution *see* intermetallic corrosion

Abrasion, abrasion mechanisms 142 ff.

Acheson process 198

AE alloys 6

AHC process 245

Alloys 3, 6

– Additions 4

– Alloying elements, effect 4 f.

– Anodic oxidation 223

– Applications 9

– Automotive engineering 19

– Composite materials 16

– Creep behaviour 116 f.

– Creep resistance 106, 116 f.

– Forging 99

– High temperature properties 106 ff.

– Joining 152 ff.

– Low temperature behaviour 98

– Parameters of the weldability 160

– Production and processing 15

– Secondary creep rates 173

– Vacuum die-casting 45

– Weight savings 19

AM alloys 6

Arc welding processes 153 ff.

– Impulsion arc 153

– Joining processes 153 ff.

– MIG 153

– Short circuit arc 153

– TIG 153

AS alloys 6

ASTM-specification 3

## B

Base metal corrosion 236 f.

Bayer-process 198

Beam welding methods 153

## C

Calculation of casting parameters 42 f.

Carbon fiber 187, 192

– Coating 192

– Castability 5 f.

Casting 93

Casting alloys 6

– Containing aluminium 122 f.

– Rare Earth elements 8

– Weldability 160 ff.

– With Ca 122

Cathodic dip coatings

– Delta Seal (DS) 235

– Deltacoll (DC) 235

– Gliss-Coat 235

Coating 243

– Process, electrochemical 242

Coatings 247 f.

Coil-solids 186

Cold chamber machines 46 f.

Cold chamber process 45

Cold deformation 2, 96

Cold forming 82

Compo-casting 204

Composite materials 15, 16, 63, 142, 184 ff.

*see also* Metal-matrix composite materials

– Boundary surfaces 192 f.

– Component quality 148

– Components 186

– Composite strength 185

– Continuously reinforced properties 186 f.,

189

– Creep properties 191

– Critical fiber length 185

– Discontinuously reinforced 173

– – Properties 186 f., 190 f.

– Drill moment 146 f.

– Drilling 146, 148 f.

– Effect on the strength properties 200

– Feed force 146 f.

– Fiber composites 274

– Fiber reinforced 184 ff.

– Fiber reinforcement 186 f.

– – Application 193

– Hybrid reinforcement 211 f.

– Inverse rule of mixture 185

– Linear rule of mixture 184 f.

– Machining 141 ff.

– – Tool wear 142 ff.

– – Wear mechanisms 142 ff.

– Manufacturing, Production 142

– – Of MMCs 186

– – Processes 187 f.

– Matrix materials 186

– Melting metallurgical manufacturing 188

– Melting metallurgical processes 204

– Metal matrix composite materials 63

– Particle reinforced 197

– – Materials 274

– – Mechanical properties 208 ff.

– – Production methods 203

- - Strength properties 199 ff.
  - Powder metallurgical manufacturing 187
  - Powder metallurgical processes 206 ff.
  - Preform 186 f.
  - Properties 184, 189 ff.
  - Reclamation 193
  - Recycling 274
  - Reinforcement materials 186 f.
  - Spray forming 16, 173, 175
  - Squeeze-casting 16
  - Strength properties 199 ff.
  - Tensile strength 191
  - Wetting 186 f.
  - Yield strength of the matrix 185
  - Young's Modulus 199 f.
  - Composite strength 185
  - Cooling concept
    - Emulsion 141
    - MLS 141
    - Oil 141
  - Cooling lubricants 131, 135 ff.
  - Corrosion 17, 218 ff., 226 ff.
    - Contact corrosion 221, 227
    - Corrosion resistance 226 ff.
    - Electrochemical 227
    - Free corrosion potentials 228
    - Galvanic 219 ff.
    - Intermetallic 227
    - Pitting Corrosion 219
    - Stress corrosion cracking 219
    - Tests for corrosion behaviour 234
  - Corrosion protection 17, 218 ff., 228 ff., 242, 249 ff.
    - Addition of specific alloying elements 221
    - Additional coatings and structural actions 238
    - Aluminium systems 237
    - Anodic oxidation 222, 229
    - ANOMAG-process 231 f.
    - Aluminium materials 238
    - Autocatalytic deposition 243
    - Cathodic dip coating 235
    - Classification of Verified Protection Systems 233
    - Coatings 228
    - DOW17-process 229
    - Duplex systems 235
    - Encapsulated with plastics 238
    - HAE process 229
    - HART-COAT 221
    - HP alloys 219, 221
    - MAGOXID 239
    - MAGOXID-COAT 222
    - Nickel/phosphor dispersion layers 249 ff.
    - Oxide ceramic layer 224
    - Plasma-physical layer 250 f.
    - PVD 230 f.
    - Surface methods 242
    - Surface protection 235
    - Surface treatment 222 ff.
    - Surface treatment with electron beam 229
    - TIG coating 229
    - Zinc alloying systems 236 f.
    - Zinc systems 235 f.
  - Corrosion resistance 5, 48, 165
    - Influences
    - Laser surface treatment
  - Creep
    - Behaviour 112
    - Die-casting alloys 115
    - Magnesium 111
    - Primary 106 ff., 115
    - Secondary 106 ff.
    - Tertiary 106 ff.
  - Creep curve 106 f.
  - Creep mechanisms
    - Diffusion creep 108
    - Dislocation creep 108 f.
    - Grain boundary creep 108
  - Creep properties 191
  - Creep rate 106
    - Precipitations 109
    - Reduction 109
    - Secondary 106 ff.
    - Solid solution crystals 109
    - Stress dependence 108
    - Temperature dependence 107 f.
  - Creep resistance 5, 7, 49, 106, 114
  - Critical fiber length 185
  - Crystal structure 2
  - Cylinder compression test 78
    - Flow curves 80
    - Plastometer 79
- 
- ## D
- Damping capacity 3
  - Deformability 165, 2, 56
  - Deformation 81
    - By crystallographic gliding 111
    - By twinning 111
    - Deformation behaviour 81 f.
    - Influences 81 f.
  - Deformation temperature 79, 81
  - Deformation-map for pure magnesium 112
  - Density 3
  - Deposit 1
  - Die-casting 10, 23 ff., 56
    - Alloys 37
    - Calculation of casting parameters 42 f.
    - Cold chamber machine 26, 46 f.
    - Costs 54 f.
    - Feeding system 41
    - Gas cubage content 57
    - Hot chamber machine 25
    - Inert gas 40
    - Mould making 38



- Process safety 42 ff.
- Proportioning furnace 40
- Safety 40
- Vacuum die-casting 45, 47 f., 49
- Die-casting alloys
  - Applications 12, 225
  - Automotive engineering 29, 50 ff.
  - Composition 220
  - Corrosion rate 37
  - Creep analysis 220
  - Creep rate 49, 114 f., 123
  - Heat resistance 49
  - High temperature properties 113
  - MAGOXID-COAT 222 ff.
  - Rare Earth elements containing 123
  - Spray forming 57
  - Squeeze-casting 56, 57
  - Tensile strength 7
  - Thixo-casting 56, 57, 65
  - Thixo-moulding 66
  - With aluminium 48
- Die-casting mould 38 f.
  - Hot chamber process 39 f.
- Die-casting processes
  - Cold chamber process 27, 45
  - Hot chamber process 25, 45
  - Vacuum die-casting 45
- Die-castings 34 ff.
  - Application examples 50 ff.
  - Application fields 29, 34
  - Automotive engineering 29, 50 ff.
  - Costs 54 f.
  - Electronic industry 34
  - Equipment 34
  - Strain Control 54
  - Tools 34
- Diffusion creep 108
- Diffusion joining
  - DB/SPF process technology 159
  - Diffusion bonding 159
  - Joining methods 159
  - Superplastic forming 159
- Drill finishing 131, 136
  - Cooling concept 141
  - Mechanical load on tool 136 ff.
  - Optimizing machining time 139
- Drilling
  - Comparison of Mg and Al alloys 132 ff.
  - Cutting parameters 132 ff.
  - Drill moment 132 ff.
  - Mechanical tool load 132 f.
  - MLS 140
  - Solid drilling 135
  - Surface and peripheral zones 149
  - Surface roughness 148
  - Temperature dependent contraction 148
  - Tool geometry 132, 134
- Drilling speed and feed Precipitation hardening AZ Alloys 4
- Ductility 56

**E**

- EA-RS alloys 171, 173
- Electrochemical corrosion 227
- Electromagnetic stirring *see* Rheo-casting
- Electromotive chain of elements 244
- Electron beam welding
  - Energy input 2
  - Joining methods 156
  - Non-vacuum electron beam welding (NV-EBW) 156
- ESMA-mapping 230
- Extrusion 90 ff.
  - Alloys 94
  - Casting 93
  - Direct 94
  - Feedstock manufacturing 92
  - Melting 92
  - Minimum wall thickness 95
  - Pressing speed 94
  - Solid and hollow profiles 94 f.

**F**

- Fiber/matrix adhesive strength 192
- Finite element method 201
- Flank-wear 144 ff.
- Floater-Nozzle process 93
- Flow curves 80
- Forging 85, 90 ff., 99 ff.
  - Alloys 99
  - Application Examples 101 ff.
  - Casting 93
  - Comparison Al and Mg forged wheel 102 ff.
  - Cubic 100
  - Feedstock manufacturing 92
  - Melting 92
  - Premises 99
  - Tensile strength, dependent on direction 100
  - Three-axial dispersing 101
- Frank-von-Mises criterion 111
- Friction welding 157 f.
  - joining methods 157
  - Of die-casting alloys 160
  - Pressure welding 157

**G**

- Galvanic corrosion 219 ff.
- Gas cubage content 14
- Gas pressure infiltration 188 f.
- Glueing, joining methods 160
- Grain boundary gliding 108
- Grain hardening 4
- Gravity casting 8, 57
  - Microstructure 178 f.
- Guiner-Preston-zones 118

**H**

- Half liquid melts 65 f.
- Hall-Petch relation 202
- Hardness increase 5
- Heat resistance 5, 7, 49
- High temperature properties 106 ff., 111
- High-Purity (HP) alloys 2, 4, 10, 23, 91 f., 219, 226
  - Corrosion rate 37
- Hollow profiles 94 f.
- Hot chamber machines 28, 46
- Hot chamber process 27, 45 f.
  - Die-casting mould 39 f.
- Hot working 90
- Hot-Top process 93
- Hydrogen overvoltage 233

**I**

- Impact strength 57
- Impulsion arc 153
- Inert gas sputtering 164 f., 166
- Infiltration
  - Melting metallurgical processes 203
  - Production of particle and hybrid preforms 204
- Ingot feeding 41
- Intermetallic corrosion 227
- Intermetallic phase 4
- Inverse rule of mixture 185, 199

**J**

- Jerky flow 119
- Joining
  - Arc welding processes 153 ff.
  - Beam welding processes 153
  - History 152
  - Joining methods 154, 156 ff.
  - Thixotropic materials 160

**L**

- Laser beam welding
  - Gas laser 154
  - Joining methods 154
  - Schematic 155
  - Solid-state laser 154
- Laser surface treatment 229
  - Gradient surface setup 229
- Laval nozzle 166, 176
- Light weight construction 33
- Linear rule of mixture 184 f.

**M**

- Machining 130 ff.
- Machining, Cutting 96
  - Properties 130
- Magnesium alloys 2, 3, 9 f., 72 ff., 81
  - Applications 9
  - As construction material 18
  - ASTM codes 3
  - Characteristic profile 18
  - Compared to aluminium 10
  - Damping capacity 3
  - Deformation 72 ff.
  - Deformation behaviour 81 f.
  - DIN-specification 3
  - Dispersion strengthened 15
  - Forging 85
  - Formed sheets 73
  - Massive forming 78 ff.
  - Processing 10
  - Recycling 18
  - Specification 3
  - Temperature dependence 85
- Magnesium composites
  - Drilling and precision boring 131
  - Machining 130
  - Safety engineering 131
  - Safety precautions 131
- Magnesium materials, deformation of 72 ff.
  - Deep drawing 75
  - Methods 73 ff.
  - Swaging of powder 74
- Magnesium, gaining 1 f.
- MAGOXID 239
- MAGOXID-COAT 229
- Massive forming 78 ff.
  - Cylinder compression tests 78
- Materials, density 24
- Maximum drawing ratio 75, 83
- Median or d50-value 198
- Melt-spun alloys 171 ff.
  - EA-RS alloys 171
  - Fracture elongation 172 f.
  - Overview 171
  - Properties 171
  - Tensile strength 172 f.
- Melt-spinning 166
  - Corrosion and creep behaviour 173
  - Schematic 166
- Metal matrix composite material 63
  - Drilling 142
  - Machining 141 ff.
  - Manufacturing 142
  - PCD 142
  - Tools 142
- Mg-alloys 4
- Micro lubrication system (MLS) 142 f.
- Microstructure inhomogeneities 57
- MIG process 153
  - Material specific difficulties 153

- Micro-cracking 142 f.
- Micro-fatigue 142 f.
- Micro-machining 122
- Micro-ploughing 142 f.
- MLS, *see* Micro lubrication system 140

**N**

- Nickel plating, electroless/chemical 244 ff.
  - AHC process 244 f.
  - Standard process 244
- Nickel/phosphor alloy coatings 242 ff.
  - Application examples 252 f.
  - Corrosion resistance 247
  - Distribution of layer thickness 247
  - Electroless deposited 242 ff.
  - Influence of the surface roughness on the coating 247 f.
  - Layer properties 246
  - Thermal cycling test 248
  - Thermal stability 248
  - Wear measurements 248
- Norton's Law 108
- NRC process 66
- NV-EBW *see* Non-vacuum electron beam welding process

**O**

- Orowan-Mechanism 200, 203
- Ostwald-Ripening 110
- Oxidation, anodic 223

**P**

- P/M materials 167
- Particle Materials
  - Boundary surface reactions 198
  - Geometry 198
  - Manufacturing 198
  - Mechanical Properties 198
  - Physical Properties 198
- Particle reinforcements 199 ff.
  - Grain refinement 199
- Passivation, behaviour 218 f.
- PCD-tools 142
- Physical Vapor Deposition (PVD) 230
- Pitting corrosion 219
- Planar Flow Cast process 166
  - Corrosion and creep behaviour 173
  - Schematic 166
- Plasma-glow discharge 231
- Plasma-physical layer 250 f.
- Plastometer 79
- Powder 206
  - Mechanical crushing 206 f.
  - Production by gas sputtering 206

- Precision boring, mechanical load on tool 136
- Preform 186 f.
- Process safety with die-casting 42 ff.
- Profiles
  - Application examples 99
  - Bending 96
  - Joining 96
  - Tensile and compression strength values 96
- Properties 2 f.

**Q**

- QE alloys 8

**R**

- Radius-effect 118
- Rapid solidification 14, 17, 164
  - Cathodic sputtering 165
  - Change of properties 164 f., 166
  - Cooling rate 165
  - CVD 165
  - Improving corrosion resistance 165
  - Improving deformability 165
  - Inert gas sputtering 166
  - Laser or electron beams 165
  - Melt-spinning 164 f.
  - Oversaturated solid solution crystals 165
  - Planar Flow Cast process (PFC) 166
  - Rapidly solidifying structures 165
  - Spray Forming 164 f., 166
  - Sputtering a metal melt 166
- Rapidly solidified materials 168 ff.
  - Profile 168
- Rare Earth elements alloys 117 ff.
  - Activation energies 119 ff.
  - Corrosion resistance 118 ff.
  - Creep behaviour 124
  - Creep of Y-containing magnesium alloys 120
  - Creep resistance 118 ff.
  - Die-casting alloys 123
  - Heat resistance 118 ff.
  - High temperature properties 117 ff.
  - Jerky flow 119
  - Mg high-performance alloys 124
  - Mg-Y-alloys 119
  - QE-alloys 119
  - Radius effect 118
  - Valence effect 118
  - WE-alloys 119, 121
  - Wrought alloys 119, 121
- Rare Earth elements casting alloys 8
- Reaming
  - Averaged roughness 137
  - Cutting edge wear 138
  - Influence of cutting speed and feed on the drilling quality 137
  - Machining 138

- Mechanical load on tool 136
  - MLS 140
  - Reboring
    - Drilling quality 138
    - MLS (micro lubrication system) 140
  - Recycling 18, 175, 254 ff.
    - Agent-free melting 268
    - Automatic sorting of automotive shredder 260 ff.
    - Casting alloys 255
    - Chippings 272
    - Composites 274 f.
    - Dry process 260
    - General schematic 260
    - Materials 265
    - Melting and refining processes with little refining salts 267
    - Melting metallurgical recycling 266
    - Melting processes 262 ff.
    - Melting processes with much refining salts 270 ff.
    - Metal sorting facility 260 ff.
    - Metallurgical cleaning methods 265
    - New scrap 255 ff.
    - Old scrap 255 ff.
    - Protection gases 264
    - Raw materials 255
    - Reactivity of magnesium 263 f.
    - Recycling Scenarios 256 ff.
    - Refining salts 263
    - Scandium 273 f.
    - Special magnesium scrap 272
    - Transportation of liquid magnesium 266
    - Wrought alloys 255
  - Reinforcement materials 198 f.
    - Melting metallurgical manufacturing 197
    - Particle reinforced 197
  - Rheo-casting 65
  - Rotation sputtered alloys 169
    - Mechanical properties 169 f.
- S**
- Sand casting 8, 15
  - Sand casting alloy 121
    - Spray formed 175
    - Tensile strength 121
  - Secondary creep rate 173
  - Self corrosion 239
  - Separation of a melt 166
  - Shear-Lag-model 201
  - Sheet metal forming 76 ff., 82 ff.
    - Cold forming 82
    - Deep drawing 76, 82
    - Deformation speed 78
    - Deformation temperature 77
    - Maximum drawing ratio 83 f.
    - n-value 76 f.
    - r-value 76 f.
  - Stretch-forming 82
  - Temperature dependent deformation behaviour 82 f.
  - Short circuit arc 153
  - Softening 110
  - Solid drilling
    - Influence of the cutting speed 135
    - Mechanical load on tool 135 f.
  - Solid profiles 94 f.
  - Solid solution hardening 4
  - Spray casting 166
  - Spray deposition 166
  - Spray formed alloys 174 ff.
    - Fracture elongation 174
    - Microstructure 178 f.
    - Profile 174
    - Tensile strength 174
    - Yield strength 174
  - Spray formed materials 175 ff.
    - Fracture elongation 178
    - Inert gas sputtering machine 175
    - Manufacturing and properties 175 ff.
    - Mechanical properties 178
    - Sputtering behaviour of different alloys 176
    - Sputtering tests 176
    - Tensile strength 178
    - Yield strength 178
      - As a function of the temperature 179
  - Spray forming 173 ff., 166
    - Melting metallurgical methods 203
  - Sputtered alloys, mechanical properties 169 f.
  - Sputtering 15
  - Squeeze-casting 16, 56, 57 f., 204
    - Composites 62 f.
    - Production 58
    - Direct squeeze-casting 59 f.
    - Indirect squeeze-casting 58 f.
    - Properties of the castings 60 ff.
  - Squeeze-casting processes 188
    - Melting metallurgical production 188
  - Strength
    - Increase 5
  - Stress corrosion cracking 219
  - Stress-Strain behaviour 57
  - Surface treatment with electron beam 229
- T**
- Tensile strength 191
  - Thixo-casting 56, 57, 65 ff.
    - Globular microstructure 65 f.
  - Thixo-moulding 57, 66, 68
    - Injection-moulding cycle 68
    - Injection-moulding machine 68
  - Thixotropic materials 160
    - Welding 160
  - TIG-coating 229
  - TIG-process 153
  - Tool load

- Comparison between non-reinforced and reinforced magnesium 146 f.
- Tool wear 142 ff.
- Coating 144 ff.
- Cutting speed 143 ff.
- Feed 144 ff.
- Feed force and drill moment 147
- Flank wear 144
- Mechanical load on tool 147

**U**

Use in cars 9, 11

**V**

- Vacuum die-casting 45, 50, 57
- Gas cubage content 57
- Valence effect 118

**W**

- Water-cooled slab casting 93
- Floater-Nozzle process 93
- Hot-Top process 93
- WE alloys 8
- Weight savings 19
- Weight, specific 92

- Weldability 160 ff.
- Welding 160 f.
- Wrought alloys 15, 56, 82, 85, 96, 119
- Alloying elements 91
- Composition and properties 9
- Creep behaviour 97
- Dynamic strength 98
- Extrusion products 91 f.
- Fatigue strength 98
- Forging 85 ff.
- Forging products 91 f.
- Fracture toughness 98
- Low temperature behaviour 98
- Massive forming 88
- Strength increase 91
- Temperature dependent deformation behaviour 82 f.
- Tensile and compression test results 96
- Tensile test results (elevated temperature) 97
- Toughness 98
- Weldability 160 ff.
- Wrought material 9
- Wrought semi products 90

**Y**

- Yield Strength of the matrix 185
- Young's Equation 186
- Young's Modulus 189